

**Development of efficient cytochrome P450-dependent
whole-cell biotransformation reactions for steroid
hydroxylation and drug discovery**

Dissertation
zur Erlangung des Grades
des Doktors der Naturwissenschaften
der Naturwissenschaftlich-Technischen Fakultät III
Chemie, Pharmazie, Bio- und Werkstoffwissenschaften
der Universität des Saarlandes
von

Tarek Hakki

Saarbrücken

2008

Index

	Publications resulting from this work	I
	Abbreviations	II
	Abstract	IV
	Zusammenfassung	V
	Summary	VI
1.	Introduction	1
1.1.	Steroid hormones and cytochromes P450	1
1.2.	Human CYP11B1 and CYP11B2	6
1.2.1.	General aspects	6
1.2.2.	Physiological role of CYP11B1 and CYP11B2	7
1.2.3.	Differences and similarities between CYP11B1 and CYP11B2	11
1.2.4.	CYP11B1 and CYP11B2 modelling	11
1.2.5.	CYP11B1 and CYP11B2 as drug targets	13
1.2.6.	General requirements for the development of CYP11B2 inhibitors	15
1.2.7.	Heterologous expression of CYP11B1 and CYP11B2 in stable cell cultures	16
1.2.8.	Heterologous expression of CYP11B1 and CYP11B2 in yeast	16
1.2.9.	Inhibitors of CYP11B1 and CYP11B2	17
1.3.	Fission yeast <i>Schizosaccharomyces pombe</i> as a model system	18
1.4.	Biotechnological applications of the 11 β -Hydroxylases	20
1.5.	Aim of the work	21
2.	Materials & Methods	23
2.1.	Materials	23
2.1.1.	Microorganism growth media	23
2.1.1.1.	Growth media for <i>Escherichia coli</i> (<i>E. coli</i>)	23
2.1.1.2.	Growth media for <i>Schizosaccharomyces pombe</i> (<i>S. pombe</i>)	24
2.1.2.	Microorganisms	26
2.1.3.	Plasmids	26
2.1.4.	Oligonucleotides	29
2.1.5.	Library of pharmacologically active compounds (LOPAC)	29
2.1.6.	Mega Block plates	30
2.2.	Methods	31
2.2.1.	Molecular biology methods	31

Index

2.2.1.1.	pNMT1- TOPO cloning	31
2.2.1.2.	Amplification of the human AdR	32
2.2.1.3.	DNA electrophoresis and manipulation	33
2.2.1.4.	DNA restriction and ligation	33
2.2.1.5.	Plasmid purification and DNA sequencing	33
2.2.2.	Microbiology methods	34
2.2.2.1.	<i>E. coli</i> cultivation and transformation	34
2.2.2.2.	<i>S. pombe</i> cultivation and transformation	34
2.2.2.3.	<i>ura4</i> gene disruption in <i>S. pombe</i>	35
2.2.3.	Biochemical methods	36
2.2.3.1.	Subcellular fractionation and protein preparation from <i>S. pombe</i>	36
2.2.3.2.	SDS (Sodium dodecylsulfate) polyacrylamid gel electrophoresis and gel blotting	37
2.2.3.3.	Immunologic detection of proteins	37
2.2.4.	Steroid hydroxylation assays	39
2.2.4.1.	Bioconversion assay in Erlenmeyer flasks	39
2.2.4.2.	Bioconversion in modified 1.5 ml tubes	39
2.2.4.3.	Steroid extraction	40
2.2.4.4.	Steroid analysing methods	41
2.2.4.4.1.	High performance liquid chromatography (HPLC)	41
2.2.4.4.2.	High performance thin layer chromatography (HPTLC)	41
2.2.4.5.	Measuring of steroid bioconversion	42
2.2.4.6.	Measuring of the inhibition of steroid bioconversion (Determination of the IC ₅₀ values)	42
2.2.5.	Structure activity relationship (SAR) study	43
2.2.6.	Statistical analysis	44
2.2.6.1.	Descriptive statistics (Measures of variation)	44
2.2.6.2.	Statistical tests	44
2.2.6.2.1.	<i>t</i> -test for independent samples	44
2.2.6.2.2.	Correlation	45
2.2.6.2.3.	Z'-Factor of assay	45
3.	Results	47
3.1.	Optimisation of a steroid hydroxylation assay for the 96-well plate format	47

Index

3.1.1.	Steroid bioconversion assay in modified 1.5 ml tubes (tip-tube format)	47
3.1.2.	Steroid bioconversion assay in 96-well plate	49
3.2.	Coexpression of the corresponding redox partners in CYP11B1-expressing fission yeast <i>Schizosaccharomyces pombe</i>	60
3.2.1.	The Coexpression of AdR and Adx through two expression vectors (Strategy I)	60
3.2.1.1.	<i>Ura4</i> gene disruption in <i>S. pombe</i> (SZ1) and the characterisation of the new strain	61
3.2.1.2.	Construction of AdR expressing vector (pTH1)	63
3.2.2.	Construction of an AdR+Adx expressing vector pTH2 (Strategy II)	63
3.2.3.	Coexpression of Adx and AdR in fission yeast	65
3.2.4.	The 11 β -hydroxylation activity of CYP11B1 in the new recombinant fission yeast strains	68
3.2.4.1.	Comparison of biotransformation activity of CYP11B1-expressing strains after coexpressing of the corresponding redox partners	69
3.2.4.2.	Quantification of hydrocortisone production in the novel strain TH75	71
3.2.4.2.1.	Optimisation of the biotransformation parameters to a achieve a high conversion rate	71
3.2.4.2.2.	Hydrocortisone production efficiency in the fission yeast strain TH75	72
3.3.	Development of a cell-based high throughput screening system for the discovery of human aldosterone synthase inhibitors	74
3.3.1.	Automated screening technology plate-format	74
3.3.2.	Optimisation of the screening assay parameters to get detectable conversion/inhibition response	76
3.3.3.	Proof of principle	81
3.3.4.	Validation of the new CYP11B2 inhibitors identified during the screening assay	88
3.3.4.1.	Toxicity in fission yeast	88
3.3.4.2.	Determination of the IC ₅₀ values against CYP11B2 and CYP11B1	89
4.	Discussion and Outlook	95
4.1.	Optimisation of steroid hydroxylation assay for the 96-well plate format	95
4.2.	Coexpression of redox partners in CYP11B1 expressing fission yeast <i>Schizosaccharomyces pombe</i>	96

Index

4.3.	The development of a cell-based high throughput screening system for the discovery of human aldosterone synthase inhibitors	100
4.4.	Testing of a library of pharmacologically active compounds using the developed screening system	103
5.	References	111
6.	Appendix	128
6.1.	Contributions to international meetings	128
6.2.	Index of Figures	129
6.3	Index of Tables	132
6.4.	Materials and Methods	133
6.4.1.	Stock solutions for EMM medium	133
6.4.2.	Oligonucleotides	134
6.4.3.	Library of pharmacologically active compounds	136
6.4.4.	Liquid class programs	165
7.	Acknowledgment	167
	Curriculum Vitae	

Publications resulting from this work

A. Manuscripts:

1. Derouet-Hümbert, E., Dragan, C. A., **Hakki, T.** and Bureik, M., 2007. ROS production by adrenodoxin does not cause apoptosis in fission yeast. *Apoptosis*. 12, 2135-2142.
2. **Hakki, T.** and Bernhardt, R., 2006. CYP17- and CYP11B-dependent steroid hydroxylases as drug development targets. *Pharmacol Ther.* 111, 27-52.
3. **Hakki, T.**, Zearo, S., Dragan, C. A., Bureik, M. and Bernhardt, R., 2008. Coexpression of redox partners increases the hydrocortisone (cortisol) production efficiency in CYP11B1 expressing fission yeast *Schizosaccharomyces pombe*. *J Biotechnol.* 133, 354-359.
4. **Hakki, T.**, Hübel, K., Waldmann, H. and Bernhardt, R., in preparation. The development of high throughput screening system for the discovery of human aldosterone synthase (CYP11B2) inhibitors.
5. Petric, S., **Hakki, T.**, Bernhardt, R., Cresnar, B. in preparation. Characterization and expression of progesterone-inducible cytochrome P450 genes in the zygomycete fungus *Rhizopus oryzae*.

B. Patent application

Tarek Hakki¹, Rita Bernhardt¹, Matthias Bureik¹, Katja Hübel², Herbert Waldmann².

Vier neue und spezifische Inhibitoren der humanen Aldosteronsynthase (Submitted)

¹Institute of Biochemistry, P. O. Box: 151150, Saarland University, D-66041 Saarbrücken, Germany

²Max Planck Institute of Molecular Physiology, Otto-Hahn-Str, 11, D-44227 Dortmund, Germany

Abbreviations

18-OH-B	18-hydroxycorticosterone
5-FOA	5 -fluoroorotic acid
A	Area
ACE	Angiotensin-converting enzyme
ACTH	Adrenocorticotrophic hormone
AdR	Adrenodoxin reductase
Adx	Adrenodoxin
Adx ^{D113Y}	Adx substitution mutant containing Tyr instead of Asp at position 113
Adx ^{S112W}	Adx substitution mutant containing Trp instead of Ser at position 112
Adx ^{WT}	Adrenodoxin wild type
AGS	Adrenogenital syndrome
Aldo	Aldosterone
ampR	Ampicillin resistance gene
arh1	Fission yeast ferredoxin reductase
ars1	Autosomal replicating sequence
B	Corticosterone
CAH	Congenital adrenal hyperplasia
C _{inh}	Inhibitor concentration
CMO	Corticosterone methyl oxidase
CPR	Cytochrome P450 reductase
CRH	Corticotropin-releasing hormone
CYP11B1	Steroid 11 β -hydroxylase, cytochrome P450c11
CYP11B2	Aldosterone synthase, cytochrome P450c11Aldo
Da	Dalton
DBH	Dopamine β - hydroxylase
DHEA	Dehydroepiandrosterone
DITIs	Disposable Tips
DMSO	Dimethyl sulfoxide
DNA	Deoxyribonucleic acid
DOC	11-deoxycorticosterone
DTE	1,4-Dithioerythritol
EMM	Edinburgh minimal medium
EPHESUS	The Eplerenone Post-Acute Myocardial Infarction Heart Failure Efficacy and Survival Study
ET	Electron transfer
EtOH	Ethanol
etp1 ^{fd}	Adrenodoxin-like ferredoxin
F	Cortisol (Hydrocortisone)
<i>f</i>	Correction factor
FAD	Flavine adenine dinucleotide
FH-I	Familial hyperaldosteronism type I

FMN	Flavine mononucleotide
GRA	Glucocorticoid-remediable aldosteronism
GSH	Glucocorticoid-suppressible hyperaldosteronism
HPLC	High performance liquid chromatography
HPTLC	High performance thin-layer chromatography
HTS	High throughput screening system
IC ₅₀	Concentration of inhibitor that gives 50% inhibition
<i>INH(P)</i>	The inhibition of the product production
<i>I_{radio}</i>	Intensity of the radioactive signal
IST	Internal standard
IZA	Inner zone antigen
kDa	kilodalton
LB	Luria-Bertani
LiAc	Lithium acetate
LOPAC	Library of pharmacologically active compounds
MAO	Monoamine oxidase
MeOH	Methanol
NaAc	Sodium acetate
NADPH	Nicotinamide adenine dinucleotide phosphate
NC	Negative control
PC	Positive control
PEG	Polyethylene glycol
PMSF	Phenyl methyl sulfonyl fluoride
PNMT	Phenylethanolamine N-methyltransferase
pNMT	no message with thiamine promoter
RALES	Randomized Aldosterone Evaluation Study trial
RNA	Ribonucleic acid
ROI	Region of interest
RSS	11-deoxycortisol
RT	Room temperature
<i>S. cerevisiae</i>	<i>Saccharomyces cerevisiae</i>
<i>S. pombe</i>	<i>Schizosaccharomyces pombe</i>
SAR	Structure-activity relationship
SCC	Side-chain cleavage
SDH	Steroid dehydrogenases
SDS-PAGE	Sodium dodecylsulfate polyacrylamid gel electrophoresis
SE	Standard error of the mean
TH	Tyrosine hydroxylase
YEA	Yeast extract and supplements

Abstract

Cytochromes P450 play a vital role in the steroid biosynthesis in the human adrenal gland, e.g. the production of hydrocortisone and aldosterone by CYP11B1 and CYP11B2, respectively. The steroid hydroxylases of the CYP11B family are important targets for drug development. Since they are very closely related, the discovery of selective inhibitors has been a focus of interest. Furthermore, hydrocortisone is a precursor for drugs with high therapeutic potential. Therefore, the purpose of this work was the development of an efficient system for CYP11B-dependent whole-cell biotransformation to facilitate the bioproduction of hydrocortisone and the discovery of selective inhibitors. The present work shows clearly that hydrocortisone production can be dramatically enhanced (3.4-fold) by coexpression of the natural redox partners of CYP11B1. Moreover, a high production efficiency has been achieved by optimisation of the reaction conditions. Additionally, in the course of this work an automated screening technology plate-format has been developed using a CYP11B2-expressing fission yeast strain. Additionally, the conditions for HPLC analysis of steroids were optimised and a high throughput screening system for the discovery of CYP11B2 inhibitors has been established. The new screening system was successfully used for the investigation of a library of pharmacologically active compounds resulting in the identification of several novel potential inhibitors of CYP11B2.

Zusammenfassung

Cytochrome P450 spielen eine entscheidende Rolle in der Steroidbiosynthese in der menschlichen Nebenniere z. B. bei der Produktion von Hydrocortison durch CYP11B1 sowie von Aldosteron durch CYP11B2. Steroidhydroxylasen der CYP11B Familie stellen Ziele für die Entwicklung von Medikamenten dar. Wegen des hohen Verwandtschaftsgrades dieser Enzyme ist die Entdeckung selektiver Inhibitoren von großem Interesse. Darüber hinaus ist Hydrocortison eine Vorstufe für Arzneimittel mit großem therapeutischem Potenzial. Das Ziel der vorliegenden Arbeit war daher die Entwicklung eines effizienten Systems für die CYP11B-abhängige Ganzzellbiotransformation, um die Herstellung von Hydrocortison sowie die Identifizierung selektiver CYP11B2-Inhibitoren zu erleichtern. Die Hydrocortisonproduktion konnte in dieser Arbeit durch die Coexpression der natürlichen Redoxpartner von CYP11B1 und durch die Optimierung der Reaktionsbedingungen deutlich gesteigert werden. Für den Nachweis von selektiven CYP11B2-Inhibitoren wurde für die Spaltheife ein automatisches hintergrundarmes Hochdurchsatz-Screening-System, basierend auf Mikrotiterplatten und HPLC-Analyse entwickelt. Dieses Verfahren wurde anschließend erfolgreich für die Untersuchung einer Bibliothek pharmakologisch aktiver Komponenten benutzt, wobei neue potentielle Inhibitoren detektiert wurden.

Summary

Cytochromes P450 play a vital role in the steroid biosynthesis pathway in the human adrenal gland, exemplified by the production of the main glucocorticoid hydrocortisone (cortisol) from 11-deoxycortisone by CYP11B1, and the production of the most important human mineralocorticoid aldosterone from 11-deoxycorticosterone by CYP11B2. CYP11B-dependent steroid hydroxylases are drug development targets, and since they are very closely related enzymes, the discovery of selective inhibitors of each one has been a hot topic. Furthermore, hydrocortisone is a precursor for drugs with high therapeutic potential. Therefore, the purpose of this work was the development of efficient CYP11Bs-dependent whole-cell biotransformation reactions for the bioproduction of hydrocortisone and the discovery of selective inhibitors of CYP11B2.

For this reason, the corresponding mitochondrial electron transfer proteins (AdR and Adx) were coexpressed with CYP11B1 in fission yeast *Schizosaccharomyces pombe*. Moreover, two mutants of Adx were investigated and coexpressed with AdR to improve the electron transport to CYP11B1 to increase the bioproduction of hydrocortisone in recombinant fission yeast. This work shows clearly that hydrocortisone production can be dramatically enhanced (3.4- fold) by coexpressing the other components of the CYP11B1 electron transfer chain and by optimising the reaction conditions to achieve a high production efficiency on the laboratory level. The new fission yeast strain TH75 coexpressing the wild type Adx and AdR displays high production efficiency at an average of 9.7 μmol hydrocortisone / 10 ml test culture over a period of 72 hours, the highest value published to date for this biotransformation.

In addition, using a CYP11B2-expressing fission yeast strain, an automated screening technology plate-format has been developed. The new screening technology is a one-point HPLC-based assay that investigates compounds regarding of their inhibitory effect against CYP11B2 at concentration of 41.6 μM . Furthermore, the HPLC was further optimised, which enabled the separation of the closely related steroids 11-deoxycorticosterone (DOC) and corticosterone (B) within 2 minutes. Hence, a high throughput screening system has been established. The new screening system displayed high reproducibility and was validated in the presence of controls. In a next step, a library of pharmacologically active compounds was investigated using this new screening system, which reported novel potential inhibitors of CYP11B2. The new inhibitors were further validated and new selective inhibitors have been discovered. Since the use of these drugs is usually combined with unexplained hypotension and severe side effects, the ability of these compounds to inhibit CYP11B2 can explain to

some extent these side effects. Furthermore, the new inhibitors are “druggable” compounds that could be used either in the treatment of hyperaldosteronism-related diseases or as lead compounds that could further optimised in the field of drug development to achieve more safe and selective inhibitors of CYP11B2.

Although the screening system was developed and validated on the laboratory level, it displayed the ability to screen up to 600 compounds per week with the possibility to increase the capacity of the test (10-fold) up to 6000 compounds per week.

Taken together, the newly developed system is a robust screening system that can be applied to investigate libraries of existing drugs to find novel CYP11B2 inhibitors. This screening enables the reposition (recycling) of existing drugs, which can save costs and billions of dollars spend to develop new CYP11B2 inhibitors.

1. Introduction

1.1. Steroid hormones and cytochromes P450

Steroid hormone research began in a broader sense with the crystallisation of several sex steroid hormones in the years 1929-1935, of the glucocorticoids in 1935-1938, and finally of aldosterone in 1953. All of these hormones possess the basic parent cyclopentanophenanthrene ring structure provided by cholesterol, which is modified by an array of enzymes expressed at various levels and in numerous tissues throughout the body.

The enzymes involved in steroid hormone metabolism can be divided into three large groups: the cytochromes P450, reductases and steroid dehydrogenases (SDH), each of which exhibits important, biochemically distinct properties (Miller 1988; Lisurek and Bernhardt 2004; Hakki and Bernhardt 2006). P450 enzymes comprise a large family of highly conserved proteins that incorporate molecular oxygen into lipophilic substrates with the provision of reducing equivalents from the cofactor NAD(P)H (Figure 1.1).

Cytochrome P450 proteins in humans are enzymes that synthesise cholesterol, steroids, and other important endogenous substrates such as prostacyclins and thromboxane A₂, and degrade xenobiotics and drugs. They catalyse many types of reactions, but the most important one is hydroxylation. These enzymes are classified as mixed function oxidases or monooxygenases, because they incorporate one atom of molecular oxygen into the substrate and one atom into water (Figure 1.1.).

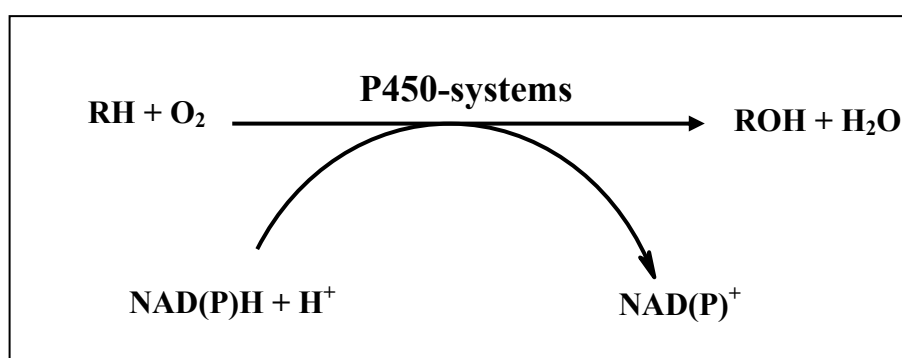


Figure 1.1. Reaction generally catalysed by cytochrome P450.

Cytochromes P450 are monooxygenases, which in contrast to dioxygenases catalyses the incorporation of a single atom of molecular oxygen into the substrate. The reduction equivalents needed for this reaction are provided by an external cofactor.

These reactions are essentially irreversible, not easily to be inhibited, and are so poised in the steroidogenic pathway that they determine the formation of each of the five major classes of

steroid hormones: progestagens, mineralocorticoids, glucocorticoids, androgens, and estrogens. To activate oxygen in the substrate binding pocket of P450s, electrons must be transferred from NAD(P)H to the P450. Although some P450s do not require any other protein component to achieve the reductive activation of molecular oxygen (Degtyarenko and Kulikova 2001), the vast majority of P450s performs the diverse range of chemical reactions after interaction with one or more redox partners to obtain the redox equivalents from electron transfer (ET) chains. A protein complex forms transiently between the P450 and the redox partner allowing the effective transfer of electrons. Although ten classes of P450 systems have been recently classified depending on the topology of the protein components involved in the electron transfer to the P450 enzyme (Hannemann *et al.*, 2007), there are only two redox protein systems involved in the steroid biosynthesis in mammals. One for the P450 enzymes anchored in the mitochondrial membrane and one for P450s located in the endoplasmic reticulum (microsomal compartment). The mitochondrial electron transfer chain consists of two components, a FAD containing flavoprotein, adrenodoxin reductase (AdR), and an iron-sulphur protein of the [2Fe-2S] ferredoxin type, adrenodoxin (Adx) (Figure 1.2) (Lambeth *et al.*, 1982; Hannemann *et al.* 2007).

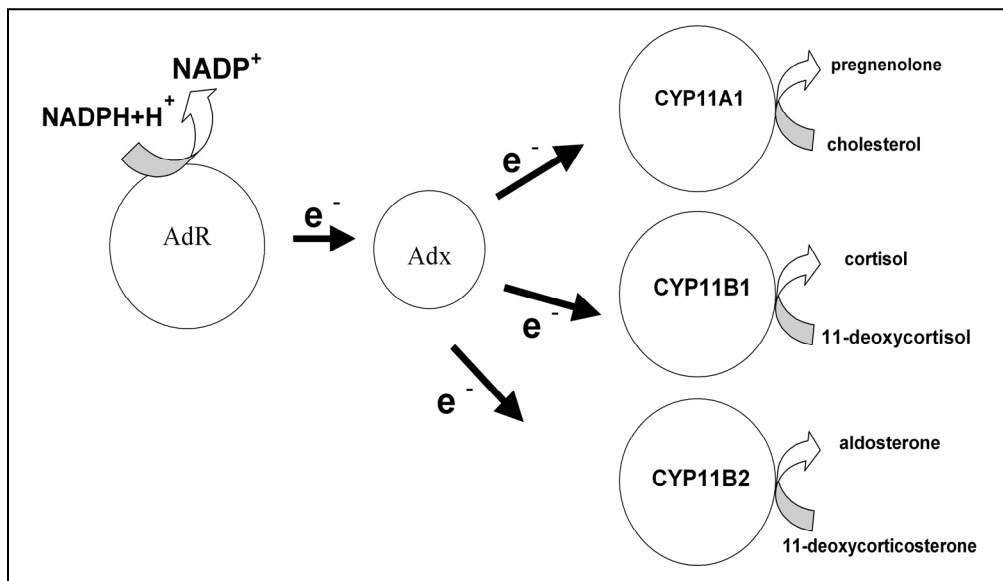


Figure 1.2. The mitochondrial steroid hydroxylase systems.

The electron transport chain for the adrenal mitochondrial steroid hydroxylases consisting of a [2Fe-2S] ferredoxin designated as adrenodoxin (Adx) and a FAD containing, NADPH-dependent ferredoxin reductase accordingly referred to as adrenodoxin reductase (AdR).

Microsomal P450s are supported by a single redox partner protein, the highly conserved FAD and FMN containing flavoprotein NADPH-cytochrome P450 reductase (CPR) (Black and

Coon 1987; Porter 1991) In some cases, also a third protein, cytochrome b5 is involved in modular protein–protein interaction and electron transport (Figure 1.3).

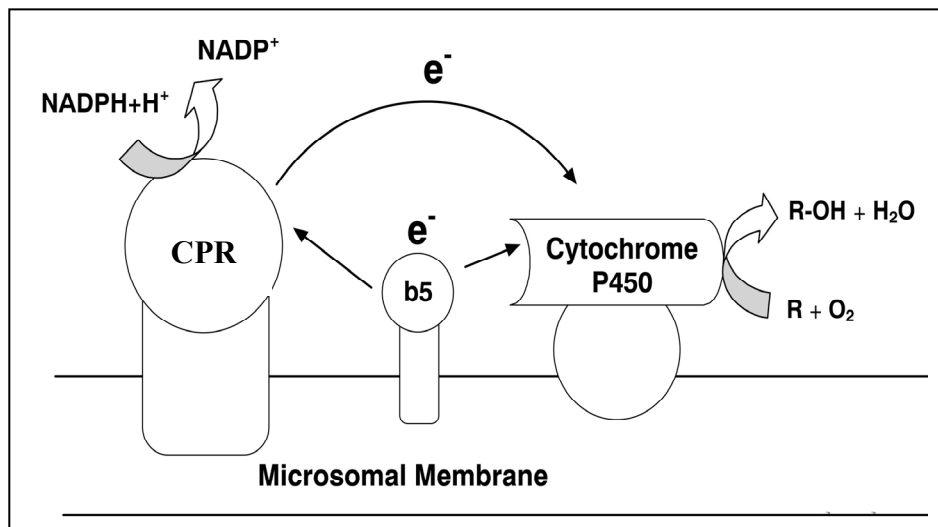


Figure 1.3. The microsomal steroid hydroxylase systems.

Microsomal hydroxylases receive the necessary electrons from an NADPH-dependent FAD- and FMN-containing reductase (CPR).

Thus, the subcellular location (Tamaoki 1973) and corresponding electron transfer or redox system also defines a subclassification of mitochondrial or microsomal cytochrome P450s involved in steroid synthesis, collectively known as the steroid hydroxylases. Within the mitochondrial class of steroid hydroxylases of most species, there are three functionally distinct P450 enzymes (Figure 1.4).

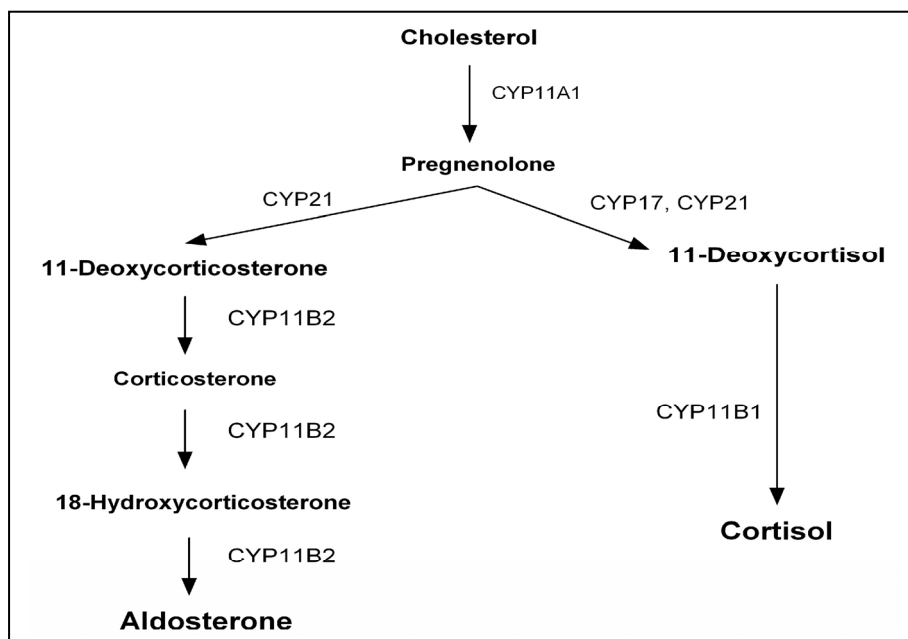


Figure 1.4. The role of cytochromes P450 in the biosynthesis of steroid hormones in the human adrenal cortex. The biosynthesis of all steroid hormones in the adrenal cortex starts with a reaction catalysed by CYP11A1, which cleaves the cholesterol side chain and forms pregnenolone. Other members of the CYP11 family (CYP11B1 and CYP11B2) are involved in the production of cortisol and aldosterone.

The first one, the cholesterol side-chain cleavage P450 (CYP11A, also known as P450_{sc}), utilizes cholesterol for the formation of pregnenolone, which is the universal precursor for all subsequent steroids. A second enzyme, which is cytochrome P450 steroid 11 β -hydroxylase (CYP11B1, also known as P450_{11 β} or P450c11) catalyses the last step in cortisol (hydrocortisone) biosynthesis (Figure 1.4). In addition, CYP11B1 catalyses the subsequent conversion of corticosterone to aldosterone in some species such as cow and pig, and therefore this enzyme is critical in mineralocorticoid metabolism in these animals. In humans, baboons, rats, mice, and guinea pigs, however, a third mitochondrial cytochrome P450, aldosterone synthase (CYP11B2, also known as P450_{aldo}), is encoded by another gene (CYP11B2), which has evolved by duplication of CYP11B1 to specifically catalyses aldosterone synthesis (Bureik *et al.*, 2002a).

The enzymes comprising the microsomal steroid hydroxylase group include three P450s involved in steroid hormone biosynthetic steps subsequent to CYP11A1 leading to both corticoid and sex steroid hormone synthesis.

CYP17 (17 α -hydroxylase/17,20-lyase, also known as P45017 α or P450c17) catalyses the 17-hydroxylation of pregnenolone and progesterone and the 17,20-lyase reaction of the corresponding 17-hydroxylated products. Progesterone and 17-hydroxyprogesterone are substrates for 21-hydroxylase cytochrome P450 (CYP21, also known as P450c21), which catalyses the formation of 11-deoxycorticosterone (DOC) and 11-deoxycortisol (RSS), intermediates in corticosterone and cortisol biosynthesis (Figure 1.4). Finally, the aromatase enzyme (CYP19, P450arom) is responsible for the aromatisation of ring A leading to estrogens. Mutations in steroid hydroxylase genes, or deficiencies of these enzymes, are responsible for several human diseases. Thus, congenital adrenal hyperplasia (CAH) (also known as adrenogenital syndrome; AGS) is mainly caused by defects of CYP21 (Migeon and Donohoue 1991; New 1992), although in 8-9% of the patients with CAH, CYP11B1 mutations are fault (Naganuma *et al.*, 1988; Migeon and Donohoue 1991; New 1992). Defects in aldosterone production caused by mutations in CYP11B2 lead to salt wasting and to failure to thrive (White 2004). Defects in the CYP17 gene exemplified by the 17-hydroxylase deficiency in which the production of sex steroids is absent, results in a compensatory increase in follicle-stimulating hormone and luteinizing hormone, comparable to menopausal levels. In humans, the CYP17 gene is expressed in the adrenal cortex, testes, and ovaries but not the placenta. The adrenals produce glucocorticoids, mineralocorticoids, and C-19 steroids. The gonads, on the other hand, predominantly produce the C-19 steroids and sex hormones. Thus, in patients with 17-hydroxylase deficiencies both adrenal and gonadal steroidogenesis

is impaired. In contrast, CYP17 overproduction leads to prostate cancer (Madigan *et al.*, 2003). Moreover, in some cases prostate cancer is stimulated by androgen production as breast cancer is by estrogens (Figure 1.5). Overproduction of cortisol can be one cause of Cushing's syndrome, which is a chronic glucocorticoid excess associated with substantial morbidity and mortality (Boscaro *et al.*, 2001; Fisher *et al.*, 2001). Overproduction of aldosterone has been shown to cause hypertension. Furthermore, hyperaldosteronism was found to be in 5 to 10% of all patients with hypertension (Young 2007) and congestive heart failure and fibrosis of the heart (Pitt *et al.*, 1999; Brilla 2000; Pitt *et al.*, 2001; Hakki and Bernhardt 2006). More recently, R-fadrozole, which has been reported as aldosterone synthase inhibitor showed the ability to reverse cardiac fibrosis in spontaneously hypertensive heart failure rats (Minnaard-Huiban *et al.*, 2008).

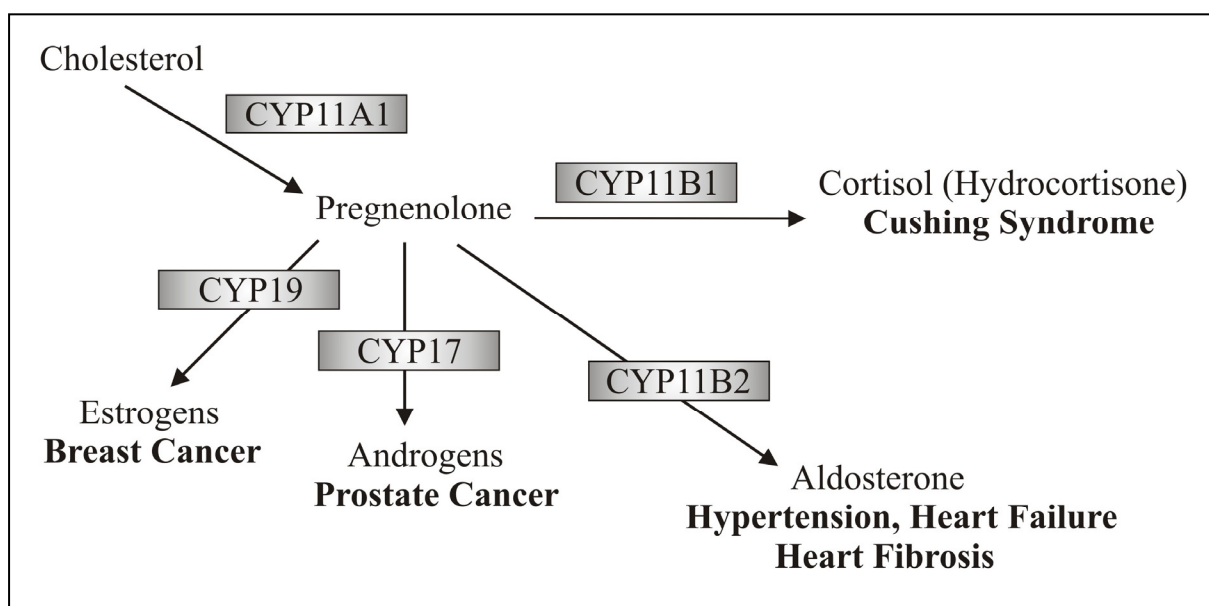


Figure 1.5. Steroid hydroxylases as drug development targets.

Steroid overproduction-related diseases can be treated or controlled by inhibiting the corresponding steroid hydroxylase.

During the past years it became obvious that cytochromes P450 not only play an exceptional role in drug and xenobiotics metabolism and in the biosynthesis of endogenous compounds, but also gain increasing importance as novel therapeutic targets for drug development (Baston and Leroux 2007; Schuster and Bernhardt 2007).

1.2. Human CYP11B1 and CYP11B2

1.2.1. General aspects

Human CYP11B1 and CYP11B2 are localised mainly in the adrenal cortex that consists of the zona glomerulosa and the zona fasciculata/reticularis, which differ from each other with regard to steroidogenic reactions catalysed by different cytochrome P450 isozymes. Glucocorticoids and adrenal androgens are synthesised in the zona fasciculata/reticularis, whereas aldosterone, the most potent natural mineralocorticoid, is synthesised in zona glomerulosa cells (Miller and Tyrell 1995). CYP11B1 is expressed at high levels in the zona fasciculata/reticularis of the adrenal cortex (Erdmann *et al.*, 1995a; Erdmann *et al.*, 1995b; Miller and Tyrell 1995) and produces cortisol, the principal human glucocorticoid. In contrast, aldosterone secretion (Miller and Tyrell 1995) and CYP11B2 expression (Pascoe *et al.*, 1995) take place at low levels in the zona glomerulosa of the adrenal cortex. Vinson argued that the zona glomerulosa in fact has many functions, including aldosterone synthesis, but is probably only a relatively poor de novo source of steroids. In vitro, CYP11B2 (aldosterone synthase) of the glomerulosa has the ability to use the products that arise from CYP11B1 activity in fasciculate cells (Vinson 2004) as substrates. This zonal distribution of expression has been further investigated with surgically removed human adrenal gland cells, showing a higher concentration of CYP11B1 in the zona fasciculata than in the zona reticularis (Mitani *et al.*, 1982). Furthermore, Mitani *et al.* identified the so-called “undifferentiated cell zone”, which could facilitate the exploration of molecular mechanisms for the differentiation and development of adrenocortical cells (Mitani *et al.*, 2003). Min *et al.* characterized the adrenal-specific inner zone antigen (IZA), which is a protein specifically expressed in the zona fasciculate/reticularis of the adrenal cortex, and reported the inhibition of adrenal steroidogenesis by the addition of an anti-IZA monoclonal antibody, and the adrenal steroidogenesis activation by IZA overexpression suggesting its importance in the steroidogenesis (Min *et al.*, 2004). CYP11B enzymes of other species have also been studied, and results indicated that bovine (Wada *et al.*, 1985), porcine (Yanagibashi and Hall 1986), and frog (Nonaka *et al.*, 1995) adrenal cortex syntheses of gluco- and mineralocorticoids are catalysed by a single enzyme, while in man (Kawamoto *et al.*, 1990a; Ogishima *et al.*, 1991), baboons (Hampf *et al.*, 1996; Brown *et al.*, 2002), rats (Matsukawa *et al.*, 1990), mice (Domalik *et al.*, 1991), and guinea pigs (Bülow *et al.*, 1996; Bülow and Bernhardt 2002) two distinct isoforms are involved in the formation of either mineralo- or glucocorticoids. The

reason for these interspecies differences is unknown. Enzymes with 11 β -hydroxylase activity have also been found in several fungi (Megges *et al.*, 1990); however, none of the genes for these enzymes has been cloned to date and their relation to the CYP11B family remains unclear.

The DNA sequence of the *CYP11B2* gene is about 95% identical to that of the *CYP11B1* gene in the coding regions and 90% identical in the introns. The 5' upstream region has, however, diverged considerably from that of *CYP11B1*, suggesting that this second gene, if expressed, may be regulated differently. Mornet *et al.* determined that the *CYP11B1* and *CYP11B2* genes both contain nine exons (Mornet *et al.*, 1989). The eight introns are identical in location to the introns of *CYP11A1*. The genes encoding the two human enzymes are arranged ~ 45 kb apart from each other on chromosome 8 (Chua *et al.*, 1987; Wagner *et al.*, 1991) and chimeric *CYP11B1/CYP11B2* genes that result from unequal crossing-over between these two genes have been found in patients suffering from familial hyperaldosteronism type I (FH-I; also called glucocorticoid-remediable hyperaldosteronism) and congenital adrenal hyperplasia (Lifton *et al.*, 1992; Pascoe *et al.*, 1992; MacConnachie *et al.*, 1998; Hampf *et al.*, 2001).

1.2.2. Physiological role of CYP11B1 and CYP11B2

Cortisol (Hydrocortisone) is the main glucocorticoid in humans. It regulates energy mobilisation and thus the stress response. In addition, it is involved in the immune response of the human body. It is formed by 11 β -hydroxylation of 11-deoxycortisol (RSS) (Figure 1.6) and is normally secreted 100-to 1000-fold in excess over aldosterone.

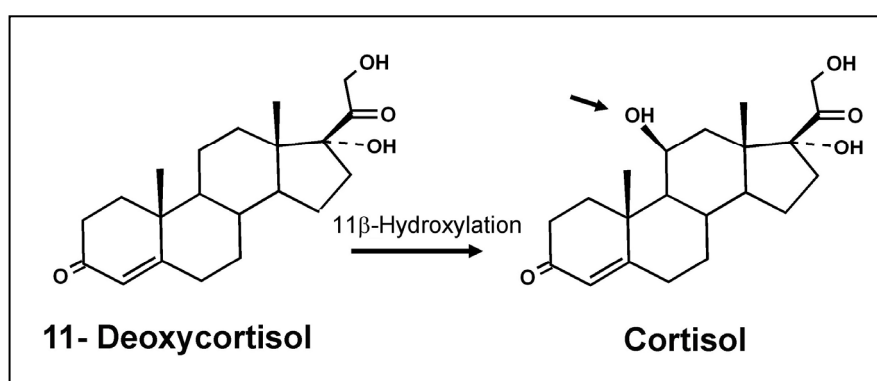


Figure 1.6. CYP11B1-dependent hydroxylation reaction.

Human CYP11B1 enzyme is a pure 11 β -hydroxylase, and catalyses the 11 β -hydroxylation reaction that produces cortisol (F) from 11-deoxycortisol (RSS).

Aldosterone, the most important human mineralocorticoid, is involved in the regulation of the salt and water household of the body and thus in the regulation of blood pressure. The terminal three steps in aldosterone biogenesis in humans are the 11 β -hydroxylation of 11-deoxycorticosterone (DOC) that leads to corticosterone (B), which is then 18-hydroxylated to yield 18-hydroxycorticosterone (18-OH-B) and finally oxidized to aldosterone (Figure 1.7).

DOC can also be first 18-hydroxylated to yield 18-hydroxy-11-deoxycorticosterone (18-OH-DOC) followed by conversions to 18-OH-B and aldosterone, but in man this pathway is unlikely to be important (Fisher *et al.* 2001). Both CYP11B1 and CYP11B2 11 β -hydroxylate RSS and DOC in vitro (Kawamoto *et al.* 1990a; Curnow *et al.*, 1991; Denner *et al.*, 1995a); however, the human CYP11B1 enzyme is a pure 11 β -hydroxylase without 18-hydroxylase or 18-oxidase activity and is even unable to 11 β -hydroxylate 18-OH-DOC (Fisher *et al.* 2001).

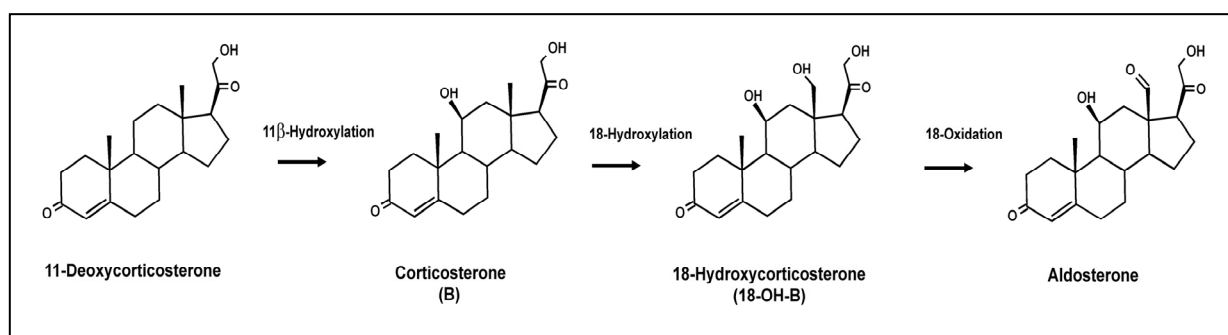


Figure 1.7. CYP11B2 converts 11-deoxycorticosterone via corticosterone and 18-OH corticosterone to aldosterone.

CYP11B2 11 β -hydroxylates 11-deoxycorticosterone (DOC) to yield corticosterone (B), which will then 18-hydroxylated to yield 18-hydroxycorticosterone and finally 18-oxidized to aldosterone.

CYP11B2 displays much weaker 11 β -hydroxylase activity towards RSS, but also 18-hydroxylates cortisol. The influence of several 18-hydroxylated steroids on human CYP11B1 and CYP11B2 activity was investigated (Fisher *et al.* 2001) using stably transfected V79 cells (Denner *et al.* 1995a; Denner *et al.*, 1995b). It was found that neither 18-hydroxycortisol nor 18-oxocortisol affected the efficiency of use of DOC or RSS as substrates by both enzymes, thus ruling out that these compounds contribute to lower 11 β -hydroxylase activity in glucocorticoid-suppressible hyperaldosteronism. In contrast, 18-OH-DOC significantly reduced the conversion rate of DOC to B and that of RSS to cortisol by both enzymes, while it increased the production rate of 18-OH-B and aldosterone by CYP11B2.

As mentioned above, there is a series of different diseases that are connected with changes in the steroid hormone production. Adrenogenital syndrome (AGS, CAH), which is a disorder affecting one in 14,000 patients, with mild forms of the disease occurring in one of every

100–1000 persons has been studied for many years (Cutler and Laue 1990; New 1992; Ohlsson *et al.*, 1998). The condition is caused by deficient synthesis of cortisol; most cases are related to 21-hydroxylase or 11 β -hydroxylase deficiency (White and Speiser 1994). The affected enzyme can be totally or partially impaired. The degree of enzyme insufficiency determines the severity of the condition (White and Speiser 1994). Steroid 11 β -hydroxylase deficiency, an autosomal recessive disorder, is the second most common cause of congenital adrenal hyperplasia (Zachmann *et al.*, 1983), and hypertension is a feature that often distinguishes this disorder from the steroid 21-hydroxylase deficiency causing virilizing adrenal hyperplasia due to the overproduction of 17-hydroxylated steroids. Before the identification and characterization of the CYP11B2 enzyme, it was thought that each of the last steps of aldosterone biosynthesis was catalysed by a separate enzyme, and in addition to the already known steroid 11 β -hydroxylase, the existence of an 18-hydroxylase called corticosterone methyl oxidase (CMO) type I and of an 18-hydroxysteroid dehydrogenase (CMO II) was postulated. Consequently, isolated deficiencies of aldosterone biosynthesis that are caused by CYP11B2 gene defects were (and still are) called CMO deficiencies. These disorders are clinically characterised by salt wasting, hyponatremia, and hyperkalemia, often presenting in infants with failure to thrive. Plasma renin activity is elevated, plasma aldosterone is low or undetectable, and the plasma levels of aldosterone precursors are elevated. While different types of gene aberrations in CYP11B1 and CYP11B2 including gene conversions, insertions, and deletions have been found in patients (Peters *et al.*, 1998; White 2004), the investigation of missense point mutations contributes most to our understanding of the structure–function relationship of these enzymes. More recently a novel missense mutation (L451F) caused by a T to C transition at position c.1351 in exon 8 was discovered in a newborn infant. This mutation showed complete aldosterone synthase deficiency type I. The L451F mutation is the first mutation found located immediately adjacent to the highly conserved heme-binding C450 of the cytochrome P450 (Nguyen *et al.*, 2008).

In normal physiology, aldosterone secretion is under the principal control of the renin–angiotensin system in a classical endocrine negative feedback loop. Renin is a proteolytic enzyme that is synthesized and stored by specialized cells in the wall of the afferent arteriole situated in the glomerulus of the kidney. These cells are anatomically and functionally associated with the cells in the wall of the distal convoluted tubules (the “macula densa”), and the whole structure is known as the juxtaglomerular apparatus. The release of renin activates a cascade system (Figure 1.8) in which renin cleaves a leucine–valine bond in the

hepatic α_2 -globulin, angiotensinogen, to form the decapeptide angiotensin I. This is subsequently converted by angiotensin-converting enzyme (ACE) to the octapeptide angiotensin II. ACE is a dipeptidyl carboxypeptidase that is found in high concentrations in pulmonary circulation; it is, however, also present in systemic vasculature and the kidney. Angiotensin II is a potent vasoconstrictor and can thus elevate blood pressure but it also stimulates aldosterone secretion, which leads to sodium retention and potassium loss. The major trigger for renin release is a decrease in perfusion pressure, and this may result from hemorrhage, hypotension, or a reduction in the extracellular fluid volume after sodium depletion. Negative feedback for aldosterone secretion is ensured; increased renin secretion increases angiotensin II and aldosterone levels, which will raise blood pressure and result in sodium retention. In turn, this will subsequently inhibit renin secretion maintaining homeostasis.

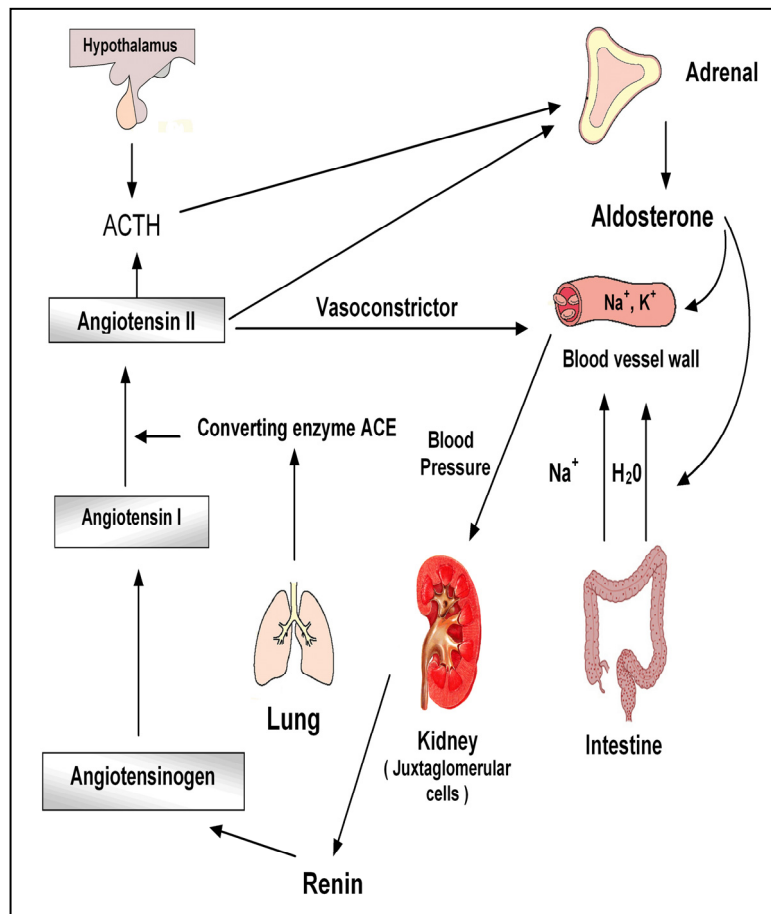


Figure 1.8. The renin–angiotensin–aldosterone system.

The release of renin activates a cascade system in which renin cleaves angiotensinogen to form angiotensin I and angiotensin II. Angiotensin II is a potent vasoconstrictor and can thus elevate blood pressure but it also stimulates aldosterone secretion, which leads to sodium retention and potassium loss.

1.2.3. Differences and similarities between CYP11B1 and CYP11B2

Human CYP11B1 and CYP11B2 are synthesised as 503 amino acids containing precursor proteins (Mornet *et al.* 1989; Kawamoto *et al.* 1990a; Kawamoto *et al.*, 1990b), both containing a 24-residue N-terminal mitochondrial targeting sequence, which is cleaved off after translocation into the mitochondrial matrix. In the mature enzymes, only 29 out of 479 residues are not identical, all of these residues seem to be located outside of the generally accepted substrate recognition sites (Gotoh 1992), and are spread throughout the protein (Böttner and Bernhardt 1996). Human mature CYP11B1 and CYP11B2 have apparent molecular masses of 50 (CYP11B1) and 48.5 (CYP11B2) kDa, respectively, and are bound to the inner mitochondrial membrane by as yet undefined protein segments (Ogishima *et al.* 1991). As mentioned above, human CYP11B1 and CYP11B2 are very similar in their primary sequence, but their catalytic properties are clearly different. To understand the structure–function relationships of these enzymes, which like all mitochondrial P450s so far have resisted all attempts at experimental structure determination, homology models were developed (Belkina *et al.*, 2001). Moreover, Böttner *et al.* suggested that the sequence spanned by amino acids 301 and 335 constitutes part of the substrate-binding site in CYP11B1 and CYP11B2 (Böttner and Bernhardt 1996; Böttner *et al.*, 1998). The effect of the C-terminal portions of both proteins was investigated as well, and it was found that diverging residues at positions 471, 472, 492, 493, and 494 were insignificant for the stereospecificity and regiospecificity of steroid hydroxylation (Böttner *et al.* 1998).

1.2.4. CYP11B1 and CYP11B2 modelling

Understanding the structure–function relationships of CYP11B enzymes requires information about their 3- dimensional structure. Protein structure determination by X-ray diffraction is often problematic in the case of membrane-bound proteins such as CYP11B1 and CYP11B2, and NMR structure determination is restricted to smaller proteins. Due to these reasons, no structure of a mitochondrial cytochrome P450 has been experimentally resolved so far. Only the structures of several bacterial cytochrome P450s and that of a few microsomal P450s solubilized by truncation and site-directed mutagenesis have been experimentally determined (for more information about the resolved 3-dimensional structures of cytochrome P450 visit: <http://www.expasy.org/>). Analysis of the structures revealed a conserved structural fold. Therefore, homology modelling studies of human CYP11B1 and CYP11B2 have been

performed. The models have been evaluated and used to explain the significance of a number of residues that were identified by mutagenesis studies or found in patients (Belkina *et al.* 2001). These models suggest that the main difference between the two proteins is the position of the heme. An angle of $\sim 20^\circ$ between the hemes of the two models has been observed, apparently dependent on the interaction of side chains forming the heme environment and the orientation of its binding loop (Figure 1.9).

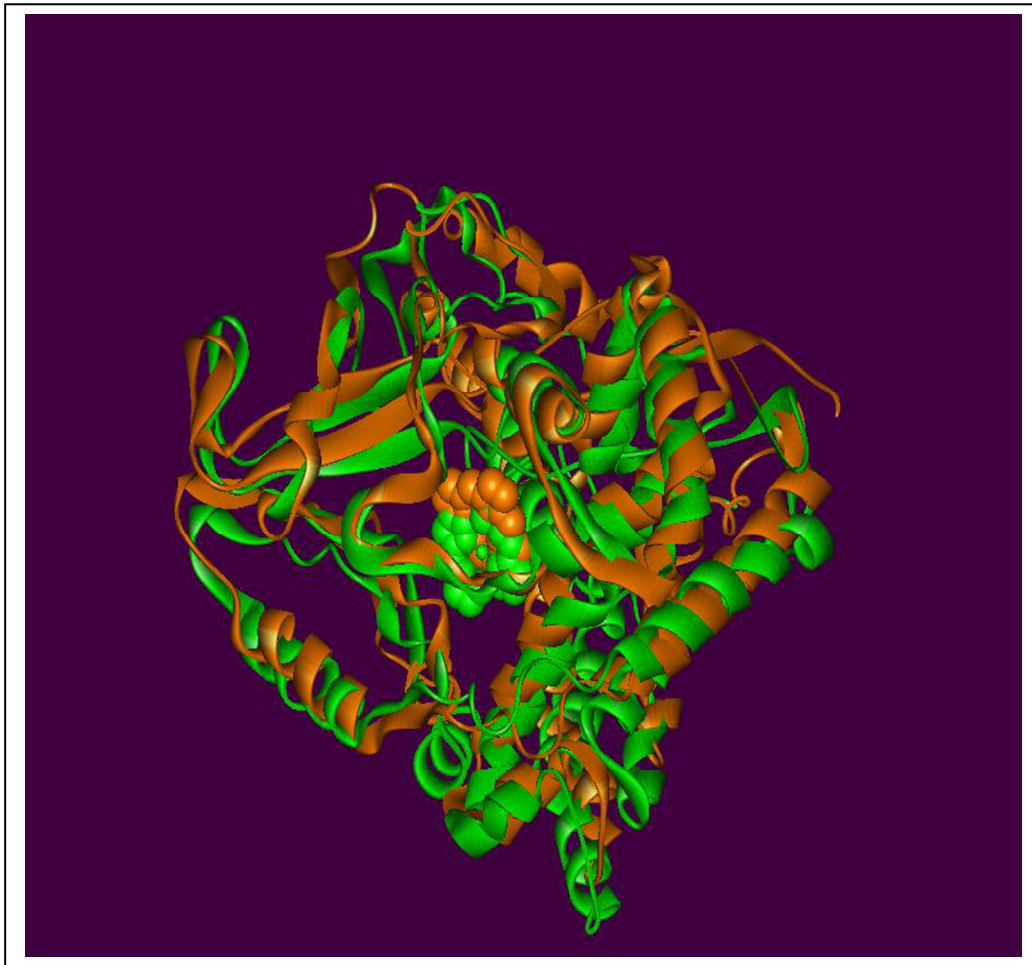


Figure 1.9. Superposition of the ribbon structures of the homology models of human CYP11B1 (green) and CYP11B2 (orange) (Belkina *et al.* 2001). While the overall structure is similar, the position of the hemes in both proteins is different.

In case of CYP11B1, one heme propionate group forms a hydrogen bond with Arg448 while the second one interacts with Arg384, whereas in CYP11B2 both heme propionate groups are involved in hydrogen bond interactions with Arg448. Both Arg384 and Arg448 have been found to be mutated in CYP11B1 of patients suffering from congenital adrenal hyperplasia (CAH) (White *et al.*, 1991; Curnow *et al.*, 1993; Nakagawa *et al.*, 1995); all known mutations in positions 384 and 448 led to a complete loss of enzyme activity, most probably due to destabilisation of the holoprotein. As a consequence of the different hydrogen bonding

network around Arg384, Arg448, and the heme propionates, the active site of CYP11B2 is predicted to be smaller than that of CYP11B1. The larger active site found in the CYP11B1 model correlates with the fact that the natural substrate of CYP11B1 (11-deoxycortisol) is larger than that of CYP11B2 (11-deoxycorticosterone) due to the presence of an additional 17 α -hydroxy group. Thus, from the structural point of view selective inhibition of one of the enzymes appears to be more probable than the extremely high homology of the protein primary sequences would suggest at first glance.

1.2.5. CYP11B1 and CYP11B2 as drug targets

As mentioned above, not only CYP11B1 and CYP11B2 deficiencies, but also abnormally increased plasma levels of aldosterone and cortisol are the cause of a variety of diseases like Cushing's syndrome which leads to chronic glucocorticoid excess. Elucidation of multiple pathogenetic mechanisms has greatly improved the management of this complex endocrine disorder. However, the syndrome is still associated with substantial morbidity and mortality (Boscaro *et al.* 2001; Fisher *et al.* 2001). Many drugs have been used in the treatment of pituitary-dependent Cushing's disease. They act at the hypothalamic–pituitary level and decrease corticotropin secretion, inhibit cortisol synthesis at adrenal level, or compete with cortisol at the receptor level. The neuromodulatory compounds used so far have shown real clinical efficacy only rarely when used as sole treatment, whereas inhibitors of steroid synthesis are effective in most cases in dose-dependent manner (Weber and Villarreal 1993; Engelhardt and Weber 1994; Hartmann *et al.*, 2002). Through their ability to correct hypercortisolism and its severe complications quickly, they are suitable for critical cases and in preparation for surgery, for patients treated with pituitary irradiation, and whenever a definitive treatment is delayed. The most common inhibitors of steroid biosynthesis in clinical use are mitotane, metyrapone, aminoglutethimide, etomidate, and ketoconazole (Gross *et al.*, 2007). While the mode of action of mitotane seems to be multifactorial, the other inhibitors of adrenal steroidogenesis that play an important role in the management of patients all reduce cortisol secretion by blocking one or more of the steroidogenic P450s. However, this mechanism of action has little selectivity and extra-adrenal effects are likely (Sonino and Boscaro 1999). For example, metyrapone treatment leads to increased concentrations of androgens (causing acne and hirsutism) and DOC (leading to hypokalaemia and oedema) as a consequence of CYP11B2 inhibition. Therefore, the development of highly selective CYP11B1 inhibitors would be a major improvement for the treatment of patients suffering

from Cushing's syndrome. The familial occurrence of primary aldosteronism was first described in 1966 by (Sutherland *et al.*, 1966), which reported a father and son with hypertension due to hyperaldosteronism that was resolved during treatment with dexamethasone. Subsequent studies confirmed an autosomal dominant mode of inheritance (New *et al.*, 1980). Today this disease is designated familial hyperaldosteronism type I [FH-I; also called glucocorticoid-suppressible hyperaldosteronism (GSH) or glucocorticoid-remediable aldosteronism (GRA)] in order to distinguish it from a non-glucocorticoidremediable form of familial hyperaldosteronism (FH-II) (Stowasser *et al.*, 1992). As mentioned above, the genetic basis for FH-I is a hybrid gene composed of 5' sequence (including regulatory sequences) derived from the *CYP11B1* gene fused to 3' sequence (which include most of the coding sequences) derived from the *CYP11B2* gene (Lifton *et al.* 1992). Like wild-type *CYP11B2*, the hybrid gene codes for an enzyme with aldosterone synthase activity, but its expression and consequently the production of aldosterone is regulated by the strong *CYP11B1* promoter (about 100- to 1000-fold stronger than the *CYP11B2* promoter) and by the Adrenocorticotrophic hormone (ACTH) (rather than angiotension II, the principal regulator of *CYP11B2* expression) by virtue of its *CYP11B1* regulatory sequences. In addition, chronic elevation of plasma aldosterone has also been diagnosed in other diseases such as adenoma, idiopathic hyperaldosteronism, as well as congestive heart failure or myocardial fibrosis (Brilla 2000; Tsybouleva *et al.*, 2004), and in cases of insufficient renal flow (Stowasser and Gordon 2001). Especially in congestive heart failure, elevated aldosterone levels lead to an increase in blood volume and may stimulate cardiac fibroblasts resulting in cardiac hypertrophy, myocardial fibrosis, ventricular arrhythmia, and other adverse effects (Ramires *et al.*, 1998; Lijnen *et al.*, 2000; Young and Funder 2000). Thus, the Randomised Aldosterone Evaluation Study trial (RALES) was done to determine whether the aldosterone antagonist spironolactone reduces mortality in patients with severe heart failure (Pitt *et al.* 1999). The study followed 1663 patients who had been diagnosed with severe heart failure for two years. During this study the patients, in addition to the standard therapy, were treated with either placebo or with 25 mg daily spironolactone. It was clearly demonstrated that the group treated with the aldosterone antagonist revealed a decreased risk of mortality of 30% and an improvement of the heart disease (Pitt *et al.* 1999). Since spironolactone is associated with severe side effects in the patients, the investigations have been repeated with another anti-mineralocorticoid, eplerenone, which is described to cause fewer side effects. The Eplerenone Post-Acute Myocardial Infarction Heart Failure Efficacy and Survival Study (EPHESUS) trial investigated the benefits of using this drug and

demonstrated a reduced mortality in acute myocardial infarction by 15% and of sudden death by 21% (Pitt *et al.* 2001). Nevertheless, treatment with steroidal antihormones is still accompanied by severe side effects (MacFadyen *et al.*, 1997; Delyani 2000; Mantero and Lucarelli 2000; Soberman and Weber 2000; Pitt *et al.* 2001).

And thus, a promising pharmacological approach alternative to spironolactone, eplerenone, and to angiotensin-II antagonists (Thai *et al.*, 1999) might be the use of specific and selective CYP11B2 inhibitors. Thus, CYP11B1 and CYP11B2 comprise new targets for drug treatment and selective inhibitors of both enzymes are of high pharmacological interest.

1.2.6. General requirements for the development of CYP11B2 inhibitors

Although Zöllner *et al.* succeeded recently in the expression and purification of functional human CYP11B1 in *E. coli* (Zöllner *et al.*, 2008), human CYP11B2 has not been heterologously expressed so far in significant amounts. Hence, it is not possible to use pure CYP11Bs enzymes for the development of screening systems, and alternative systems have had to be developed. Thus, some clues toward the CYP11B reaction mechanism's and potential inhibition have only been drawn from data obtained from their animal counterparts, although differences between different organisms have to be taken into account (Wada *et al.* 1985; Yanagibashi and Hall 1986; Matsukawa *et al.* 1990; Domalik *et al.* 1991; Nonaka *et al.* 1995; Bülow *et al.* 1996), or by using recombinant mammalian cell cultures (Denner *et al.* 1995a; Denner *et al.* 1995b). The main challenges to develop specific and selective inhibitors of the two mitochondrial CYP11B enzymes are the following: (1) to overcome the high similarity of both proteins for producing inhibitors with sufficient selectivity; for example, inhibitors, which strongly bind to CYP11B1 and not to CYP11B2 and vice versa; and (2) to create convenient test systems for the analysis of the potential inhibitors. As mentioned before, the high similarity between CYP11B1 and CYP11B2 makes the development of selective inhibitors of each one a big challenge for pharmacists and chemists. Furthermore, the 3 dimensional structures are not available yet making the development of inhibitors difficult, but the computer models (Belkina *et al.* 2001; Ulmschneider *et al.*, 2005a; Ulmschneider *et al.*, 2005b; Roumen *et al.*, 2007) of both enzymes may help to design and synthesise new and efficient inhibitors.

1.2.7. Heterologous expression of CYP11B1 and CYP11B2 in stable cell cultures

In 1995, two cell lines that express human CYP11B1 and CYP11B2 in a stable and constitutive manner have been established in our group, the cells were derived from V79 Chinese hamster cells, designated V79MZh11B1 and V79MZh11B2, respectively (Denner *et al.* 1995a; Denner *et al.* 1995b). Interestingly, the recombinant V79 cells were able to support CYP11B1- and CYP11B2-dependent steroid conversion without additional heterologous expression of the corresponding electron donor system (AdR and Adx) in these non-steroidogenic lung fibroblast cells. As expected, metyrapone strongly inhibited CYP11B1 and to a lesser extent CYP11B2 activity when tested using these cell lines. When several pharmaceutically important azole derivatives were tested, it was shown for the first time that the inhibitory effect of fluconazole is minor compared with clotrimazole, ketoconazole, and miconazole (Denner and Bernhardt 1998). These results demonstrated the usefulness of V79MZh11B1 and V79MZh11B2 cell lines for investigating pharmaceutically important compounds for interference with human CYP11B1 and CYP11B2 activity. Spironolactone, which has been described as an inhibitor of rat aldosterone synthase (Weindel *et al.*, 1991), and bovine CYP11B1 (Cheng *et al.*, 1976) showed no inhibitory effect against human CYP11B2 using V79MZh11B2 cells even when used at high concentrations (Denner and Bernhardt 1998). This suggested that the rat enzyme is not an appropriate tool for the evaluation of inhibitors of the human enzyme. Furthermore, this finding indicated that the pharmacological activity of spironolactone is not caused by enzyme inhibition as had been speculated (Cheng *et al.* 1976) but is only due to its antagonistic property. Interestingly, the cell lines are still active and in use for testing potential inhibitors of CYP11B1 and CYP11B2 (Fisher *et al.* 2001; Ehmer *et al.*, 2002; Bureik *et al.*, 2004; Bureik *et al.*, 2005; Ulmschneider *et al.* 2005a; Ulmschneider *et al.* 2005b; Roumen *et al.* 2007).

1.2.8. Heterologous expression of CYP11B1 and CYP11B2 in yeast

It can be generally stated that mitochondrial cytochrome P450s are more difficult to express in microorganisms than their microsomal relatives. While some mitochondrial P450s like bovine CYP11A1 (Wada *et al.* 1985), rat CYP24 (Akiyoshi-Shibata *et al.*, 1994), and CYP27 (Pikuleva *et al.*, 1997) can be readily expressed in *Escherichia coli*, expression of human CYP11B2 in bacteria has not been successful so far and that of the rat counterparts was achieved with only a very low yield (Nonaka *et al.*, 1998).

Our group succeeded in the functional expression of human CYP11B2 and CYP11B1, using the fission yeast *Schizosaccharomyces pombe* (Bureik *et al.*, 2002b; Dragan *et al.*, 2005). The transformed yeasts displayed steroid hydroxylase activity *in vivo* without additional heterologous expression of the corresponding electron donor system (AdR and Adx) in these nonsteroidogenic cells. Our group found an adrenodoxin-like ferredoxin (etp1^{fd}) in this yeast, which was shown to be able to support substrate conversion of different cytochrome P450s (Bureik *et al.* 2002b; Schiffler *et al.*, 2004). Meanwhile etp1^{fd} has been cloned, isolated, and characterized. It was demonstrated to be able to transfer electrons to CYP11B1 and was shown to resemble the mammalian adrenodoxin in many aspects (Schiffler *et al.* 2004). Furthermore, our group confirmed recently the existence of a corresponding fission yeast ferredoxin reductase, which was characterised and called arh1 (Ewen *et al.*, 2008).

1.2.9. Inhibitors of CYP11B1 and CYP11B2

As described above, two systems for evaluating compounds with respect to their inhibitory effect on human CYP11Bs have been established in our group, the yeast system using recombinant *S. pombe* (Bureik *et al.* 2002b; Ehmer *et al.* 2002; Dragan *et al.* 2005), and the mammalian cell culture system using recombinant V79 cells (Denner *et al.* 1995a; Denner *et al.* 1995b). The availability of the recombinant yeast system allows a convenient and effective testing of potential CYP11B1 and CYP11B2 inhibitors. Since candidate compounds can be tested in the fission yeast system, a medium throughput screening system seems to be possible but has not been realized yet. Repeated steroid hydroxylation measurements testing several compounds with fission yeast strains expressing both CYP11B1 and CYP11B2 showed very good reproducibility of the inhibitory effects (Bureik *et al.* 2002b; Ehmer *et al.* 2002; Dragan *et al.* 2005).

Using both expression systems, it was clearly demonstrated that inhibitors can be identified with higher selectivity towards CYP11B2 or towards CYP11B1 (Denner and Bernhardt 1998; Ehmer *et al.* 2002), supporting the initial idea that although both proteins show an extremely high identity, the differences (as shown by the two models of CYP11B1 and CYP11B2) are nevertheless big enough to cause differences in the inhibitor binding. Moreover, the two testing systems were compared and evaluated and it was remarkable that all compounds that displayed an effective inhibitory effect in the cell culture assay were also active in the fission yeast system (Bureik *et al.* 2004).

Although several compounds were reported using these two testing systems as selective inhibitors of CYP11B2, the reported compounds were not ‘druggable’ compounds, which make their use as drugs or lead compounds difficult.

In conclusion, each one of the two test systems mentioned before possess advantages and disadvantages (Table 1.1). So far neither of them could be considered as high or even medium throughput screening system, as they are radioactive-dependent typical inhibition assays, in which the enzyme activity is monitored, and a multiple concentration-response curve is used to generate the IC₅₀ values. Using such multiple-concentrations assays at early (screening) stages of drug discovery is very time-and resource-intensive; therefore, further work is still needed to improve the fission yeast system for higher sensitivity and to allow medium or high throughput screening conditions.

Table 1.1. Comparison of the yeast and mammalian recombinant systems for the development and analysis of potential selective inhibitors

System	Advantages	Disadvantages
V79 cells	Mammalian cell lines	Expensive
	Widely used for drug evaluation	
<i>S. pombe</i>	Low cost	Non mammalian cells
	Medium-high throughput possible	Cell wall can cause problems

1.3. Fission yeast *Schizosaccharomyces pombe* as a model system

Fission yeast *Schizosaccharomyces pombe* is a unicellular eukaryote belonging to the Ascomycetes (Sipiczki 2000). P. Lindner first described it in 1893, and since it was originally isolated in millet beer from eastern Africa, the yeast was called pombe which means *beer* in Swahili, and it was called also fission yeast as it divides by fission as opposed to budding spores.

In comparison to baker’s yeast *Saccharomyces cerevisiae* (*S. cerevisiae*), the whole genome of *S. pombe* is only slightly bigger in size (13.8 Mb), and is distributed between chromosomes I (5.7 Mb), II (4.6 Mb) and III (3.5 Mb) (Smith *et al.*, 1987), together with a 20 kb mitochondrial genome (Lang *et al.*, 1987). Fission yeast has only 4824 different genes (Wood *et al.*, 2002), which is significantly less than the number of genes in the human genome (about 23,000) (Pennisi 2003). It is also substantially lower than the 6200 different genes found in *S. cerevisiae*.

Fission yeast *S. pombe* is a harmless, rapidly growing eukaryote. The cells are cylindrical, oval or round, with a diameter of 3-4 μm and a length of up to 7-15 μm (Figure 1.10).

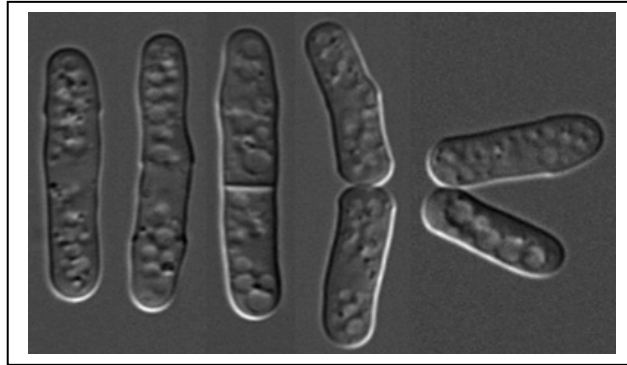


Figure 1.10. Picture of the fission yeast *Schizosaccharomyces pombe* from Steve's place (see http://www.steve.gb.com/science/model_organisms.html).

Fission yeast cells grow quickly, have a generation time between two and four hours and are easy to manipulate on the laboratory level, and since some features such as chromosome structure, cell cycle, and ribonucleic acid (RNA)-splicing are more similar between mammalian cells and *S. pombe* than between mammalian cells and *S. cerevisiae* (Moreno *et al.*, 1991; Box *et al.*, 2008; Miyoshi *et al.*, 2008; Takeda *et al.*, 2008), studying *S. pombe* gives the opportunity to understand what happens in mammalian system, which is more complex and experimentally more difficult to deal with.

Moreover, the works carried out in *S. pombe* have greatly improved our knowledge about the eukaryotic cell (Nurse 2000) and its regulation (Moser and Russell 2000), and added to many related areas, such as microtubule formation (Hagan and Petersen 2000), cellular morphogenesis (Brunner and Nurse 2000), stress response mechanisms (Toone and Jones 1998), and the response to deoxyribonucleic acid (DNA) damage (Zhou and Elledge 2000).

Furthermore, *S. pombe* is an interesting model for studying mitochondria (Chiron *et al.*, 2007), and has been reported to be an interesting host for recombinant expression of P450 (Yamazaki *et al.*, 1993; Bureik *et al.* 2002b; Dragan *et al.* 2005; Dragan *et al.*, 2006; Peters *et al.*, 2007). Therefore, this work will focus on the use of recombinant *S. pombe* as a whole-cell system to develop efficient P450-dependent biotransformation reactions for steroid hydroxylation and drug discovery.

1.4. Biotechnological applications of the 11 β -Hydroxylases

Hydrocortisone (cortisol) is an important starting molecule for the synthesis of drugs with potent anti-inflammatory or antiproliferative actions. The industrial synthesis of hydrocortisone and other glucocorticoids depends currently on hemi-synthesis, which involves multiple chemical and biotransformation reactions in order to introduce the functionally essential 11 β -hydroxy group directly into the steroid scaffold. Several decades ago, studies were carried out to identify 11 β -hydroxylating microorganisms and, as a result, several suitable species such as *Cunninghamella blakesleeana*, *Curvularia lunata* and *Cochliobolus lunatus* have been reported (Hanson *et al.*, 1953; Fried *et al.*, 1955; Zakelj-Mavric *et al.*, 1990).

The 11 β -position is axial and therefore more strongly hindered than the 11 α -position by 1,3-diaxial interactions with the C18- and C19-methyl groups and the 8 β -hydrogen atom. This can explain why the microbial steroid 11 β -hydroxylases generally proceed at lower yields and with more side-reactions (Megges *et al.* 1990). The 11 β -hydroxylases of *Curvularia lunata* is an extremely labile enzyme (Zuidweg 1968) and seems to catalyse in addition to the 11 β -hydroxylation, the 10 β and 14 α hydroxylation when 19-nortestosterone is used as substrate (Lin and Smith 1970). However, this enzyme was first purified and characterized in 1993. It showed a turnover rate of 207 nmol/min per nmol P450 (Suzuki *et al.*, 1993). *Cochliobolus lunatus* was shown to efficiently hydroxylate progesterone at both 11 β - and 14 α -positions into mono- and dihydroxy-products. In addition, this fungus displays other minor hydroxylation and side-chain cleavage reactions.

In the case of the 11 α -hydroxylase, a comparison of 11 β -hydroxylase on the basis of their specific activity was not possible, but comparative studies demonstrated *C. lunata* to be more effective than *Streptomyces fradia* and *C. blakesleeana*.

1.5. Aim of the work

To apply cytochrome P450s in biotechnology either whole-cell systems expressing the P450 isoforms of interest have to be developed or self-sufficient systems avoiding NAD(P)H regeneration have to be used. In general, whole-cell systems are used more often than (partly) isolated enzymes in biotechnological processes (Straathof *et al.*, 2002).

The main topic of this work consisted in the development of an efficient hydrocortisone-producing whole-cell system.

Hydrocortisone (Cortisol) is used as all other glucocorticoids as important anti-inflammatory agent and generally requires an 11 β -hydroxy group as a functionally essential entity. During the industrial synthesis of glucocorticoids, the microbiological introduction of the 11 β -hydroxy group into the steroid scaffold not only represents the most costly synthesis step, but also the step whereby most of the losses occur due to the formation of by-products (Dragan *et al.* 2005).

In recent years, it has been demonstrated that the fission yeast *Schizosaccharomyces pombe* is a very suitable model system for the investigation of P450 dependent steroid hydroxylases (Bureik *et al.* 2002a; Bureik *et al.* 2002b; Dragan *et al.* 2005; Dragan *et al.* 2006). During these studies, the construction of recombinant fission yeast strains that functionally express human CYP11B1 was reported. In these strains (named CAD1 (Bureik *et al.* 2004) and SZ1 (Dragan *et al.* 2005), respectively), 11 β -hydroxylation of RSS was accomplished without the need for coexpression of the other components of the mitochondrial P450 electron transfer chain (Adx and AdR).

While the hydrocortisone production efficiency using strain SZ1 is considerably higher than the values reported for production by other steroid 11 β -hydroxylation systems with recombinant microorganisms (e.g. those from bovine CYP11B1 expressed in baker's yeast *Saccharomyces cerevisiae* (Dumas *et al.*, 1996; Dragan *et al.* 2005)), all bioconversion activities published to date appear to still be not competitive enough for the consideration of their use for industrial applications. Therefore, the purpose of this work was to improve the efficiency of hydrocortisone bioproduction in the CYP11B1-expressing fission yeast. In this context, it is of special interest to determine whether the coexpression of the corresponding mitochondrial electron transfer partners (AdR, Adx) is capable of directly improving the 11 β -hydroxylation activity of CYP11B1-expressing fission yeast strains.

In addition to the wild type of Adx, two mutants that were previously reported by our group to have enhanced affinity for the cytochrome P450 (Schiffler *et al.*, 2001; Bichet *et al.*, 2007) were also included in this work to determine whether a higher 11 β -hydroxylation activity of CYP11B1 can be achieved by substituting Adx^{WT} with the Adx mutants.

The second part of this work consisted in the development of a medium or high throughput screening system for the discovery of aldosterone synthase inhibitors. These inhibitors can be used as lead compounds or drugs for the treatment of aldosterone overproduction-related diseases (Hakki and Bernhardt 2006; Baston and Leroux 2007; Schuster and Bernhardt 2007). As mentioned before (see subsection 1.2.9) two systems for evaluating compounds with respect to their inhibitory effect on human CYP11Bs have been developed in our group, the yeast system using recombinant *S. pombe* (Bureik *et al.* 2002b; Ehmer *et al.* 2002; Dragan *et al.* 2005), and the mammalian cell culture system using recombinant V79 cells (Denner *et al.* 1995a; Denner *et al.* 1995b). Although fission yeast test system allows a convenient and effective testing of CYP11Bs inhibitors, no screening system has been reported. Moreover, the established testing system is a radioactive-dependent typical inhibition assay, in which the enzyme activity is monitored, and a multiple concentration-response curve is used to generate the IC₅₀ value. Using such multiple-concentrations assays at early (screening) stages of drug discovery is very time-and resource-intensive; therefore, the target of this work was to develop a medium or a high throughput screening system (HTS) for the discovery of aldosterone synthase inhibitors.

To accomplish this goal, to develop and execute an efficient, rapid, and reproducible *S. pombe* screening assay, an automated screening technology plate-format had to be established. In this context, it is of special interest to optimise the steroid hydroxylation assay for the 96-well plate format and to determine whether a one-point assay can be developed and used instead of the multiple points assay. The use of one-point assay will increase the throughput of the screening system.

Additionally, the steroid detection method has to be investigated and optimised in order to allow the screening of large numbers of compounds and to achieve a high or even medium throughput screening system.

2. Materials & Methods

2.1. Materials

2.1.1. Microorganism growth media

All following media were prepared and sterilised by autoclaving on a liquid cycle (20 min at 121 °C) and stored in cold room. Solid form was obtained by setting up a 2% (w/v) agar concentration.

2.1.1.1. Growth media for *Escherichia coli* (*E. coli*)

- **LB medium (Luria-Bertani)**

25 g powder from Difco™ LB Broth, Miller (Luria-Bertani) (Becton, Dickinson and company) was dissolved in 1 L of distilled water and the pH was adjusted to 7.5 with drop NaOH or HCl.

LB formula per litter is shown in Table 2.1 below.

Table 2.1. Composition of LB medium

Tryptone	10 g
Yeast extract	5 g
Sodium chloride	10 g

When needed, ampicillin was added to a final concentration of 100 µg/ml.

- **SOC medium**

SOC is a suitable medium for use in the final step of cell transformation to obtain maximal transformation efficiency of *E. coli* (Hanahan 1983).

Table 2.2. Composition of SOC medium

Tryptone	2.0 %
Yeast extract	0.5 %
KCl	2.5 mM
MgCl ₂ •6H ₂ O	10.0 mM
Mg SO ₄	10.0 mM
NaCl	10.0 mM
Glucose	20.0 mM

2.1.1.2. Growth media for *Schizosaccharomyces pombe* (*S. pombe*)

- **EMM (Edinburgh minimal medium)**

EMM is a minimal medium for the culturing of *S. pombe*, and is prepared with the following composition as shown in the Table below.

Table 2.3. Composition of EMM medium

Potassium hydrogen phthalate	12.0 g (14.7 mM)
Na ₂ HPO ₄	8.8 g (15.5 mM)
NH ₄ Cl	20.0 g (93.5 mM)
Glucose	80.0 g (111.0 mM)
The pH must be adjusted to be 5.4- 5.8; subsequently the vitamins, minerals and salt have to be added as shown in the table below, and filled up to 4 L with distilled water.	
Salt stock (x50)*	80.0 ml
Vitamin stock (x1000)*	4.0 ml
Mineral stock (x10,000)*	0.4 ml

* For supplements, see appendix

For culturing of *S. pombe* the needed supplements have to be added for each strain (as shown in Tables 2.6, 3.6) with an end concentration of 0.01% (w/v) for each supplement. When needed, thiamine with final concentration of 5 μ M was added to suppress the *nmt1* promoter.

- **YEA: yeast extract medium and supplements**

YEA medium is a rich and complete medium for the culturing of *S. pombe*, and is prepared as shown below in the Table.

Table 2.4. Composition of YEA medium

Yeast extract	5.0 g (0.5% w/v)
Glucose	30.0 g (3.0% w/v)
adenine, histidine, leucine, uracil	0.1 g each (0.01% w/v)
Distilled water	Up to 1.0 L

- **2X YEA with 25 % glycerol**

This medium is used to prepare glycerol stock cultures from *S. pombe* strains, in order to freeze them by -80°C.

Table 2.5. Composition of 2X YEA with 25 % glycerol medium

Yeast extract	1.0 g
Glucose	6.0 g
adenine, histidine, leucine, uracil	0.02 g each
Distilled water	75.0 ml
Glycerol	25.0 ml

2.1.2. Microorganisms

Microorganisms used in this work are summarised in Table 2.6 below.

Table 2.6. Microorganisms used in this work

Name (Organism)	Genotype	Supplements	Reference
TOP10F ['] (<i>E. coli</i>)	F- mcrA Δ (mrr-hsdRMS-mcrBC) Φ 80lacZ Δ M15 Δ lacX74 recA1deoR araD139 Δ (araleu)7697 galU galK rpsL (Str ^R) endA1 nupG	-	US Patent 5,487,993 (Invitrogen; Carlsbad, CA)
MB164 (<i>S. pombe</i>)	NCYC2036/pINT5-CYP11B2 integrant	leucine	(Bureik <i>et al.</i> 2002b)
SZ1 (<i>S. pombe</i>)	h ⁻ ura4-dl18 leu1::pCAD1-CYP11B1	leucine	(Dragan <i>et al.</i> 2005)
1445 (<i>S. pombe</i>)	h- ade6.M210 leu1.32 ura4.dl18 his3. Δ 1	adenine, leucine, uracil, histidine	(Burke and Gould 1994)

2.1.3. Plasmids

▪ pNMT1-TOPO[®]

Fission yeast vector pNMT1-TOPO (Invitrogen; Carlsbad, CA) was used for all subcloning steps for the development of AdR expression plasmids, and as a starting point for the construction of a new expression vector bearing two expression cassettes for Adx and AdR, respectively.

This vector uses the TOPO I ligation strategy and is mainly designed to be used for expression of cDNA in *S. pombe* under the control of the *nmt1* promoter (Maundrell 1990), which is the strongest known inducible promoter of *S. pombe* (Forsburg 1993). An autosomal replicating sequence (*ars1*) directs the high-copy maintenance in *S. pombe*. The LEU2 ORF from *S. cerevisiae* under the control of the *SV40* promoter allows auxotrophic selection in *leu1⁻* hosts. Biological amplification in *E. coli* is possible due to a pUC ORI and an ampicillin resistance ORF enables the selection of transformed *E. coli* colonies in the presence of ampicillin. An additional feature represents the opportunity of tagging the protein of interest with the Pk tag (Craven *et al.*, 1998) for immunologic detection and a hexahistidine (his6) tag

for purification with metal-chelating resins. Moreover, the addition of polyhistidine tags has sometimes a stabilising effect on the expressed protein (Nonaka *et al.* 1998). Further information can be extracted from Figure 2.1.

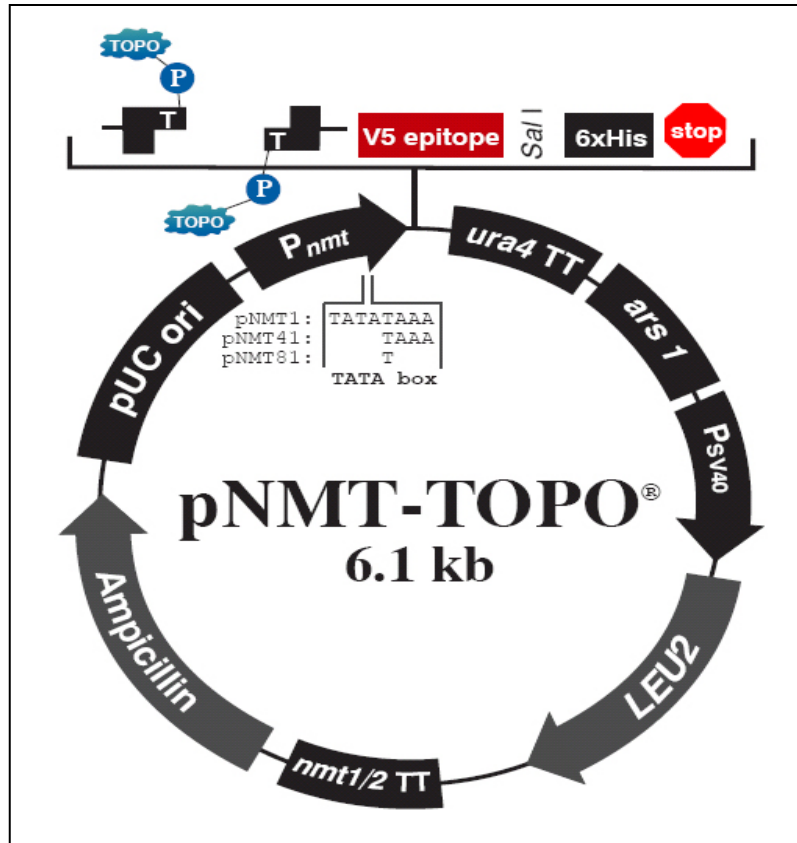


Figure 2.1. pNMT1-TOPO vector map (Invitrogen; Carlsbad, CA). Pk tag is the C-terminal peptide containing the V5 epitope, P_{nmt} is *nmt1* promoter, *S. pombe ars1* origin of replication for non-integrative high-copy maintenance of the plasmid in *S. pombe* cells, *S. cerevisiae LEU2* auxotrophic marker for selection of yeast transformants.

▪ pREP42 Pk C

A vector for the expression of tagged proteins in *Ura4⁻ S. pombe* strains under the control of the *nmt1* promoter (Craven *et al.* 1998). An autosomal replicating sequence (*ars1*) directs the high-copy maintenance in *S. pombe*. The *Ura4* ORF allows auxotrophic selection in *Ura4⁻* hosts. Furthermore, this vector enables the tagging of the protein of interest with the Pk tag for immunologic detection (Figure 2.2).

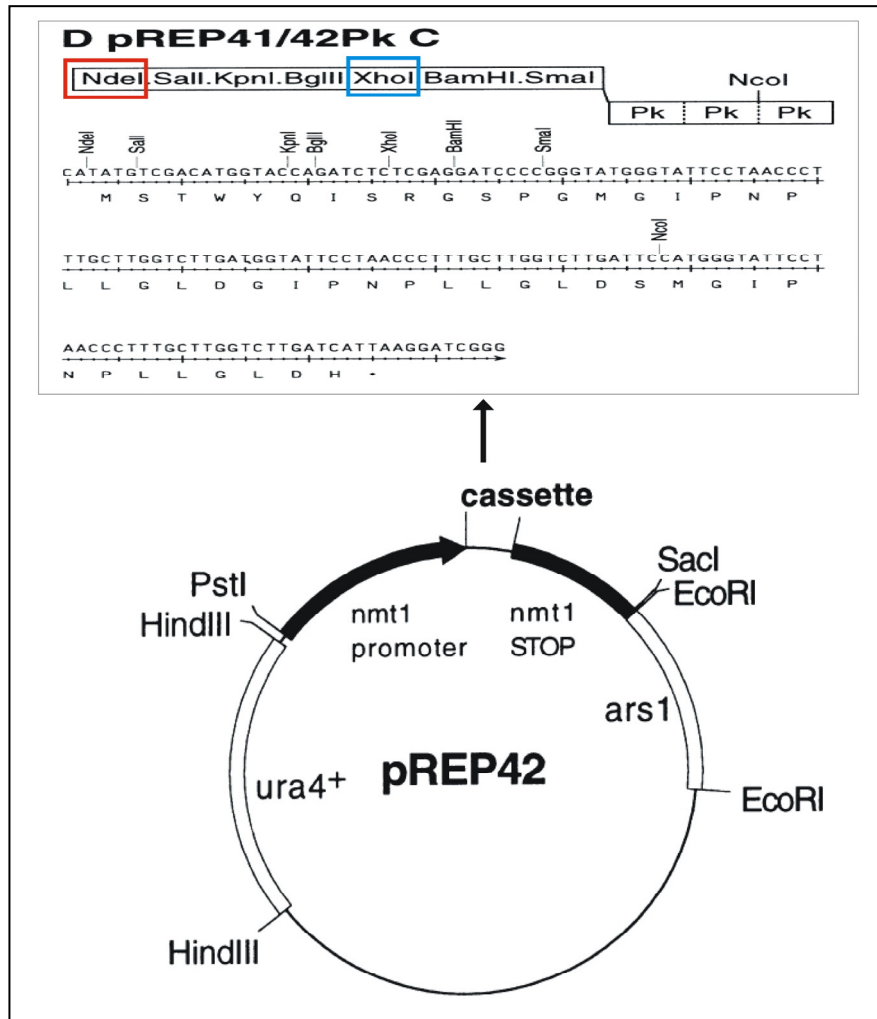


Figure 2.2. pREP42 Pk C vector map.

▪ Adx expression plasmids

Adx expression plasmids were a kind gift of Dipl. Biol. Calin-Aurel Dragan. (Derouet-Hümbert *et al.*, 2007) and are listed in the Table below. For the construction of Adx expression plasmids, the cDNA of bovine wild-type Adx was PCR-amplified and cloned into the fission yeast expression vector pNMT1-TOPO to yield pNMT1-Adx^{WT}. Subsequently plasmid pNMT1-Adx^{WT} was subjected to site-directed mutagenesis yielding pNMT1-Adx^{S112W} and pNMT1-Adx^{D113Y} (Derouet-Hümbert *et al.* 2007).

Table 2.7. Adx expressing plasmids used in this work (Derouet-Hümbert *et al.* 2007)

Plasmid	Insert	Selection marker
pNMT1-Adx ^{WT}	Adx ^{WT}	<i>LEU2</i>
pNMT1-Adx ^{D113Y}	Adx ^{D113Y}	<i>LEU2</i>
pNMT1-Adx ^{S112W}	Adx ^{S112W}	<i>LEU2</i>

2.1.4. Oligonucleotides

All primers used during this work were obtained from the company BioTeZ (Berlin-Buch, Deutschland) and purified via HPLC. The sequences as well as the purpose of each oligonucleotide used in this work are given in the appendix section.

5' fluorescence labelled oligonucleotides (fluorophore IR800) used for DNA sequencing with a LicorTM-DNA sequencer 4000 were purchased from MWG Biotech. The applied sequencing primers are also listed in the appendix section.

2.1.5. Library of pharmacologically active compounds (LOPAC)

A library of 1268 compounds from the LOPAC¹²⁸⁰ library (Library of pharmacologically active compounds) was obtained from SIGMA (Deisenhofen, Germany) and is shown in the appendix section. The library is a collection of high quality, innovative molecules that span a broad range of cell signalling and neuroscience areas.

The complexion of the investigated library reflects the most commonly screened targets in the field of drug discovery, and it contains marketed drugs, failed development candidates and “gold standards” that have well-characterised activities. These compounds are the result of lead optimisation efforts and thus, possess a great deal of value, having been rationally designed by structure activity relationship (SAR) studies. For more information about the LOPAC¹²⁸⁰ library see

<http://www.sigmaaldrich.com/catalog/search/ProductDetail/SIGMA/LO1280>

2.1.6. Mega Block plates

Two different kinds of Mega Block plates from VWR (Darmstadt, Germany) were used as shown below in Figure 2.3.

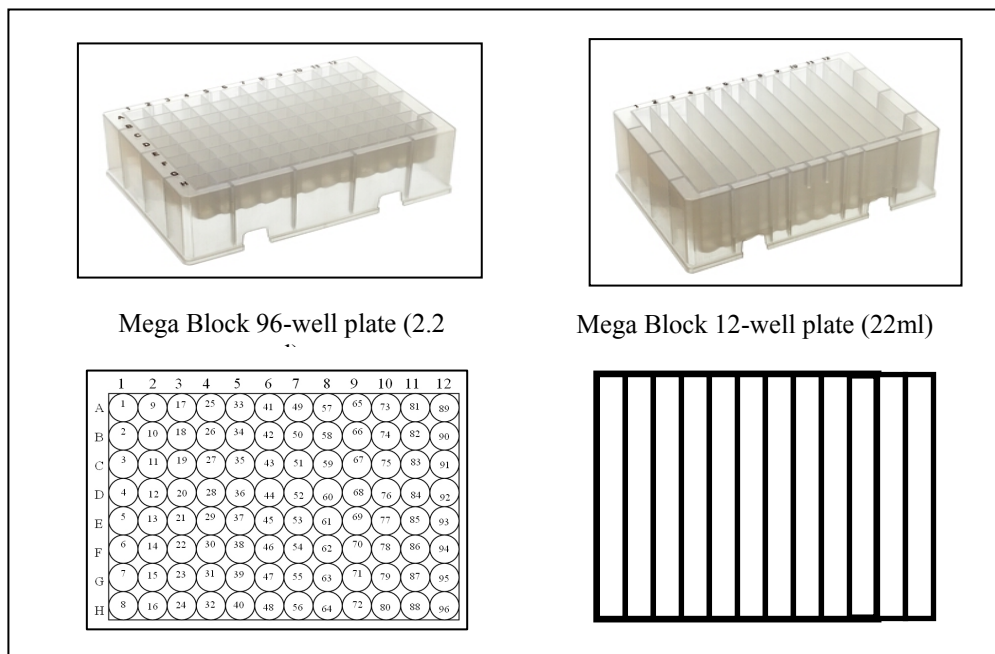


Figure 2.3. The Mega Block plates from VWR used during this work. The 96-well plate was used to perform the hydroxylation assay, whereas the 12-well plate was applied essentially for the preparation of the test as will be described in details below.

Since the 96-well plates are used to perform the steroid hydroxylation, an automated liquid handling system is needed to manipulate the 96-well plates. For this reason, the pipetting robot (Tecan Aquarius, Switzerland) (Figure 2.4) was used and several programs that enable the manipulation of plates were developed in this work.



Figure 2.4 The pipetting robot (Tecan Aquarius, Switzerland).

2.2. Methods

2.2.1. Molecular biology methods

Unless otherwise noted, all genetic methods applied during this work were carried out according to the standard methods as described previously (Sambrook and Russell 2001).

2.2.1.1. pNMT1- TOPO cloning

TOPO[®] Cloning depends on the DNA topoisomerase I enzyme, which functions both as a restriction enzyme and as a ligase. Its biological role is to cleave and rejoin DNA during replication. *Vaccinia* virus topoisomerase I specifically recognizes the pentameric sequence 5'-(C/T)CCTT-3' and forms a covalent bond with the phosphate group of the 3' thymidine. It cleaves one DNA strand, enabling the DNA to unwind. The enzyme then religates the ends of the cleaved strand and releases itself from the DNA (Shuman 1994). To harness the religating activity of topoisomerase, pNMT-TOPO[®] vector is provided linearized with topoisomerase I covalently bound to each 3' phosphate. This enables the vector to ligate DNA sequences with compatible ends (Figure 2.5) (Shuman 1994). In only five minutes at room temperature, the ligation is complete and ready for transformation into *E. coli*.

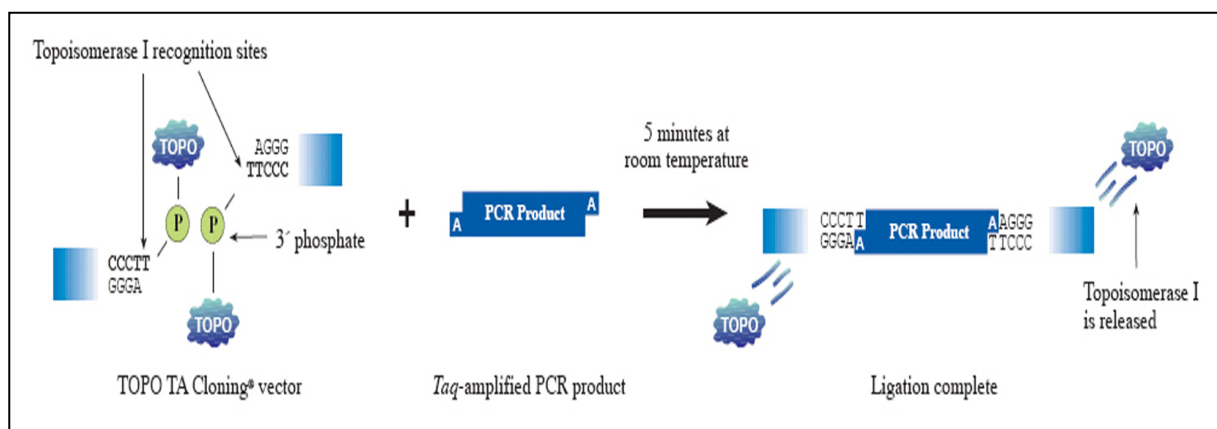


Figure 2.5. TOPO TA Cloning[®] of Taq-amplified DNA (Invitrogen; Carlsbad, CA).

The amplification of cDNA prior to cloning was carried out with PCR and the *PfuTurbo*[®] DNA Polymerase from Stratagene. Since an A-3' overhang is needed to perform the TOPO[®] cloning, the PCR product was then incubated at 72°C for ten minutes with the DNA

polymerase *Taq*, which has a nontemplate-dependent terminal transferase activity that adds a single deoxyadenosine (A) to the 3' ends of PCR product.

The DNA was then analysed by agarose gel electrophoresis and precipitated as described in subsection 2.2.1.3, dissolved in water and used for the TOPO[®] cloning.

To perform the TOPO[®] cloning 4 µl from the DNA suspension was incubated with 1 µl pNMT1-TOPO[®] Vector and 1 µl salt solution for 5 minutes at room temperature, finally 2 µl from the reaction mixture was then used to transform *E. coli*. The transformation was carried out using the TOP10 chemically competent *E. coli*, and heat-shock method at 42°C for 30 seconds. The transformed cells were then resuspended in SOC medium, plated on ampicillin-containing LB medium plates and incubated at 37°C for 24 hours. Positive clones were identified and isolated after performing colony PCR.

2.2.1.2. Amplification of the human AdR

The AdR cDNA was PCR-amplified using *PfuTurbo*[®] DNA Polymerase from Stratagene. The compositions of a typical reaction as well as the applied PCR-conditions are shown below.

Sample composition:

Pfu -polymerase Buffer (10x)	5.0 µl
dNTP (5 mM)	1.0 µl
Forward primer (10 µM)	1.0 µl
Reverse primer (10 µM)	1.0 µl
Template (100 ng/µl)	1.0 µl
<i>Pfu</i> -polymerase (3 u/µl)	0.5 µl
dest.H ₂ O	40.5 µl

PCR-program:

Segment	Number of cycles	Temperature	Duration
1	1	95°C	5 minutes
2	35	95°C	30 seconds
		48°C	30 seconds
		72°C	4 minutes
3	1	72°C	10 minutes

The PCR amplification product was then analysed on 1% (w/v) agarose gel, isolated from the gel and precipitated as shown below.

2.2.1.3. DNA electrophoresis and manipulation

Products from PCR and endonuclease reactions were analysed by agarose gel electrophoresis using agarose mass concentrations ranging from 0.7 % to 1.5 % (w/v) in 0.5X TBE. The Smart Ladder from Eurogentec (Liège, Belgium) was used as reference DNA.

The ethidium bromide stained DNA fragment of interest was then isolated from the agarose gel by cutting the band of interest. The band was then transferred to a bottom perforated 0.5 mL flask filled with saline treated glass wool (Supelco, Bellefonte, PA, USA). The 0.5 ml flask containing the gel and the glass wool was set on an empty 1.5 ml flask. This assembly was centrifuged at 8×10^3 g for 10 min at 4°C. Subsequently the DNA in the flow-through was precipitated with ethanol (EtOH) and sodium acetate (NaAc) (Sambrook and Russell 2001).

DNA concentration was determined spectroscopically by measuring the absorption at 260 nm. According to Hagemann (Hagemann 1990) 1 AU₂₆₀ corresponds to a DNA concentration of 50 µg/ml.

2.2.1.4. DNA restriction and ligation

Restriction endonucleases were from NEB (New England Biolabs, Beverly, MA, USA), Roche Diagnostics (Basel, Switzerland), and from Promega (Madison, WI, USA). All restriction reactions were performed according to the manufactures instructions in the recommended buffers. Double restrictions were simultaneously performed in the most appropriate buffers. Ligation of DNA fragments were performed using the commercially available T4 DNA ligase™ from NEB (New England Biolabs, Beverly, MA, USA). The ligation reactions were performed according to the manufactures instructions, at different molar ratios of linker to insert (Sambrook and Russell 2001).

2.2.1.5. Plasmid purification and DNA sequencing

Plasmid purification was performed using a commercially available kit from Macherey-Nagel (Nucleobond® midi plasmid preparation kit) according to the manufacturer's instructions.

After purification, the plasmid concentration was determined spectroscopically by measuring the absorption at 260 nm as mentioned before.

Correctness of all DNA inserts was verified by automatic sequencing using a slightly modified protocol of the dideoxynucleotide method developed by Sanger *et al.* (Sanger *et al.*, 1977). Primers used for DNA sequencing were 5' fluorescence labelled (MWG Biotech) enabling a laser-scan detection on an automated DNA sequencer (Licor™ 4000 DNA sequencer). PCRs were performed with the Thermo-Sequenase™ Cycle Sequencing Kit from Amersham according to the manufactures instructions. Mrs. Natalie Lenz or Mrs. Katharina Bompais thankfully carried out all DNA sequencing reactions being part of this work.

2.2.2. Microbiology methods

2.2.2.1. *E. coli* cultivation and transformation

Unless otherwise noted, *E. coli* cells were grown in LB medium (see 2.1.1.1) and incubated at 37°C and 200 rpm. Media used for the cultivation of transformed *E. coli* cells always contained 100 µg/ml ampicillin. Transformation of competent *E. coli* cells after addition of approximately 50 ng plasmid-DNA was performed via heat-shock (30 seconds at 42°C; (Sambrook and Russell 2001)). Chemically Competent *E. coli* cells were from invitrogen or generated following a protocol published by Sambrook *et al.* (Sambrook and Russell 2001).

2.2.2.2. *S. pombe* cultivation and transformation

The starting point for all *S. pombe* cultures was a fresh plate, which was prepared by streaking an agar plate containing the desired solid medium from a glycerol stock, and incubated at 30°C for approximately two to three days. The colony of interest was transferred to a 10 ml EMM medium containing the needed supplements (see Tables 2.6, 3.6) to prepare a pre-culture, which was incubated at 30°C and 180 rpm overnight. The pre-culture was then centrifuged and the pellet was used to inoculate a 100 ml fresh medium, this 100 ml main culture was then incubated under the same condition like the pre-culture.

In order to transform fission yeast *S. pombe*, a certain number of cells are needed to perform the transformation. For this reason, a culture of 100 ml was prepared as mentioned before and the cell density (δ_{cell}) was determined microscopically by using a haemocytometer for optical

counting. Cells were only used if $\delta_{\text{cell}} \in [5 \cdot 10^6 - 10^7]$ cells/ml, whereby the total number of cells used for transformation had to be 10^9 to $2 \cdot 10^9$ cells.

The following steps describe the process that was applied to make the *S. pombe* cells competent in order to perform the transformation. The first step comprised a centrifugation step at $3 \cdot 10^3$ g for 5 min and a washing step with 5 ml distilled water. After a second centrifugation step under the same condition as above, the cells were resuspended in 1 ml of 0.1 M LiAc pH 4.9 and transferred to a 1.5 ml flask. A volume of 100 μ l of the above cell suspension was used for each transformation. An amount of 10 μ g of DNA solution was added to each transformation. Following incubation at RT for 10 min, 260 μ l of 40% PEG 4000 in 0.1 M LiAc pH 4.9 solution were added and gently mixed with the cell suspension. After one hour incubation at 30°C and 10³ rpm, 43 μ l DMSO was added, mixed and a heat shock was applied at 42°C for 5 min. Quickly, 500 μ l water was mixed with the cell suspension that was then centrifuged at $3 \cdot 10^3$ g for 5 min and washed again with 500 μ l water. After a second centrifugation step ($3 \cdot 10^3$ g, 5 min) the cells were resuspended in 500 μ l water and 100 μ l were streaked on the desired plate. The plates were then incubated at 30°C for 3-4 days. The resulted colonies were then analysed by colony PCR.

2.2.2.3. *ura4* gene disruption in *S. pombe*

A gene disruption process was carried out to disrupt the *ura4* gene in fission yeast SZ1, in order to create a new *S. pombe* strain that already express CYP11B1 (Dragan *et al.* 2005), and posses in addition to leucine, uracil as second auxotrophic marker. This process will enable then the transformation of a new strain with two plasmids at the same time.

The gene disruption was done essentially according to Akio Tohe-e (Toh-e 1995). The transformed yeast cells were selected depending on the new auxotrophic marker by multiple replica plating in the presence of 5-fluoroorotic acid (5-FOA), which generates a toxic metabolite in *ura4*⁺ strains (Boeke *et al.*, 1987).

The *Hind* III fragment containing the *ura4* disruption cassette was excised from the plasmid pAT539 and used as donor for the transformation of SZ1 from *ura4*⁺ to *ura4*⁻ (Toh-e 1995). The transformation of *S. pombe* (SZ1) was carried out as described in subsection 2.2.2.2, and transformed cells were then plated on EMM containing 0.01% leucine, 0.01% uracil and 1 mg/ml fluoroorotic acid (5-FOA) as selection factor (Boeke *et al.* 1987). Multiple replica plating was carried out to isolate the *ura4*⁻ fission yeast strain.

B2

Sorbitol	1.2 M
KH ₂ PO ₄ , pH 7.4	20.0 mM

Protein extraction buffer

Tris-HCl, pH 7.5	1.0 M	
MgCl ₂	1.0 M	
EDTA	0.5 M	
DTT	1.0 M	
IGEPAL CA-630	100% (w/v)	from Sigma [®] (Steinheim, Germany)

2.2.3.2. SDS (Sodium dodecylsulfate) polyacrylamid gel electrophoresis and gel blotting

Separation of proteins according to their molecular mass was carried out using the Laemmli discontinuous gel electrophoresis (SDS-PAGE) method (Laemmli 1970). Gels used for the separation of Adx and AdR consisted of a 15 % acrylamide containing separation gel superimposed with a stacking gel (5 % acrylamide). Sample buffer composition was as described by Sambrook *et al.* (Sambrook and Russell 2001).

The reference protein mix for molecular weight identification was the pre-stained broad range protein marker purchased from NEB (New England Biolabs, Beverly, MA, USA).

Blotting of proteins separated on a SDS gel onto a nitrocellulose membrane (pore size 0.2 µm) was performed using a semi-dry electrophoretic unit from BIO-RAD[®] (München, Germany).

Blotting of mini gels (8*8 cm) was carried out for 15-30 min and 10-15 V, whereas middle gels (16*17cm) were blotted for 30-60 min and 15-25V according to the manufactures instructions.

2.2.3.3. Immunologic detection of proteins**▪ Antibodies**

The detection of proteins after blotting onto nitrocellulose was performed using a monoclonal anti-Pk tag antibody (MCA1360, Serotec; Oxford, UK) or polyclonal rabbit antibodies

(Biogenes; Berlin, Germany) raised against bacterially expressed Adx, and peroxidase-conjugated secondary antibodies (Dako; Glostrup, Denmark).

▪ Western Blotting

The nitrocellulose membrane bearing the transferred proteins (see 2.2.3.2) was blocked with Blotto1 for 1h. The primary antibody was added 1:10³ diluted for α -Pk tag and 1:2*10³ diluted for α -Adx, respectively, in TBST (Pk tag) for 2 h, in Blotto1 (Adx) for 45 min. After the binding reaction, three washing steps with TBST were followed by incubation with the secondary antibody, 1:500 diluted in TBST (Pk tag), Blotto1 (Adx) for 30 min. A second washing process was carried out twice to remove the excess secondary antibody.

TBST

Tris-Cl, pH = 8	10.00 mM
NaCl	150.00 mM
Tween 20	0.05 % (v/v)

The Blotto1 solution is TBST buffer with 1 % of lyophilised milk powder.

The staining of immunolabelled protein bands was carried out by chloronaphthol in presence of H₂O₂ via horseradish peroxidase.

The nitrocellulose membrane from the previous step above was washed twice with PBS. To perform the visualization of targeted proteins, 25 ml fresh PBS was added on the membrane, 10 mg of chloronaphthol was solved in 2 ml absolute ethanol and mixed with 10 μ l H₂O₂ (30 %) prior to be added on the membrane. After shaking for 10-30 minutes at room temperature, the targeted proteins became visible and membrane was then washed and scanned.

PBS, pH 7.3

NaCl	137.0 mM
KCl	2.7 mM
Na ₂ HPO ₄ .2H ₂ O	8.0 mM
KH ₂ PO ₄	1.5 mM

2.2.4. Steroid hydroxylation assays

The starting point for all bioconversion assays including IC_{50} determinations was fission yeast main culture set up as described in subsection 2.2.2.2. Main cultures with cell densities in the range of 10^7 to $5 \cdot 10^7$ cells/ml were used for bioconversion assays. Cells from the main culture were washed with EMM, centrifuged ($3 \cdot 10^3$ g, 5 min, 4°C) and resuspended in the appropriate assay medium as described in details below.

The bioconversion assays were initiated by adding the appropriate substrate. After shaking at 30°C, steroids were extracted with chloroform and measured.

2.2.4.1. Bioconversion assay in Erlenmeyer flasks

In order to follow the time course of the bioconversion process, the bioconversion assay was carried out in 300 ml wide-neck Erlenmeyer flasks covered by a cellulose-pot, where multiple sampling can be done.

A fission yeast cell suspension with cell density of 10^8 cells/ml was prepared using fresh EMM medium. A volume of 9.75 ml cell suspension was transferred to the Erlenmeyer and the substrate concentration was set up to 1 mM using 250 μ l from a 40 mM ethanolic steroid stock solution. The flask was then incubated at 30°C and 180 rpm, and multiple samples of 500 μ l were taken at defined time points and stored at -20°C until steroid extraction was carried out.

2.2.4.2. Bioconversion in modified 1.5 ml tubes

This bioconversion method is based on 500 μ l cultures. In contrast to the method described in 2.2.4.1, the use of such low-volume cultures allows only the sampling of one time point of the bioconversion period and was mainly designed to determine the IC_{50} values of CYP11Bs inhibitors.

The system requires a simple modification of a conventional 1.5 ml tube (Figure 2.6) in order to add an exhaust to the culture flask. A fission yeast cell suspension with cell density of $5 \cdot 10^7$ cells/ml was prepared using fresh EMM medium and steroid concentration was set to be 100 nM. The incubation was carried out at 30°C and 1400 rpm using a tube shaker (thermomixer). After the required assay period, the whole tip-tube content was extracted with chloroform (see subsection 2.2.4.3) or stored at -20°C until steroid extraction.

Inhibitors were dissolved in DMSO at different concentrations, and equal volumes were used in all cases (including controls). Final concentrations of inhibitors ranged from 100 nM to 25 μ M. Cells were pre-incubated with the respective inhibitor solutions for 15 min prior to the addition of 100 nM steroid substrate (11-deoxycortisol or 11-deoxycorticosterone in the case of CYP11B1 or CYP11B2, respectively). For the detection of CYP11Bs-dependent steroid bioconversion, 0.15 μ Ci [3 H] 11-deoxycortisol or 2.5 nCi [14 C] 11-deoxycorticosterone were added to each vial, respectively. After 6 h incubation at 30°C and 1400 rpm, steroids were extracted with chloroform. The detection of steroid bioconversion or inhibition was performed using the high performance thin-layer chromatography (HPTLC) as described below.

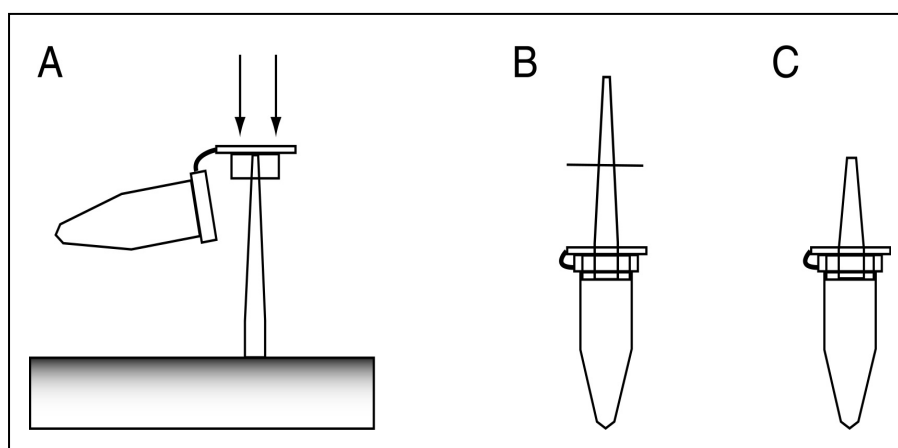


Figure 2.6. The construction of a modified 1.5 ml tube (tip-tube). This tip-tube format was developed by Dipl. Biol. Calin-Aurel Dragan.. The exhaust channel is made of a 200 μ l pipette tip that was pressed through the cap of the 1.5 ml tube (A). To avoid plastic material blocking the air pathway, a cut was done at the line indicated (B) to finally yield a tip-tube (C).

2.2.4.3. Steroid extraction

Samples (500 μ l) gained from bioconversion assays mentioned before were twice completely extracted with 500 μ l CHCl_3 except where indicated. After vigorous shaking, the aqueous phase was pulled out while the organic phase was dried under vacuum. An amount of 10 μ l of 10 mM internal standard steroid was given to the cell suspension prior to steroid extraction in case of subsequent non-radioactive HPLC-based quantification assay.

2.2.4.4. Steroid analysing methods

2.2.4.4.1. High performance liquid chromatography (HPLC)

After evaporation of the chloroform phase, the steroids were resuspended in acetonitril and separated on a Jasco reversed phase HPLC system (Tokyo, Japan) composed of an auto-sampler AS-2050 plus, pump PU-2080, gradient mixer LG-2080-02 and an UV-detector UV-2075 plus equipped with a reversed phase Nova-Pak® C18 60Ao 4 µm column from Waters (Milford, MA, USA). The column temperature was kept constant at 25°C with a peltier oven. The mobile phase used for steroid separation was a mixture of MeOH:H₂O(60:40) with flow velocity of 0.5 ml/min. Steroids were detected at 240 nm, and peak identification was done using the ChromPass software (V.1.7.403.1, Jasco), pure steroids (>99%) were used as standards to identify the peaks on HPLC and to construct calibration curve or as internal standard to normalize the steroid extraction efficiency.

2.2.4.4.2. High performance thin layer chromatography (HPTLC)

Extracted, dried, radioactive samples were dissolved in 10 µl chloroform and applied on the concentrating zone of an HPTLC silica gel 60 F254 plate (Merck, Darmstadt, Germany). The mobile phase for chromatography was CHCl₃:MeOH:H₂O (300:20:1). Radioactive decay signals were exposed to BAS-TR2040 (³H) or BAS-IIIS (¹⁴C) imaging plates (IP) from Fuji (Tokyo, Japan), and scanned with the BAS-2500 phosphoimager (BAS-2500, Fuji; Stamford, CT). Pure 10 mM steroid solutions dissolved in EtOH were used as reference substances for the identification of bands on the scanned IP.

Quantification data analysis procedures were performed using the open-source analysis software TINA v2.10g. The intensity (*I*) of a region of interest (ROI) on the imaging plate was reported in PSL (phosphostimulated luminescence) units, whereby the background exposure signal was subtracted from the raw PSL values prior to conversion calculations by the internal background quantification function. The intensity of the radioactive signal (*I*_{radio}) caused by a certain steroid is proportional to the amount of radioactively labelled steroid (*n*_{radio}).

2.2.4.5. Measuring of steroid bioconversion

Since, the steroids present in sample are chemically and physically very similar molecules, it was assumed that the relative loss of steroids during the extraction procedure is equal for all steroids. Therefore, the ratio of product formation can be calculated depending on the intensity signal (I) of steroid of interest as shown below.

$$R(\text{Pr oduct})\% = \frac{I(\text{Pr oduct})}{I(\text{Pr oduct}) + I(\text{Substrate})} * 100$$

The intensity signal of a steroid is the radioactive signal (I_{radio}) in the case of HPTLC or the peak Area (A) of a certain steroid in the chromatogram with dimension mV.min. in the case of non radioactive HPLC.

This kind of calculation displays the relative ratio of product formation and enables the direct comparison of different *S. pombe* strains and the investigation of the inhibitory effect of compounds compared with a negative control. Furthermore, a quantification assay was also applied to determine the hydrocortisone (Cortisol) production efficiency over time in the “hit” fission yeast strain developed during this work in comparison with the parental strain SZ1.

The quantification assay was carried out in Erlenmeyer flasks as described in subsection 2.2.4.1. Steroid extraction was carried out with chloroform in the presence of DOC as internal standard to normalize the steroid extraction efficiency. Therefore, the correction factor f , defined by the peak areas of the internal standard (IST) as

$$f := \frac{A_{\text{IST,non-extracted}}}{A_{\text{IST,sample}}}$$

was applied to correct the measured peak area of every detected steroid in a particular sample. The data analysis relies on the peak area as a function of molar amount that can be easily established on the used HPLC system by relating A to different n . The linear function was determined for hydrocortisone in the range $n \in [0.1, 10]$ nmol pure hydrocortisone (>99 %).

2.2.4.6. Measuring of the inhibition of steroid bioconversion (Determination of the IC₅₀ values)

The ratio of a certain steroid product P can be regarded as a function of the inhibitor concentration c_{inh} . The inhibition of the production of P ($\text{INH}(P)$) from the substrate is therefore defined as

$$INH(P) = 1 - \frac{R(P, c_{inh})}{R(P, c_{inh} = 0)}$$

Where $R(P, c_{inh} = 0)$ is the ratio of product in the control reaction without inhibitor. From the above formula one can clearly see that when $c_{inh} = 0$ or when the inhibitor shows no effect at all then $R(P, c_{inh} = 0) = R(P, c_{inh})$ for all c_{inh} and the inhibition is 0.

Multiplying $INH(P)$ by 100 displays the result in percent inhibition of the control reaction. The presentation of the data requires the following substitutions

$$y := INH(P),$$

$$x := \log(c_{inh}).$$

After inserting the data in a two dimensional scatter plot a function of the form

$$y = ax + b$$

is fitted by linear regression. The IC_{50} value is the inhibitor concentration $c_{inh,50}$ where $INH = 0.5$ for the production of P. Therefore we rearrange the equation above to

$$x = \frac{0.5 - b}{a}.$$

After back substitution and minor rearrangement we finally get

$$c_{inh,50} = 10^{\frac{0.5 - b}{a}}, \quad \text{Where } IC_{50} = c_{inh,50}.$$

2.2.5. Structure activity relationship (SAR) study

Structure activity relationship study was performed using the BenchwareHTS DataMiner (Tripos). Only the new selective CYP11B2 inhibitors defined in this work were included in this SAR study. SAR analysis being part of this work were thankfully carried out by Dr. Katja Hübel (Max-Planck-Institute of Molecular Physiology, Dortmund, Germany).

2.2.6. Statistical analysis

To evaluate the results; descriptive statistics were applied using the “Statistica” computer program. Moreover, *t*-test for independent samples was applied to evaluate the differences in means between two groups (fission yeast strains), whereas the correlation coefficient Pearson *r*, was applied to measure the relation between two or more variables. The results of these statistical tests are considered significant when $p < 0.05$. Furthermore, the *Z*'-Factor (Zhang *et al.*, 1999) was used for the evaluation and validation of the screening system developed in this work.

2.2.6.1. Descriptive statistics (Measures of variation)

Descriptive statistics were calculated separately for each variable to provide basic information as the mean, standard deviation as well as data about the shape of the distribution of the variable.

It is already known that standard deviation σ is a measure of the average deviation of measured values around the mean \bar{t} and is called in the case of single measurement “error of single measurement”. In practice, it is not interesting to know with which probability the result of a single measurement is within the range $\bar{t} \pm \sigma$, more important is the question of how reliable and reproducible is the mean \bar{t} , which was found with a series of measurements and which represents the result of measurement. For this reason the standard deviation of the mean, which is often called “standard error of the mean (SE)” will be used in this work to measure the standard deviation of the results. The standard deviation of mean say with which probability would the mean of a second measurement series found in a given interval around the mean found by the first measurement.

2.2.6.2. Statistical tests

2.2.6.2.1. *t*-test for independent samples

The *t*-test is the most commonly used method to evaluate the differences in means between two groups. For example, the *t*-test was used in this work to test for a difference in hydrocortisone bioproduction efficiency between fission yeast strain that coexpresses the

complete mitochondrial chain (CYP11B1+Adx+AdR) and the parental fission yeast strain that expresses only the cytochrome CYP11B1.

2.2.6.2.2. Correlation

Correlation is a measure of the relation between two or more variables. Correlation coefficients can range from -1.00 to +1.00. The value of -1.00 represents a perfect negative while a value of +1.00 represents a perfect positive correlation. A value of 0.00 represents a lack of correlation.

The most widely used type of correlation coefficient Pearson r was applied to determine the extent to which values of the two variables are "proportional" to each other. The value of correlation (i.e., correlation coefficient) does not depend on the specific measurement units used. Proportional means linearly related; that is, the correlation is high if it can be "summarised" by a straight line (sloped upwards or downwards).

This line is called the regression line or least squares line, because it is determined such that the sum of the squared distances of all the data points from the line is the lowest possible.

This test was applied in this work to investigate the correlation between the inhibition and concentration of inhibitor in different test media.

2.2.6.2.3. Z'-Factor of assay

To evaluate the robustness and reliability of the developed screening system the Z' -factor known as "screening window coefficient" (Zhang *et al.* 1999) that compares the assay's dynamic range to data variation was applied.

The Z' -factor was determined from the inhibition assays of ketoconazole, clotrimazole and miconazole against CYP11B2 in recombinant fission yeast. The calculation of Z' -factor was carried out using the following formula:

$$Z' = 1 - \frac{(3 * \sigma_{PC} + 3 * \sigma_{NC})}{|\bar{t}_{PC} - \bar{t}_{NC}|}$$

Where \bar{t} and σ are the mean and standard deviation of mean, respectively. PC refers to the positive control and NC to negative control.

A Z' -factor equal to 1 indicates a perfect assay whereas a Z' -factor above 0.5 indicates an excellent screening assay for whole cell systems (Zhang *et al.* 1999).

3. Results

The main topic of this work consisted in the improvement of hydrocortisone bioproduction using new recombinant fission yeast strains coexpressing additionally to CYP11B1 the corresponding electron transfer partners. In addition to this, a second project focussing on the CYP11B2-expressing fission yeast test system was carried out to develop a high throughput screening system for the discovery of selective CYP11B2 inhibitors.

In order to address each project separately the results presented in this section as well as the subsequent discussion were divided into independent sections with the following titles:

- Optimisation of steroid hydroxylation assay for the 96-well plate format
- Coexpression of the corresponding redox partners in the CYP11B1-expressing fission yeast *Schizosaccharomyces pombe*
- The development of a cell-based high throughput screening system for the discovery of human aldosterone synthase (CYP11B2) inhibitors

3.1. Optimisation of a steroid hydroxylation assay for the 96-well plate format

The goal of this part of work was to optimise the steroid hydroxylation assay in fission yeast described above in the Material and Methods section in order to use the 96-well plate to perform the assay in low-volume culture without the need to use radioactive-labelled substrates. This optimisation will give the opportunity to develop a screening assay that does not require the use of radioactively substances that need an especial area in the laboratory.

3.1.1. Steroid bioconversion assay in modified 1.5ml tubes (tip-tube format)

The hydroxylation assay described in subsection 2.2.4 involved the use of radioactive labelled substrates when the bioconversion assay is carried out in low-volume culture (tip-tube format). Therefore, the aim of this part of work was the optimisation of the hydroxylation assay for low-volume cultures without the need to use radioactively labelled substrates. This optimisation was carried out using the CYP11B1-expressing fission yeast strain SZ1, and the tip-tube format described in subsection 2.2.4.2. The assay was designed to be carried out as described in subsection 2.2.4.2 with a cell density of 5×10^7 cells/ml and 100 nM non-

radioactive RSS as substrate. After 24 hours incubation at 30°C and 1400 rpm, the steroid extraction was carried out with chloroform and the HPLC technique was applied as described in subsection 2.2.4.4.1. The HPLC measurement displayed no steroid bioconversion under the conditions described before. In order to optimise the hydroxylation assay to get detectable conversion on HPLC, the substrate concentration was increased but no conversion was detected even after increasing the concentration by 1000-fold (from 100 nM to 100 µM) (Table 3.1). In a next step, the cell density of the assay culture was investigated and a 2-fold concentrated culture was investigated with different concentrations of the substrate as mentioned before. Increasing the cell density and the concentration of substrate to 10⁸ cells/ml and 100 µM, respectively, (Table 3.1) displayed detectable steroid bioconversion of RSS into F (Figure 3.1) in the tip-tube format.

Table 3.1. Steroid bioconversion parameters (tip-tube format)

Test Volume	500 µl					
Incubation time	24 hours					
Shaking velocity	1400 rpm (Thermo mixer)					
Cell density Cells/ml	5*10 ⁷	5*10 ⁷	5*10 ⁷	10 ⁸	10 ⁸	10 ⁸
Substrate concentration	100 nM	500 nM	100 µM	100 nM	500 nM	100 µM
Result	No conversion	No conversion	No conversion	No conversion	No conversion	Conversion

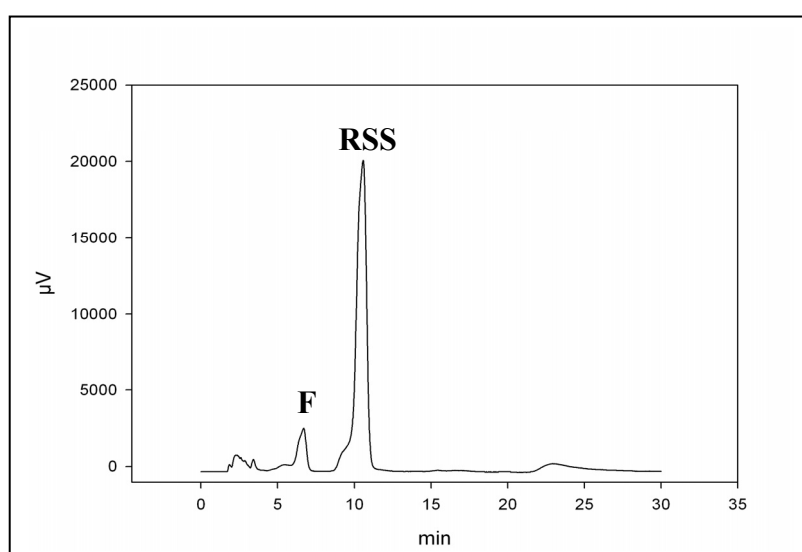


Figure 3.1. HPLC chromatogram of CYP11B1-dependent bioconversion of RSS into F carried out using the tip-tube format. The bioconversion was carried out in the tip-tube format using the CYP11B1-expressing strain SZ1 with cell density of 10⁸ cells/ml and 100 µM RSS. Steroids extraction was performed manually with chloroform.

This first optimisation step enabled the coupling of the tip-tube format (low-volume culture) with the HPLC technique to perform steroid hydroxylation assay in low-volume culture and to measure the steroid bioconversion efficiency using the HPLC technique.

3.1.2. Steroid bioconversion assay in 96-well plate

The hydroxylation assay parameters established in subsection 3.1.1 (Table 3.1) were the starting point to develop a hydroxylation assay in 96-well plates.

Since the hydroxylation assay will be performed in plates, an automated steroid extraction technology plate-format had to be developed. This automated technology should enable the manipulation of low-volume cultures on large scale and the performance of efficient steroid extraction in order to get detectable steroid bioconversion on the HPLC. For this reason, several protocols (Script) were developed during this work to perform the preparation of test plates and steroid extraction using the Aquarius 96 Multichannel pipetting robot (Tecan Aquarius, Switzerland).

The main idea behind using the Aquarius pipetting robot is to mix the culture with the chosen organic solvent, which should not be miscible with water in order to extract the steroids from the culture. This mixing process must be various enough to resemble a strong shaking effect with the ability to separate finally the organic phase in order to perform an efficient HPLC measurement. For the development of an Aquarius script that enables the extraction of steroids from a 96-well plate, two kinds of organic solvents that have different densities and boiling points were investigated. The high boiling range (114-117°C) of 4-Methyl-2-pentanone disables the fast evaporation of the solvent during the extraction process, which prevents any significant loss in the solvent volume. For this reason, it is expected heir to recover almost all the solvent that was added to extract the steroids after mixing the two phases using the pipetting robot. However the low density of 4-Methyl-2-pentanone (0.8) make it lighter than water and, as a result, it forms the upper phase above the culture after mixing the two phases. In contrast to this, chloroform has a boiling point of 61.2 °C and a density of 1.48, and, as a result, the solvent evaporation is higher in the case of chloroform whereas the high density of chloroform locates it under the aqueous phase. For this reason, it is important to determine the tip height at which the organic phase is dispensed to perform the mixing process and the height at which only the organic phase is aspirated to get pure organic phase in order to dray the steroids for the HPLC measurement.

Figure 3.2 below illustrates the different Z positions for a tube in a 96-well plate. This coordinates were taken into consideration to develop an Aquarius script to extract the steroids.

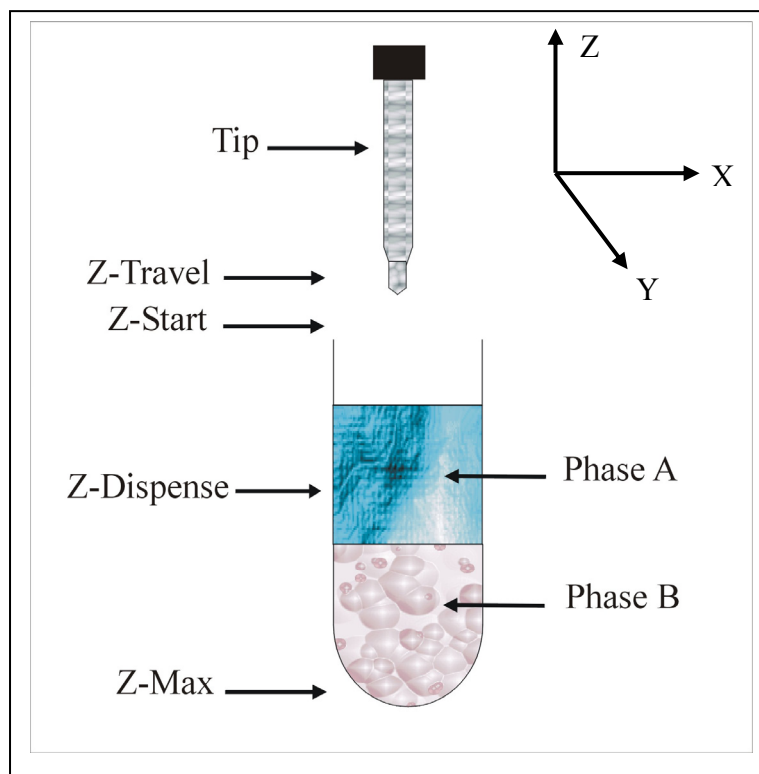


Figure 3.2. Z-positions for a tube.

Z-Travel is the height at which the tip moves from one position to another, Z-Start is usually slightly above the rim of the liquid container. Z-dispense is the tip height at which liquid is dispensed. Z-Max is the position in the lowest point of the well/tube of the rack and is the lowest possible position the tip is allowed to reach.

Since the test culture is incubated for 24 hours at 30°C, the volume of the aqueous phase (test culture) will decrease. This is due to the evaporation of water and, as a result, 4-Methyl-2-pentanone (Phase A, Figure 3.2) will display different Z positions above the aqueous phase after mixing them prior to perform the steroid extraction process. Hence, it is difficult in the case of an organic solvent, which is lighter than water to determine the tip height at which the organic phase is aspirated/dispensed to mix the two phases and the height at which only the organic phase is aspirated to get pure organic phase. For this reason, chloroform was chosen to develop the Aquarius script as it forms the lower phase (Phase B, Figure 3.2) and no changes in the Z position are expected. The Aquarius script developed in this work (Table 3.2) performs several aspirating and dispensing steps in order to mix the organic phase (chloroform) with the assay culture. For this reason, several types of programs that determine the liquid class were developed. These programs are sets of liquid handling parameters that specify speed, airgaps, tip height, etc. Furthermore, and as shown below in Table 3.2 the

Aquarius scrip performs the steroids extraction process on two levels. In the first level, the first volume of chloroform (400 μ l) added in Steps 6-9 is strongly mixed with the test culture for 50 times (steps 10-13). This strong mixing process resembles a various shaking effect that should be enough to extract almost all the steroids from the test culture. The strong mixing process is followed by a slow mixing process (steps 14-17) that enables the separation of the two phases by getting rid of the air bubbles formed between the two phases during the former mixing process. This first extraction level is ended by transferring 200 μ l organic phase on the HPLC 96-well plate. A second extraction process begins by step 26 in which the culture plate receives 200 μ l fresh chloroform. The second extraction process is also carried out like in the first level. Finally, 150 μ l organic phase will be transferred to the HPLC plate. This extraction program recovers 350 μ l organic phase from the 600 μ l chloroform added during the extraction process (Table 3.2).

Table 3.2. Steroid extraction script developed during this work. Red and blue sentences represent the liquid class programs and positions in the Tecan working area, respectively (Figure 3.3). For more information about the liquid class programs, see appendix

Step			Purpose
1	Get DITIs*	Grid1; site: 4 (TeMO_Diti_200 μ l)	Getting Tips
2	Begin loop	5 times "Chloroform transfer"	
	3	Aspirate 200 μ l (Program 1) "Chloroform pool"	Filing up a 96-well plate with chloroform
	4	Dispense 200 μ l (Program 1) "Chloroform plate"	
5	End loop	"Chloroform transfer"	
6	Begin loop	2 times "Chloroform transfer"	
	7	Aspirate 200 μ l (Program 1) "Chloroform plate"	Adding 400 μ l chloroform (1st time extraction)
	8	Dispense 200 μ l (Program 1) "Test plate"	
9	End loop	"Chloroform transfer"	
10	Begin loop	50 times "Chloroform mixing"	
	11	Aspirate 200 μ l (Program 2) "Test plate"	Strong mixing to extract the steroids (Shaking-like effect)
	12	Dispense 200 μ l (Program 2) "Test plate"	
13	End loop	"Chloroform mixing"	
14	Begin loop	20 times "Chloroform relaxing"	

	15		Aspirate	200 μ l (Program 3) "Test plate"	Getting raid of the air bubbles formed between the organic and aqueous phases during the extraction process
	16		Dispense	200 μ l (Program 3) "Test plate"	
17		End loop	"Chloroform relaxing"		
18		Wait timer	Timer 1: 300 sec		
19		Start timer	1		
20		Begin loop	1 time "Transfer of extract"		
	21		Aspirate	200 μ l (Program 1) "Test plate"	Checking if the 200 μ l organic phase pure is, unless the process can be stopped at this step and repeated by step14
	22		Dispense	200 μ l (Program 1) "Test plate"	
	23		Aspirate	200 μ l (Program 1) "Test plate"	Transfer of 200 μ l to the HPLC plate
	24		Dispense	200 μ l (Program 1) "HPLC plate"	
25		End loop	"Transfer of extract"		
26			Aspirate	200 μ l (Program 1) "Chloroform plate"	Adding 200 μ l chloroform (2nd time extraction)
27			Dispense	200 μ l (Program 1) "Test plate"	
28		Begin loop	20 times "Chloroform mixing"		
	29		Aspirate	200 μ l (Program 2) "Test plate"	Strong mixing to perform steroid extraction (Second time)
	30		Dispense	200 μ l (Program 2) "Test plate"	
31		End loop	"Chloroform mixing"		
32		Begin loop	10 times "Chloroform relaxing"		
	33		Aspirate	200 μ l (Program 3) "Test plate"	Getting raid of the air bubbles formed between the organic and
	34		Dispense	200 μ l (Program 3) "Test plate"	
35		End loop			
36		Wait timer	Timer 2: 150 sec		

37	Start timer	2	aqueous phases during the extraction process
38		Aspirate 150 μ l (Program 1) "Test plate"	Checking if the 150 μ l organic phase pure is, unless the process can be stopped at this step and repeated by step 32
39		Dispense 150 μ l (Program 1) "Test plate"	
40		Aspirate 150 μ l (Program 1) "Test plate"	Transfer of 150 μ l to the HPLC plate
41		Dispense 150 μ l (Program 1) "HPLC plate"	
42	Drop DITIs	Grid1; site: 4 (TeMO_Diti_200 μ l)	

*DITIs: Disposable Tip

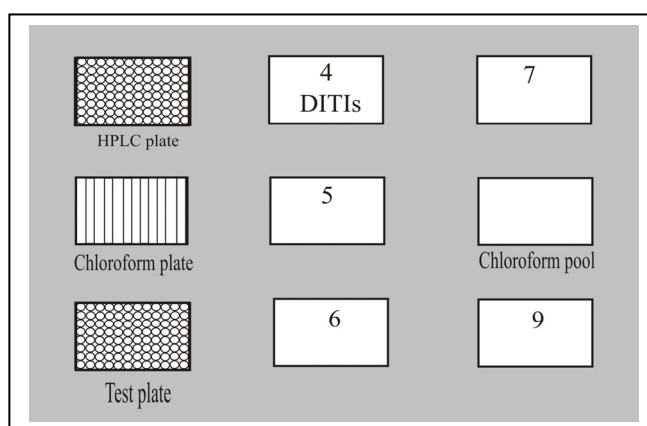


Figure 3.3. Tecan working area during the extraction process

The automated extraction program developed in this work performs the several tasks mentioned above (Table 3.2) in ca 20 min. To investigate the efficiency of this program, a test was carried out to determine the steroid extraction efficiency when a 500 μ l EMM with 100 μ M steroid concentration (RSS or DOC) is extracted automatically in comparison with the manual method.

Since the automated extraction program recovers only 350 μ l organic phase from the 600 μ l chloroform added during the extraction process, a 2 ml tube with 500 μ l EMM with steroid

concentration of 100 μM RSS or DOC was extracted manually with 600 μl chloroform (by shaking strongly for 3 min) whereas only 350 μl organic phase was transferred to be analysed on the HPLC. At the same time, another tube was extracted under the same conditions and the whole recoverable amount of chloroform (500 μl) was transferred to be analysed. After drying under vacuum, the steroids were resolved and measured with HPLC as described above in subsection 2.2.4.4.1.

Figure 3.4 below shows the original HPLC chromatograms of the extracted steroids, which were obtained using the automated method that was applied in a 96-well plate. It is clearly to notice that the peak areas of the extracted steroids do not display any significant difference between the several wells.

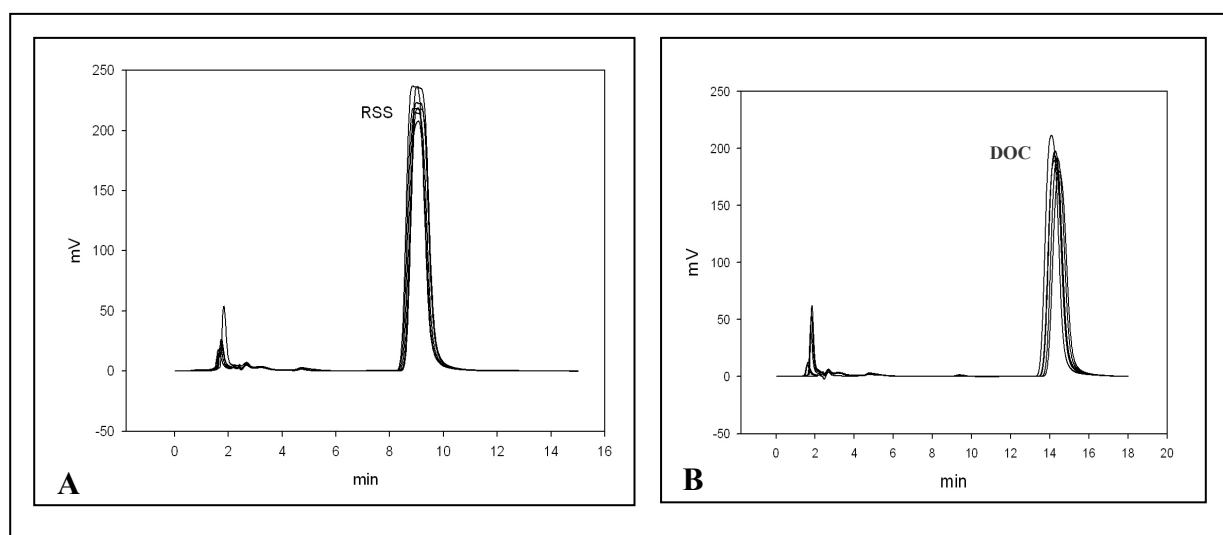


Figure 3.4. HPLC chromatograms of extracted steroids obtained using the automated extraction method applied in a 96-well plate.

96-well plate was filled with 500 μl EMM per well and steroid concentration was set to be 100 μM . Steroid extraction was carried out using the automated method described above. (A) Extracted RSS, (B) Extracted DOC.

Moreover, peak areas of the steroids obtained with the automated extraction method were compared with the steroid peak areas obtained with the manual method, as well as with the same amount of steroids that was given directly on the HPLC without extraction (Figure 3.5). It is clearly to notice that 350 μl of the organic phase in the automated method displays higher steroid content in comparison with the same volume of organic phase obtained using the manual extraction method after mixing with the same volume of chloroform. Moreover, the steroid amount recovered with 350 μl organic phase in the automated method is still more than the amount of steroid recovered with 500 μl organic phase in the manual method.

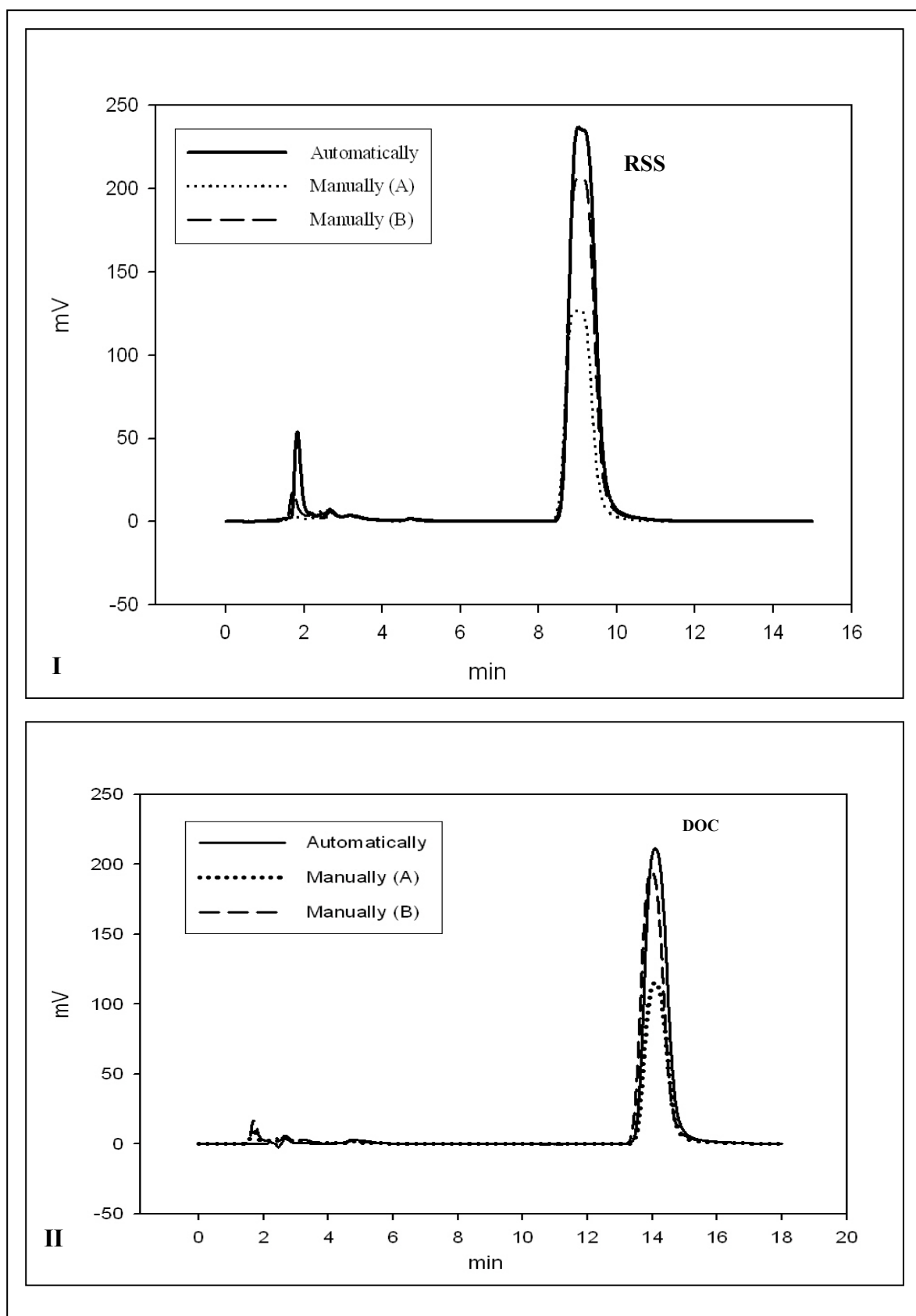


Figure 3.5. HPLC chromatograms of steroids extracted automatically or manually.

(I); RSS, (II); DOC. All samples were mixed with 600 μ l chloroform, whereas different volumes of the organic phase were then analysed on the HPLC (Automatically; 350 μ l, Manually (A); 350 μ l, Manually (B); 500 μ l).

These observations mean that the steroids extraction efficiency of the automated method is significantly higher than the manual method (Figure 3.6). Although the automated method displays high efficiency to extract steroids in comparison with the manual method, only a fraction and not all the organic phase will be transferred to the HPLC plate to be analysed. For this reason, the hydrocortisone ratio (R(F)) will be used to compare the 11 β -hydroxylation activity between the different samples (wells), as it presents proportionally the hydrocortisone production (see 2.2.4.5).

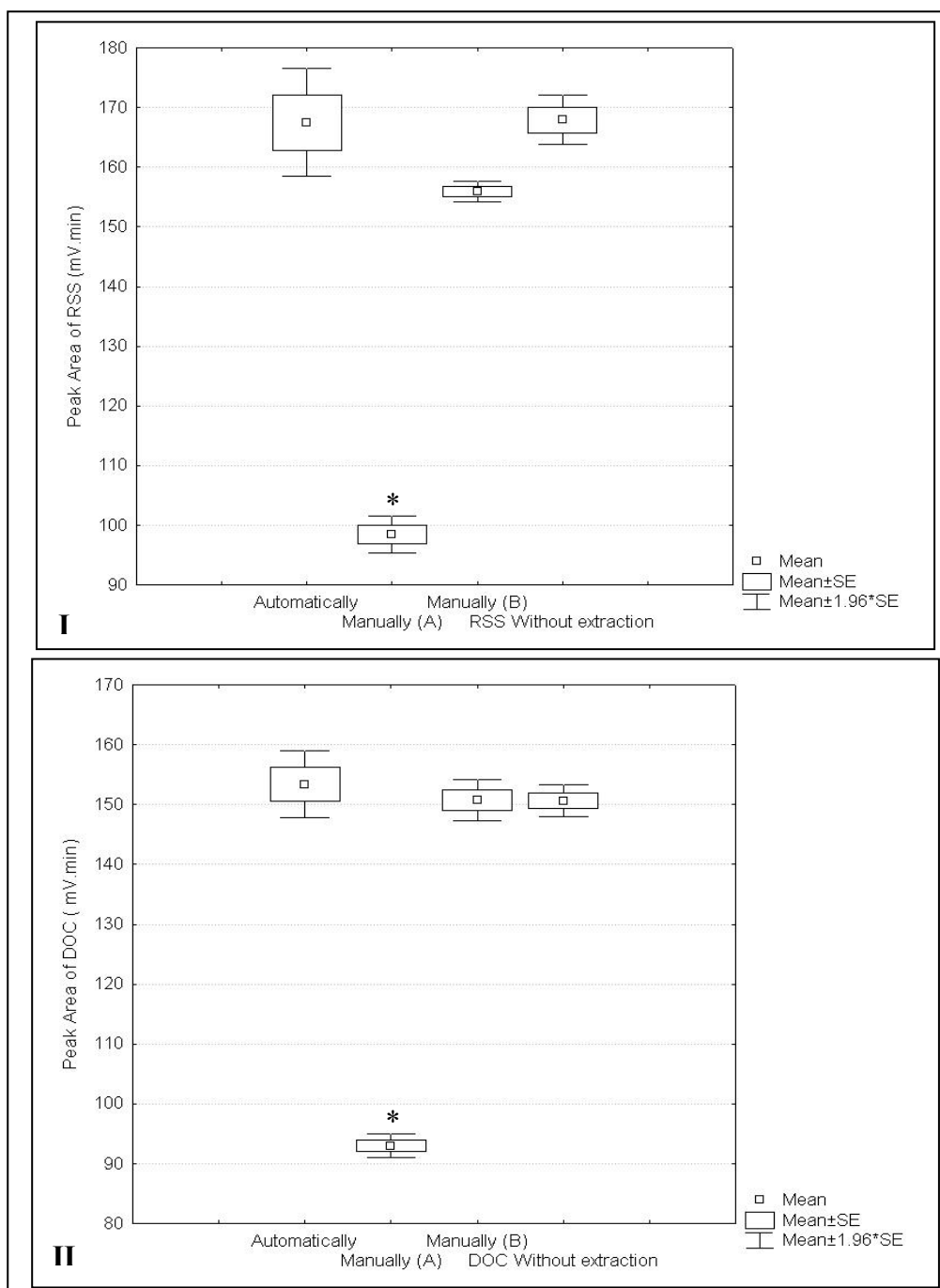


Figure 3.6. Direct comparison of the recovered steroids obtained using different extraction methods in comparison with the same amount of steroids that were given on the HPLC without extraction. (I); RSS, (II); DOC. The samples were mixed with 600 μ l chloroform, whereas different volumes of the organic phase were then analysed on the HPLC (Automatically; 350 μ l, Manually (A); 350 μ l, Manually (B); 500 μ l). Values presented as mean \pm standard error of mean. Asterisks above boxes indicate a significant difference to RSS without extraction ($p < 0.05$).

To validate the 96-well plate hydroxylation assay and the extraction method, the fission yeast strain SZ1 was investigated under the parameters established in subsection 3.1.1. The test was carried out in a 96-well plate, which was shaken at 30°C and 1400 rpm for 24 hours. The HPLC measurement did not show any detectable steroid bioconversion, whereas increasing the test volume and the shaking velocity to 600 μ l and 480 rpm, respectively, play an important role and detectable steroid bioconversion of RSS into F was achieved under these conditions (Table 3.3, Figures 3.7, 3.9).

Table 3.3. Steroid bioconversion parameters (96-well plat format)

Cell density (cells/ml)	10 ⁸
Substrate concentration (RSS)	100 μ M
Test volume	600 μl
Incubation time	24 hours
Shaking (Incubator)	480 rpm

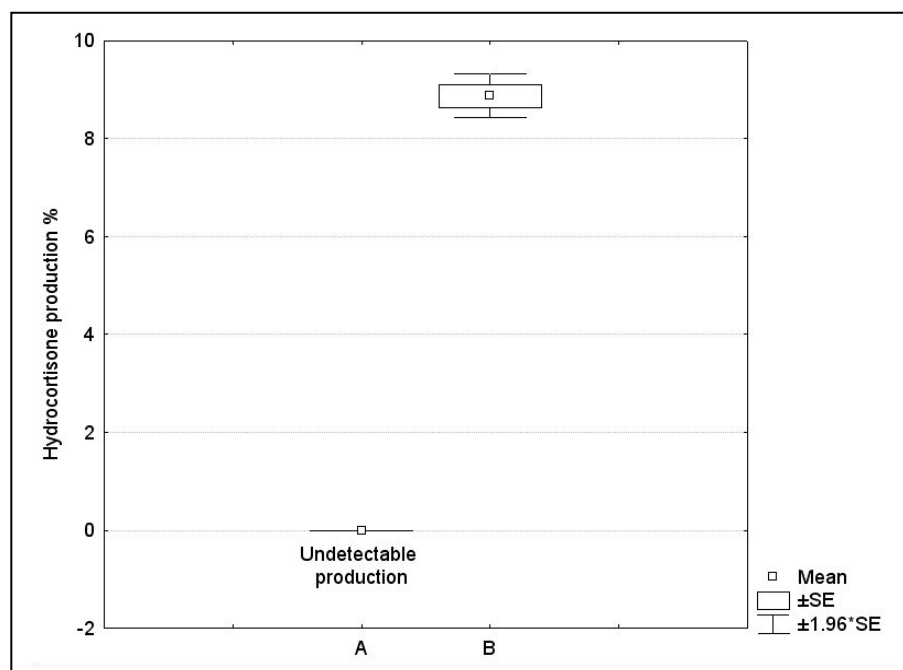


Figure 3.7. Steroid 11 β -hydroxylation activity of SZ1 in a 96-well plate format.

The test was carried out with 100 μ M RSS under different conditions. (A); 500 μ l test volume incubated at 1800 rpm for 24h. (B); 600 μ l test volume incubated at 480 rpm for 24h. Values were calculated from three independent experiments and are presented as mean \pm standard error of mean.

Furthermore, and since each assay plate contains 96 samples, the HPLC parameters described in subsection 2.2.4.4.1 had to be optimised in order to increase the throughput of the HPLC

assay. For this reason, the flow velocity of the mobile phase was increased in order to decrease the time needed for the separation of RSS and F.

Figure 3.8 below shows the separation of RSS and F using a mixture of MeOH:H₂O(60:40) as mobile phase with different flow velocities. Increasing the flow velocity from 0.5 to 1 ml/min decreased the retention times of RSS and F from 9.5 min and 6.7 min (Figure 3.1) to 5.32 min and 3.35 min, respectively (Figure 3.8 A). Moreover, RSS and F displayed with flow velocity of 1.2 ml/min retention times of 4.45 min and 2.8 min (Figure 3.8 B). Whereas increasing the flow velocity up to 1.5 ml/min decreased the time needed to separate RSS and F to less than 5 min (Figures 3.8 C, 3.9) increasing the throughput of the HPLC assay by more than 2-fold. Hence, these new HPLC parameters (Table 3.4) will be applied when a steroid bioconversion assay is carried out in a 96-well plate.

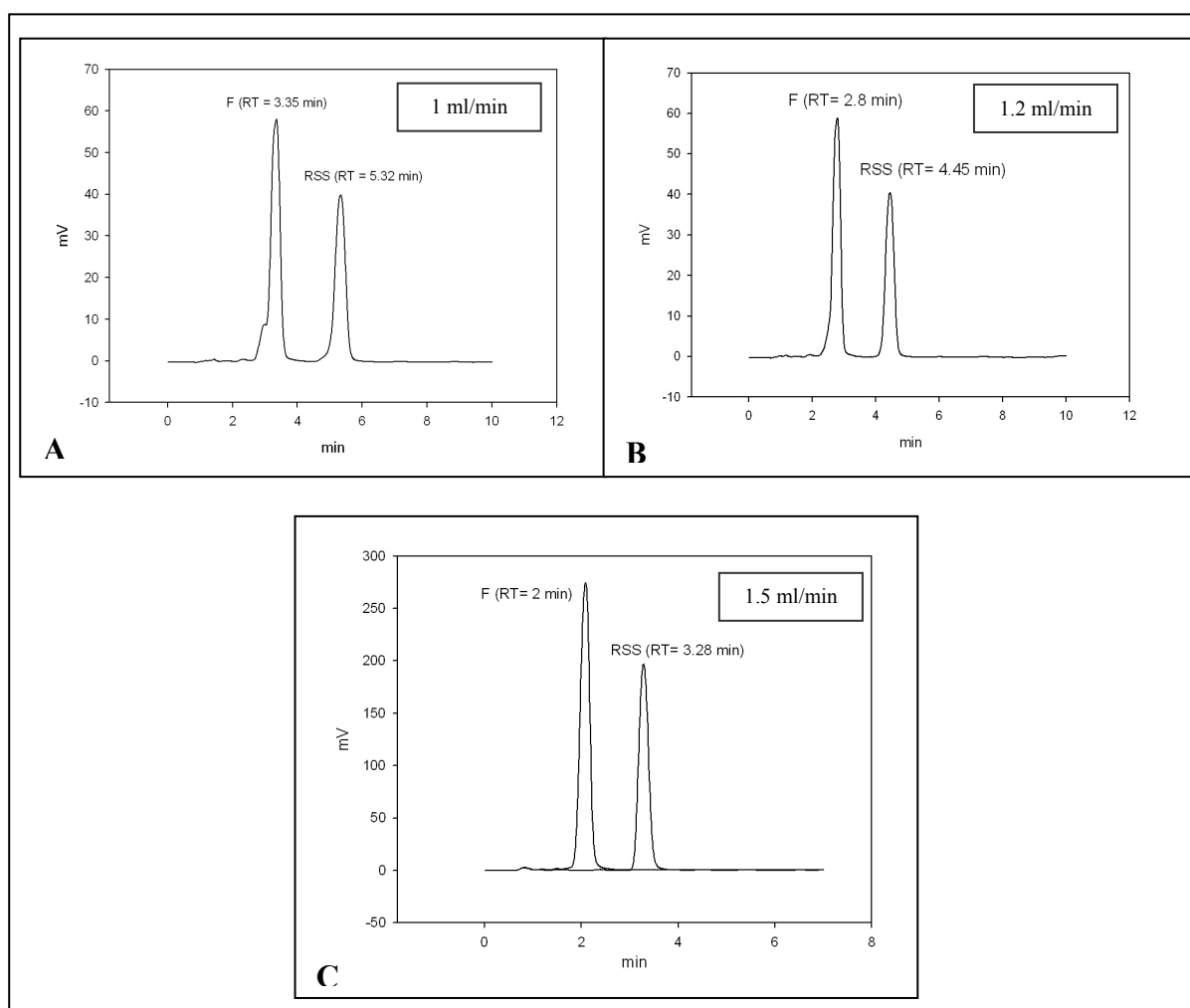
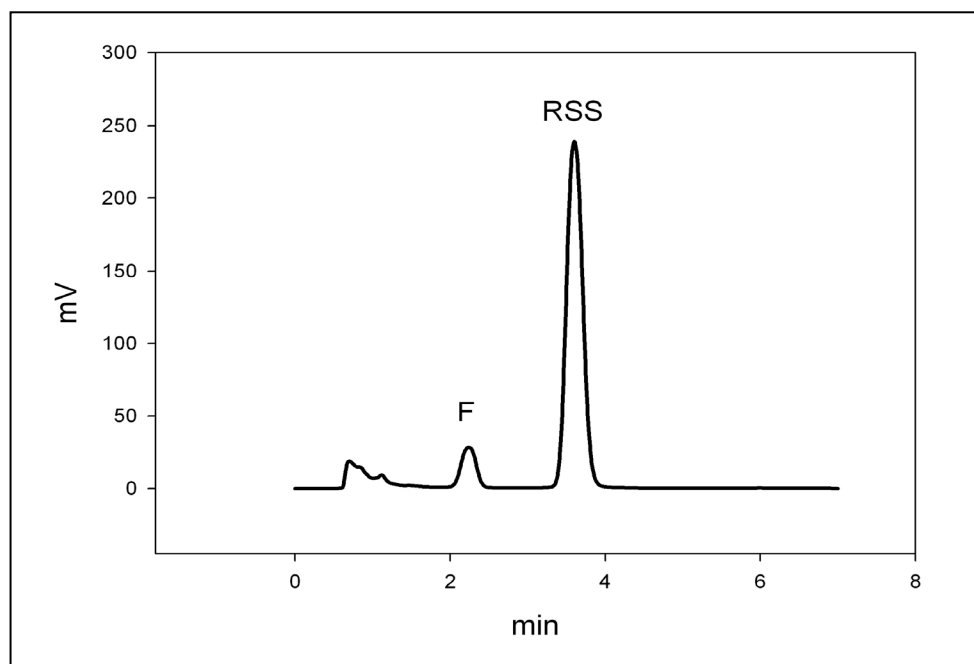


Figure 3.8. HPLC Chromatograms show the separation of RSS and F under different HPLC conditions.

The HPLC was carried out using a mixture of MeOH:H₂O(60:40) as mobile phase with different flow velocities (A; 1 ml/min, B; 1.2 ml/min, C; 1.5 ml/min).

Table 3.4. HPLC parameters to separate RSS and F in less than 5 min

Mobile phase	MeOH:H ₂ O (60:40)
Flow velocity	1.5 ml/min
Column temperature	25 °C
Time per sample	< 5 min

**Figure 3.9. HPLC chromatogram of the CYP11B1-dependent bioconversion of RSS into F carried out using the 96-well plate format.**

The bioconversion was carried out in 96-well plate, using the CYP11B1-expressing strain SZ1 with cell density of 10^8 cells/ml and 100 μ M RSS. Steroid extraction was carried out with chloroform using the pipetting robot as described above.

Moreover, the steroid hydroxylation assay in 96-well plate did not show any significant difference in the bioconversion efficiency between the several wells (*t*-test, $p < 0.05$) (As will be shown below in subsection 3.2.4). Therefore, this 96-well hydroxylation assay is an efficient screening tool to investigate and compare the steroid hydroxylation activity in the recombinant strains that will be developed during this work.

3.2. Coexpression of the corresponding redox partners in CYP11B1-expressing fission yeast *Schizosaccharomyces pombe*

As mentioned before, recombinant fission yeast strains that functionally express human CYP11B1 have been developed in our group (Bureik *et al.* 2002b; Dragan *et al.* 2005). Although these strains display 11 β -hydroxylation of RSS without the need for coexpression of Adx and AdR, the hydrocortisone production is considerably higher than the values reported by other steroid 11 β -hydroxylation systems, but still not competitive enough for industrial applications. Therefore, the purpose of this part of work was to coexpress the corresponding mitochondrial electron chain (Adx and AdR) to improve the activity of CYP11B1 and, as a result, the efficiency of hydrocortisone bioproduction at the laboratory level. In order to achieve this aim, two strategies were selected: one involved a gene disruption based method while the other involved the construction of an expression plasmid that could bear the Adx and the AdR expression cassette. Additionally, the Adx wild type was substituted by two Adx mutants, Adx^{S112W} (Schiffler *et al.* 2001) and Adx^{D113Y} (Bichet *et al.* 2007), in the coexpression strain which were suspected to further improve the electron transport chain and, as a result, the efficiency of steroid 11 β -hydroxylation and hydrocortisone production.

3.2.1. The Coexpression of AdR and Adx through two expression vectors (Strategy I)

Since Adx expression vectors used in the work are derived from the pNMT1- TOPO vector (see subsection 2.1.3), and since the latter possesses a *Leu2* gene from *S. cerevisiae* that complements functionally each *leu1* mutant strain and enables the selection of yeast transformants (Andreadis *et al.*, 1984), the transformation of the Adx plasmid in fission yeast strain SZ1 is possible through the (*leu1*⁻) auxotrophy. Since SZ1 contains only a single selection marker (*leu1*⁻), the creation of a second marker was a necessary prerequisite to accomplish the coexpression of AdR on a second plasmid.

3.2.1.1. *Ura4* gene disruption in *S. pombe* (SZ1) and the characterisation of the new strain

A gene disruption process was carried out to knockout the *ura4* gene inserted by the pCAD1-hCYP11B1 plasmid (Figure 3.10) in the fission yeast strain SZ1 (Dragan *et al.* 2005) in order to create a strain that expresses the human CYP11B1, and possesses *ura4⁻* and *leu1⁻* auxotrophies. The resulting strain then can be used as a host for the assembly of the human electron transfer chain. The *ura4* gene disruption was done according to Akio Tohe-e (Tohe-e 1995). The *Hind* III fragment containing the *ura4* disruption cassette was excised from the plasmid pAT539 and used as a donor for the transformation of SZ1 from *ura4⁺* to *ura4⁻*. Transformed cells were plated on agar plates containing EMM, leucine, uracil and 5-FOA. After three days incubation in the presence of 5-FOA, and replica plating on selective media, positive colonies were checked for the presence of selection marker.

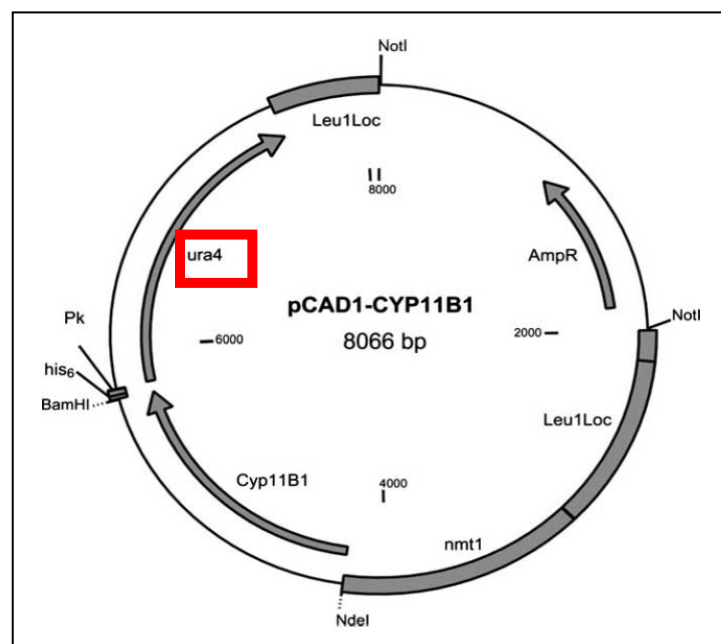


Figure 3.10. Vector map of pCAD1_CYP11B1. Leu1Loc: gene fragments of the *leu1* gene that serve as integration target sequences, *ura4*: ORF for orotidine monophosphate decarboxylase, complements *ura4.dl18* in *S. pombe* (Dragan *et al.*, 2005).

The transformation procedure yielded strain TH1, which was characterised as a new fission yeast strain that already expresses CYP11B1 and needs the addition of leucine and uracil to grow (Figure 3.11).

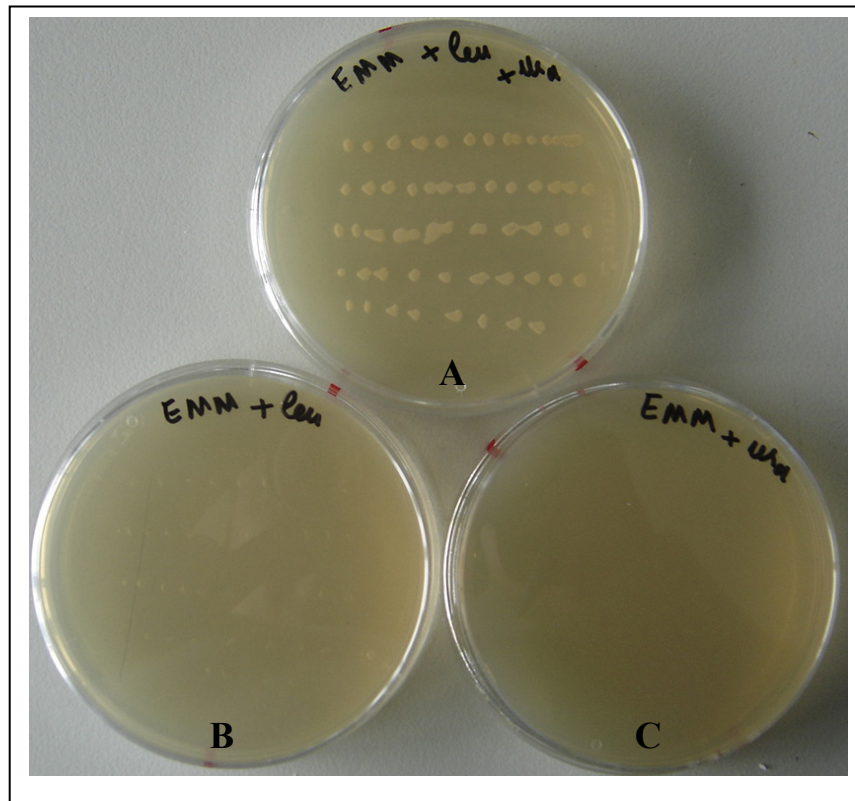


Figure 3.11. Fission yeast TH1 plated on different EMM plates.

The new fission yeast TH1 shows no growth without the addition of leucine and uracil to the medium (A; EMM + leucine + uracil, B; EMM+ leucine, C; EMM + uracil).

Furthermore, strain TH1 displayed the ability to grow in the presence of 1% 5-FOA in contrast to SZ1 that showed an altered phenotype in comparison with TH1 after incubation with 5-FOA (data not shown). The morphologic differences between SZ1 and TH1 could indicate that the *ura4* gene in TH1 is not functional, whereas the intact *ura4* gene in strain SZ1 generates toxic metabolites (Boeke *et al.* 1987) that could be responsible for the morphological changes of the cells after incubation with 5-FOA. Since the *ura4* gene is located near the cloned *CYP11B1* in strain SZ1 (Dragan *et al.* 2005) (Figure 3.10) further validation was carried out to investigate the CYP11B1 activity in TH1.

The CYP11B1 activity in the new *S. pombe* strain TH1 was investigated in comparison with the parental strain SZ1. The test was performed in the tip-tube format as described in subsection 2.2.4.2. The hydroxylation assay showed that strain TH1 still retains the 11 β activity of SZ1 and no significant differences were noticed ($p < 0.05$) (Figure 3.12). This observation indicates that the *CYP11B1* gene in TH1 is still intact rendering TH1 as a potential host for the construction of the electron transfer chain in fission yeast.

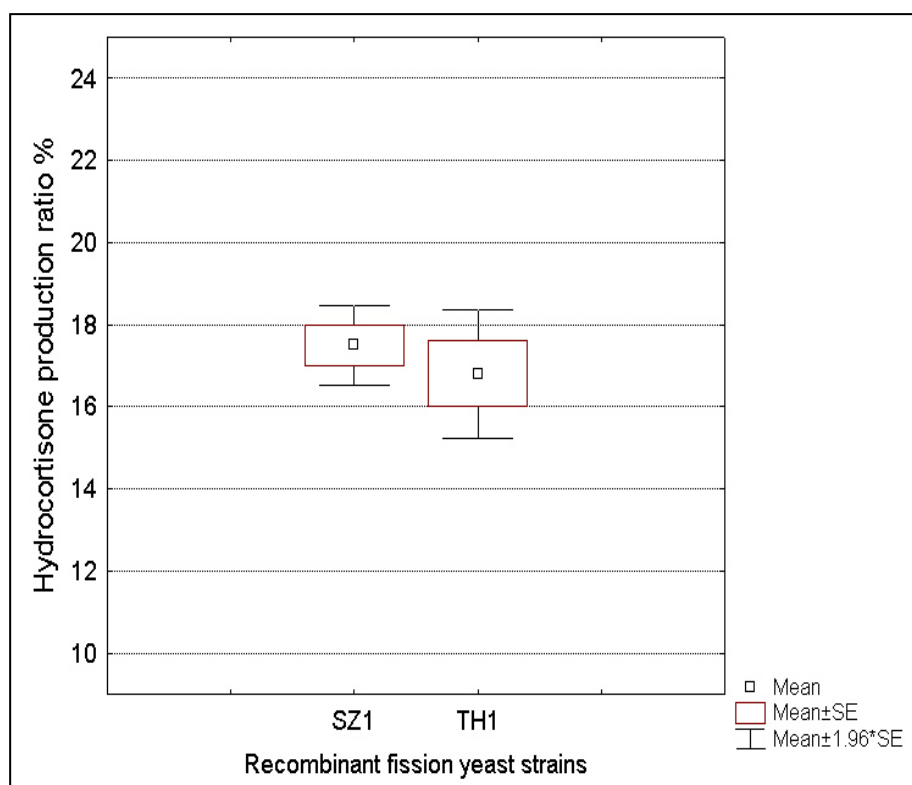


Figure 3.12. Steroid 11 β -hydroxylation activity of TH1 and SZ1.

The bioconversion assay was carried out in tip-tube with 100 nM RSS. Values were calculated from three independent experiments and are presented as mean \pm standard error of mean.

3.2.1.2. Construction of AdR expressing vector (pTH1)

The *Hsa*AdR cDNA was PCR-amplified with the primers Pr₁, Pr₂ that introduce *NdeI/XhoI* restriction sites (see the appendix), and sub-cloned into the pNMT1-TOPO vector as described in subsection 2.2.1.1. After transformation of *E. coli* and plasmid purification, the fragment was cut out using *NdeI* and *XhoI*. The *Hsa*AdR fragment was then cloned into the *NdeI/XhoI* -digested pREP42 Pk C vector to yield pTH1. The developed vector pTH1 was sequenced and it was shown that AdR revealed no alteration compared to the wild type sequence. In this way a vector for the expression of Pk tagged-AdR in *ura4⁻ S. pombe* strains is constructed, and will be used to transform the fission yeast strain TH1.

3.2.2. Construction of an AdR+Adx expressing vector pTH2 (Strategy II)

The aim of this cloning strategy was to develop an expression vector that coexpresses both, wild type Adx and AdR, under the control of the strong inducible *nmt1* promoter. The construction of this expression vector enables the coexpression of the complete mitochondrial

electron transfer partners through one single plasmid. For the construction of the Adx-AdR expression plasmid a cloning strategy was carried out as shown below in Figure 3.13. The $HsaAdR$ cDNA was PCR-amplified with the primers Pr_3, Pr_4 (see the appendix). The PCR product was isolated, purified and subsequently subcloned into the pNMT1-TOPO vector. After transformation of *E. coli*, a colony PCR was carried out to isolate the positive colonies with the correct orientation of the inserted *AdR* gene downstream the *nmt1* promoter. The colony PCR was performed using Primer Pr_4 as forward primer and primer Pr_6 as reverse primer.

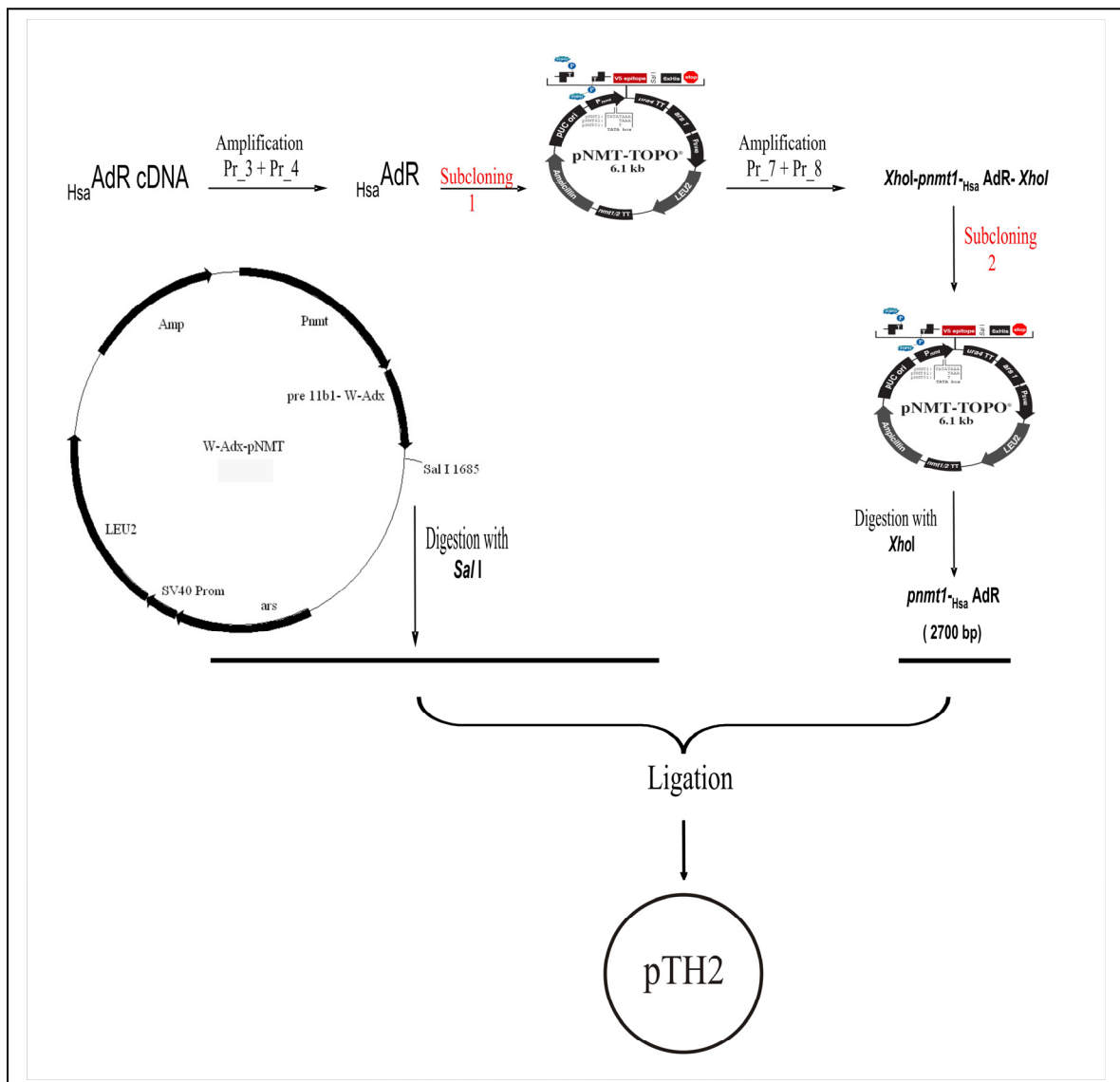


Figure 3.13. The cloning strategy used to create the Adx_AdR expression vector pTH2.

The $HsaAdR$ cDNA was PCR-amplified and subcloned in the PNMT1-TOPO, the resulting plasmid was then used as template to amplify the (*nmt1* promoter + AdR expression cassette) with two *XhoI* sites as overhangs. The *XhoI* digested fragment was then isolated and cloned in the *SalI* site in the pNMT1-Adx^{WT} to yield pTH2.

Subsequently the resulting plasmid from last step with the correct orientation was used as a template to PCR-amplify the (*nmt1* promoter + AdR expression cassette). For this target, primers Pr_7, Pr_8 were used that introduced 5' and 3' terminal *XhoI* sites. The amplified product was then subcloned in pNMT1-TOPO, and finally cloned into the *SalI* site in pNMT1-Adx^{WT} to yield pTH2 (Figure 3.14), which accordingly allows the coexpression of Adx and Pk-tagged AdR in *leu1* hosts.

The developed vector pTH2 was validated by performing Adx colony PCR using primers Pr_9, Pr_10. Furthermore, sequencing of the *nmt1* promoter-AdR expression cassettes in pTH2 revealed no alteration compared to the wild type sequence. Restriction analysis of pTH2 confirmed the construction of the plasmid as shown in Figure 3.14 A, B.

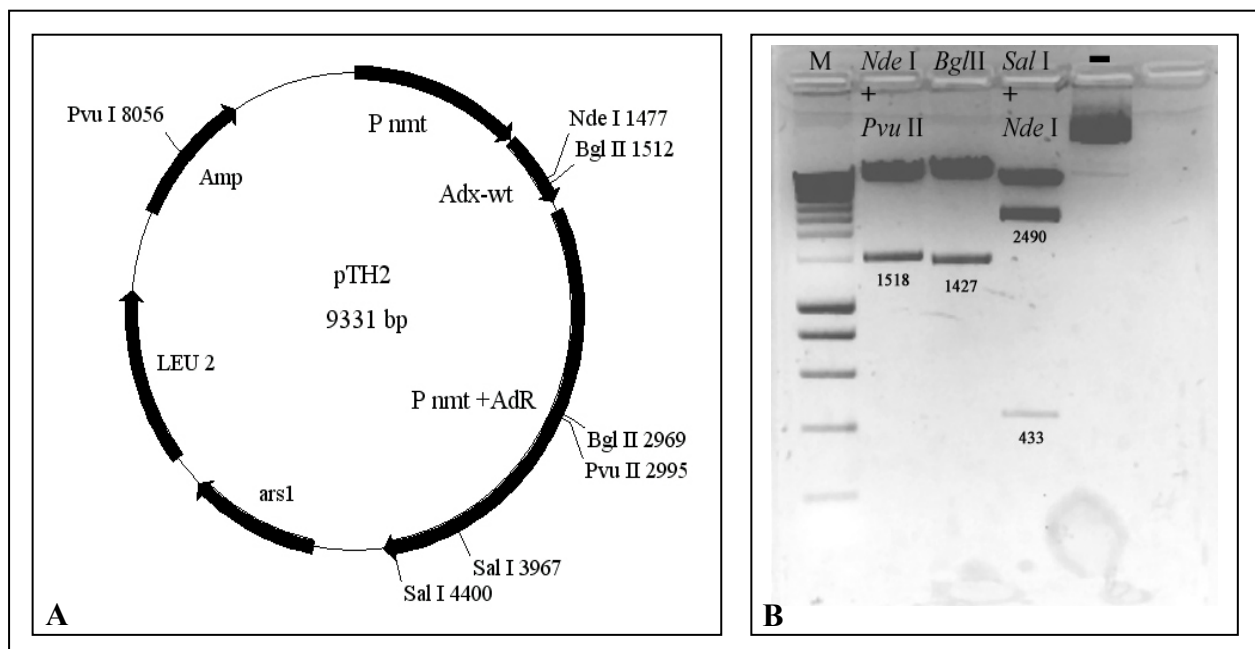


Figure 3.14. A: Vector map of pTH2. Relevant restriction sites are shown, P nmt: *nmt1* promoter. **B. Restriction analysis of pTH2 confirming the existence of the two expression cassettes.** *NdeI* and *PvuII* are unique sites that cut in Adx and AdR, respectively, whereas *Bgl II* cuts in Adx and AdR as shown. Numbers at bands indicate the theoretical sizes calculated from the pTH2 vector map.

3.2.3. Coexpression of Adx and AdR in fission yeast

The Adx expressing plasmids described in subsection 2.1.3, and the new developed plasmids pTH1 and pTH2 (Table 3.5) were then used to transform CYP11B1-expressing strains as well as the control strain 1445 as shown in Table 3.6.

Table 3.5. Fission yeast expression plasmids used in this work

Plasmid	Insert(s)	Selection marker	Reference
pNMT1-Adx ^{WT}	Adx ^{WT}	<i>LEU2</i>	(Derouet-Hümbert <i>et al.</i> 2007)
pNMT1-Adx ^{D113Y}	Adx ^{D113Y}	<i>LEU2</i>	(Derouet-Hümbert <i>et al.</i> 2007)
pNMT1-Adx ^{S112W}	Adx ^{S112W}	<i>LEU2</i>	(Derouet-Hümbert <i>et al.</i> 2007)
pTH1	AdR ^{WT}	<i>ura4</i>	(Hakki <i>et al.</i> , 2008)
pTH2	Adx ^{WT} + AdR ^{WT}	<i>LEU2</i>	(Hakki <i>et al.</i> 2008)

Table 3.6. Fission yeast strains created in this work

Name	Parental strain	Expression construct(s)	Expressed Protein(s)	Required supplement(s)
TH1	SZ1	pAT539	CYP11B1	leucine + uracil
TH2	TH1	pNMT1-Adx ^{WT}	CYP11B1 + Adx ^{WT}	uracil
TH3	TH1	pTH1	CYP11B1 + AdR ^{WT}	leucine
TH4	TH1	pNMT1-Adx ^{WT} + pTH1	CYP11B1 + Adx ^{WT} + AdR ^{WT}	none
TH6	TH1	pNMT1-Adx ^{S112W} + pTH1	CYP11B1 + Adx ^{S112W} + AdR ^{WT}	none
TH7	TH1	pNMT1-Adx ^{D113Y} + pTH1	CYP11B + Adx ^{D113Y} + AdR ^{WT}	none
TH75	SZ1	pTH2	CYP11B + Adx ^{WT} + AdR ^{WT}	none
TH175	1445	pTH2	Adx ^{WT} + AdR ^{WT}	adenine, uracil, histidine

Since the molecular mass of the Pk-tagged human AdR of 50 kDa could interfere with the very similar mass of the Pk-tagged human CYP11B1 (59 kDa), an approach was used to

confirm expression from the double cassette plasmid pTH2. A wild type *leu1⁻* fission yeast strain (1445) was transformed with pTH2 in order to eliminate the Pk signal background introduced by the CYP11B1 in SZ1. Western blot analysis using α -Pk and α -Adx antibodies to detect AdR and Adx, respectively, showed that pTH2 is able to coexpress AdR and Adx with mitochondrial localisation in fission yeast (Figure 3.15 A and B).

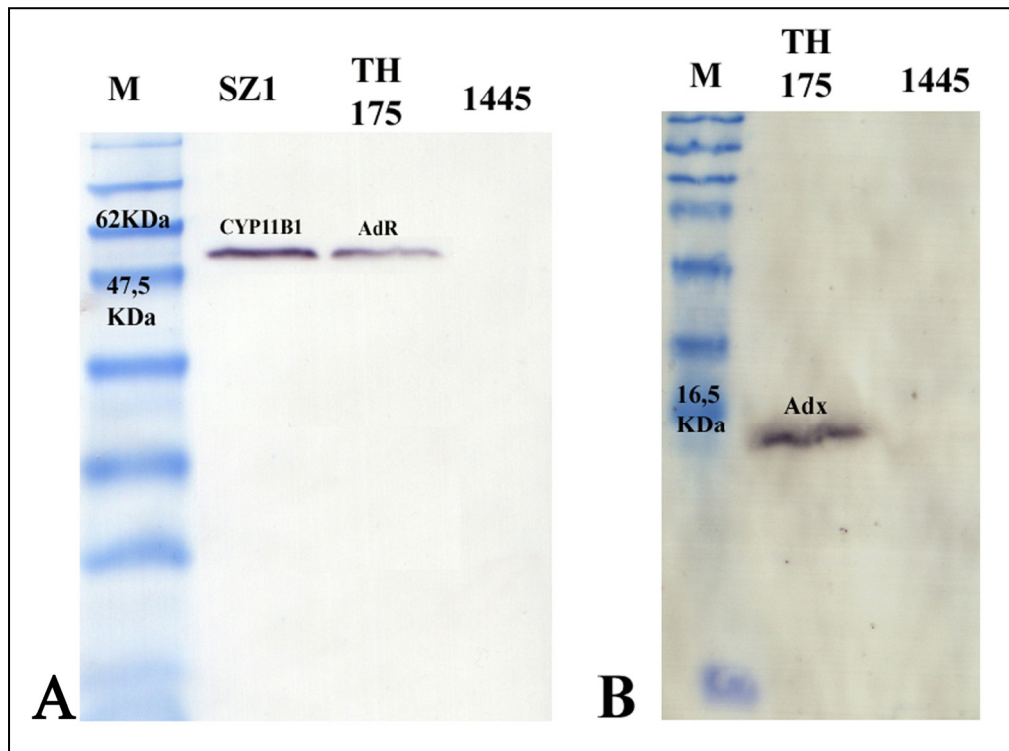


Figure 3.15. Detection of AdR^{WT} (A) and Adx^{WT} (B) in mitochondrial lysates of strain TH175 by Western blot analysis. Mitochondrial lysates of TH175 and its parental strain 1445 were separated by SDS/PAGE and blotted onto nitrocellulose membranes. Immunologic protein detection was carried out using α -Pk and α -Adx antibodies as described by materials and methods. M: Protein standard.

As expected, the signals could not be detected in the parental wild type strain 1445. The apparent molecular weight of AdR and Adx expressed from pTH2 are displayed at approximately 56 and 15 KDa and are in good agreement with the calculated masses of 50 and 13.8 KDa, respectively (Figure 3.15. A, B). For each of the Adx expressing plasmids used in this work, correct subcellular localisation of the expressed Adx in fission yeast strains was previously confirmed by Western blot analysis of mitochondrial protein lysates (Figure 3.16) (Derouet-Hümbert *et al.* 2007).

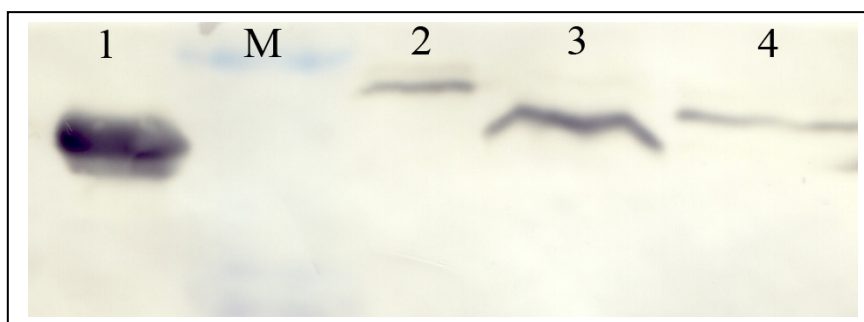


Figure 3.16. Immunological detection of adrenodoxin (Adx) expressed in *S. pombe*. Mitochondrial lysates were prepared and analyzed by SDS-PAGE and Western blot using an α -Adx antibody. Lane 1; purified mature bovine Adx (positive control), lane 2; Adx^{WT}-expressing fission yeast strain, lane 3; Adx^{S112W}-expressing fission yeast strain, lane 4; Adx^{D113Y}-expressing fission yeast strain.

Wild type of Adx (Adx^{WT}) migrates at a higher molecular weight than the positive control because it contains an additional mitochondrial localisation signal (Derouet-Hümbert *et al.* 2007). The calculated molecular weight of mutant Adx^{S112W} is lower (about 2.2 kDa) than that of Adx^{WT}, which is in good agreement with these results. Mutant Adx^{D113Y}, however, should theoretically have a slightly higher mass than Adx^{WT}, but migrates much faster during SDS-PAGE. The reason for this discrepancy is not known, but rarely other point mutations in Adx also cause a change in migration behavior during SDS-PAGE that cannot be explained by their mass difference (Hannemann, unpublished observation). Expression of the activated Adx mutants also did not lead to slower growth of the cells or to a pronounced phenotype (Derouet-Hümbert *et al.* 2007).

3.2.4. The 11 β -hydroxylation activity of CYP11B1 in the new recombinant fission yeast strains

The hydroxylation assay in the 96-well plate format developed in this work (subsection 3.1.2) was further validated. The validation was carried out to investigate the reliability of the assay. For this reason, the bioconversion efficiencies between the several wells in one plate were investigated for any differences. The test was carried out using the new fission strain TH4 with a cell density of 10⁸ cells/ml. The bioconversion was initiated by adding RSS (substrate) to give a final concentration of 100 μ M. After 24h shaking at 480 rpm and 30°C, steroids were extracted with chloroform, resolved in acetonitrile and analysed by HPLC as mentioned before in subsection 3.1.2.

Figure 3.17 below shows the bioconversion results of 66 wells. It is clearly to see that the majority of results belong to the range (Mean \pm 1.96*SD) which is an acceptable normal distribution for any measurement. Therefore, this 96-well hydroxylation assay is an efficient screening tool and can be applied to investigate the steroid hydroxylation activity in the recombinant strains developed during this work.

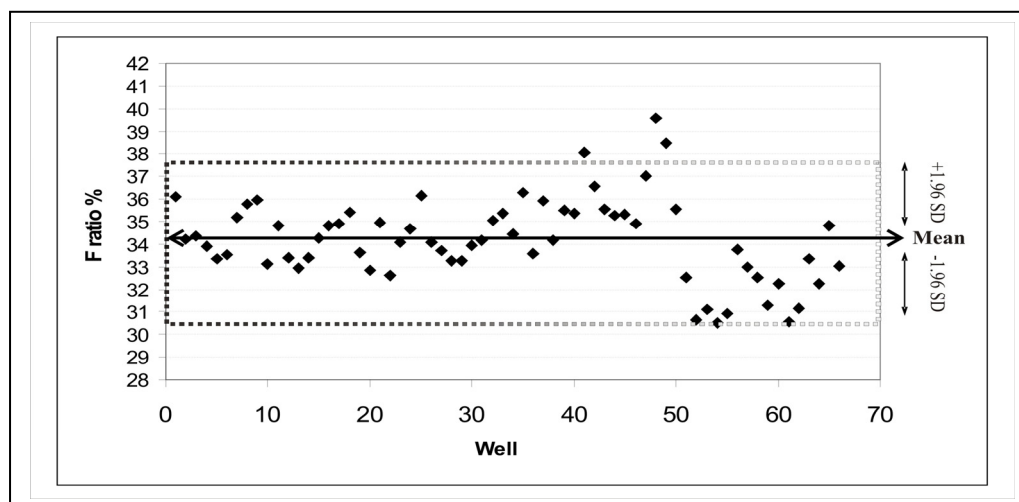


Figure 3.17. The biotransformation of RSS into F investigated in 66 wells using the newly developed hydroxylation assay.

The test was carried out in a 96-well plate using the recombinant fission yeast TH4. 66 wells were analysed and presented as hydrocortisone production ratio (F ratio).

3.2.4.1. Comparison of biotransformation activity of CYP11B1-expressing strains after coexpressing of the corresponding redox partners

To compare the activities of CYP11B1 in the newly developed fission yeast strains, the hydroxylation assay in 96-well plate format developed in this work (subsection 3.1.2) was applied. To perform the steroid hydroxylation assay, fission yeast cell suspensions with a cell density of 10^8 cells/ml were prepared. The bioconversion was initiated by adding RSS (substrate) to give a final concentration of 100 μ M. After 24h shaking at 480 rpm and 30°C, steroids were extracted with chloroform, resolved in acetonitrile and analysed by HPLC as mentioned before in subsection 3.1.2. Steroid 11 β -hydroxylation activity was investigated in all fission yeast strains, which coexpressed Adx and/or AdR and compared with the parental strain SZ1 (Figure 3.18). These experiments clearly demonstrate that coexpression of Adx^{WT} increases the biotransformation activity, with the hydrocortisone ratio increasing significantly from 12% in SZ1 to 25% in TH2 (*t*-test, *p*<0.05). As expected, 11 β -hydroxylation activity in strain TH3 (CYP11B1 + AdR) did not show any improvement over the parental strain SZ1

due to the fact that Adx plays a central role in the electron transfer chain (Figures 1.2, 4.1). A further increase in steroid hydroxylation activity could, however, be achieved in the strain TH4, which coexpresses AdR, Adx^{WT} and CYP11B1, and displays a hydrocortisone production ratio of 40%. Since it was previously shown by our group that mutants of Adx are able to stimulate 11 β -hydroxylation, I attempted to further increase the biotransformation efficiency by substituting Adx^{WT} with the Adx mutants. The first mutant chosen was Adx^{S112W}, which lacks the 16 carboxy terminal amino acids and features a terminal tryptophane, leading to enhanced affinity for the cytochrome P450 and also to a lower redox potential (-334 mV) (Schiffler *et al.* 2001). The second mutant, Adx^{D113Y}, is a full-length Adx mutant with enhanced cytochrome P450 binding ability and a slightly changed redox potential (-298 mV) (Bichet *et al.* 2007). However, as can be seen in Figure 3.18, fission yeast strains TH6 and TH7 that coexpress AdR and either Adx^{S112W} or Adx^{D113Y} did not show any improvement in the 11 β -hydroxylation activity compared with the strain TH4. Moreover, strains TH6 and TH7 even displayed a slightly lower activity than the strain TH4.

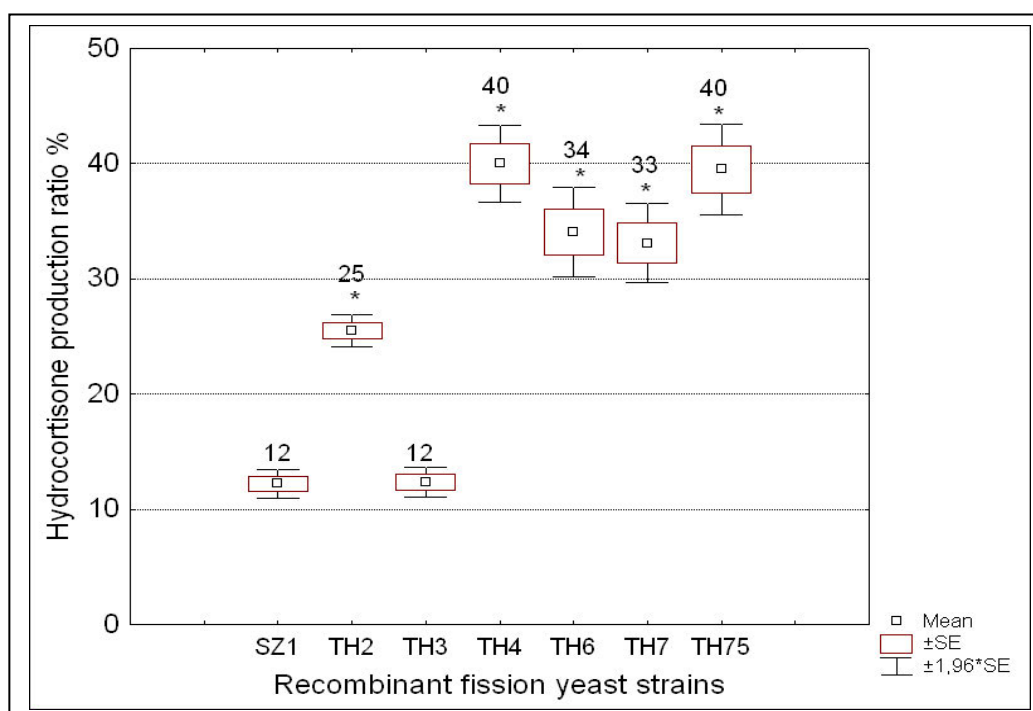


Figure 3.18. Direct comparison of the bioconversion rates of fission yeast strains coexpressing CYP11B1 and electron transfer proteins. SZ1 (CYP11B1), TH2 (CYP11B1+Adx^{WT}), TH3 (CYP11B1+AdR^{WT}), TH4 (CYP11B1+Adx^{WT}+AdR^{WT}), TH6 (CYP11B1+Adx^{S112W}+AdR^{WT}), TH7 (CYP11B1+Adx^{D113Y}+AdR^{WT}), TH75 [CYP11B1+(Adx^{WT}+AdR^{WT})]. Values were calculated from three independent experiments and are presented as mean \pm standard error of mean. Asterisks above boxes indicate a significant difference to the parental strain SZ1 (*t*-test, $p < 0.05$).

The second approach for the construction of a reconstituted CYP11B1 electron transfer chain in fission yeast involved the fusion of the Adx and the AdR expression cassettes on one

plasmid (pTH2). This approach bypasses the need for gene disruption and speeds up the process of strain generation by offering a more convenient way of adding two proteins at once. The coexpression of the wild type Adx and AdR from pTH2 in TH75 resulted in an 11 β -hydroxylation activity in the same range of the strain TH4, thereby confirming the functionality of pTH2 in fission yeast.

3.2.4.2. Quantification of hydrocortisone production in the novel strain TH75

3.2.4.2.1. Optimisation of the biotransformation parameters to achieve a high conversion rate

To achieve a high production rate of hydrocortisone using the fission yeast strain TH75, biotransformation conditions were investigated and optimised. The cell density displayed an important factor to influence the hydrocortisone production in this system, since a cell suspension from strain TH75 with a cell density of 10^9 cell/ml displayed significant higher hydrocortisone production efficiency in comparison with low-density suspensions when investigated with 1 mM RSS (Figure 3.19).

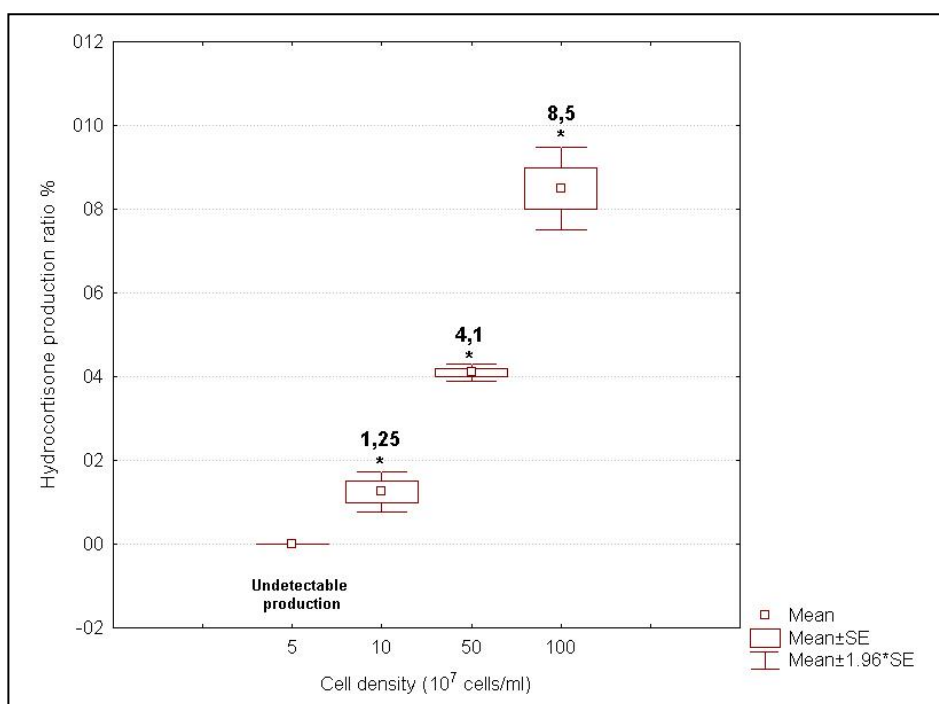


Figure 3.19. The influence of cell density of the recombinant fission yeast on the hydrocortisone production. The assay was carried out with 1 mM RSS, and different cell densities from TH75. Values were calculated from three independent experiments and are presented as mean \pm standard error of mean. Asterisks above boxes indicate a significant difference (*t*-test, $p < 0.05$).

Simultaneously increasing the substrate concentration up to 5 mM RSS increased the biotransformation efficiency, whereas 10 mM RSS displayed a negative effect and less hydrocortisone production was reported in comparison with 5 mM RSS (data not shown).

3.2.4.2.2. Hydrocortisone production efficiency in the fission yeast strain TH75

Hydrocortisone production efficiency was investigated in the new strain TH75 in comparison with the parental strain SZ1. The assay was designed to be carried out in 300-ml Erlenmeyer flasks with 10 ml assay culture under the optimal conditions (10^9 cells/ml with 5 mM RSS) reported in subsection 3.2.4.2.1. During shaking for 72 hours at 180 rpm and 30°C, samples of 500 µl were extracted with chloroform at several time points after adding DOC as an internal standard to normalize the steroid extraction efficiency. A calibration curve was used to quantify the hydrocortisone amount produced over time. The calibration curve was constructed using pure hydrocortisone and displayed a high correlation between the amount of hydrocortisone injected on the HPLC and the corresponding peak areas. Depending on the internal standard and the hydrocortisone calibration curve, a quantitative measurement was carried out, and the hydrocortisone production was investigated over time in the two fission yeast strains.

The assay demonstrated clearly that the new fission yeast strain TH75 possesses higher 11β-hydroxylation activity in comparison with the parental strain SZ1 (Figure 3.20), although no differences in the steroid extraction efficiency between the two investigated strains had occurred (Figure 3.21).

Additionally, the time course presented a steady increase in hydrocortisone production from the beginning up to maximum activity of 9.7 µmol/10ml test culture measured after 72 hours, in contrast to the parental strain that produce 3.2 µmol/10ml over the same time (Figure 3.20).

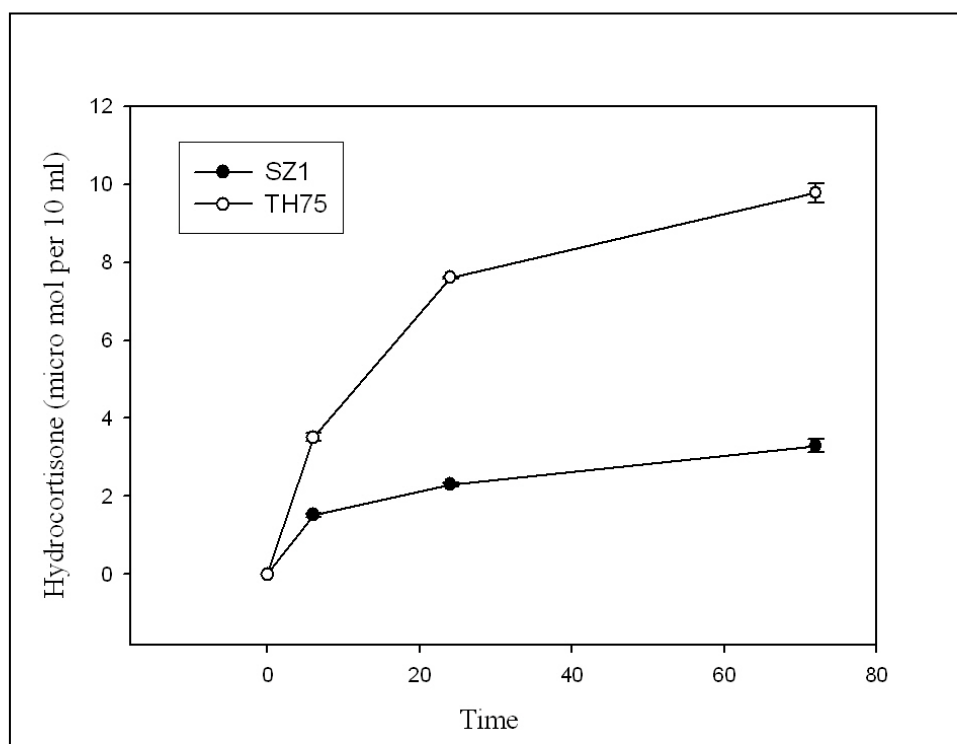


Figure 3.20. Time course of the hydrocortisone production efficiency by SZ1 (CYP11B1) and TH75 (CYP11B1 + Adx + AdR). Data shown are mean values for triplicate measurements and standard deviations are too small to be displayed. The assay was performed in 300-ml Erlenmeyer flasks with a cell density of 10^9 cells/ml with 10 ml assay culture and 5 mM RSS. During shaking for 72 hours at 180 rpm and 30°C, samples of 500 μ l were extracted with chloroform at several time points after adding DOC as an internal standard to normalize the steroid extraction efficiency.

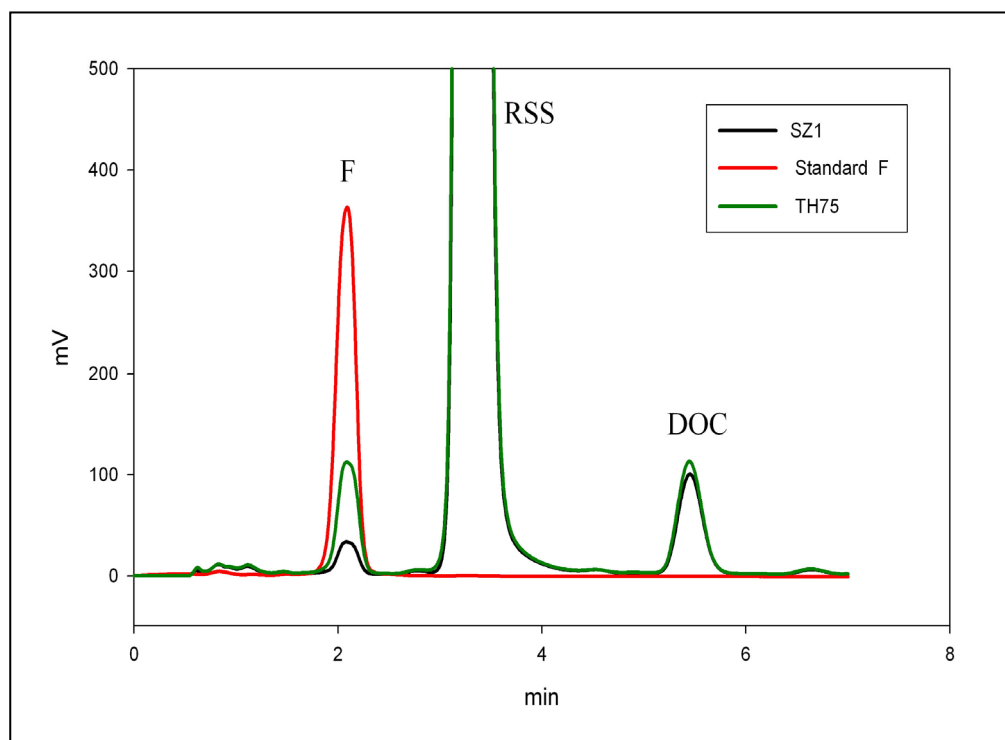


Figure 3.21. HPLC chromatograms of CYP11B1-dependent substrate conversion using the novel strain in comparison with the parental strain. Chromatograms were obtained from extracted samples after adding DOC as internal standard, black and green chromatograms represent the CYP11B1-dependent substrate conversions obtained with SZ1 and TH75 respectively, whereas the red chromatogram represents the pure hydrocortisone injected on HPLC under the same condition.

This demonstrates clearly that the 11β -hydroxylation activity in TH75 is significantly higher than in the parental strain SZ1.

3.3. Development of a cell-based high throughput screening system for the discovery of human aldosterone synthase inhibitors

In order to successfully develop and execute an efficient, rapid, and reproducible cell-based HTS assay in the field of drug discovery, one must have access to (1) automated screening technology plate-format, (2) detectable conversion and inhibition response.

3.3.1. Automated screening technology plate-format

The steroid bioconversion assay in the 96-well format established in this work (subsection 3.1.2) was adapted to develop a CYP11B2 activity screening system. Plate preparation and steroid extraction programs were applied as described before. Taken into consideration the technical limitations and the capacity of the available HPLC instrument; 192 samples (two 96-well plates) can be analysed per run, and since the HPLC parameters described in subsection 3.1.2 enable the separation of DOC and its hydroxylated products within 7 minutes (Figures 3.21, 3.22 A), the time needed to analyse 192 samples is 1344 min = 22.4 h. Hence, the HPLC parameters had to be further optimised to increase the throughput of the assay. For this reason, acetonitrile (ACN), which is more polar than methanol was used in a mixture with water as mobile phase. The new mobile phase was used to separate DOC and B and different flow velocities were investigated (Figure 3.22 B, C, D).

It is clearly shown that a mixture of ACN:H₂O (60:40) with flow velocity of 0.5 ml/min separates DOC and B within the same time that a mixture of MeOH:H₂O (60:40) needs to separate them with a higher flow velocity (1.2 ml/min). Increasing the flow velocity of ACN:H₂O mixture reduced the time needed to separate DOC and B (Figure 3.22 B, C, D).

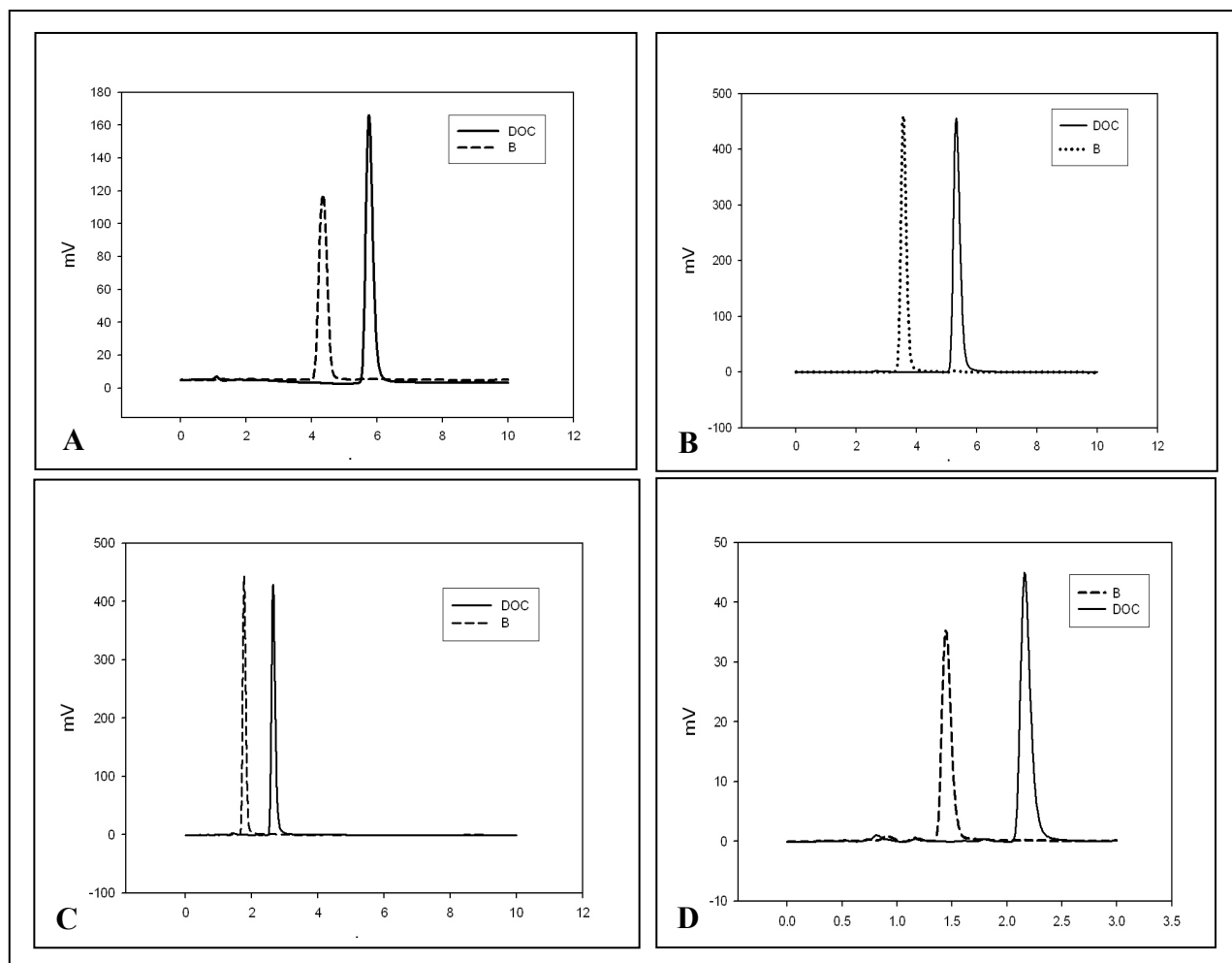


Figure 3.22. HPLC Chromatograms show the separation of DOC and B under different HPLC parameters. A; 1.2 ml/min MeOH:H₂O (60:40), B; 0.5 ml/min ACN:H₂O (60:40), C; 1 ml/min ACN:H₂O (60:40), D; 1.2 ml/min ACN:H₂O (60:40).

As a result, the mixture of ACN:H₂O (60:40) with a flow velocity of 1.2 ml/min displays an efficient separation of DOC and B within 3 min (Figure 3.22 D). This HPLC conditions (Table 3.7) decreased the time needed to analyse 196 samples from 22.4 h to 9.6 h, which increases the throughput of the HPLC by more than 2-fold.

Table 3.7. Optimised HPLC parameters to separate DOC and B within 3 min

Mobile phase	ACN:H ₂ O (60:40)
Flow velocity	1.2 ml/min
Column temperature	25 °C
Time per sample	3 min

3.3.2. Optimisation of the screening assay parameters to get detectable conversion/inhibition response

In order to get reproducible conversion/inhibition response using a whole-cell-based assay, several parameters should be taken into consideration and optimised to achieve a reliable screening assay. These parameters include the amount of enzyme, substrate concentration, incubation time and the optimal test medium needed to get reproducible conversion and inhibition. For this reason, and in order to estimate the optimal conditions where reproducible screening can be performed, the CYP11B2-expressing *S. pombe* strain MB164 was used to investigate the parameters mentioned above. Moreover, this strain has already been used to test compounds for their CYP11B2 inhibitory effect and several compounds were identified to inhibit CYP11B2 in recombinant fission yeast with different IC₅₀ values (Table 3.8).

Table 3.8. The IC₅₀ values of CYP11B2 inhibitors determined using recombinant *S. pombe* strain MB164 (Bureik *et al.* 2004)

Compound	IC ₅₀ against CYP11B2
Clotrimazole	0.20 µM
Ketoconazole	3.50 µM
Miconazole	5.60 µM

As addressed below, several optimisation steps were carried out in the presence of the known inhibitors of CYP11B2 (Table 3.8) as positive controls, in addition to mock-treated control. The starting point was the setting of assay time (duration of incubation) needed to get detectable conversion and inhibition. Hence, three hours incubation was suggested for the conversion of DOC into B and for the detection of a possible inhibition. For this reason, 600

μl cell suspension from MB164 with cell density of 10^8 cell/ml was investigated with different concentrations of substrate and inhibitors. Furthermore, different test media were also investigated to estimate the optimal environment to get reproducible detection and inhibition in the presence of negative and positive controls.

- **Substrate concentration**

Although $100\ \mu\text{M}$ substrate concentration described in subsection 3.1.2 displayed detectable conversion of DOC into B, no inhibition response was observed after incubation with even high concentrations of the well-known inhibitors of CYP11B2 (ketoconazole, clotrimazole). For this reason, the substrate concentration had to be reduced to a minimal level where detectable conversion and inhibition can take place and can be followed in the screening system. The investigation showed that $5\ \mu\text{M}$ DOC is a minimal concentration that gives detectable conversion of DOC into B (Figure 3.23). Hence, the test will be carried out with $5\ \mu\text{M}$ DOC as substrate. In a next step, the inhibitor concentration must be estimated to get reproducible inhibition in the present of the CYP11B2 inhibitors.

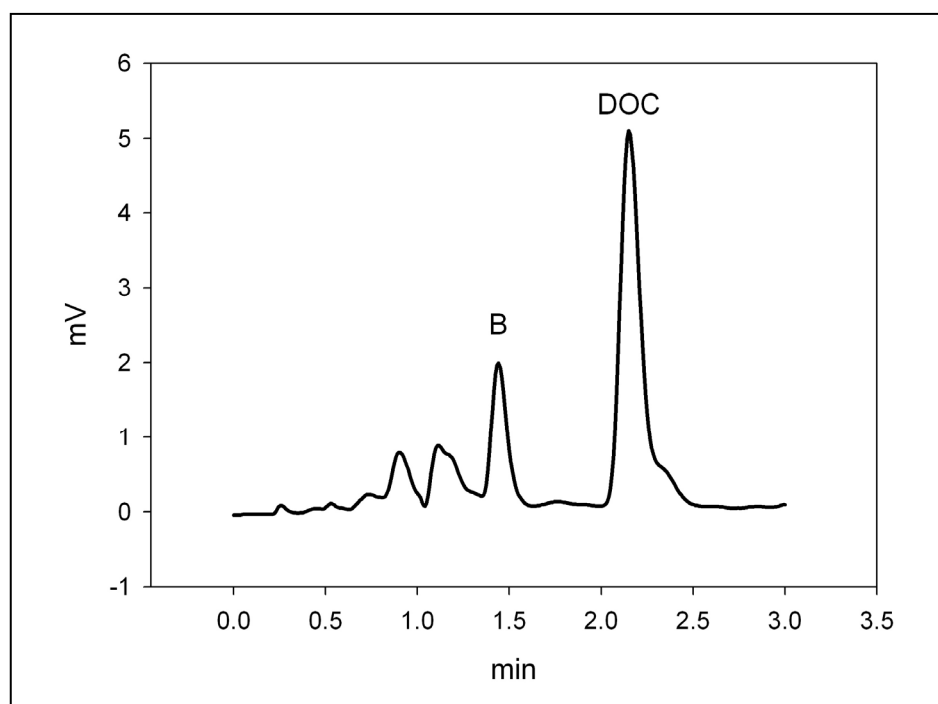


Figure 3.23. HPLC chromatogram of the CYP11B2-dependent bioconversion using the 96-well plate format.

The bioconversion was carried out in a 96-well plate using the CYP11B2-expressing fission yeast strain MB164 incubated with $5\ \mu\text{M}$ Doc for three hours. Steroid extraction was carried out with chloroform using the pipetting robot as described before (see subsection 3.1.2).

- **Inhibitor concentration**

To estimate the inhibitor concentration that has to be applied in the screening system, the inhibition profile of the CYP11B2 inhibitor ketoconazole was investigated in different test media. Although fission yeast cells used for each bioconversion assay in this work are prepared from a main culture, in which we expect that the cells achieved the stationary phase, performing the bioconversion/inhibition assay in fresh growth medium can give the cells the opportunity to grow and to use the fresh added glucose, which could influence the inhibition profile of the inhibitor during the assay. Hence, the aim of this part of work was to investigate the influence of different test media on the inhibition profile of ketoconazole, and the correlation between the concentration of inhibitor and inhibition.

Fission yeast strain MB164 with cell density of 10^8 cells/ml was incubated in a 96-well plate with 5 μ M substrate (DOC). Ketoconazole was added to achieve final concentrations in the range from 5 to 60 μ M. Different test media including EMM, simple potassium phosphate buffer (50 mM) with different pH values (5.8, 7, 7.4) were investigated. After three hours incubation, steroid extraction and subsequent HPLC measurements were carried out as described before. The ketoconazole inhibition profile in EMM showed bad correlation between the inhibitor concentration and inhibition ($r = 0.548$). Furthermore, unexplained activation was observed with 5, 10, and 40 μ M ketoconazole (Figure 3.24 A). This result shows clearly that the inhibition profile of ketoconazole in EMM is not reliable to perform reproducible screenings under our test condition since the correlation between the inhibitor concentrations and inhibition is very low (Figure 3.24 A). In contrast, it is clearly shown that the inhibition profile of ketoconazole displays better correlation between inhibitor concentration and inhibition when the test is performed in a simple phosphate buffer (Figure 3.24 B, C, D). Although high correlations were observed in the different pH-variants of the simple buffer, the physiological pH (7.4) will be used as test medium to develop the screening assay during this work.

As mentioned before; the use of multiple-concentrations assay at early (screening) stages of drug discovery is very time- and resource-intensive, and when conducting the CYP11B2-inhibition assay in a high-throughput format to support early drug discovery, inaccuracies in IC_{50} values determination are less problematic, because we are trying to quickly identify strong inhibitors, and we are less concerned with minor inhibition. Furthermore, in the early stages of drug development, before the *in vivo* pharmacokinetics and pharmacodynamics are

known, CYP inhibition assay results are often interpreted in board terms and used to classify compounds into three categories as potent, moderate or weak inhibitors (Lin *et al.*, 2007).

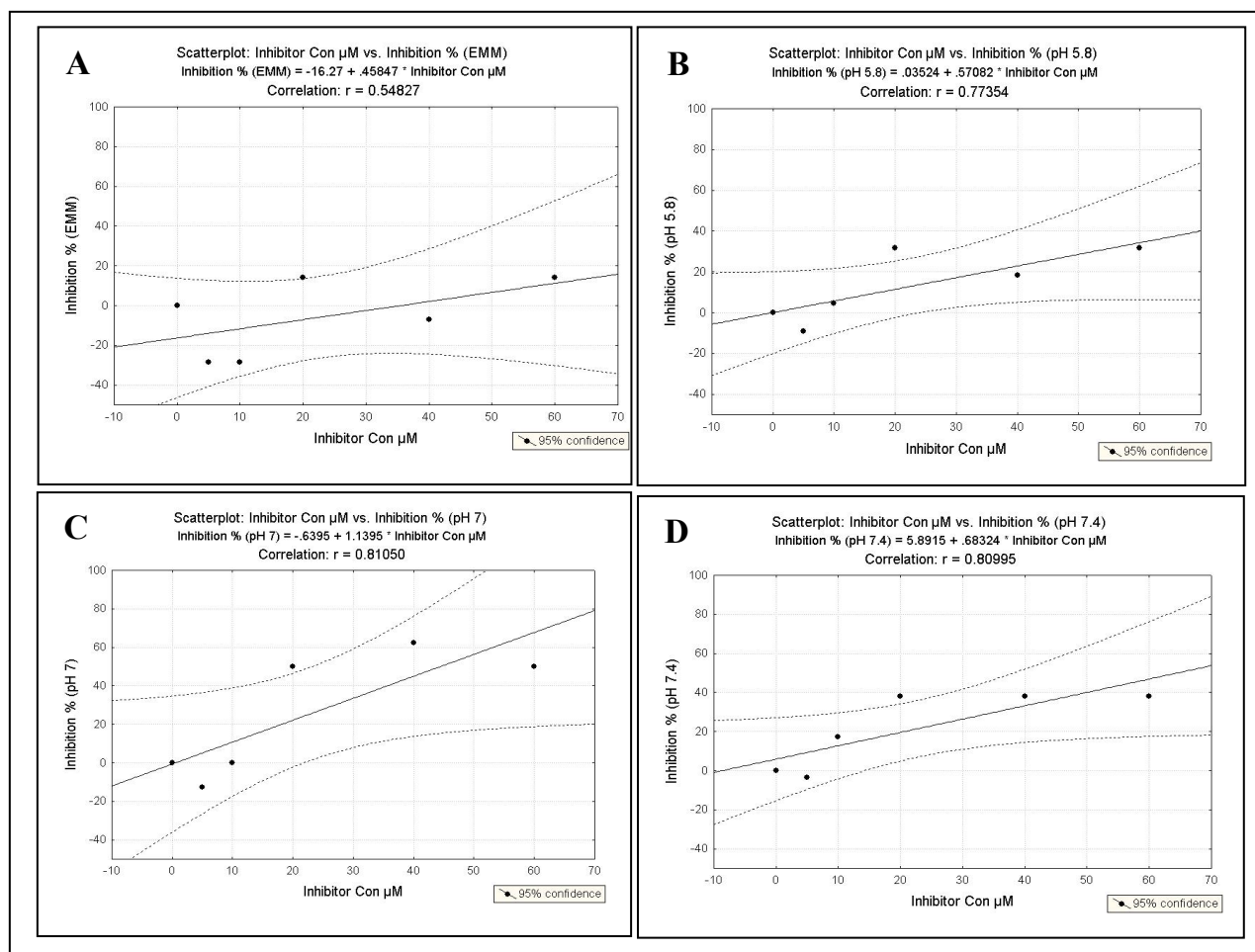


Figure 3.24. Correlation between the concentration of ketoconazole and inhibition in different test media. (A; EMM) [B, C, D; Potassium phosphate buffer 50 mM (B; pH 5.8), (C; pH 7), (D; pH 7.4)].

Therefore, the aim of this part of work was the development of a one-point method to estimate the CYP11B2 inhibitory profile. Bureik *et al.* reported the high inhibition effect of clotrimazole and ketoconazole against the expressed CYP11B2 in recombinant fission yeast, with IC_{50} values of $0.20 \mu\text{M}$ and $3.50 \mu\text{M}$, respectively, whereas miconazole was reported to inhibit CYP11B2 with a relatively higher IC_{50} value of $5.6 \mu\text{M}$ and to be a less potent inhibitor of CYP11B2 (Bureik *et al.* 2004). These observations enable the classification of these known inhibitors of CYP11B2 into two groups; potent inhibitors (clotrimazole and ketoconazole), and less potent inhibitors (miconazole).

To develop a one-point assay, a concentration of $41.6 \mu\text{M}$ ($10 \mu\text{l}$ from a 2.5 mM stock solution) of each inhibitor was tested under the conditions established above. A cell suspension from MB164 with a cell density of 10^8 cells/ml and final volume of $600 \mu\text{l}$ was

incubated in a 96-well plate in potassium phosphate buffer (50 mM, pH 7.4) as test medium with 5 μM DOC as substrate. In addition to DMSO-mock treated samples; ketoconazole, clotrimazole and miconazole were added to achieve final concentrations of 41.6 μM (10 μl from 2.5 mM stock solutions in DMSO). After three hours incubation, steroid extraction and subsequent HPLC measurement were carried out as described before.

The CYP11B2 inhibitors displayed different inhibition profiles during this test. The mock-treated samples (DMSO) displayed CYP11B2 activity with B production ratio of 11.5 %, whereas the presence of miconazole decreased the CYP11B2 activity and B production ratio to 6.5 % showing 44 % inhibition. Furthermore, clotrimazole or ketoconazole displayed total inhibition (100 %) of CYP11B2 under the test conditions (Figure 3.25).

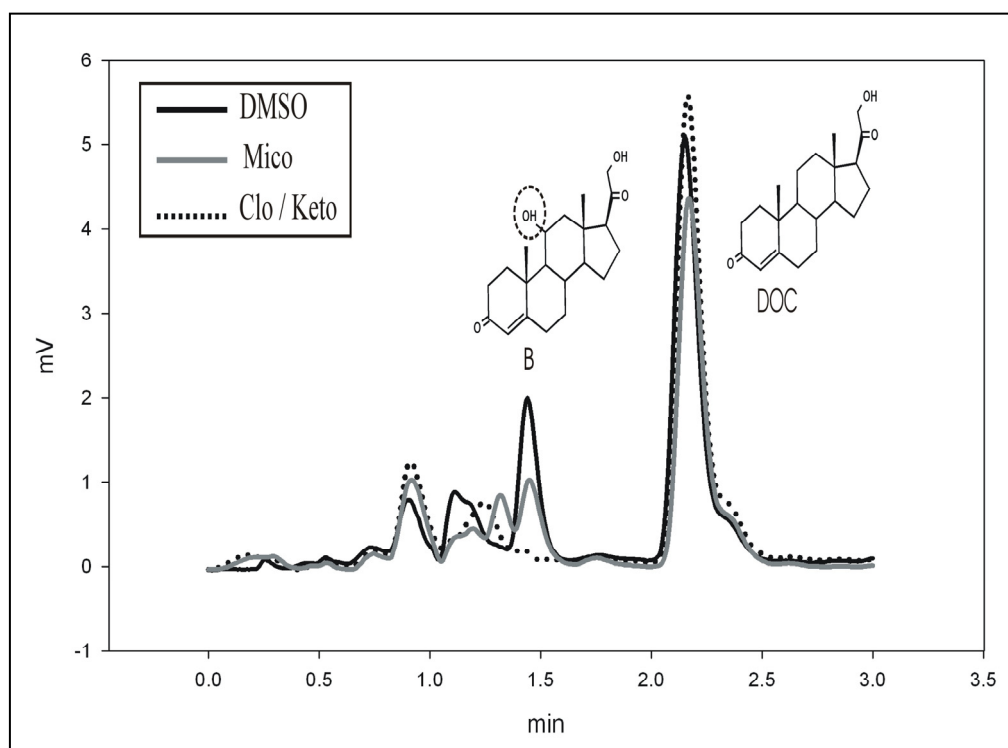


Figure 3.25. HPLC Chromatograms of the CYP11B2-dependent conversion of DOC into B using MB164 in the presence of positive and negative controls. The presence of clotrimazole (Clo) or ketoconazole (Keto) causes total inhibition of CYP11B2, whereas the less potent inhibitor miconazole (Mico) inhibits partially CYP11B2 under these test conditions.

These results confirm clotrimazole/ketoconazole and miconazole as potent and less potent inhibitors of CYP11B2, respectively. Moreover, these observations display a significant and logical correlation between the multiple-point assay reported before (Bureik *et al.* 2004) and the one-point assay developed in this work. Hence, and since clotrimazole/ketoconazole display total inhibition of CYP11B2 under these test conditions, each compound with similar

inhibition profile will be defined during the screening assay as clotrimazole-like inhibitor of CYP11B2, whereas compounds with less inhibition effect resembling the miconazole effect will be defined as miconazole-like inhibitors.

3.3.3. Proof of principle

For the validation of the newly developed screening system, a library of pharmacologically active compounds (LOPAC) was investigated as kindly provided by Prof. Herbert Waldmann (Max-Planck-Institute of Molecular Physiology, Dortmund, Germany). For controls, entire DMSO-treated and positive controls wells were incorporated in each plate (Figure 3.26) in order to have a kind of internal quality control along the screening process, and to enable the interpretation of results.

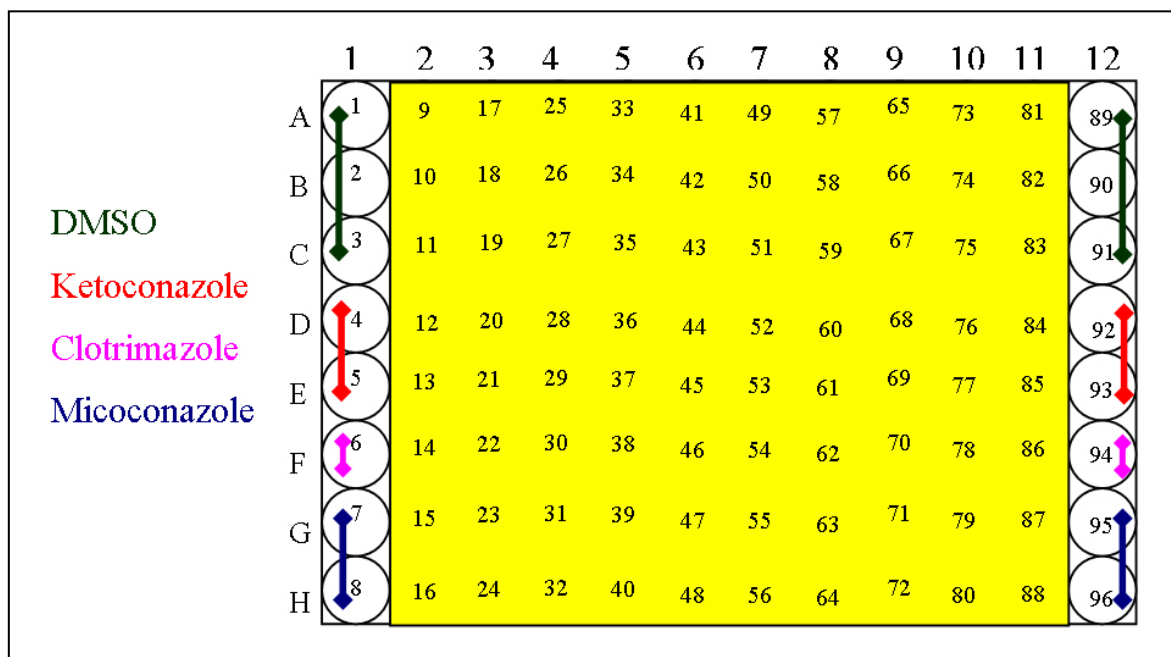


Figure 3.26. Schematic overview of the 96-well plate during the screening assay of the investigated library (LOPAC). The yellow area presents the wells with the investigated compounds (one compound per well); 2.5 mM of stock solution of the individual compounds was prepared in DMSO to be tested at once per plate. Furthermore, mock-treated wells (DMSO) and well-known inhibitors of CYP11B2 as positive controls were incorporated in each plate as shown in the Figure.

Moreover, further optimisation was carried out in order to increase the throughput of the HPLC system. This was achieved by using a 70 mm high-speed column packed with 3 μ m counterparts (reversed NUCLEODUR 100-3 C18) from MACHEREY-NAGEL (Düren, Germany). This column is shorter than the one mentioned by Materials and Methods, which decrease the time of separation whereas the smaller particles size packing allows the use of this short column for rapid separation without loss of resolution. This column decreased the

HPLC time needed to separate DOC and B from 3 min to 1.6 min per each sample (Figure 3.27) under the HPLC parameters mentioned in Table 3.7. This optimisation increased further the throughput of the HPLC and, as a result, the throughput of the developed screening system by 2-fold. An additional benefit in this rapid resolution column is the remarkable reduction of solvent consumption.

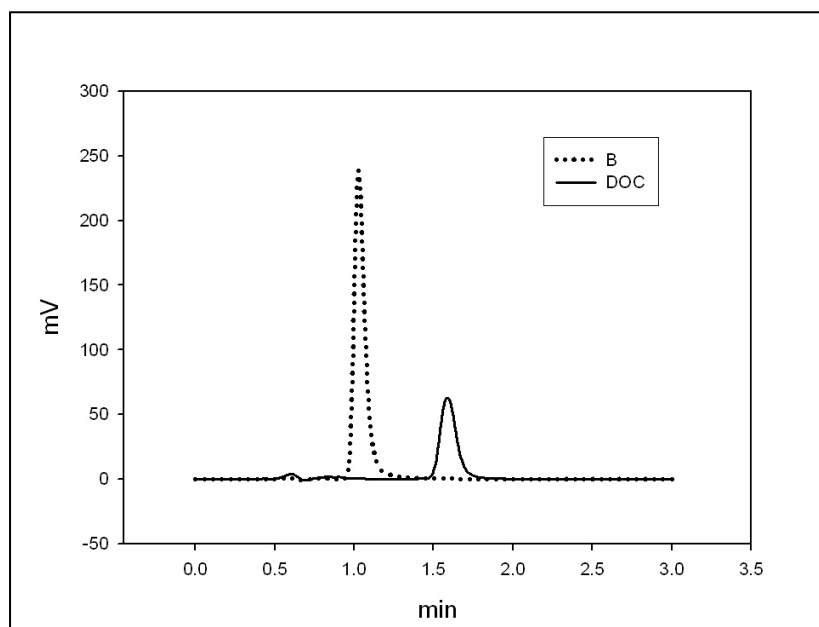


Figure 3.27. HPLC chromatograms show the separation of DOC and B using a high-speed column.

The HPLC separation was performed using pure steroids and the HPLC parameters mentioned in Table 3.7. The separation of DOC and B was done within 1.6 min, which increases the throughput of the HPLC system.

Cells from a main culture of MB164 were washed with EMM, centrifuged (3×10^3 g, 5 min, 4°C) and resuspended in 50 mM potassium phosphate buffer (pH 7.4) to cell density of 10^8 cells/ml with final volume of 600 μl of cell suspension per well. All assay steps were carried out using the pipetting robot Tecan. The assay was initiated by adding 10 μl from a 2.5mM stock solution of the investigated compound to give a final concentration of 41.66 μM . After 20 min shaking at 480 rpm and 30°C , the substrate (DOC) was added to give a final concentration of 5 μM (10 μl from a 0.3 mM stock solution in DMSO). Once again, the assay plate was shaken at 480 rpm and 30°C for three hours the steroids were extracted with chloroform using the extraction program mentioned in subsection 3.1.2 and dried under vacuum. The dried steroids were then dissolved in acetonitril and analysed by HPLC using the high-speed column mentioned above and the HPLC parameters described in Table 3.7.

Figure 3.28 below shows the HPLC separation of the CYP11B2-dependent bioconversion of DOC into B analysed using the high-speed column mentioned above. In contrast to Figure

3.27, the HPLC chromatogram in Figure 3.28 displays an unknown peak with retention time of 0.6 min. This peak was also detected when a 500 μ l water mixed with 20 μ l DMSO was extracted with chloroform and analysed with HPLC under the same condition (Figure 3.29).

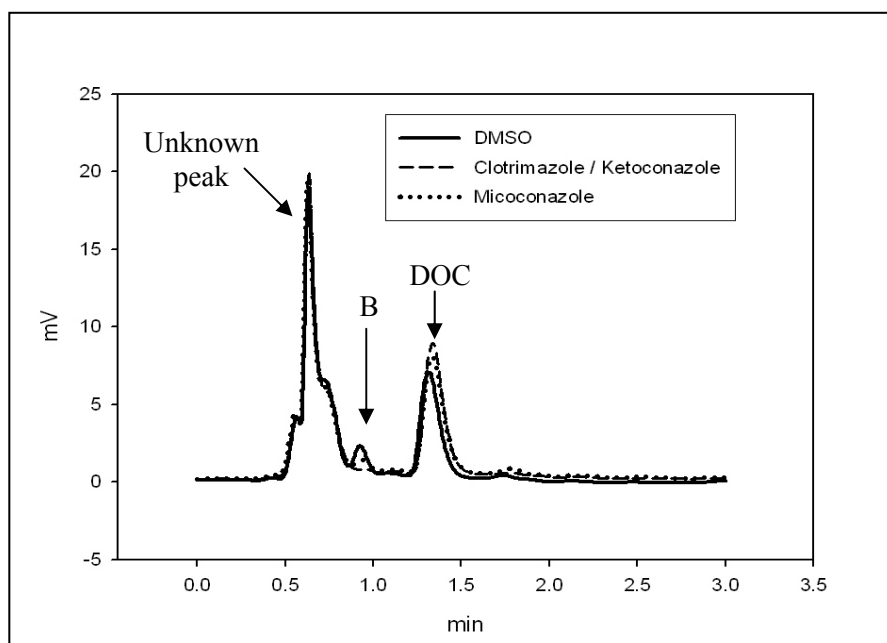


Figure 3.28. HPLC Chromatograms of the CYP11B2-dependent bioconversion of DOC into B analysed using the high-speed column. The bioconversion was carried out as described before using fission yeast strain MB164 in the presence of positive and negative controls. Unknown peak with retention time of 0.6 min was observed.

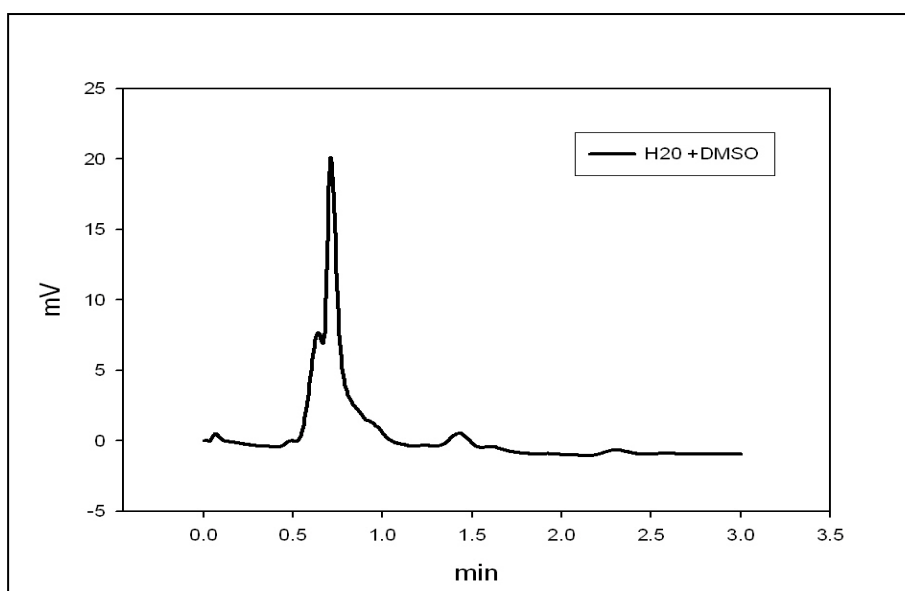


Figure 3.29. HPLC chromatogram of an extracted sample that consists of water and DMSO.

The chromatogram shows that the unknown peak reported in Figure 3.28 is a medium noise peak. This noise peak is obviously better separated using this high-speed column in comparison with the long column mentioned above by Materials and Methods.

The results of controls obtained from 32 independent assays using the one-point assay (41.6 μM) displayed reproducible results, and were statistically analysed using *t*-test ($p < 0.05$). The mock-treated samples (DMSO) displayed CYP11B2 activity with B production ratio of 11.5%, whereas the presence of miconazole decreased significantly ($p < 0.05$) the activity of CYP11B2 and B production ratio to 6.5% showing 44 % inhibition under our test condition. Furthermore, the presence of either clotrimazole or ketoconazole displayed total inhibition of CYP11B2 (100%) (Figure 3.30, Table 3.9).

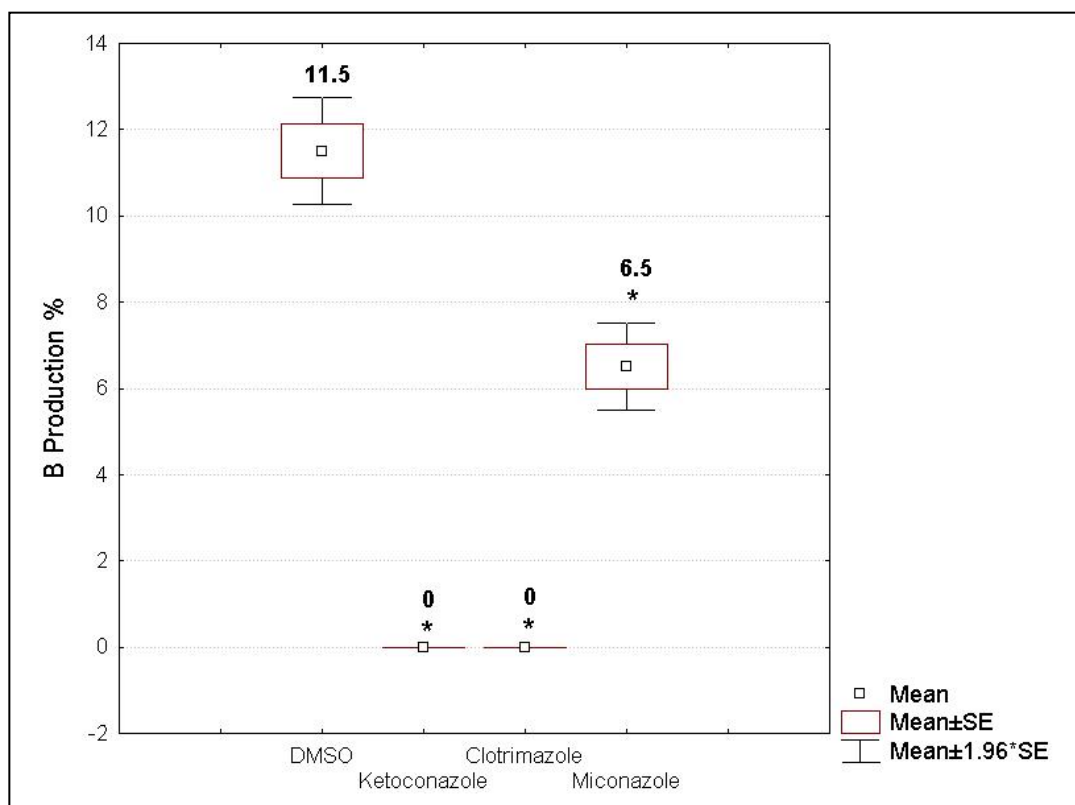


Figure 3.30 Direct comparisons of the CYP11B2-dependent conversion rates of DOC into B during the screening assay. Values were calculated from 32 independent experiments and are presented as mean \pm standard error of mean. Asterisks above boxes indicate a significant difference to the mock treated sample (DMSO) (*t*-test, $p < 0.05$).

Table 3.9. The inhibition profiles of the CYP11B2 inhibitors tested using the six-point inhibition assay and the one-point assay developed in this work

Compound	IC ₅₀ against CYP11B2 (μM) ^a	B ratio (%) ^b	Inhibition (%) ^b
Clotrimazole	0.20	0	100
Ketoconazole	3.50	0	100
Miconazole	5.60	6.5	44

^a(Bureik *et al.* 2004)

^b This work

The Z' -factor of the screening system was determined from the inhibition assay for clotrimazole, ketoconazole and miconazole as positive controls and DMSO as negative control. The Z' -factor was calculated using the formula mentioned in subsection 2.2.6.2.3.

The screening assay gave a Z' -factor of 1.0 for clotrimazole, 1.0 for ketoconazole and 0.85 for miconazole, showing that the screening system is robust.

In a next step, the LOPAC library was tested on triplicate. Additionally to ketoconazole, clotrimazole already supplied in the library, the screening assay reported two clotrimazole-like inhibitors (e.g. Compound Co_TH1, Figure 3.31), whereas nine compounds were defined regarding to our definition as miconazole-like inhibitors (Table 3.10, Figure 3.32).

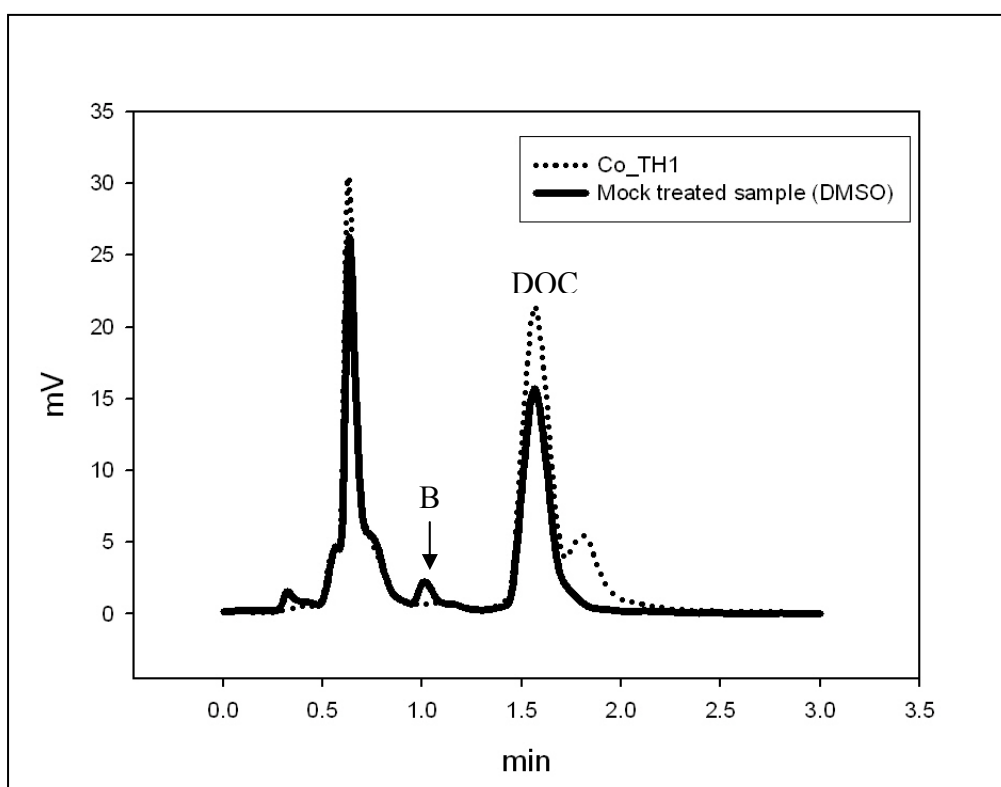


Figure 3.31. HPLC chromatograms of CYP11B2-dependent bioconversion in the presence of Co_TH1 during the screening assay.

Compound Co_TH1 displayed total inhibition of CYP11B2 under the test conditions. For this reason, Co_TH1 can be defined as clotrimazole-like inhibitor of CYP11B2.

Table 3.10. The new CYP11B2 inhibitors identified during the screening assay in this work

Compound code in this work	Compound code by SIGMA®	Name	Screening assay result	Description
Co_TH1	A5791	4-Androsten-4-ol-3,17-dione	Clotrimazole-like inhibitor	Aromatase inhibitor
Co_TH2	A9630	4-Androstene-3,17-dione	Miconazole-like inhibitor	Testosterone precursor and metabolite with androgenic activity
Co_TH3	C3635	DL-p-Chlorophenylalanine methyl ester hydrochloride	Miconazole-like inhibitor	Tryptophan hydroxylase inhibitor
Co_TH4	E3380	Ellipticine	Miconazole-like inhibitor	Cytochrome P450 (CYP1A1) and DNA topoisomerase II inhibitor
Co_TH5	I0782	Imazodan	Miconazole-like inhibitor	Selective phosphodiesterase II (PDEII) inhibitor
Co_TH6	L3791	Lamotrigine	Miconazole-like inhibitor	Anticonvulsant
Co_TH7	V1889	VER-3323 hemifumarate salt	Miconazole-like inhibitor	5-HT _{2C} /5-HT _{2B} serotonin receptor agonist.
Co_TH8	L131	L-745,870 hydrochloride	Miconazole-like inhibitor	Selective D ₄ dopamine receptor antagonist
Co_TH9	P6777	Phenelzine sulfate salt	Miconazole-like inhibitor	Non-selective MAO-A/B inhibitor
Co_TH10	P8765	Ammonium pyrrolidinedithiocarbamate	Miconazole-like inhibitor	Prevents induction of nitric oxide synthase (NOS) by inhibiting translation of NOS mRNA
Co_TH11	T7313	1-[2-(Trifluoromethyl)phenyl]imidazole	Clotrimazole-like inhibitor	Potent nitric oxide synthase (NOS) inhibitor

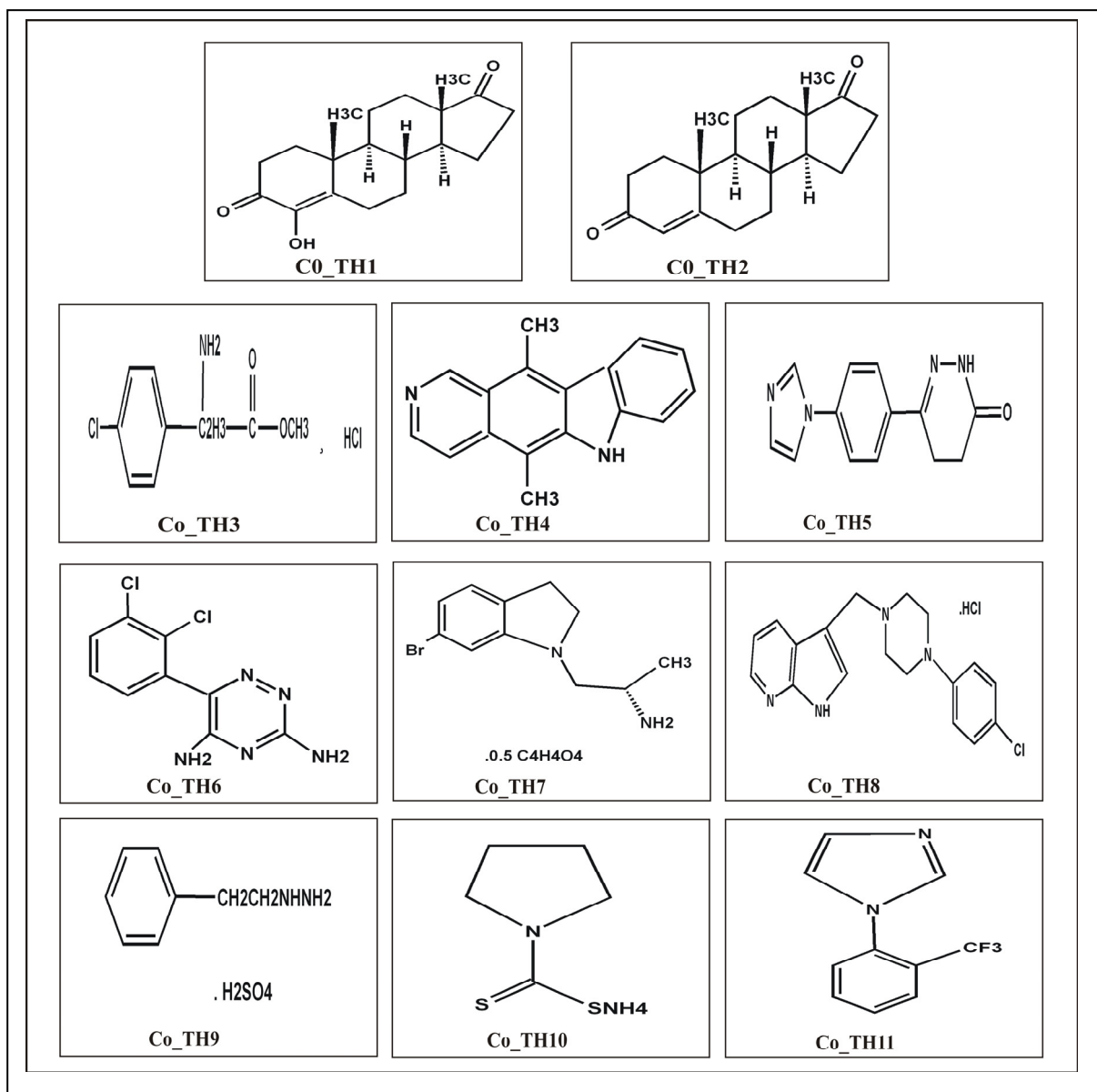


Figure 3.32. Structures of the new CYP11B2 inhibitors identified during the screening assay in this work.

Although fission yeast *S. pombe* has a cell wall, which could disable the transport of the investigated compound to the cell in the fission yeast test system, the new screening system reported in addition to ketoconazole, clotrimazole and miconazole eleven potential inhibitors of CYP11B2. These observations demonstrate clearly that these 14 compounds could pass the cell wall since they inhibited the mitochondria-localised CYP11B2 in the recombinant fission yeast although they have different molecular weight values (Figure 3.33). For this reason, it is clearly to say that the cell wall of fission yeast does not form any disadvantages in the fission yeast test system.

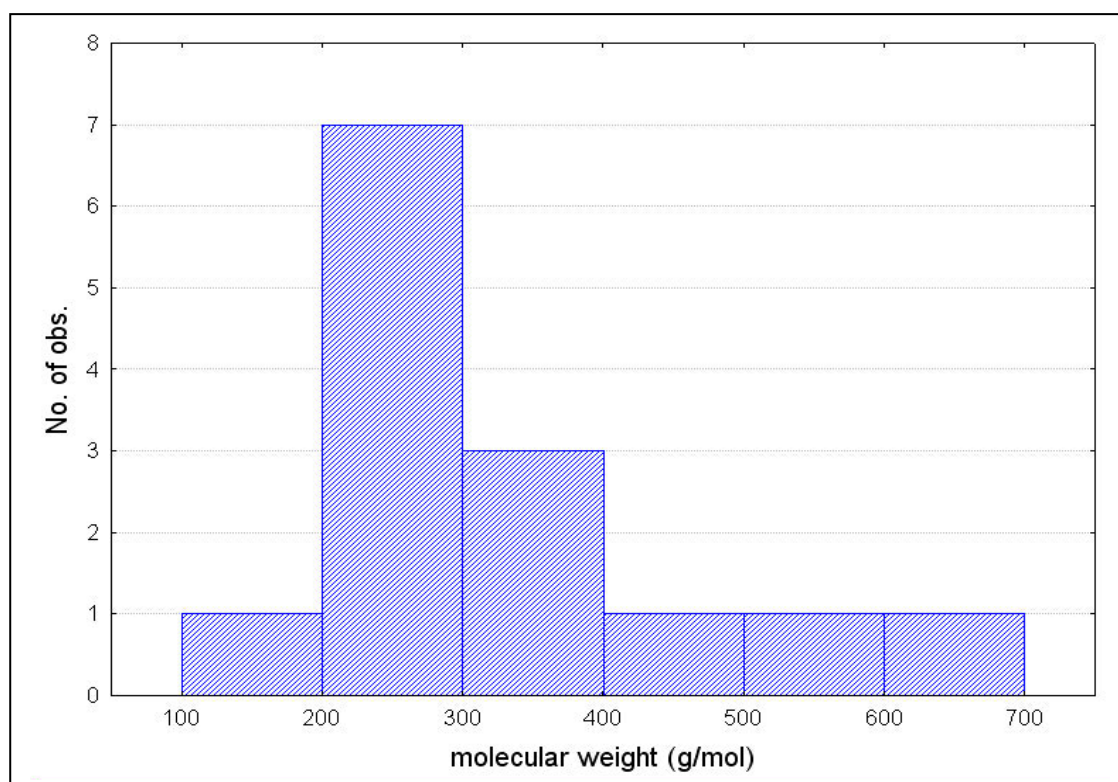


Figure 3.33. Distributions graph of the new inhibitors of CYP11B2 vs. their molecular weight.

3.3.4. Validation of the new CYP11B2 inhibitors identified during the screening assay

The potential inhibitors of CYP11B2 identified during the screening system (Table 3.10, Figure 3.32) were defined as active compounds (“hits”) and selected for further validation on the basis of commercial availability and clinical interest.

3.3.4.1. Toxicity in fission yeast

Since, the screening assay is an inhibition assay; further investigations had to be done to investigate if the detected inhibition is due to the inhibitory effect and not to the toxicity of the compound.

After incubation of fission yeast cultures with the different “hits” under the same conditions like in the screening assay, no morphological changes were observed (colour and shape). Moreover, a cell viability assay was carried out, and no significant changes ($p < 0.05$) were observed in comparison with mock-treated samples (Figure 3.34).

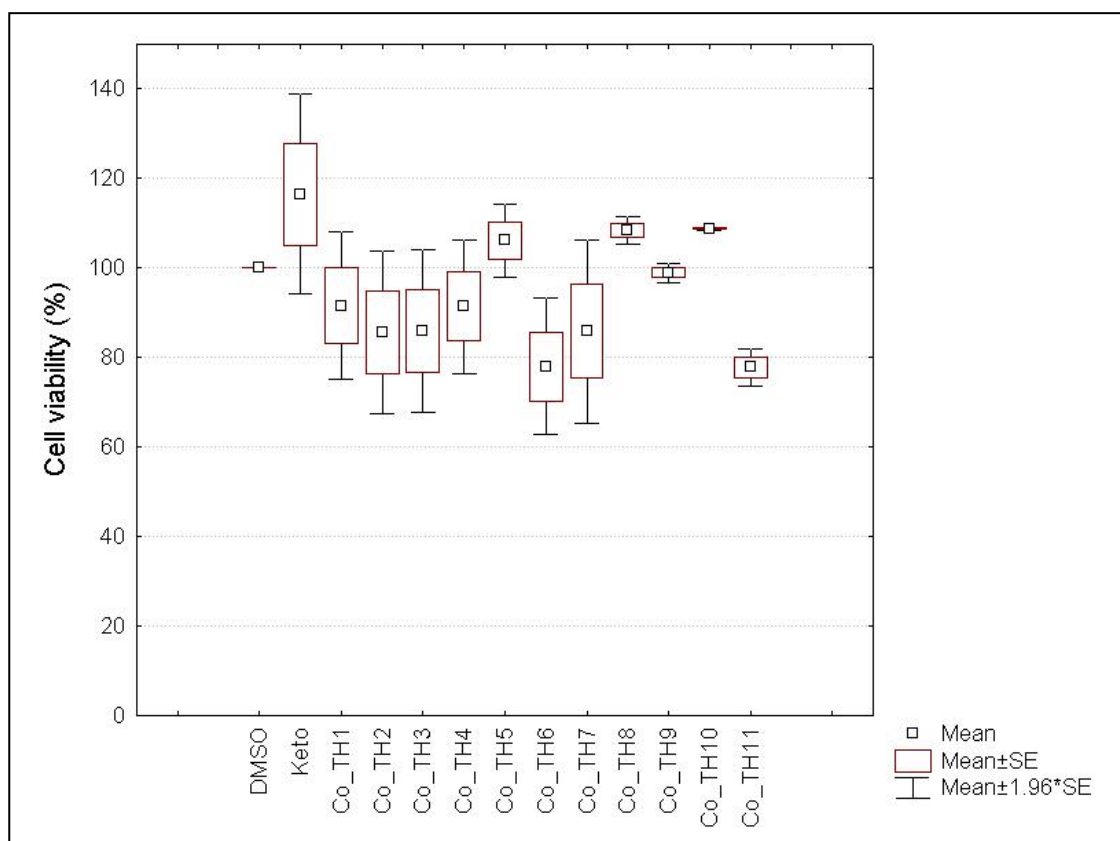


Figure 3.34. Cell viability shown as a percentage of negative control (DMSO).

The fission yeast cultures were incubated with 41.6 μM from each hit under the same condition like in the screening assay. Diluted samples were taken and plated on the desired plates. Colonies were calculated after 48 hours incubation at 30°C. Each *bar* represents the average of triplicate data points.

Although some compounds displayed less cell viabilities in comparison with the negative control, no significant differences were reported (*t*-test, $p < 0.05$). This result displays clearly that the “hits” are not toxic against the fission yeast cells during the screening assay. Hence, the detected inhibition is due to the inhibitory effect of these compounds under the test conditions. Further validation had to be done to investigate the selectivity of these compounds and to calculate the IC_{50} values against CYP11B2 and CYP11B1.

3.3.4.2. Determination of the IC_{50} values against CYP11B2 and CYP11B1

For the determination of the IC_{50} values, the six-point method described previously (Bureik *et al.* 2004) was applied. This radioactive assay possesses high sensitivity to test the effect of the compound of interest in low concentration ranges (100 nM – 25 μM) to determine the IC_{50} value in the presence of 100 nM substrate. This low concentration of the substrate does not allow a detectable bioconversion using HPLC, giving the radioactive method the advantage to perform the assay with low concentrations to determine the IC_{50} value. For this reason, fission yeast strains SZ1 and MB164 expressing human CYP11B1 and CYP11B2, respectively, were

used to perform the assay in the tip-tube format as described in subsection (2.2.4.2). The potassium phosphate buffer 50 mM (pH 7.4) was used as test medium, and the “hits” were tested with final concentrations ranging from 100 nM to 25 μ M. Radioactive substrate was applied to detect the steroid conversion and inhibition with a final concentration of 100 nM. Clotrimazole with 25 μ M was applied as positive control during the assay.

Repeated steroid hydroxylation measurements with both CYP11B2- or CYP11B1-expressing fission yeast systems, were carried out, and only highly correlative data sets ($R^2 > 0.75$) were used for the determination of the IC_{50} values. Comparing the inhibitor’s effect on the two enzymes using identical conditions is an appropriate strategy to evaluate their selectivity (Bureik *et al.* 2004). In this way, it was possible to identify highly selective inhibitors of CYP11B2 (Table 3.11).

Table 3.11. The inhibition profiles of the active compounds against CYP11B2 and CYP11B1 in the validation assay

Compound code *	Name	Validation assay	
		CYP11B2	CYP11B1
Co_TH1	4-Androsten-4-ol-3,17-dione	$IC_{50} = 2.4 \mu\text{M}$ $R^2 = 0.92$	-
Co_TH2	4-Androstene-3,17-dione	$IC_{50} = 3.11 \mu\text{M}$ $R^2 = 0.95$	-
Co_TH3	DL-p-Chlorophenylalanine methyl ester hydrochloride	$IC_{50} = 40 \mu\text{M}$ $R^2 = 0.90$	-
Co_TH4	Ellipticine	$IC_{50} = 8.9 \mu\text{M}$ $R^2 = 0.93$	-
Co_TH5	Imazodan	#	#
Co_TH6	Lamotrigine	-	-
Co_TH7	VER-3323 hemifumarate salt	-	-
Co_TH8	L-745,870 hydrochloride	-	-
Co_TH9	Phenelzine sulfate salt	$IC_{50} = 48 \mu\text{M}$ $R^2 = 0.75$	-
Co_TH10	Ammonium pyrrolidinedithiocarbamate	-	-
Co_TH11	1-[2-(Trifluoromethyl)phenyl]imidazole	$IC_{50} = 1.37 \mu\text{M}$ $R^2 = 0.97$	$IC_{50} = 0.7 \mu\text{M}$ $R^2 = 0.85$

* In this work

(-) No significant inhibitory action was detectable under the conditions described

(#) Nonspecific inhibitory action was detected, and no IC₅₀ value was calculated

The validation assay reported five selective inhibitors of CYP11B2 and two inhibitors of both, CYP11B2 and CYP11B1. Furthermore, four compounds showed no inhibitory effect against CYP11Bs under the validation assay conditions (Table 3.11). Co_TH1 and Co_TH11 reported as clotrimazole-like inhibitors in the screening assay, showed in the validation assay different inhibition profiles. Compound Co_TH1 showed selective inhibitory effect against CYP11B2, whereas Co_TH11 showed inhibitory effects against both isoforms of enzyme.

Interestingly, out of the nine compounds defined during the screening assay as miconazole-like inhibitors, four compounds showed selective inhibition against CYP11B2. For this reason, it is important to include all miconazole-like inhibitors defined during the screening assay into the validation assay when the screening is carried out to discover selective inhibitors of CYP11B2.

The new CYP11B2 inhibitors reported in this work are pharmacologically active compounds. Co_TH1 is already known as formestane (sold as Lentaron®) and described as an injectable steroidal aromatase inhibitor with significant activity against metastatic breast cancer (Wiseman and Goa 1996). Figure 3.35 below shows the autoradiographic detection of steroid hydroxylation activity in the case of increased concentrations of Co_TH1 in comparison with positive (clotrimazole) and negative (DMSO) controls.

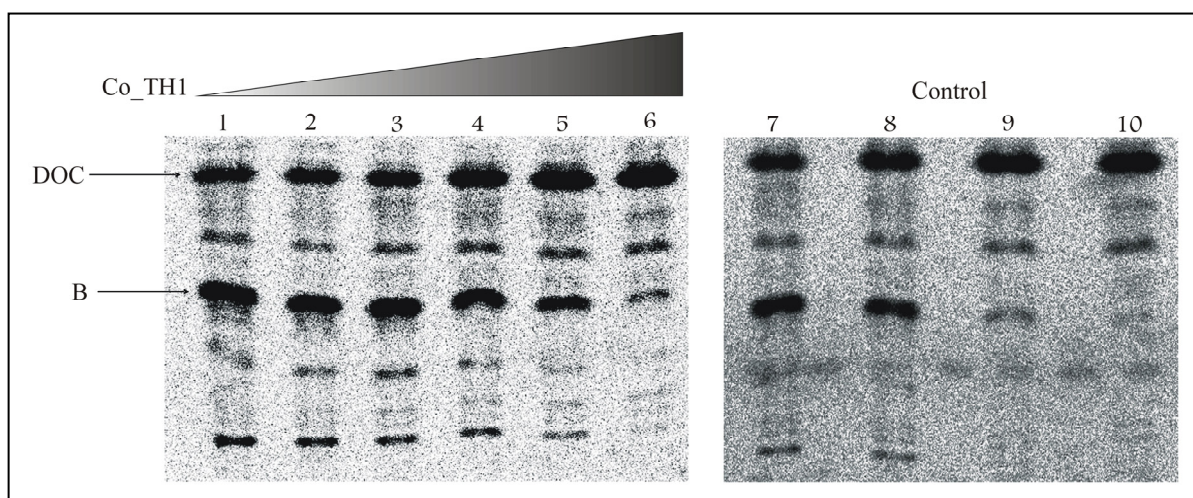


Figure 3.35. Autoradiographic detection of steroid hydroxylation activity. Steroid hydroxylation assay using strain MB164 and different concentrations of Co_TH1 was carried out as described in Section 2.2.4. Co_TH1 concentrations were as follows: (line 1) 100 nM; (line 2) 200 nM; (line 3) 500 nM; (line 4) 2 μ M; (line 5) 5 μ M; (line 6) 25 μ M; (lines 7, 8) mock-treated cells (DMSO); (line 9, 10) 25 μ M clotrimazole (positive control).

The plot of the CYP11B2 inhibition against the concentration of Co_TH1 shows a high correlation as shown in Figure 3.36 below, and was used to calculate the IC_{50} value for Co_TH1 against CYP11B2. This result displays that formestane (Co_TH1) inhibits selectivity CYP11B2 with an IC_{50} of 2.4 μM , whereas no significant inhibition was detected against CYP11B1.

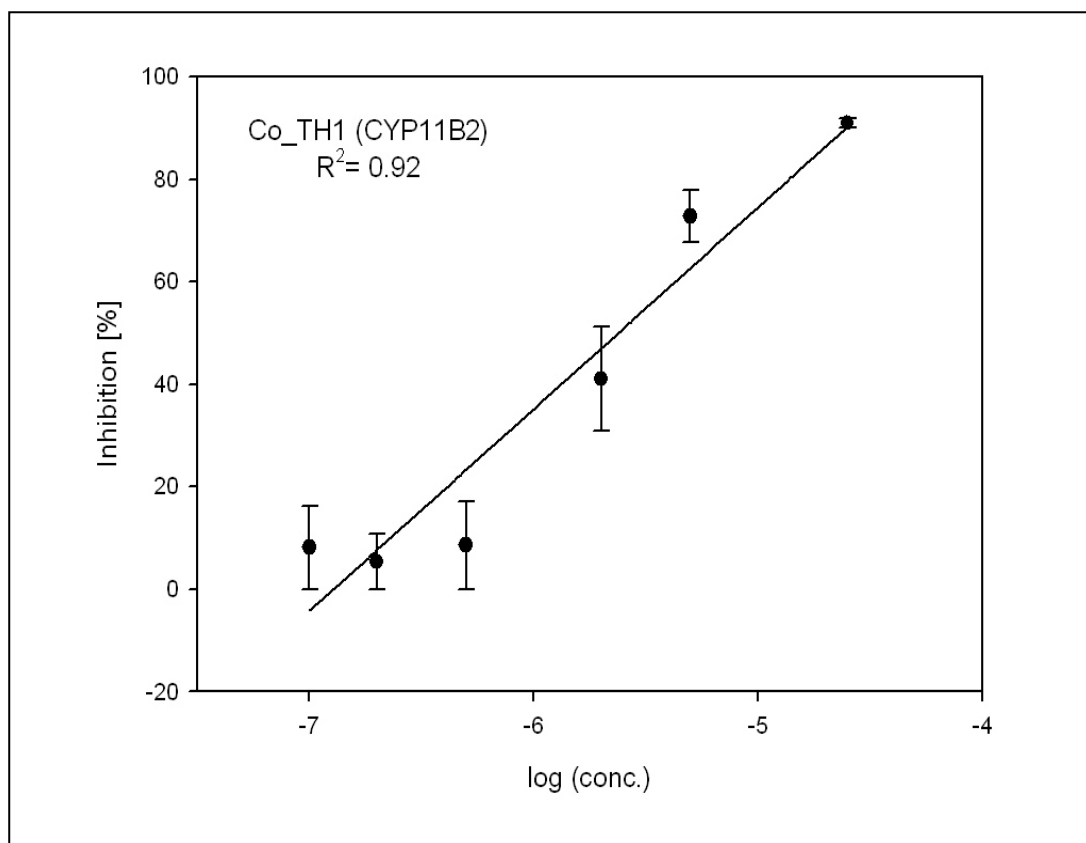


Figure 3.36. The inhibitory effect of Co_TH1 on the activity of CYP11B2.

The closely related compound Co_TH2, which is androstendion is a testosterone precursor and metabolite with androgenic activity. Interestingly, Co_TH1 and Co_TH2 were identified during the screening assay as clotrimazole-like and miconazole-like inhibitors of CYP11B2, respectively. These results were confirmed through the validation assay, where the miconazole-like inhibitor displayed relatively higher IC_{50} value (Co_TH2; $IC_{50} = 3.11 \mu\text{M}$) (Figure 3.37) in comparison with the clotrimazole-like inhibitor Co_TH1 ($IC_{50} = 2.4 \mu\text{M}$) (Figure 3.36). Although the difference between the two IC_{50} values is not very high, a difference has been reported that confirms the screening results.

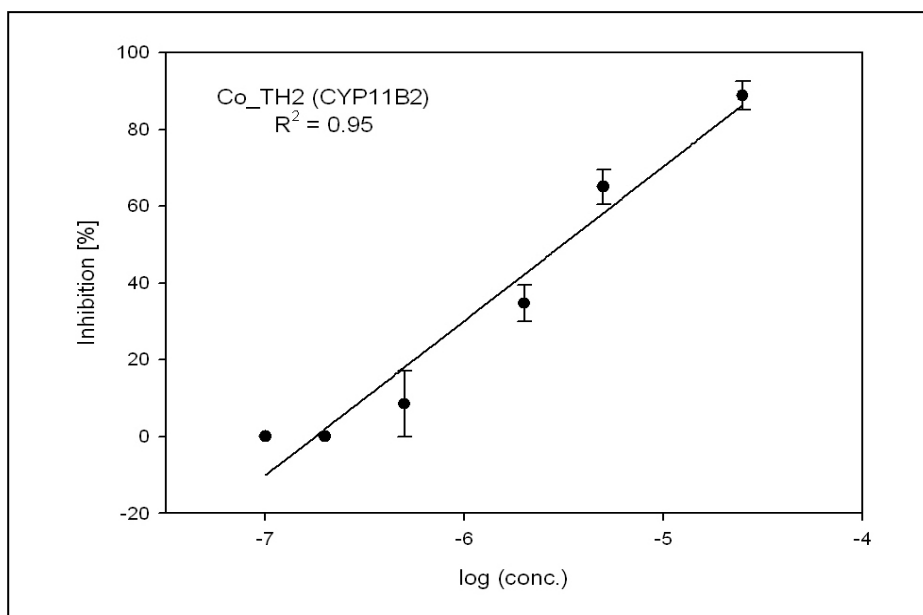


Figure 3.37. The inhibitory effect of Co_TH2 on the activity of CYP11B2.

Regarding the steroidal scaffold of 4-androsterone-4-ol-3, 17-dione the structure activity analysis revealed that the ketone in position 17 (D-ring) is beneficial for the activity, and an OH- residue at position 4 (A-ring) is necessary for potent inhibition of CYP11B2 (Figure 3.32). Although the nitric oxide synthase inhibitor Co_TH11 (1-[2-(Trifluoromethyl)phenyl]imidazole) was defined in the screening assay as clotrimazole-like inhibitor of CYP11B2, this compound displayed in the validation assay and in contrast to Co_TH1 a strong and unselective inhibition effect against CYP11B2 and CYP11B1 with IC_{50} values of 1.37 μ M and 0.7 μ M, respectively (Table 3.11, Figure 3.38).

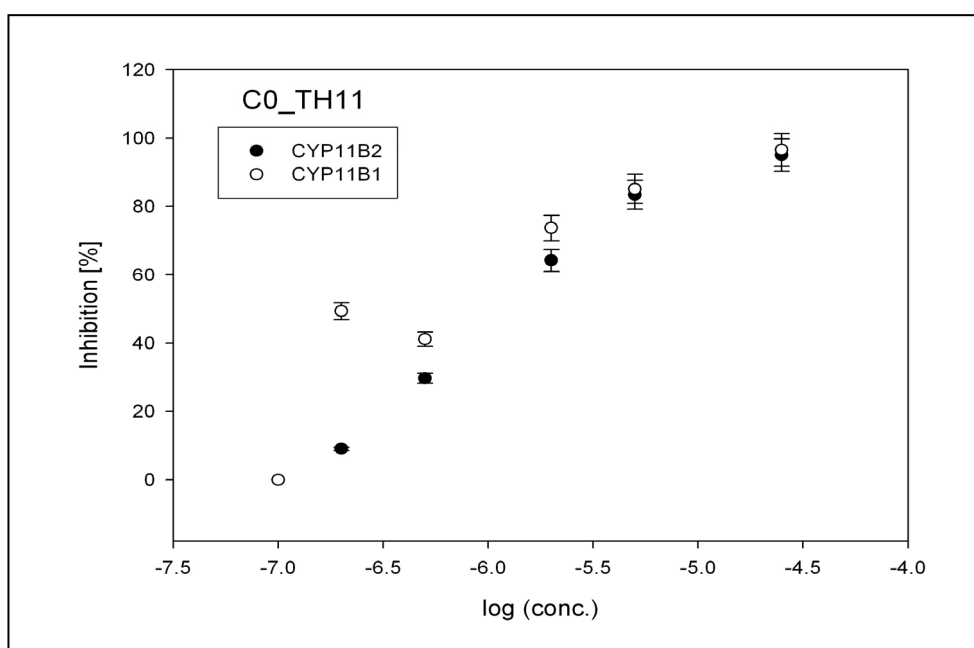


Figure 3.38. The inhibitory effect of Co_TH11 on the activity of CYP11B1 (opened symbols) and CYP11B2 (closed symbols).

In contrast to this, Co_TH3, Co_TH4 and Co_TH9 which were defined as miconazole-like inhibitors in the screening assay showed in the validation assay selective inhibition against CYP11B2 with IC₅₀ values of 40 µM, 8.9 µM and 48 µM respectively (Table 3.11).

The new CYP11B2 inhibitors defined in this work are pharmacologically active compounds which make them “druggable” lead compounds that could further optimised during the drug development process to achieve more selective and safe inhibitors of CYP11B2. Furthermore, some of these compounds are already commercial drugs and are applied clinically with unexplained side effects and severe complications. These unexplained complications could be explained to some extent because of their inhibitory effect against CYP11B2 as will be discussed in details below.

4. Discussion and Outlook

Since, the overall target of this work was the development of efficient P450-dependent whole-cell biotransformation reactions for steroid hydroxylation and drug discovery, the CYP11Bs-expressing fission yeast systems mentioned above were investigated and optimised in order to achieve this target.

The optimisation of the fission yeast systems was carried out on two different levels; the optimisation of the whole-cell system itself to increase the activity of the steroid hydroxylase and the optimisation of the hydroxylation assay parameters to achieve efficient reactions with biotechnological and pharmaceutical impacts.

4.1. Optimisation of the steroid hydroxylation assay for the 96-well plate format

Although fission yeast *Schizosaccharomyces pombe* was previously reported as an efficient host to express human CYP11Bs and to perform a whole-cell-based hydroxylation reaction (Bureik *et al.* 2002b; Bureik *et al.* 2004; Dragan *et al.* 2005), the ability to perform a CYP11B-dependent steroid hydroxylation assay in a 96-well plate has not yet been reported.

Performing the steroid hydroxylation assay in 96-well plate will give the opportunity to perform the assay on a relatively large scale in comparison with the tip-tube format or with Erlenmeyer flasks, which enables the comparison of the 11 β activity of several recombinant fission yeast strains at the same time. Furthermore, the plate-format method can be used to develop a screening system to check the steroid hydroxylation activity in a recombinant fission yeast strain under different conditions (inhibitor, medium, pH, etc.).

In order to perform a steroid hydroxylation assay in a 96-well plate a steroid bioconversion had to be achieved using a low-volume culture of fission yeast and a non-radioactive substrate, in which the steroid bioconversion can be measured with the HPLC. For this reason, the hydroxylation parameters were investigated and optimised to perform the reaction in low-volume culture in the tip-tube format and then in the 96-well plate format.

This work showed clearly the ability to get steroid bioconversion using a low-volume culture of the CYP11B1-expressing fission yeast and without the need to use radioactive-labelled substrate (Figure 3.1). Although the test was optimised for low-volume culture and carried out in the tip-tube format, no steroid bioconversion was detected when the test was performed in a 96-well plate. Taking into consideration the similarities and differences between the two test

formats (tip-tube and 96-well plate), it turns out that each format has its own test shape, which could influence the shaking process and aeration during the assay. Moreover, the tip-tube format assay was carried out using a thermomixer whereas the plate was shaken using an incubator. The investigations showed clearly the influence of the shaking velocity and assay volume on steroid bioconversion since increasing the shaking velocity to 480 rpm and assay volume to 600 μ l displayed detectable steroid bioconversion on the HPLC when the test was carried out in a 96-well plate (Figure 3.9). Furthermore, using the pipetting robot to manipulate the 96-well plates showed high efficiency to perform the hydroxylation assay on a relatively large scale in comparison with other test formats described above. The extraction program developed in this work (Table 3.2) enables the extraction of steroids from 96 samples in ca. 20 min, which is significantly shorter than the manual extraction process. In addition to this, and since no significant differences were observed between several wells, this hydroxylation assay provides an efficient screening tool to investigate the P450-dependent steroid hydroxylases in recombinant fission yeast strains (in the case of CYP11B1 (Dragan *et al.* 2005), CYP11B2 (Bureik *et al.* 2002b), CYP17 or CYP21 (Dragan *et al.* 2006)) and can be further optimised to develop a high or medium throughput screening system.

4.2. Coexpression of redox partners in CYP11B1-expressing fission yeast *Schizosaccharomyces pombe*

The biotechnological production of hydrocortisone is a complex process, which requires many different optimisation steps in order to significantly increase the product formation.

Although fission yeast *Schizosaccharomyces pombe* has been reported to be a very suitable model system for the investigation of P450 dependent steroid hydroxylases, hydrocortisone production efficiency using CYP11B1-expressing fission yeast strain SZ1 is not competitive enough for the consideration of its use for industrial applications.

As mentioned above and although the human CYP11B1 is able to accept electrons from the yeast Adx homologue, it has been demonstrated that the electron transfer to the cytochrome P450 can be rate limiting in various P450 systems (Grinberg *et al.*, 2000; Bernhardt 2006; Hannemann *et al.* 2007). For this reason, the target of this part of work was the improvement of the electron transfer pathway that supplies electrons to CYP11B1 in the recombinant fission yeast in order to increase the CYP11B1-mediated 11 β -hydroxylation activity to produce more hydrocortisone. Hence, the corresponding mammalian electron transfer partners (Adx and AdR) were coexpressed with CYP11B1, and different mutants of Adx were

investigated to achieve a recombinant fission yeast strain with the highest hydrocortisone bioproduction efficiency.

This work shows clearly that hydrocortisone production can be dramatically enhanced (3.4-fold) by coexpressing the other components of the CYP11B1 electron transfer chain and by optimising the reaction conditions to achieve high production efficiency on the laboratory level.

The CYP11B1-expressing fission yeast strains developed during this work were classified into four types according to the presence of the electron transfer proteins (Figure 4.1).

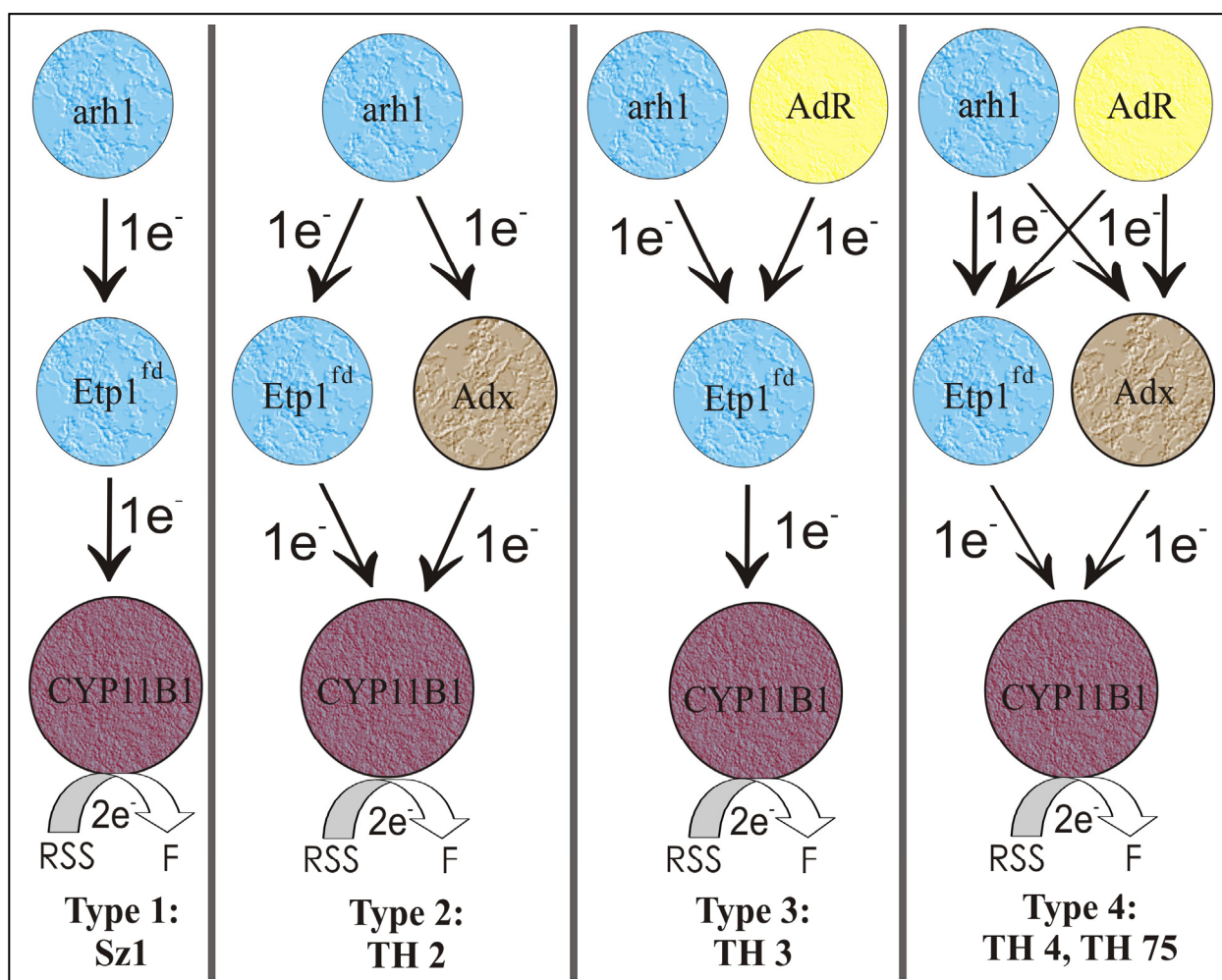


Figure 4.1. Schematic overview of the recombinant fission yeast types according to the availability of the electron transfer proteins in the fission yeast strains used in this study.

The fission yeast strain SZ1, which expresses the cytochrome CYP11B1 belongs to the first type, since this strain expresses only the P450. Nevertheless, this strain is capable of efficiently performing 11 β -hydroxylation reaction and produces 12% hydrocortisone under the test conditions mentioned before (Figure 3.18), which confirms earlier reports that the

P450 is supplied with reducing equivalents presumably from the endogenous electron transfer proteins *etp1^{fd}* (Bureik *et al.* 2002b; Dragan *et al.* 2005) and *arh1* (Ewen *et al.* 2008) (Figure 4.1, type I). Strain TH2 belongs to the second type in which the cytochrome CYP11B1 is heterologously coexpressed together with *Adx^{WT}*. This strain displayed an increased 11 β -hydroxylation activity compared to SZ1 (Type I electron transfer chain) with a hydrocortisone production of 25% (Figure 3.18) indicating a participation of *Adx* in the electron transfer to CYP11B1 also in fission yeast (Type II electron transfer chain). The third type implemented in the strain TH3 heterologously coexpresses *AdR^{WT}* and CYP11B1. The strain showed no increase in 11 β -hydroxylation activity compared to the SZ1 strain, which clearly demonstrated that *AdR^{WT}* alone can not improve the electron transfer efficiency in recombinant fission yeast. These findings could indicate a lack in cooperation between the heterologous *AdR* and the host ferredoxin *etp1^{fd}* in the presence of its putative natural host partner *arh1* or a maximum of electron transfer efficiency between the autologous redox partners (see Figure 4.1, compare type I and type III). Furthermore, it shows that the efficiency of substrate conversion depends mainly on the ferredoxin employed in the reaction (Ewen *et al.* 2008).

Strains TH4 and TH75 which coexpressed CYP11B1, *Adx^{WT}*, and *AdR^{WT}* (Type IV electron transfer chain) displayed a 3.4-fold higher activity (40% of initial RSS converted, Figure 3.18) with respect to the parental strain SZ1. In this way, TH75 is a highly efficient recombinant organism that can be used for the biotechnological conversion of RSS to hydrocortisone.

The investigations of *Adx* mutations that were assumed to improve the 11 β -hydroxylation activity in the context of a complete electron transfer chain could not further improve the hydrocortisone production compared to TH4 or TH75. This could be due to the distinct interaction forms between the different types of *Adx* and *AdR* in the yeast or to other limitations in the reaction process apart from the electron transfer.

Although human CYP11B1 in SZ1 was already optimised on the enzyme level and a site-directed mutagenesis was performed at positions 52 and 78 of CYP11B1, which showed that the presence of an isoleucine at position 78 increased the 11 β -hydroxylation activity (3.5-fold) (Hakki *et al.* 2008), the 11 β -hydroxylation activity could be further optimised (3.4-fold) by the coexpression of the corresponding electron transfer partners. These results demonstrated clearly the opportunity to optimise the steroid hydroxylases by optimising the whole-cell system itself. Moreover, and additionally to the coexpression of *Adx* and *AdR* optimising the bioconversion conditions enabled a high bioconversion efficiency on the laboratory level in comparison with the parental strain (Figure 3.20).

Thus it can be clearly demonstrated that the new fission yeast strain TH75 (Figure 4.2) coexpressing the complete electron transfer chain of the mitochondrial cytochrome CYP11B1 displays a significantly higher 11 β -hydroxylation activity than the parental strain SZ1. This new fission yeast strain TH75 displayed a high hydrocortisone production efficiency at an average of 9.7 μ mol hydrocortisone per 10ml test culture over a period of 72 hours (Figure 3.20), the highest value published to date for this biotransformation. Moreover, it can be expected that optimising the fermentation conditions in order to perform a sophisticated high-cell-density process can further enhance the efficiency of hydrocortisone bioproduction using TH75.

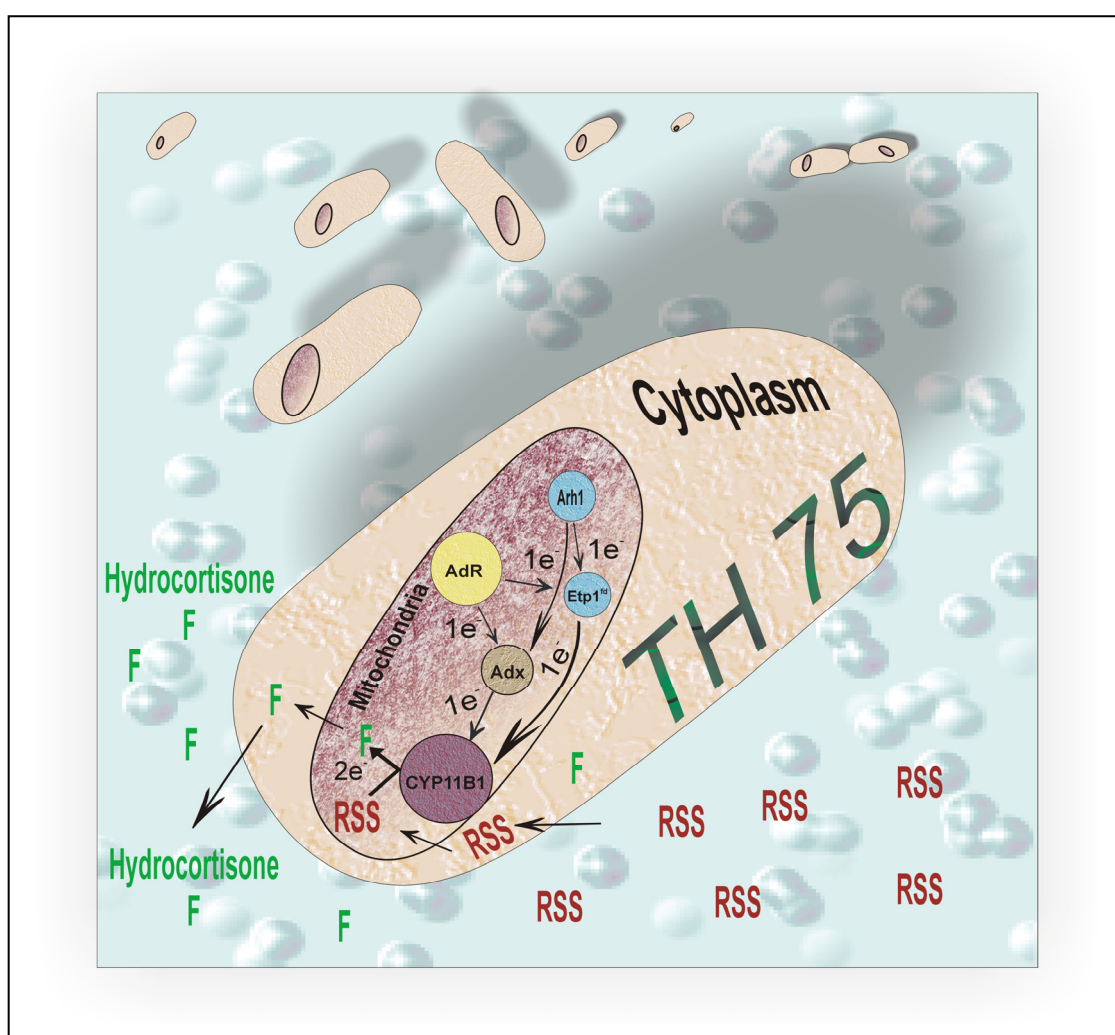


Figure 4.2. Schematic overview of the recombinant fission yeast strain TH75. The electron transfer proteins involved in the CYP11B1-dependent steroid hydroxylation in the fission yeast strain TH75.

Additionally, the newly developed vector pTH2 (Figure 3.14 A) has proven to be an important tool in combination with the integration vector pCAD1. Whereas the use of the integration vector pCAD1 enables the expression of a mitochondrial cytochrome of interest via chromosomal expression, the use of pTH2 enables the autosomal coexpression of the

complete mitochondrial electron transfer partners. This demonstrates an interesting way of functionally assembling the complete P450 system including the mitochondrial electron transfer chain by using only two expression vectors (pCAD1 and pTH2).

4.3. The development of a cell-based high throughput screening system for the discovery of human aldosterone synthase inhibitors

As mentioned before, the principal function of aldosterone is the maintenance of salt and water homeostasis and it therefore has a pivotal role in the regulation of blood pressure. It is unsurprising therefore that excessive aldosterone secretion has been reported in several cases of hypertension and has been correlated with higher mortality in congestive heart failure and fibrosis of the heart (Pitt *et al.* 1999; Brilla 2000; Pitt *et al.* 2001; Hakki and Bernhardt 2006). In addition to this, chronic elevation of aldosterone has also been implicated in adenoma, idiopathic hyperaldosteronism and insufficient renal flow (Stowasser and Gordon 2001). Although the use of aldosterone antagonists shows clinical benefit in the treatment of these diseases, it also leads to severe side effects like gynaecomastia and endocrinal dysregulation. Therefore, trials to inhibit the synthesis of aldosterone directly have been published (Denner *et al.* 1995b; Ehmer *et al.* 2002; Bureik *et al.* 2004; Ulmschneider *et al.* 2005a; Ulmschneider *et al.* 2005b; Hakki and Bernhardt 2006; Baston and Leroux 2007). Thus, CYP11B2 comprises a new target for drug treatment and selective inhibitors of the aldosterone producing CYP11B2 enzyme is of high pharmacological interest (Hakki and Bernhardt 2006; Baston and Leroux 2007; Schuster and Bernhardt 2007).

Although two systems (recombinant V79 cells, recombinant fission yeast) have been already established for evaluating compounds with respect to their inhibitory effect on human CYP11B1 and CYP11B2 (Bureik *et al.* 2004), neither of these two systems mentioned before could be considered as high or even medium throughput screening system. For this reason, the target of this part of work was the development of a high throughput screening system (HTS) for the discovery of aldosterone synthase inhibitors.

The development of the screening system was carried out on two levels; the development of a one point hydroxylation assay in fission yeast and the optimisation of the HPLC measurement in order to increase the throughput of the screening system.

Using the CYP11B2-expressing *S. pombe* system, a rapid, reliable and reproducible whole-cell-based HTS has been developed during this work. Furthermore, a new testing strategy has

been established to be applied in the field of drug discovery to discover CYP11B2 inhibitors for both academic and pharmaceutical purposes.

This new testing strategy consisted of a high throughput screening system followed by secondary validation assays for the further characterisation of the potential inhibitors of CYP11B2 (Figure 4.3).

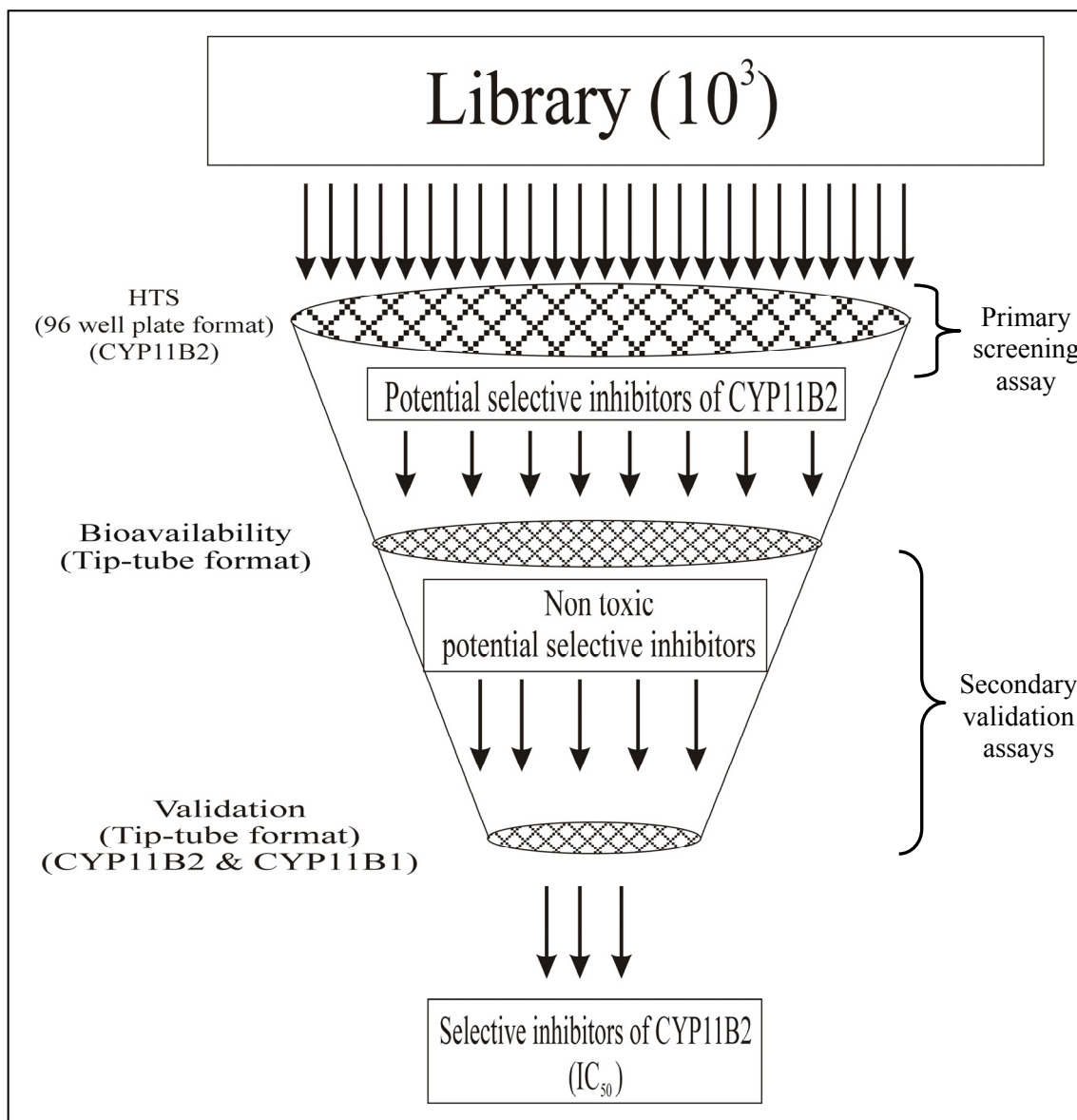


Figure 4.3. Schematic overview of the CYP11B2 testing strategy developed in this work. The new testing strategy consists of a primary screening assay, in which potential inhibitors will be investigated using the one point method to define the active compounds “hits. The hit will then go under secondary validation assays to investigate the toxicity of the compound and to define the selectivity against CYP11B2 and CYP11B1 using the multiple point method.

To develop a one-point whole-cell assay, the CYP11B2-expressing fission yeast strain MB164 was investigated in the presence of the known inhibitors of CYP11B2 (Table 3.8).

The target of these investigations was the determination of the optimal conditions for a one-point method, which gives reproducible results of conversion and inhibition in the presence of negative and positive controls.

The results demonstrated clearly that 5 μM DOC is an optimal concentration to get detectable conversion of DOC into B after three hours incubation in a 96-well plate (Figure 3.23). Moreover, test media were investigated to define the optimal medium in which the model inhibitor of CYP11B2 (ketoconazole) gives reproducible and highly correlated inhibition with its concentration. This investigation showed that simple potassium phosphate buffer (50 mM) is an optimal test medium to perform the screening assay (Figure 3.24). Although the different pH values showed high correlation between the concentration of ketoconazole and inhibition, the physiological pH 7.4 was chosen in order to test the compounds in a mammalian cell culture-resembling pH-environment.

Although the industry standard for initial CYP screening is 10 μM (Lin *et al.* 2007), the one-point assay developed in this work was designed to be carried out at 41.6 μM . This high concentration was chosen since this new developed screening assay is a whole cell-based assay and no information about the transport of compounds through the fission yeast cell wall is available. Moreover, it was assumed that the investigated compounds would be considered as uninteresting when no inhibition is detected even with this high concentration. Interestingly, this one-point method displayed reproducible results when the model inhibitors of CYP11B2 were tested. The mock- treated (DMSO) samples showed bioconversion ratio of 11.5%, whereas the presence of the CYP11B2 inhibitors showed significant inhibition profiles. The potent CYP11B2 inhibitors ketoconazole and clotrimazole showed total inhibition under the test conditions. Furthermore, the less potent CYP11B2 inhibitor miconazole showed 44% inhibition (Figure 3.30, Table 3.9). The results of controls are well correlated with the literature results reported before since significant differences between the potent and less potent inhibitors of CYP11B2 were noticed when tested using the one-point method. This one-point assay enables the classification of the CYP11B2 inhibitors (“hits”) defined during the primary screening into potent and less potent inhibitors of CYP11B2. For this reason, the controls were considered as internal quality control parameters along the screening process and were incorporated in each plate.

Moreover, the HPLC parameters were further optimised which enabled the separation of DOC and B within 2 min (Figures 3.27) reducing the solvent consumption and increasing the throughput of the HPLC by more than 2-fold.

4.4. Testing a library of pharmacologically active compounds using the developed screening system

Drug companies try to conserve efforts, years of time and money they have put into drugs that failed to reach the market for a variety of reasons like poor safety profile or unexplained side effects. However, recouping losses of billions of dollars spent to develop a drug could be simply done by finding a different disease to treat with it, or by taking drugs already existing on the market for one indication, and trying to find other possible indications to make more money with the existing drug, or in other words; recycling of existing drugs.

Although repositioning of existing drugs has appeared in the early 1990s, it has only existed in its current form since the beginning of the decade and only very few companies looked at existing drugs or retooled themselves to do repositioning sprouted up (Table 4.1).

Table 4.1. Selected long-standing pharmaceuticals that had been repositioned during or prior to 2004 (Ashburn and Thor 2004)

Generic Name	Trade Name, Original Indication (originator)	Trade Name, Repositioned Indication (repositioner)
Celecoxib	Celebrex, osteoarthritis and rheumatoid arthritis (Pfizer)	Celebrex, familial adenomatous polyposis, colon & breast cancer
Minoxidil	trade name N/A, hypertension (Pharmacia & Upjohn)	Rogaine, hair loss (Pfizer)
Topiramate	Topamax, epilepsy (Johnson & Johnson)	trade name N/A, obesity (Johnson & Johnson)
Lidocaine	Xilocaine, local anesthesia (AstraZeneca)	trade name N/A, Oral corticosteroid-dependent asthma (Corus Pharma)
Bupropion	Wellbutrin, depression (GlaxoSmithKline)	Zyban, smoking cessation (GlaxoSmithKline)
Fluoxetine	Prozac, depression (Eli Lilly)	Sarafem, premenstrual dysphoria (Eli Lilly)
Duloxetine	Cymbalta, depression (Eli Lilly)	Duloxetine SUI, stress urinary incontinence (Eli Lilly)

In fact, of the top 50 selling pharmaceuticals in 2004, 84% have had additional indications approved since their initial US licensure. For this reason, the target of this part of work was to screen a library of pharmacologically active compounds using the newly developed screening system. The screening was carried out to validate the system itself and to check if a

repositioning process can be carried out on these existing pharmaceuticals to add the inhibition of CYP11B2 as a new indication.

The results of controls displayed reproducible results using the one-point concentration method (41.6 μ M), and showed significant differences between the controls and the mock-treated samples ($p < 0.05$). The mock-treated samples (DMSO) displayed CYP11B2 activity with B production ratio of 11.5%, whereas the presence of miconazole decreased significantly ($p < 0.05$) the activity of CYP11B2 and B production ratio to 6.5% showing 44% inhibition under the test conditions. Moreover, the presence of either clotrimazole or ketoconazole displayed total inhibition of CYP11B2 (100%). Hence, each compound with similar inhibition profile will be defined during this screening assay as clotrimazole-like inhibitor of CYP11B2, whereas compounds with less inhibition effect resembling the miconazole effect will be defined as miconazole-like inhibitors.

The results of control showed high reproducibility during the screening assay and confirmed the reliability of the screening system. Furthermore, the screening assay showed high robustness when the Z' -factor was calculated for the several known CYP11B2 inhibitors as positive controls and DMSO as negative control. The Z' -factor of 1.0 for clotrimazole and ketoconazole show that the screening assay is perfect to identify clotrimazole-like inhibitors, and is an excellent assay to identify miconazole-like inhibitors since the Z' -factor for miconazole was 0.85.

The investigated library contains 1268 proven pharmacologically active compounds (see appendix) and is distributed in different kinds of drug classes as shown in Figure 4.4.

Although 35% of the compounds in the library are inhibitors of different enzymes, only 13 compounds were reported during the screening assay as potential inhibitors of CYP11B2. The two novel clotrimazole-like inhibitors reported in this work belong to the inhibitors class, whereas the miconazole-like inhibitors belong to different classes (Table 3.10, Figure 4.4).

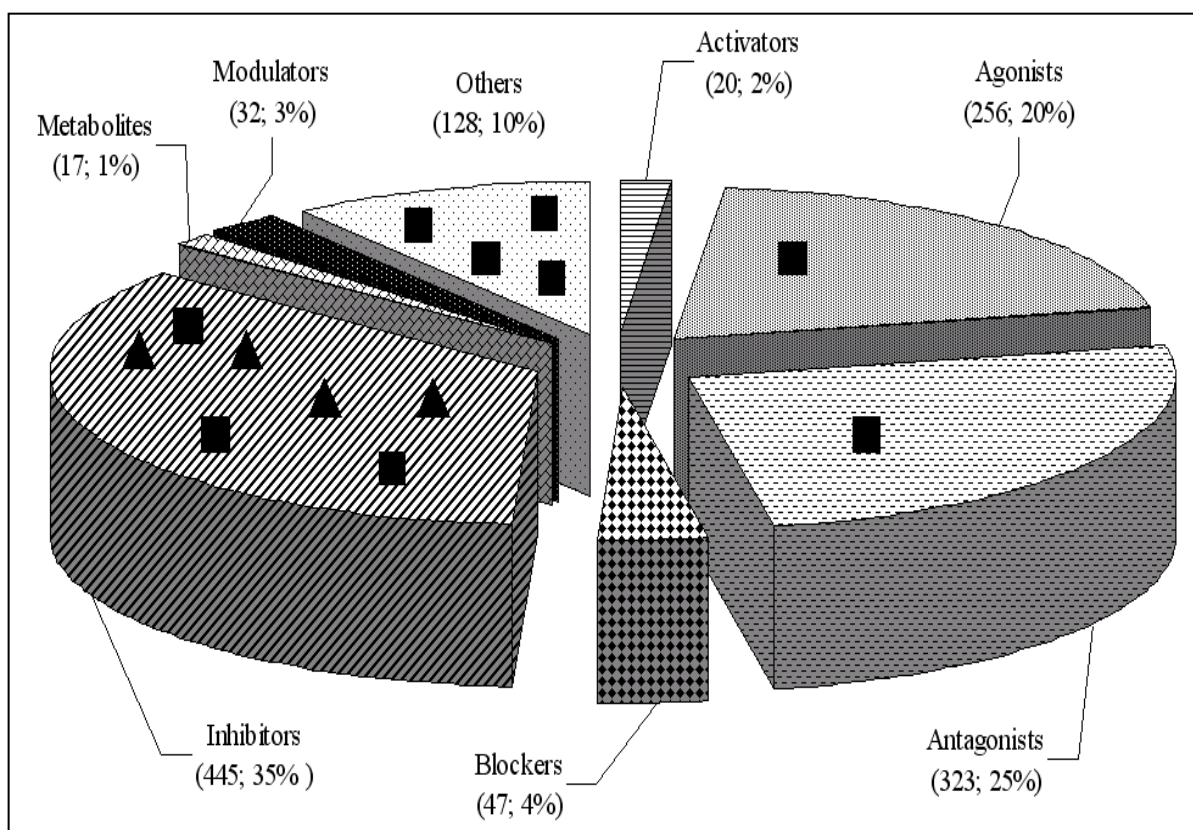


Figure 4.4. Pie chart depicting the composition of the investigated library.

The LOPAC library contains different classes of compounds. The screening assay reported four clotrimazole-like inhibitors, whereas nine miconazole-like inhibitors were also reported. The new inhibitors of CYP11B2 belong to different classes as shown (▲ clotrimazole-like inhibitor, ■ miconazole-like inhibitor).

Since the new CYP11B2 inhibitors are pharmacologically active compounds, the unexplained side effects associated with the therapeutic application of these drugs can be explained to some extent according to the results of this work.

Co_TH1 is formestane (sold as Lentaron®) and described as an injectable steroidal aromatase inhibitor with significant activity against metastatic breast cancer. In the clinical trials, formestane has been generally well tolerated following intramuscular administration at doses of up to 500 mg weekly (Goss *et al.*, 1986).

Previous studies showed that systemic adverse effects occurred in about 12% of patients following intramuscular drug administration (Coombes *et al.*, 1992). Many of these such as hot flushes, vaginal spotting and emotional lability were related to the mechanism of action of formestane i.e. estrogen suppression. Lethargy, rash, nausea, dizziness, indigestion, ataxia, cramps and facial swelling have also been reported with an incidence of <7% (Hoffken *et al.*, 1990). Moreover, it was reported recently that formestane treatment is also associated with changes in bile composition, which may predispose to gallstone formation (Czerny *et al.*,

2005). Our results display that formestane (Co_TH1) inhibits selectively CYP11B2 (IC_{50} : 2.4 μ M) (Figure 3.32). This observation could explain some of the side effects associated with formestane i.e. nausea and dizziness.

The closely related compound Co_TH2 is androstendion, which is a testosterone precursor and metabolite with androgenic activity. Interestingly Co_TH1 and Co_TH2 were identified during the primary screening assay as clotrimazole-like and miconazole-like inhibitors of CYP11B2, respectively. This result was confirmed through the validation assay, where the miconazole-like inhibitor displayed higher IC_{50} value (Co_TH2; IC_{50} = 3.11 μ M) in comparison with the clotrimazole-like inhibitor Co_TH1 (IC_{50} = 2.4 μ M). Regarding the steroidal scaffold of 4-androsterone-4-ol-3, 17-dione the structure activity analysis revealed that the ketone in position 17 (D-ring) is beneficial for activity, and an OH- residue at position 4 (A- ring) is necessary for potent inhibition of CYP11B2.

Since androstendion (Co_TH2) is a dehydroepiandrosterone (DHEA) metabolite, it might be of special interest that hormonal replacement therapy increasing DHEA will increase androstendion. Therefore, DHEA replacement performed as anti-aging therapy (Ohnaka and Takayanagi 2007), should take into consideration the possibility to develop salt depletion and unexplained hypotension.

The anti cancer drug Ellipticine (Co_TH4) identified during the primary assay as miconazole-like inhibitor of CYP11B2 showed selective inhibition of CYP11B2 with an IC_{50} of 8.9 μ M ($R^2 = 0.93$). Ellipticine (5,11-dimethyl-6H-pyrido[4,3-b]carbazole) and several of its derivatives isolated from Apocyanaceae plants (i.e. *Ochrosia borbonica*, *Excavatia coccinea*) are alkaloids exhibiting significant antitumor and anti-HIV activities. Ellipticine and its more soluble derivatives (9-hydroxyellipticine, 9-hydroxy-N2-methylellipticinium, 9-chloro-N2-methylellipticinium and 9-methoxy-N2-methylellipticinium) exhibit promising results in the treatment of osteolytic breast cancer metastases, kidney sarcoma, tumors of brain and myeloblastic leukemia (Stiborova *et al.*, 2001). The main reason for the interest in ellipticine and its derivatives for clinical purposes is their high efficiencies against several types of cancer, their rather limited toxic side effects and their complete lack of hematological toxicity (Auclair 1987).

Many suggestions were reported about the mechanisms of action that ellipticines follow as anticancer drugs, taken into consideration that the prevalent mechanisms of antitumor activities are (1) intercalation into DNA (Chu and Hsu 1992; Singh *et al.*, 1994), and (2) inhibition of DNA topoisomerase II activity (Monnot *et al.*, 1991; Fosse *et al.*, 1992).

Recently, it has been demonstrated that ellipticine covalently binds to DNA after being enzymatically activated. Cytochromes P450 (CYPs) are the major enzymes catalysing the ellipticine oxidation and its activation to more efficient metabolites forming DNA adducts (Aimova and Stiborova 2005). Furthermore, ellipticine was found to be a substrate of CYP1A1 and CYP1A2 (Auclair 1987; Frei *et al.*, 2002), and an inducer of several CYPs (Aimova *et al.*, 2007). On the other hand, this compound was previously reported to be a strong inhibitor of CYP1A1/2 (Auclair 1987). We found an inhibitory effect of ellipticine against the human CYP11B2. For this reason, it should be taken into consideration that the clinical application of ellipticine in the treatment of cancer could be associated with blood hypotension.

Compound Co_TH9 known as phenelzine (Sold as Nardil®) is a potent, irreversible inhibitor of monoamine oxidase (MAO)-A and -B, that has been used to treat depression since the late 1950s (Furst 1959). There has been a recent resurgence of interest in this drug class for patients with severe depression (Shelton Clauson *et al.*, 2004; Sokolski and Brown 2006).

Phenelzine toxicity is normally characterised by agitation, seizures, sweating, tachycardia and hypertension (Ciocatto *et al.*, 1972; Bhugra and Kaye 1986; Henry and Antao 1992), although hypotension has also been described (Linden *et al.*, 1984; Breheny *et al.*, 1986). Furthermore, the unexplained phenelzine-induced hypotension could be treated successfully with salt tablets (Munjack 1984). Moreover, several studies reported phenelzine-overdose induced complications, these complications include severe and unexplained hypotension, impaired left ventricular function and acute myocarditis, death was also reported and should be considered in patients who develop unexplained hypotension after phenelzine overdose (Linden *et al.* 1984; Waring and Wallace 2007).

Since it was found in this work that phenelzine inhibits the aldosterone synthase (CYP11B2) with an IC_{50} value of 48 μ M hence, the side effect of this drug concerning salt loss and hypotension can be explained with this result. As a result of CYP11B2 inhibition, the renin-angiotension system will be activated in a classical endocrine negative feedback loop, this activation will increase the amount of converted angiotension II (AT II), the potent vasoconstrictor, which elevate thus the blood pressure, and could be the reason for the hypertension usually characterizing phenelzine toxicity. Furthermore, AT II has a direct stimulating action on the corticotropin-releasing hormone (CRH) (Ganong 1993; Jezova *et al.*, 1998), which induces in addition to steroidogenesis the catecholamine synthesis via the induction of tyrosine hydroxylase (TH) (Dermitzaki *et al.*, 2007), dopamine β -hydroxylase

(DBH) and phenylethanolamine N-methyltransferase (PNMT) (Lima and Sourkes 1987). Moreover, CRH stimulates the catecholamine release and poses a trophic effect on chromaffin cells (Hoheisel *et al.*, 1998).

Thus, depending on the results of this work and the previous clinical observations mentioned above, it can be suggested that the unexplained hypotension after a massive phenelzine overdose is due to the CYP11B2 inhibition.

The massive overdose could inhibit totally the aldosterone synthase, and, as a result, aldosterone, the primary hormone responsible for Na⁺ retention by the kidney, will disappear causing hypotension. Moreover, the activation of the renin-angiotension system stimulates the corticotropin-releasing factor (CRF) and adrenocorticotrophic hormone (ACTH), which stimulate the adrenal gland, and since CYP11B2 is inhibited, more cortisol will be produced.

The increased CRH will enhance also the epinephrine synthesis through the stimulation of tyrosine hydroxylase and dopamine-β-hydroxylase. Moreover, the increased cortisol will increase the expression level of phenylethanolamine N-methyltransferase (PNMT) in chromaffin cells, enhancing also the synthesis of epinephrine (Isobe *et al.*, 2000; Wong 2006) (Figure 4.5).

Unlike many other hormones, epinephrine as well as the other catecholamines does not exert any negative feedback, and therefore the overdose of phenelzine increases the epinephrine synthesis, whether on the production level by enhancing indirectly the activity of the enzymes involved in catecholamine synthesis, or directly by inhibiting the monoamin oxidase enzymes involved in the epinephrine metabolism process (Figure 4.5).

minimize the influence of any aldosterone decrease in depressed patients receiving phenelzine. Whereas an overdose from phenelzine can lead to a total inhibition of CYP11B2 and to a dramatic decrease in the aldosterone concentration. These findings could play an important role in the management of depressed patients receiving phenelzine by monitoring the aldosterone concentration and blood pressure. Furthermore, phenelzine overdose-induced death could be prevented by rapid infusion of normal saline and aldosterone replacement therapy.

Finally, the tryptophan hydroxylase inhibitor Co_TH3 (4-Chloro-DL-phenylalanine methyl ester hydrochloride) defined during the screening assay as miconazole-like inhibitor, showed during the validation assay a selective inhibition of CYP11B2 with an IC_{50} of 40 μ M ($R^2=0.90$). In contrast, the nitric oxide synthase inhibitor Co_TH11 (1-[2-(Trifluoromethyl)phenyl]imidazole) defined during the screening assay as clotrimazole-like inhibitor displayed strong inhibition effect against both, CYP11B2 and CYP11B1 with IC_{50} values of 1.37 and 0.7 μ M, respectively (Table 3.11, Figure 3.38). It is, thus, not specific enough as a “lead” for the development of CYP11B2 inhibitors. For this reason, the miconazole-like inhibitors of CYP11B2 defined during the screening assay should be taken into consideration and included in the validation assays when the screening is carried out to discover selective inhibitors of CYP11B2.

Concluding, these results indicate that the new screening system developed in this work (Figure 4.3) is a robust screening system that can be applied to investigate libraries of existing drugs to find novel CYP11B2 inhibitors. This screening enables the reposition of existing drugs, which can save costs and billions of dollars spend to develop new CYP11B2 inhibitors.

Although the test was developed and validated on the laboratory level, it displayed the ability to screen up to 600 compounds per week. The throughput of the system can further increased by testing 10 compounds per well, which will increase the throughput of the system up to 6000 compounds per week.

Finally, this screening system can be modified and established for the use on the industrial level, especially when the required equipments are offered to enable the manipulation of large numbers of plates. Furthermore, the novel CYP11B2 inhibitors identified in this work are “druggable” compounds that can be repositioned to be used in the treatment of hyperaldosteronism-related diseases or as lead compounds that could further optimised in the field of drug development to achieve more safe and selective inhibitors of CYP11B2.

5. References

- Aimova, D. and Stiborova, M., 2005. Antitumor drug ellipticine inhibits the activities of rat hepatic cytochromes P450. *Biomed Pap Med Fac Univ Palacky Olomouc Czech Repub.* 149, 437-440.
- Aimova, D., Svobodova, L., Kotrbova, V., Mrazova, B., Hodek, P., Hudecek, J., Vaclavikova, R., Frei, E. and Stiborova, M., 2007. The anticancer drug ellipticine is a potent inducer of rat cytochromes P450 1A1 and 1A2, thereby modulating its own metabolism. *Drug Metab Dispos.* 35, 1926-1934.
- Akiyoshi-Shibata, M., Sakaki, T., Ohyama, Y., Noshiro, M., Okuda, K. and Yabusaki, Y., 1994. Further oxidation of hydroxycalcidiol by calcidiol 24-hydroxylase. A study with the mature enzyme expressed in *Escherichia coli*. *Eur J Biochem.* 224, 335-343.
- Andreadis, A., Hsu, Y. P., Hermodson, M., Kohlhaw, G. and Schimmel, P., 1984. Yeast LEU2. Repression of mRNA levels by leucine and primary structure of the gene product. *J Biol Chem.* 259, 8059-8062.
- Ashburn, T. T. and Thor, K. B., 2004. Drug repositioning: identifying and developing new uses for existing drugs. *Nat Rev Drug Discov.* 3, 673-683.
- Auclair, C., 1987. Multimodal action of antitumor agents on DNA: the ellipticine series. *Arch Biochem Biophys.* 259, 1-14.
- Baston, E. and Leroux, F. R., 2007. Inhibitors of steroidal cytochrome p450 enzymes as targets for drug development. *Recent Patents Anticancer Drug Discov.* 2, 31-58.
- Belkina, N. V., Lisurek, M., Ivanov, A. S. and Bernhardt, R., 2001. Modelling of three-dimensional structures of cytochromes P450 11B1 and 11B2. *J Inorg Biochem.* 87, 197-207.
- Bernhardt, R., 2006. Cytochromes P450 as versatile biocatalysts. *J Biotechnol.* 124, 128-145.
- Bhugra, D. K. and Kaye, N., 1986. Phenelzine induced grand mal seizure. *Br J Clin Pract.* 40, 173-174.
- Bichet, A., Hannemann, F., Rekowski, M. and Bernhardt, R., 2007. A new application of the yeast two-hybrid system in protein engineering. *Protein Eng Des Sel.* 20, 117-123.
- Black, S. D. and Coon, M. J., 1987. P-450 cytochromes: structure and function. *Adv Enzymol Relat Areas Mol Biol.* 60, 35-87.
- Boeke, J. D., Trueheart, J., Natsoulis, G. and Fink, G. R., 1987. 5-Fluoroorotic acid as a selective agent in yeast molecular genetics. *Methods Enzymol.* 154, 164-175.

- Bogdanski, D. F., Weissbach, H. and Udenfriend, 1958. Pharmacological studies with the serotonin precursor, 5-hydroxytryptophan. *J Pharmacol Exp Ther.* 122, 182-194.
- Boscaro, M., Barzon, L., Fallo, F. and Sonino, N., 2001. Cushing's syndrome. *Lancet.* 357, 783-791.
- Böttner, B. and Bernhardt, R., 1996. Changed ratios of glucocorticoids/mineralocorticoids caused by point mutations in the putative I-helix regions of CYP11B1 and CYP11B2". *Endocr Res.* 22, 455-461.
- Böttner, B., Denner, K. and Bernhardt, R., 1998. Conferring aldosterone synthesis to human CYP11B1 by replacing key amino acid residues with CYP11B2-specific ones. *Eur J Biochem.* 252, 458-466.
- Box, J. A., Bunch, J. T., Zappulla, D. C., Glynn, E. F. and Baumann, P., 2008. A flexible template boundary element in the RNA subunit of fission yeast telomerase. *J Biol Chem.* 283, 23.
- Breheny, F. X., Dobb, G. J. and Clarke, G. M., 1986. Phenelzine poisoning. *Anaesthesia.* 41, 53-56.
- Brilla, C. G., 2000. Aldosterone and myocardial fibrosis in heart failure. *Herz.* 25, 299-306.
- Brown, N., Swart, P., Fenhalls, G., Stevens, L., Kolar, N. W. and Swart, A. C., 2002. Baboon CYP11B1: the localization and catalytic activity in baboon adrenal tissue. *Endocr Res.* 28, 477-484.
- Brunner, D. and Nurse, P., 2000. New concepts in fission yeast morphogenesis. *Philos Trans R Soc Lond B Biol Sci.* 355, 873-877.
- Bülow, H. E. and Bernhardt, R., 2002. Analyses of the CYP11B gene family in the guinea pig suggest the existence of a primordial CYP11B gene with aldosterone synthase activity. *Eur J Biochem.* 269, 3838-3846.
- Bülow, H. E., Mobius, K., Bahr, V. and Bernhardt, R., 1996. Molecular cloning and functional expression of the cytochrome P450 11B- hydroxylase of the guinea pig. *Biochem Biophys Res Commun.* 221, 304-312.
- Bureik, M., Hübel, K., Dragan, C. A., Scher, J., Becker, H., Lenz, N. and Bernhardt, R., 2004. Development of test systems for the discovery of selective human aldosterone synthase (CYP11B2) and 11beta-hydroxylase (CYP11B1) inhibitors. Discovery of a new lead compound for the therapy of congestive heart failure, myocardial fibrosis and hypertension. *Mol Cell Endocrinol.* 217, 249-254.
- Bureik, M., Lisurek, M. and Bernhardt, R., 2002a. The human steroid hydroxylases CYP11B1 and CYP11B2. *Biol Chem.* 383, 1537-1551.

- Bureik, M., Mion, A., Kenyon, C. J. and Bernhardt, R., 2005. Inhibition of aldosterone biosynthesis by staurosporine. *Biol Chem.* 386, 663-669.
- Bureik, M., Schiffler, B., Hiraoka, Y., Vogel, F. and Bernhardt, R., 2002b. Functional expression of human mitochondrial CYP11B2 in fission yeast and identification of a new internal electron transfer protein, etp1. *Biochemistry.* 41, 2311-2321.
- Burke, J. D. and Gould, K. L., 1994. Molecular cloning and characterization of the *Schizosaccharomyces pombe* his3 gene for use as a selectable marker. *Mol Gen Genet.* 242, 169-176.
- Cheng, S. C., Suzuki, K., Sadee, W. and Harding, B. W., 1976. Effects of spironolactone, canrenone and canrenoate-K on cytochrome P450, and 11beta- and 18-hydroxylation in bovine and human adrenal cortical mitochondria. *Endocrinology.* 99, 1097-1106.
- Chiron, S., Gaisne, M., Guillou, E., Belenguer, P., Clark-Walker, G. D. and Bonnefoy, N., 2007. Studying mitochondria in an attractive model: *Schizosaccharomyces pombe*. *Methods Mol Biol.* 372, 91-105.
- Chu, Y. and Hsu, M. T., 1992. Ellipticine increases the superhelical density of intracellular SV40 DNA by intercalation. *Nucleic Acids Res.* 20, 4033-4038.
- Chua, S. C., Szabo, P., Vitek, A., Grzeschik, K. H., John, M. and White, P. C., 1987. Cloning of cDNA encoding steroid 11 beta-hydroxylase (P450c11). *Proc Natl Acad Sci U S A.* 84, 7193-7197.
- Ciocatto, E., Fagiano, G. and Bava, G. L., 1972. Clinical features and treatment of overdose of monoamine oxidase inhibitors and their interaction with other psychotropic drugs. *Resuscitation.* 1, 69-72.
- Coombes, R. C., Hughes, S. W. and Dowsett, M., 1992. 4-hydroxyandrostenedione: a new treatment for postmenopausal patients with breast cancer. *Eur J Cancer.* 28A, 1941-1945.
- Craven, R. A., Griffiths, D. J., Sheldrick, K. S., Randall, R. E., Hagan, I. M. and Carr, A. M., 1998. Vectors for the expression of tagged proteins in *Schizosaccharomyces pombe*. *Gene.* 221, 59-68.
- Curnow, K. M., Slutsker, L., Vitek, J., Cole, T., Speiser, P. W., New, M. I., White, P. C. and Pascoe, L., 1993. Mutations in the CYP11B1 gene causing congenital adrenal hyperplasia and hypertension cluster in exons 6, 7, and 8. *Proc Natl Acad Sci U S A.* 90, 4552-4556.

- Curnow, K. M., Tusie-Luna, M. T., Pascoe, L., Natarajan, R., Gu, J. L., Nadler, J. L. and White, P. C., 1991. The product of the CYP11B2 gene is required for aldosterone biosynthesis in the human adrenal cortex. *Mol Endocrinol.* 5, 1513-1522.
- Cutler, G. B., Jr. and Laue, L., 1990. Congenital adrenal hyperplasia due to 21-hydroxylase deficiency. *N Engl J Med.* 323, 1806-1813.
- Czerny, B., Teister, M., Juzyszyn, Z., Modrzejewski, A. and Pawlik, A., 2005. Effect of 4-hydroxyandrost-4-ene-3,17-dione (formestane) on the bile secretion and metabolism of 4-(14)C-cholesterol to bile acids. *Pharmacol Rep.* 57, 896-900.
- Degtyarenko, K. N. and Kulikova, T. A., 2001. Evolution of bioinorganic motifs in P450-containing systems. *Biochem Soc Trans.* 29, 139-147.
- Delyani, J. A., 2000. Mineralocorticoid receptor antagonists: the evolution of utility and pharmacology. *Kidney Int.* 57, 1408-1411.
- Denner, K. and Bernhardt, R., Eds. (1998). Inhibition studies of steroid conversions mediated by human CYP11B1 and CYP11B2 expressed in cell cultures. Oxygen Homeostasis and Its Dynamics. Tokyo/ Berlin/ Heidelberg/New York, Springer-Verlag.
- Denner, K., Doehmer, J. and Bernhardt, R., 1995a. Cloning of CYP11B1 and CYP11B2 from normal human adrenal and their functional expression in COS-7 and V79 Chinese hamster cells. *Endocr Res.* 21, 443-448.
- Denner, K., Vogel, R., Schmalix, W., Doehmer, J. and Bernhardt, R., 1995b. Cloning and stable expression of the human mitochondrial cytochrome P45011B1 cDNA in V79 Chinese hamster cells and their application for testing of potential inhibitors. *Pharmacogenetics.* 5, 89-96.
- Dermitzaki, E., Tsatsanis, C., Minas, V., Chatzaki, E., Charalampopoulos, I., Venihaki, M., Androulidaki, A., Lambropoulou, M., Spiess, J., Michalodimitrakis, E., Gravanis, A. and Margioris, A. N., 2007. Corticotropin-releasing factor (CRF) and the urocortins differentially regulate catecholamine secretion in human and rat adrenals, in a CRF receptor type-specific manner. *Endocrinology.* 148, 1524-1538.
- Derouet-Hümbert, E., Dragan, C. A., Hakki, T. and Bureik, M., 2007. ROS production by adrenodoxin does not cause apoptosis in fission yeast. *Apoptosis.* 12, 2135-2142.
- Domalik, L. J., Chaplin, D. D., Kirkman, M. S., Wu, R. C., Liu, W. W., Howard, T. A., Seldin, M. F. and Parker, K. L., 1991. Different isozymes of mouse 11 beta-hydroxylase produce mineralocorticoids and glucocorticoids. *Mol Endocrinol.* 5, 1853-1861.

- Dragan, C. A., Hartmann, R. W. and Bureik, M., 2006. A fission yeast-based test system for the determination of IC₅₀ values of anti-prostate tumor drugs acting on CYP21. *J Enzyme Inhib Med Chem.* 21, 547-556.
- Dragan, C. A., Zearo, S., Hannemann, F., Bernhardt, R. and Bureik, M., 2005. Efficient conversion of 11-deoxycortisol to cortisol (hydrocortisone) by recombinant fission yeast *Schizosaccharomyces pombe*. *FEMS Yeast Res.* 5, 621-625.
- Dumas, B., Cauet, G., Lacour, T., Degryse, E., Laruelle, L., Ledoux, C., Spagnoli, R. and Achstetter, T., 1996. 11 beta-hydroxylase activity in recombinant yeast mitochondria. In vivo conversion of 11-deoxycortisol to hydrocortisone. *Eur J Biochem.* 238, 495-504.
- Ehmer, P. B., Bureik, M., Bernhardt, R., Müller, U. and Hartmann, R. W., 2002. Development of a test system for inhibitors of human aldosterone synthase (CYP11B2): screening in fission yeast and evaluation of selectivity in V79 cells. *J Steroid Biochem Mol Biol.* 81, 173-179.
- Engelhardt, D. and Weber, M. M., 1994. Therapy of Cushing's syndrome with steroid biosynthesis inhibitors. *J Steroid Biochem Mol Biol.* 49, 261-267.
- Erdmann, B., Denner, K., Gerst, H., Lenz, D. and Bernhardt, R., 1995a. Human adrenal CYP11B1: localization by in situ-hybridization and functional expression in cell cultures. *Endocr Res.* 21, 425-435.
- Erdmann, B., Gerst, H., Lenz, D., Bähr, V. and Bernhardt, R., 1995b. Zone-specific localization of cytochrome P45011B1 in the human adrenal cortex by PCR-derived riboprobes. *Histochemistry Cell Biol.* 104, 301-307.
- Ewen, K. M., Schiffler, B., Uhlmann-Schiffler, H., Bernhardt, R. and Hannemann, F., 2008. The endogenous adrenodoxin reductase-like flavoprotein arh1 supports heterologous cytochrome P450-dependent substrate conversions in *Schizosaccharomyces pombe*. *FEMS Yeast Res.* 8, 432-441.
- Fisher, A., Friel, E. C., Bernhardt, R., Gomez-Sanchez, C., Connell, J. M., Fraser, R. and Davies, E., 2001. Effects of 18-hydroxylated steroids on corticosteroid production by human aldosterone synthase and 11beta-hydroxylase. *J Clin Endocrinol Metab.* 86, 4326-4329.
- Forsburg, S. L., 1993. Comparison of *Schizosaccharomyces pombe* expression systems. *Nucleic Acids Res.* 21, 2955-2956.

- Fosse, P., Rene, B., Charra, M., Paoletti, C. and Saucier, J. M., 1992. Stimulation of topoisomerase II-mediated DNA cleavage by ellipticine derivatives: structure-activity relationship. *Mol Pharmacol.* 42, 590-595.
- Frei, E., Bieler, C. A., Arlt, V. M., Wiessler, M. and Stiborova, M., 2002. Covalent binding of the anticancer drug ellipticine to DNA in V79 cells transfected with human cytochrome P450 enzymes. *Biochem Pharmacol.* 64, 289-295.
- Fried, J., Thom, R. W., Perlman, D., Herz, J. E. and Bormann, A., 1955. The use of microorganisms in the synthesis of steroid hormones and hormone analogues. *Recent Prog Horm Res.* 11, 149-181.
- Furst, W., 1959. Therapeutic re-orientation in some depressive states: clinical evaluation of a new mono-amine oxidase inhibitor (W-1554-A, phenelzine, Nardil). *Am J Psychiatry.* 116, 429-434.
- Ganong, W. F., 1993. Blood, pituitary, and brain renin-angiotensin systems and regulation of secretion of anterior pituitary gland. *Front Neuroendocrinol.* 14, 233-249.
- Goss, P. E., Powles, T. J., Dowsett, M., Hutchison, G., Brodie, A. M., Gazet, J. C. and Coombes, R. C., 1986. Treatment of advanced postmenopausal breast cancer with an aromatase inhibitor, 4-hydroxyandrostenedione: phase II report. *Cancer Res.* 46, 4823-4826.
- Gotoh, O., 1992. Substrate recognition sites in cytochrome P450 family 2 (CYP2) proteins inferred from comparative analyses of amino acid and coding nucleotide sequences. *J Biol Chem.* 267, 83-90.
- Green, H. and Erickson, R. W., 1962. Further studies with tranlycypromine (monamine oxidase inhibitor) and its interaction with reserpine in rat brain. *Arch Int Pharmacodyn Ther.* 135, 407-425.
- Grinberg, A. V., Hannemann, F., Schiffler, B., Muller, J., Heinemann, U. and Bernhardt, R., 2000. Adrenodoxin: structure, stability, and electron transfer properties. *Proteins.* 40, 590-612.
- Gross, B. A., Mindea, S. A., Pick, A. J., Chandler, J. P. and Batjer, H. H., 2007. Medical management of Cushing disease. *Neurosurg Focus.* 23, E10.
- Hagan, I. M. and Petersen, J., 2000. The microtubule organizing centers of *Schizosaccharomyces pombe*. *Curr Top Dev Biol.* 49, 133-159.
- Hagemann (1990). Gentechnologische Arbeitsmethoden.
- Hakki, T. and Bernhardt, R., 2006. CYP17- and CYP11B-dependent steroid hydroxylases as drug development targets. *Pharmacol Ther.* 111, 27-52.

- Hakki, T., Zearo, S., Dragan, C. A., Bureik, M. and Bernhardt, R., 2008. Coexpression of redox partners increases the hydrocortisone (cortisol) production efficiency in CYP11B1 expressing fission yeast *Schizosaccharomyces pombe*. *J Biotechnol.* 133, 351-359.
- Hampf, M., Dao, N. T., Hoan, N. T. and Bernhardt, R., 2001. Unequal crossing-over between aldosterone synthase and 11beta-hydroxylase genes causes congenital adrenal hyperplasia. *J Clin Endocrinol Metab.* 86, 4445-4452.
- Hampf, M., Swart, A. C. and Swart, P., 1996. Sequence of the 11 beta-hydroxylase gene from the Cape baboon (*Papio ursinus*). *Endocr Res.* 22, 495-499.
- Hanahan, D., 1983. Studies on transformation of *Escherichia coli* with plasmids. *J Mol Biol.* 166, 557-580.
- Hannemann, F., Bichet, A., Ewen, K. M. and Bernhardt, R., 2007. Cytochrome P450 systems-biological variations of electron transport chains. *Biochim Biophys Acta.* 1770, 330-344.
- Hanson, F. R., Mann, K. M., Nielson, E. D., Anderson, H. V., Brunner, M. P., Karnemaat, D. R., Colingworth, D. R. and Haines, W. J., 1953. Microbiological transformations of steroids. 8. Preparation of 17-a-hydroxycorticosterone. *J Amer Chem Soc.* 75, 5369-5370.
- Hartmann, R. W., Ehmer, P. B., Haidar, S., Hector, M., Jose, J., Klein, C. D., Seidel, S. B., Sergejew, T. F., Wachall, B. G., Wachter, G. A. and Zhuang, Y., 2002. Inhibition of CYP 17, a new strategy for the treatment of prostate cancer. *Arch Pharm (Weinheim).* 335, 119-128.
- Henry, J. A. and Antao, C. A., 1992. Suicide and fatal antidepressant poisoning. *Eur J Med.* 1, 343-348.
- Hoffken, K., Jonat, W., Possinger, K., Kolbel, M., Kunz, T., Wagner, H., Becher, R., Callies, R., Friederich, P., Willmanns, W. and et al., 1990. Aromatase inhibition with 4-hydroxyandrostenedione in the treatment of postmenopausal patients with advanced breast cancer: a phase II study. *J Clin Oncol.* 8, 875-880.
- Hoheisel, G., Schauer, J., Scherbaum, W. A. and Bornstein, S. R., 1998. The effect of corticotropin-releasing hormone (CRH) on the adrenal medulla in hypophysectomized rats. *Histol Histopathol.* 13, 81-87.
- Isobe, K., Nakai, T., Yashiro, T., Nanmoku, T., Yukimasa, N., Ikezawa, T., Suzuki, E., Takekoshi, K. and Nomura, F., 2000. Enhanced expression of mRNA coding for the

- adrenaline-synthesizing enzyme phenylethanolamine-N-methyl transferase in adrenaline-secreting pheochromocytomas. *J Urol.* 163, 357-362.
- Jezova, D., Ochedalski, T., Kiss, A. and Aguilera, G., 1998. Brain angiotensin II modulates sympathoadrenal and hypothalamic pituitary adrenocortical activation during stress. *J Neuroendocrinol.* 10, 67-72.
- Jones, A. B., Pare, C. M., Nicholson, W. J., Price, K. and Stacey, R. S., 1972. Brain amine concentrations after monoamine oxidase inhibitor administration. *Br Med J.* 1, 17-19.
- Kawamoto, T., Mitsuuchi, Y., Ohnishi, T., Ichikawa, Y., Yokoyama, Y., Sumimoto, H., Toda, K., Miyahara, K., Kuribayashi, I., Nakao, K. and et al., 1990a. Cloning and expression of a cDNA for human cytochrome P-450_{aldo} as related to primary aldosteronism. *Biochem Biophys Res Commun.* 173, 309-316.
- Kawamoto, T., Mitsuuchi, Y., Toda, K., Miyahara, K., Yokoyama, Y., Nakao, K., Hosoda, K., Yamamoto, Y., Imura, H. and Shizuta, Y., 1990b. Cloning of cDNA and genomic DNA for human cytochrome P-450_{11 beta}. *FEBS Lett.* 269, 345-349.
- Laemmli, U. K., 1970. Cleavage of structural proteins during the assembly of the head of bacteriophage T4. *Nature.* 227, 680-685.
- Lambeth, J. D., Seybert, D. W., Lancaster, J. R., Jr., Salerno, J. C. and Kamin, H., 1982. Steroidogenic electron transport in adrenal cortex mitochondria. *Mol Cell Biochem.* 45, 13-31.
- Lang, B. F., Cedergren, R. and Gray, M. W., 1987. The mitochondrial genome of the fission yeast, *Schizosaccharomyces pombe*. Sequence of the large-subunit ribosomal RNA gene, comparison of potential secondary structure in fungal mitochondrial large-subunit rRNAs and evolutionary considerations. *Eur J Biochem.* 169, 527-537.
- Lifton, R. P., Dluhy, R. G., Powers, M., Rich, G. M., Cook, S., Ulick, S. and Lalouel, J. M., 1992. A chimaeric 11 beta-hydroxylase/aldosterone synthase gene causes glucocorticoid-remediable aldosteronism and human hypertension. *Nature.* 355, 262-265.
- Lijnen, P. J., Petrov, V. V. and Fagard, R. H., 2000. Induction of cardiac fibrosis by angiotensin II. *Methods Find Exp Clin Pharmacol.* 22, 709-723.
- Lima, L. and Sourkes, T. L., 1987. Effect of corticotropin-releasing factor on adrenal DBH and PNMT activity. *Peptides.* 8, 437-441.
- Lin, T., Pan, K., Mordenti, J. and Pan, L., 2007. In vitro assessment of cytochrome P450 inhibition: strategies for increasing LC/MS-based assay throughput using a one-point

- IC(50) method and multiplexing high-performance liquid chromatography. *J Pharm Sci.* 96, 2485-2493.
- Lin, Y. Y. and Smith, L. L., 1970. Microbial hydroxylations. VII. Kinetic studies on the hydroxylation of 19-norsteroids by *Curvularia lunata*. *Biochim Biophys Acta.* 218, 515-525.
- Linden, C. H., Rumack, B. H. and Strehlke, C., 1984. Monoamine oxidase inhibitor overdose. *Ann Emerg Med.* 13, 1137-1144.
- Lisurek, M. and Bernhardt, R., 2004. Modulation of aldosterone and cortisol synthesis on the molecular level. *Mol Cell Endocrinol.* 215, 149-159.
- MacConnachie, A. A., Kelly, K. F., McNamara, A., Loughlin, S., Gates, L. J., Inglis, G. C., Jamieson, A., Connell, J. M. and Haites, N. E., 1998. Rapid diagnosis and identification of cross-over sites in patients with glucocorticoid remediable aldosteronism. *J Clin Endocrinol Metab.* 83, 4328-4331.
- MacFadyen, R. J., Barr, C. S. and Struthers, A. D., 1997. Aldosterone blockade reduces vascular collagen turnover, improves heart rate variability and reduces early morning rise in heart rate in heart failure patients. *Cardiovasc Res.* 35, 30-34.
- Mackell, M. A., Case, M. E. and Poklis, A., 1979. Fatal intoxication due to tranlycypromine. *Med Sci Law.* 19, 66-68.
- Madigan, M. P., Gao, Y. T., Deng, J., Pfeiffer, R. M., Chang, B. L., Zheng, S., Meyers, D. A., Stanczyk, F. Z., Xu, J. and Hsing, A. W., 2003. CYP17 polymorphisms in relation to risks of prostate cancer and benign prostatic hyperplasia: a population-based study in China. *Int J Cancer.* 107, 271-275.
- Mantero, F. and Lucarelli, G., 2000. Aldosterone antagonists in hypertension and heart failure. *Ann Endocrinol (Paris).* 61, 52-60.
- Matsukawa, N., Nonaka, Y., Ying, Z., Higaki, J., Ogihara, T. and Okamoto, M., 1990. Molecular cloning and expression of cDNAs encoding rat aldosterone synthase: variants of cytochrome P-450(11 beta). *Biochem Biophys Res Commun.* 169, 245-252.
- Maundrell, K., 1990. nmt1 of fission yeast. A highly transcribed gene completely repressed by thiamine. *J Biol Chem.* 265, 10857-10864.
- Megges, R., Müller-Frohne, M., Pfeil, D. and Ruckpaul, K. (1990). Microbial steroid hydroxylation enzymes in glucocorticoid production. Frontiers in Biotransformation, Vol. 3. K. Ruckpaul and H. Rein. Berlin, Akademie Verlag: 204-251.

- Migeon, C. J. and Donohoue, P. A., 1991. Congenital adrenal hyperplasia caused by 21-hydroxylase deficiency. Its molecular basis and its remaining therapeutic problems. *Endocrinol Metab Clin North Am.* 20, 277-296.
- Miller, W. L., 1988. Molecular biology of steroid hormone synthesis. *Endocr Rev.* 9, 295-318.
- Miller, W. L. and Tyrell, J. B. (1995). The adrenal cortex. *Endocrinology and Metabolism*. P. Felig, J. Baxter and L. Frohman. New York, USA, McGraw-Hill Press: 555-711.
- Min, L., Takemori, H., Nonaka, Y., Katoh, Y., Doi, J., Horike, N., Osamu, H., Raza, F. S., Vinson, G. P. and Okamoto, M., 2004. Characterization of the adrenal-specific antigen IZA (inner zone antigen) and its role in the steroidogenesis. *Mol Cell Endocrinol.* 215, 143-148.
- Minnaard-Huiban, M., Emmen, J. M., Roumen, L., Beugels, I. P., Cohuet, G. M., van Essen, H., Ruijters, E., Pieterse, K., Hilbers, P. A., Ottenheijm, H. C., Plate, R., de Gooyer, M. E., Smits, J. F. and Hermans, J. J., 2008. Fadrozole reverses cardiac fibrosis in spontaneously hypertensive heart failure rats: discordant enantioselectivity versus reduction of plasma aldosterone. *Endocrinology.* 149, 28-31.
- Mitani, F., Mukai, K., Miyamoto, H., Suematsu, M. and Ishimura, Y., 2003. The undifferentiated cell zone is a stem cell zone in adult rat adrenal cortex. *Biochim Biophys Acta.* 1619, 317-324.
- Mitani, F., Shimizu, T., Ueno, R., Ishimura, Y., Izumi, S., Komatsu, N. and Watanabe, K., 1982. Cytochrome P-450_{11β} and P-450_{scc} in adrenal cortex: zonal distribution and intramitochondrial localization by the horseradish peroxidase-labeled antibody method. *J Histochem Cytochem.* 30, 1066-1074.
- Miyoshi, T., Kanoh, J., Saito, M. and Ishikawa, F., 2008. Fission yeast Pot1-Tpp1 protects telomeres and regulates telomere length. *Science.* 320, 1341-1344.
- Monnot, M., Mauffret, O., Simon, V., Lescot, E., Psaume, B., Saucier, J. M., Charra, M., Belehradek, J., Jr. and Femandjian, S., 1991. DNA-drug recognition and effects on topoisomerase II-mediated cytotoxicity. A three-mode binding model for ellipticine derivatives. *J Biol Chem.* 266, 1820-1829.
- Moreno, S., Klar, A. and Nurse, P., 1991. Molecular genetic analysis of fission yeast *Schizosaccharomyces pombe*. *Methods Enzymol.* 194, 795-823.
- Mornet, E., Dupont, J., Vitek, A. and White, P. C., 1989. Characterization of two genes encoding human steroid 11 beta- hydroxylase (P-450(11) beta). *J Biol Chem.* 264, 20961-20967.

- Moser, B. A. and Russell, P., 2000. Cell cycle regulation in *Schizosaccharomyces pombe*. *Curr Opin Microbiol.* 3, 631-636.
- Munjack, D. J., 1984. The treatment of phenelzine-induced hypotension with salt tablets: case report. *J Clin Psychiatry.* 45, 89-90.
- Murck, H., Held, K., Ziegenbein, M., Kunzel, H., Koch, K. and Steiger, A., 2003. The renin-angiotensin-aldosterone system in patients with depression compared to controls--a sleep endocrine study. *BMC Psychiatry.* 3, 15.
- Naganuma, H., Ojima, M. and Sasano, N., 1988. 11 beta-Hydroxylase in mitochondrial fractions of functioning and non- functioning adrenocortical tumors. *Tohoku J Exp Med.* 155, 81-96.
- Nakagawa, Y., Yamada, M., Ogawa, H. and Igarashi, Y., 1995. Missense mutation in CYP11B1 (CGA[Arg-384]-->GGA[Gly]) causes steroid 11 beta-hydroxylase deficiency. *Eur J Endocrinol.* 132, 286-289.
- New, M. I., 1992. Genetic disorders of adrenal hormone synthesis. *Horm Res.* 37, 22-33.
- New, M. I., Oberfield, S. E., Levine, L. S., Dupont, B., Pollack, M., Gill, J. R., Jr. and Bartter, F. C., 1980. Autosomal dominant transmission and absence of HLA linkage in dexamethasone suppressible hyperaldosteronism. *Lancet.* 1, 550-551.
- Nguyen, H. H., Hannemann, F., Hartmann, M. F., Wudy, S. A. and Bernhardt, R., 2008. Aldosterone synthase deficiency caused by a homozygous L451F mutation in the CYP11B2 gene. *Mol Genet Metab.* 93, 458-467.
- Nonaka, Y., Fujii, T., Kagawa, N., Waterman, M. R., Takemori, H. and Okamoto, M., 1998. Structure/function relationship of CYP11B1 associated with Dahl's salt-resistant rats--expression of rat CYP11B1 and CYP11B2 in *Escherichia coli*. *Eur J Biochem.* 258, 869-878.
- Nonaka, Y., Takemori, H., Halder, S. K., Sun, T., Ohta, M., Hatano, O., Takakusu, A. and Okamoto, M., 1995. Frog cytochrome P-450 (11 beta,aldo), a single enzyme involved in the final steps of glucocorticoid and mineralocorticoid biosynthesis. *Eur J Biochem.* 229, 249-256.
- Nurse, P., 2000. A long twentieth century of the cell cycle and beyond. *Cell.* 100, 71-78.
- Ogishima, T., Shibata, H., Shimada, H., Mitani, F., Suzuki, H., Saruta, T. and Ishimura, Y., 1991. Aldosterone synthase cytochrome P-450 expressed in the adrenals of patients with primary aldosteronism. *J Biol Chem.* 266, 10731-10734.
- Ohlsson, G., Muller, J. R. and Schwartz, M., 1998. [Adrenogenital syndrome--molecular biology and prenatal diagnosis]. *Ugeskr Laeger.* 160, 803-807.

- Ohnaka, K. and Takayanagi, R., 2007. [Hormone replacement Up-to-date. Adrenopause and DHEA replacement therapy]. *Clin Calcium*. 17, 1334-1340.
- Pascoe, L., Curnow, K. M., Slutsker, L., Connell, J. M., Speiser, P. W., New, M. I. and White, P. C., 1992. Glucocorticoid-suppressible hyperaldosteronism results from hybrid genes created by unequal crossovers between CYP11B1 and CYP11B2. *Proc Natl Acad Sci U S A*. 89, 8327-8331.
- Pascoe, L., Jeunemaitre, X., Lebrethon, M. C., Curnow, K. M., Gomez-Sanchez, C. E., Gasc, J. M., Saez, J. M. and Corvol, P., 1995. Glucocorticoid-suppressible hyperaldosteronism and adrenal tumors occurring in a single French pedigree. *J Clin Invest*. 96, 2236-2246.
- Pennisi, E., 2003. Bioinformatics. Gene counters struggle to get the right answer. *Science*. 301, 1040-1041.
- Peters, F. T., Dragan, C. A., Wilde, D. R., Meyer, M. R., Zapp, J., Bureik, M. and Maurer, H. H., 2007. Biotechnological synthesis of drug metabolites using human cytochrome P450 2D6 heterologously expressed in fission yeast exemplified for the designer drug metabolite 4'-hydroxymethyl-alpha-pyrrolidinobutyrophenone. *Biochem Pharmacol*. 74, 511-520.
- Peters, J., Hampf, M., Peters, B. and Bernhardt, R., Eds. (1998). Molekularbiologie, Klinik und Therapie steroidbedingter Hypertonien. Handbuch der Molekularen Medizin. Berlin/ Heidelberg/ New York, Springer-Verlag.
- Pikuleva, I. A., Bjorkhem, I. and Waterman, M. R., 1997. Expression, purification, and enzymatic properties of recombinant human cytochrome P450c27 (CYP27). *Arch Biochem Biophys*. 343, 123-130.
- Pitt, B., Williams, G., Remme, W., Martinez, F., Lopez-Sendon, J., Zannad, F., Neaton, J., Roniker, B., Hurley, S., Burns, D., Bittman, R. and Kleiman, J., 2001. The EPHEBUS trial: eplerenone in patients with heart failure due to systolic dysfunction complicating acute myocardial infarction. Eplerenone Post-AMI Heart Failure Efficacy and Survival Study. *Cardiovasc Drugs Ther*. 15, 79-87.
- Pitt, B., Zannad, F., Remme, W. J., Cody, R., Castaigne, A., Perez, A., Palensky, J. and Wittes, J., 1999. The effect of spironolactone on morbidity and mortality in patients with severe heart failure. Randomized Aldactone Evaluation Study Investigators. *N Engl J Med*. 341, 709-717.
- Porter, T. D., 1991. An unusual yet strongly conserved flavoprotein reductase in bacteria and mammals. *Trends Biochem Sci*. 16, 154-158.

- Ramires, F. J., Sun, Y. and Weber, K. T., 1998. Myocardial fibrosis associated with aldosterone or angiotensin II administration: attenuation by calcium channel blockade. *J Mol Cell Cardiol.* 30, 475-483.
- Reid, D. D. and Kerr, W. C., 1969. Phenelzine poisoning responding to phenothiazine. *Med J Aust.* 2, 1214-1215.
- Roumen, L., Sanders, M. P., Pieterse, K., Hilbers, P. A., Plate, R., Custers, E., de Gooyer, M., Smits, J. F., Beugels, I., Emmen, J., Ottenheijm, H. C., Leysen, D. and Hermans, J. J., 2007. Construction of 3D models of the CYP11B family as a tool to predict ligand binding characteristics. *J Comput Aided Mol Des.* 21, 455-471.
- Sambrook, J. and Russell, D. W. (2001). Molecular Cloning. A Laboratory Manual, Cold Spring Harbor Laboratory Press, Cold Spring Harbor, NY.
- Sandler, S. A., 1959. Iproniazid used in attempted suicide. *Dis Nerv Syst.* 20, 79.
- Sanger, F., Nicklen, S. and Coulson, A. R., 1977. DNA sequencing with chain-terminating inhibitors. *Proc Natl Acad Sci U S A.* 74, 5463-5467.
- Schiffler, B., Bureik, M., Reinle, W., Muller, E. C., Hannemann, F. and Bernhardt, R., 2004. The adrenodoxin-like ferredoxin of *Schizosaccharomyces pombe* mitochondria. *J Inorg Biochem.* 98, 1229-1237.
- Schiffler, B., Kiefer, M., Wilken, A., Hannemann, F., Adolph, H. W. and Bernhardt, R., 2001. The interaction of bovine adrenodoxin with CYP11A1 (cytochrome P450_{scc}) and CYP11B1 (cytochrome P450_{11beta}). Acceleration of reduction and substrate conversion by site-directed mutagenesis of adrenodoxin. *J Biol Chem.* 276, 36225-36232.
- Schuster, I. and Bernhardt, R., 2007. Inhibition of cytochromes p450: existing and new promising therapeutic targets. *Drug Metab Rev.* 39, 481-499.
- Shelton Clauson, A., Elliott, E. S., Watson, B. D. and Treacy, J., 2004. Coadministration of phenelzine and methylphenidate for treatment-resistant depression. *Ann Pharmacother.* 38, 508.
- Shuman, S., 1994. Novel approach to molecular cloning and polynucleotide synthesis using vaccinia DNA topoisomerase. *J Biol Chem.* 269, 32678-32684.
- Singh, M. P., Hill, G. C., Peoc'h, D., Rayner, B., Imbach, J. L. and Lown, J. W., 1994. High-field NMR and restrained molecular modeling studies on a DNA heteroduplex containing a modified apurinic abasic site in the form of covalently linked 9-aminoellipticine. *Biochemistry.* 33, 10271-10285.

- Sipiczki, M., 2000. Where does fission yeast sit on the tree of life? *Genome Biol.* 1, REVIEWS1011.
- Smith, C. L., Matsumoto, T., Niwa, O., Klco, S., Fan, J. B., Yanagida, M. and Cantor, C. R., 1987. An electrophoretic karyotype for *Schizosaccharomyces pombe* by pulsed field gel electrophoresis. *Nucleic Acids Res.* 15, 4481-4489.
- Soberman, J. E. and Weber, K. T., 2000. Spironolactone in congestive heart failure. *Curr Hypertens Rep.* 2, 451-456.
- Sokolski, K. N. and Brown, B. J., 2006. Quetiapine for insomnia associated with refractory depression exacerbated by phenelzine. *Ann Pharmacother.* 40, 567-570.
- Sonino, N. and Boscaro, M., 1999. Medical therapy for Cushing's disease. *Endocrinol Metab Clin North Am.* 28, 211-222.
- Stiborova, M., Bieler, C. A., Wiessler, M. and Frei, E., 2001. The anticancer agent ellipticine on activation by cytochrome P450 forms covalent DNA adducts. *Biochem Pharmacol.* 62, 1675-1684.
- Stowasser, M. and Gordon, R. D., 2001. Familial hyperaldosteronism. *J Steroid Biochem Mol Biol.* 78, 215-229.
- Stowasser, M., Gordon, R. D., Tunny, T. J., Klemm, S. A., Finn, W. L. and Krek, A. L., 1992. Familial hyperaldosteronism type II: five families with a new variety of primary aldosteronism. *Clin Exp Pharmacol Physiol.* 19, 319-322.
- Straathof, A. J., Panke, S. and Schmid, A., 2002. The production of fine chemicals by biotransformations. *Curr Opin Biotechnol.* 13, 548-556.
- Sutherland, D. J., Ruse, J. L. and Laidlaw, J. C., 1966. Hypertension, increased aldosterone secretion and low plasma renin activity relieved by dexamethasone. *Can Med Assoc J.* 95, 1109-1119.
- Suzuki, K., Sanga, K., Chikaoka, Y. and Itagaki, E., 1993. Purification and properties of cytochrome P-450 (P-450_{lun}) catalyzing steroid 11 beta-hydroxylation in *Curvularia lunata*. *Biochim Biophys Acta.* 1203, 215-223.
- Takeda, J., Uematsu, N., Shiraishi, S., Toyoshima, M., Matsumoto, T. and Niwa, O., 2008. Radiation induction of delayed recombination in *Schizosaccharomyces pombe*. *DNA Repair.* 9, 9.
- Tamaoki, B., 1973. Steroidogenesis and cell structure. Biochemical pursuit of sites of steroid biosynthesis. *J Steroid Biochem.* 4, 89-118.

- Thai, H. M., Van, H. T., Gaballa, M. A., Goldman, S. and Raya, T. E., 1999. Effects of AT1 receptor blockade after myocardial infarct on myocardial fibrosis, stiffness, and contractility. *Am J Physiol.* 276, H873-880.
- Toh-e, A., 1995. Construction of a marker gene cassette which is repeatedly usable for gene disruption in yeast. *Curr Genet.* 27, 293-297.
- Toone, W. M. and Jones, N., 1998. Stress-activated signalling pathways in yeast. *Genes Cells.* 3, 485-498.
- Tsybouleva, N., Zhang, L., Chen, S., Patel, R., Lutucuta, S., Nemoto, S., DeFreitas, G., Entman, M., Carabello, B. A., Roberts, R. and Marian, A. J., 2004. Aldosterone, through novel signaling proteins, is a fundamental molecular bridge between the genetic defect and the cardiac phenotype of hypertrophic cardiomyopathy. *Circulation.* 109, 1284-1291.
- Ulmschneider, S., Muller-Vieira, U., Klein, C. D., Antes, I., Lengauer, T. and Hartmann, R. W., 2005a. Synthesis and evaluation of (pyridylmethylene)tetrahydronaphthalenes/-indanes and structurally modified derivatives: potent and selective inhibitors of aldosterone synthase. *J Med Chem.* 48, 1563-1575.
- Ulmschneider, S., Muller-Vieira, U., Mitrenga, M., Hartmann, R. W., Oberwinkler-Marchais, S., Klein, C. D., Bureik, M., Bernhardt, R., Antes, I. and Lengauer, T., 2005b. Synthesis and evaluation of imidazolymethylenetetrahydronaphthalenes and imidazolymethyleneindanes: potent inhibitors of aldosterone synthase. *J Med Chem.* 48, 1796-1805.
- Vinson, G. P., 2004. Glomerulosa function and aldosterone synthesis in the rat. *Mol Cell Endocrinol.* 217, 59-65.
- Wada, A., Ohnishi, T., Nonaka, Y., Okamoto, M. and Yamano, T., 1985. Synthesis of aldosterone by a reconstituted system of cytochrome P- 45011 beta from bovine adrenocortical mitochondria. *J Biochem (Tokyo).* 98, 245-256.
- Wagner, M. J., Ge, Y., Siciliano, M. and Wells, D. E., 1991. A hybrid cell mapping panel for regional localization of probes to human chromosome 8. *Genomics.* 10, 114-125.
- Waring, W. S. and Wallace, W. A., 2007. Acute myocarditis after massive phenelzine overdose. *Eur J Clin Pharmacol.* 63, 1007-1009.
- Weber, K. T. and Villarreal, D., 1993. Aldosterone and antialdosterone therapy in congestive heart failure. *Am J Cardiol.* 71, 3A-11A.

- Weindel, K., Lewicka, S. and Vecsei, P., 1991. Interference of C17-spirosteroids with late steps of aldosterone biosynthesis. Structure-activity studies. *Arzneimittelforschung*. 41, 1082-1091.
- White, P. C., 2004. Aldosterone synthase deficiency and related disorders. *Mol Cell Endocrinol*. 217, 81-87.
- White, P. C., Dupont, J., New, M. I., Leiberman, E., Hochberg, Z. and Rosler, A., 1991. A mutation in CYP11B1 (Arg-448----His) associated with steroid 11 beta- hydroxylase deficiency in Jews of Moroccan origin. *J Clin Invest*. 87, 1664-1667.
- White, P. C. and Speiser, P. W., 1994. Steroid 11 beta-hydroxylase deficiency and related disorders. *Endocrinol Metab Clin North Am*. 23, 325-339.
- Wiseman, L. R. and Goa, K. L., 1996. Formestane. A review of its pharmacological properties and clinical efficacy in the treatment of postmenopausal breast cancer. *Drugs Aging*. 9, 292-306.
- Wong, D. L., 2006. Epinephrine biosynthesis: hormonal and neural control during stress. *Cell Mol Neurobiol*. 26, 891-900.
- Wood, V., Gwilliam, R., Rajandream, M. A., Lyne, M., Lyne, R., Stewart, A., Sgouros, J., Peat, N., Hayles, J., Baker, S., Basham, D., Bowman, S., Brooks, K., Brown, D., Brown, S., Chillingworth, T., Churcher, C., Collins, M., Connor, R., Cronin, A., Davis, P., Feltwell, T., Fraser, A., Gentles, S., Goble, A., Hamlin, N., Harris, D., Hidalgo, J., Hodgson, G., Holroyd, S., Hornsby, T., Howarth, S., Huckle, E. J., Hunt, S., Jagels, K., James, K., Jones, L., Jones, M., Leather, S., McDonald, S., McLean, J., Mooney, P., Moule, S., Mungall, K., Murphy, L., Niblett, D., Odell, C., Oliver, K., O'Neil, S., Pearson, D., Quail, M. A., Rabinowitsch, E., Rutherford, K., Rutter, S., Saunders, D., Seeger, K., Sharp, S., Skelton, J., Simmonds, M., Squares, R., Squares, S., Stevens, K., Taylor, K., Taylor, R. G., Tivey, A., Walsh, S., Warren, T., Whitehead, S., Woodward, J., Volckaert, G., Aert, R., Robben, J., Grymonprez, B., Weltjens, I., Vanstreels, E., Rieger, M., Schafer, M., Muller-Auer, S., Gabel, C., Fuchs, M., Fritzc, C., Holzer, E., Moestl, D., Hilbert, H., Borzym, K., Langer, I., Beck, A., Lehrach, H., Reinhardt, R., Pohl, T. M., Eger, P., Zimmermann, W., Wedler, H., Wambutt, R., Purnelle, B., Goffeau, A., Cadieu, E., Dreano, S., Gloux, S., Lelaure, V., Mottier, S., Galibert, F., Aves, S. J., Xiang, Z., Hunt, C., Moore, K., Hurst, S. M., Lucas, M., Rochet, M., Gaillardin, C., Tallada, V. A., Garzon, A., Thode, G., Daga, R. R., Cruzado, L., Jimenez, J., Sanchez, M., del Rey, F., Benito, J., Dominguez, A., Revuelta, J. L., Moreno, S., Armstrong, J., Forsburg, S. L., Cerrutti, L., Lowe, T.,

- McCombie, W. R., Paulsen, I., Potashkin, J., Shpakovski, G. V., Ussery, D., Barrell, B. G. and Nurse, P., 2002. The genome sequence of *Schizosaccharomyces pombe*. Nature. 415, 871-880.
- Yamazaki, S., Sato, K., Sahara, K., Sakaguchi, M., Mihara, K. and Omura, T., 1993. Importance of the proline-rich region following signal-anchor sequence in the formation of correct conformation of microsomal cytochrome P-450s. J Biochem. 114, 652-657.
- Yanagibashi, K. and Hall, P. F., 1986. Role of electron transport in the regulation of the lyase activity of C21 side-chain cleavage P-450 from porcine adrenal and testicular microsomes. J Biol Chem. 261, 8429-8433.
- Young, M. and Funder, J. W., 2000. Aldosterone and the heart. Trends Endocrinol Metab. 11, 224-226.
- Young, W. F., Jr., 2007. Adrenal causes of hypertension: pheochromocytoma and primary aldosteronism. Rev Endocr Metab Disord. 8, 309-320.
- Zachmann, M., Tassinari, D. and Prader, A., 1983. Clinical and biochemical variability of congenital adrenal hyperplasia due to 11 beta-hydroxylase deficiency. A study of 25 patients. J Clin Endocrinol Metab. 56, 222-229.
- Zakelj-Mavric, M., Plemenitas, A., Komel, R. and Belic, I., 1990. 11 beta-hydroxylation of steroids by *Cochliobolus lunatus*. J Steroid Biochem. 35, 627-629.
- Zhang, J. H., Chung, T. D. and Oldenburg, K. R., 1999. A Simple Statistical Parameter for Use in Evaluation and Validation of High Throughput Screening Assays. J Biomol Screen. 4, 67-73.
- Zhou, B. B. and Elledge, S. J., 2000. The DNA damage response: putting checkpoints in perspective. Nature. 408, 433-439.
- Zöllner, A., Kagawa, N., Waterman, M. R., Nonaka, Y., Takio, K., Shiro, Y., Hannemann, F. and Bernhardt, R., 2008. Purification and functional characterization of human 11beta hydroxylase expressed in *Escherichia coli*. Febs J. 275, 799-810.
- Zuidweg, M. H., 1968. Hydroxylation of Reichstein's compound S with cell-free preparations from *Curvularia lunata*. Biochim Biophys Acta. 152, 144-158.

6. Appendix

6.1. Contributions to international meetings

1. **July 2004:** Workshop “3000 and more Cytochromes P450: where to go now?” Saarbrücken, Germany.
2. **June 2007:** 15th International conference on Cytochromes P450, Bled, Slovenia.
Tarek Hakki, Silvia Zearo, Calin-Aurel Dragan, Matthias Bureik & Rita Bernhardt (Poster presentation)
3. **June 2008:** 9th International Symposium on Cytochrome P450 Biodiversity and Biotechnology, Nice, France
 - **Tarek Hakki**, Matthias Bureik & Rita Bernhardt (Poster presentation)
 - Spela Petric, Tarek Hakki, Rita Bernhardt & **Bronislava Cresnar** (Oral presentation)
4. **July 2008:** 17th International Symposium on Microsomes and Drug Oxidations, Saratoga Sprins, New York, USA.
 - Cornelia Virus, Tarek Hakki, Matthias Bureik, Michael Lisurek, Calin-Aurel Dragan, Benjamin Böttner, Iris Antes, Frank Hannemann and **Rita Bernhardt.** (Oral presentation)

6.2. Index of Figures

Figure	Description	Page
1.1.	Reaction generally catalysed by cytochrome P450.	1
1.2	The mitochondrial steroid hydroxylase systems.	2
1.3.	The microsomal steroid hydroxylase systems.	3
1.4.	The role of cytochromes P450 in the biosynthesis of steroid hormones in the human adrenal cortex.	3
1.5.	Steroid hydroxylases as drug development targets.	5
1.6.	CYP11B1-dependent hydroxylation reaction.	7
1.7.	CYP11B2 converts 11-deoxycorticosterone via corticosterone and 18-OH corticosterone to aldosterone.	8
1.8.	The renin– angiotensin–aldosterone system.	10
1.9.	Superposition of the ribbon structures of the homology models of human CYP11B1 (green) and CYP11B2 (orange) (Belkina <i>et al.</i> 2001).	12
1.10.	Picture of the fission yeast <i>Schizosaccharomyces pombe</i> from Steve’s place.	19
2.1.	pNMT1-TOPO vector map (Invitrogen; Carlsbad, CA).	27
2.2.	pREP42 Pk C vector map.	28
2.3.	The Mega Block plates from VWR used during this work.	30
2.4.	The pipetting robot (Tecan Aquarius, Swizerland).	30
2.5.	TOPO TA Cloning® of <i>Taq</i> -amplified DNA (Invitrogen; Carlsbad, CA).	31
2.6.	The construction of a modified 1.5 ml tube (tip-tube).	40
3.1.	HPLC chromatogram of CYP11B1-dependent bioconversion of RSS into F carried out using the tip-tube format.	48
3.2.	Z-positions for a tube.	50
3.3.	Tecan working area during the extraction process.	53
3.4.	HPLC chromatograms of extracted steroids obtained using the automated extraction method applied in a 96-well plate.	54
3.5.	HPLC chromatograms of steroids extracted automatically or manually.	55
3.6.	Direct comparison of the recovered steroids obtained using different extraction methods in comparison with the same amount of steroids that were given on the HPLC without extraction.	56
3.7.	Steroid 11 β -hydroxylation activity of SZ1 in a 96-well plate format.	57
3.8.	HPLC Chromatograms show the separation of RSS and F under different	58

HPLC conditions.	
3.9. HPLC chromatogram of the CYP11B1-dependent bioconversion of RSS into F carried out using the 96-well plate format.	59
3.10. Vector map of pCAD1_CYP11B1(Dragan <i>et al.</i> 2005).	61
3.11. Fission yeast TH1 plated on different EMM plates.	62
3.12. Steroid 11 β -hydroxylation activity of TH1 and SZ1.	63
3.13. The cloning strategy used to create the Adx_AdR expression vector pTH2.	64
3.14. A. Vector map of pTH2. Relevant restriction sites are shown, P nmt: <i>nmt1</i> promoter. B. Restriction analysis of pTH2 confirming the existence of the two expression cassettes.	65
3.15. Detection of AdR ^{WT} (A) and Adx ^{WT} (B) in mitochondrial lysates of strain TH175 by Western blot analysis.	67
3.16. Immunological detection of bovine adrenodoxin (Adx) expressed in <i>S. pombe</i> .	68
3.17. The biotransformation of RSS into F investigated in 66 wells using the newly developed hydroxylation assay.	69
3.18. Direct comparison of the bioconversion rates of fission yeast strains coexpressing CYP11B1 and electron transfer proteins.	70
3.19. The influence of cell density of the recombinant fission yeast on the hydrocortisone production.	71
3.20. Time course of the hydrocortisone production activity by SZ1 (CYP11B1) and TH75 (CYP11B1 + Adx + AdR).	73
3.21. HPLC chromatograms of CYP11B1-dependent substrate conversion using the novel strain in comparison with the parental strain.	73
3.22. HPLC Chromatograms show the separation of DOC and B under different HPLC parameters.	75
3.23. HPLC chromatogram of the CYP11B2-dependent bioconversion using the 96-well plate format.	77
3.24. Correlation between the concentration of ketoconazole and inhibition in different test media.	79
3.25. HPLC Chromatograms of the CYP11B2-dependent conversion of DOC into B using MB164 in the presence of positive and negative controls.	80

3.26.	Schematic overview of the 96-well plate during the screening assay of the investigated library (LOPAC).	81
3.27.	HPLC chromatograms show the separation of DOC and B using a high-speed column.	82
3.28.	HPLC Chromatograms of the CYP11B2-dependent bioconversion of DOC into B analysed using the high-speed column.	83
3.29.	HPLC chromatogram of an extracted sample that consists of water and DMSO.	83
3.30	Direct comparisons of the CYP11B2-dependent conversion rates of DOC into B during the screening assay.	84
3.31	HPLC chromatograms of CYP11B2-dependent bioconversion in the presence of Co_TH1 during the screening assay.	85
3.32.	Structures of the new CYP11B2 inhibitors identified during the screening assay in this work.	87
3.33	Distributions graph of the new inhibitors of CYP11B2 vs. their molecular weight.	88
3.34.	Cell viability shown as a percentage of control (DMSO).	89
3.35.	Autoradiographic detection of steroid hydroxylation activity.	91
3.36.	The inhibitory effect of Co_TH1 on the activity of CYP11B2.	92
3.37.	The inhibitory effect of Co_TH2 on the activity of CYP11B2.	93
3.38.	The inhibitory effect of Co_TH11 on the activity of CYP11B1 (opened symbols) and CYP11B2 (closed symbols).	93
4.1.	Schematic overview of the recombinant fission yeast types according to the availability of the electron transfer proteins in the fission yeast strains used in this study.	97
4.2.	Schematic overview of the recombinant fission yeast strain TH75.	99
4.3.	Schematic overview of the CYP11B2 testing strategy developed in this work.	101
4.4.	Pie chart depicting the composition of the investigated library.	105
4.5.	Schematic representation of catecholamine and adrenal hormone biosynthesis, and the speculated influence of an overdose of phenelzine (Co_TH9).	109

6.3. Index of Tables

Table	Description	Page
1.1.	Comparison of the yeast and mammalian recombinant systems for the development and analysis of potential selective inhibitors	18
2.1.	Composition of LB medium	23
2.2.	Composition of SOC medium	24
2.3.	Composition of EMM medium	24
2.4.	Composition of YEA medium	25
2.5.	Composition of 2X YEA with 25 % glycerol medium	25
2.6.	Microorganisms used in this work	26
2.7.	Adx expressing plasmids used in this work (Derouet-Hümbert <i>et al.</i> 2007)	29
3.1.	Steroid bioconversion parameters (tip-tube format)	48
3.2.	The steroid extraction script developed during this work.	51
3.3.	Steroid bioconversion parameters (96-well plat format)	57
3.4.	HPLC parameters to separate RSS and F in less than 5 min	59
3.5.	Fission yeast expression plasmids used in this work	66
3.6.	Fission yeast strains created in this work	66
3.7.	Optimised HPLC parameters to separate DOC and B within 3 min	76
3.8.	The IC ₅₀ values of CYP11B2 inhibitors determined using recombinant <i>S. pombe</i> strain MB164 (Bureik <i>et al.</i> 2004)	76
3.9.	The inhibition profiles of the CYP11B2 inhibitors tested using the six-point inhibition assay and the one-point assay developed in this work	84
3.10.	The new CYP11B2 inhibitors identified during the screening assay in this work.	86
3.11.	The inhibition profiles of the active compounds against CYP11B2 and CYP11B1 in the validation assay	90
4.1.	Selected long-standing pharmaceuticals that had been repositioned during or prior to 2004 (Ashburn and Thor 2004)	103

6.4. Materials and Methods

6.4.1. Stock solutions for EMM medium

o Vitamin stock solution (x1000)

Content	Amount [g/L]	Final concentration
Sodium pantothenate	1.00	4.2 mM
Nicotinic acid	10.00	81.2 mM
Inositol	10.00	55.5 mM
Biotin	0.01	40.8 μ M

o Salt stock solution (x50)

Content	Amount [g/L]	Final concentration
MgCl ₂ •6H ₂ O	52.500	0.26 M
CaCl ₂ •2H ₂ O	0.735	4.99 mM
KCl	50.000 g	0.67 M
Na ₂ SO ₄	2.000	14.10 mM

o Mineral stock solution (x10,000)

Content	Amount [g/L]	Final concentration
H ₃ BO ₃	5.0	80.90 mM
MnSO ₄	4.0	23.70 mM
ZnSO ₄ •7H ₂ O	4.0	13.90 mM
FeCl ₃ •6H ₂ O	2.0	7.40 mM
H ₂ MoO ₄	1.6	2.47 mM
KI	1.0	6.02 mM
CuSO ₄ •5H ₂ O	0.4	1.60 mM

Citric acid	10.0	47.60 mM
-------------	------	----------

6.4.2. Oligonucleotides

All primers used during this work were obtained from the company BioTeZ (Berlin-Buch, Deutschland) and purified via HPLC. The sequences as well as the purpose of each oligonucleotide used in this work are given below:

Code	Name	Purpose	Sequence (5'→3')
Pr_1	PR(_{Hsa} AdR_cra ven) _{for}	Forward primer for the amplification of _{Hsa} AdR with <i>NdeI</i> restriction site	GGC GGT GGC CAT ATG GCT TCG CGC TGC TGG
Pr_2	PR(_{Hsa} AdRXST OP_cra ven) _{rev}	Reverse primer for the amplification of _{Hsa} AdR with <i>XhoI</i> restriction site	GCC ACC GCC CTC GAG A GTG GCC CAG GAG GCG CAG
Pr_3	5'-hAdR	Forward primer for the amplification of _{Hsa} AdR	AGA GAG GGA TCC ATG GCT TCG CGC TGC TGG
Pr_4	hSdR3PK	Reverse primer for the amplification of _{Hsa} AdR	GTG GCC CAG GAG GAG GCG CAG C
Pr_5	NMT pombe Forward	Forward primer for the sequencing of cloned insert in pNMT1-TOPO vector	TTT CAA TCT CAT TCT CAC TTT CTG A
Pr_6	URA4 pombe reverse	Reverse primer for the sequencing of cloned insert in pNMT1-TOPO vector	ACA AGG CAT CGA CTT TTT CAA TA
Pr_7	PNMT1XhoI_F OR	Forward primer for the amplification of the <i>nm1</i> promoter with <i>XhoI</i> restriction site	AGA GAG AGA CTC GAG GAC AGA ATA AGT CAT CAG CGG TTG
Pr_8	ura4XhoI_REV	Reverse primer for the amplification of _{Hsa} AdR with <i>XhoI</i> restriction site	AGA GAG AGA CTC GAG ACA AGG CAT CGA CTT TTT CAA TA

Pr_9	K22-24Q (For)	Forward primer for the amplification of Adx (Colony PCR)	CAC TTT ATA AAC CGT GAT GGT GAA ACA TTA ACA ACC CAA GGA CAA ATT GGT GAC
Pr_10	Adx S117A rück	Reverse primer for the amplification of Adx (Colony PCR)	CAT ATC AAT GGC CTC TCT GGC
Pr_11	AdR_F	Forward primer for the sequencing of _{Hsa} AdR	ATG GCT TCG CGC TGC TGG CGC TG
Pr_12	AdR_R	Reverse primer for the sequencing of _{Hsa} AdR	GTG GCC CAG GAG GCG CAG CAT CT
Pr_13	AdR_F_+600	Forward primer for the sequencing of _{Hsa} AdR	CAC CTG GAG GCC CTC CTT TTG TGC

6.4.3. Library of pharmacologically active compounds

Lab_code	mol weight Structure	Name	Class	Action
Sigma_120693	195.22	DL-alpha-Methyl-p-tyrosine	Neurotransmission	Inhibitor
Sigma_144509	213.24	N-Phenylanthranilic acid	Cl- Channel	Blocker
Sigma_190047	373.23	S(-)-p-Bromotetramisole oxalate	Phosphorylation	Inhibitor
Sigma_194336	153.61	5-Aminovaleric acid hydrochloride	GABA	Antagonist
Sigma_211672	129.16	(±)-Nipecotic acid	GABA	Inhibitor
Sigma_246379	188.23	Azelaic acid	DNA Metabolism	Inhibitor
Sigma_246557	196.68	Tryptamine hydrochloride	Serotonin	Ligand
Sigma_265128	179.15	5-Fluoroindole-2-carboxylic acid	Glutamate	Antagonist
Sigma_291552	202.26	6-Methoxy-1,2,3,4-tetrahydro-9H-pyrido[3,4b]indole	Neurotransmission	Inhibitor
Sigma_861669	434.43	S-(4-Nitrobenzyl)-6-thioguanosine	Adenosine	Inhibitor
Sigma_861804	432.00	TMB-8 hydrochloride	Intracellular Calcium	Antagonist
Sigma_A 0152	94.12	4-Aminopyridine	K+ Channel	Blocker
Sigma_A 0257	676.83	Atropine sulfate	Cholinergic	Antagonist
Sigma_A 0382	366.42	Atropine methyl nitrate	Cholinergic	Antagonist
Sigma_A 0384	270.31	Arcaïne sulfate	Glutamate	Antagonist
Sigma_A 0430	137.57	1-Aminocyclopropanecarboxylic acid hydrochloride	Glutamate	Agonist
Sigma_A 0500	59.07	Acetamide	Biochemistry	Inhibitor
Sigma_A 0666	349.28	N-(4-Aminobutyl)-5-chloro-2-naphthalenesulfonamide hydrochloride	Intracellular Calcium	Antagonist
Sigma_A 0760	101.11	L-azetidine-2-carboxylic acid	Biochemistry	Inhibitor
Sigma_A 0779	281.57	p-Aminoclonidine hydrochloride	Adrenoceptor	Agonist
Sigma_A 0788	136.15	3-aminobenzamide	Apoptosis	Inhibitor
Sigma_A 0937	319.27	(±)-Norepinephrine (+)bitartrate	Adrenoceptor	Agonist
Sigma_A 0966	212.21	4-Amino-1,8-naphthalimide	Apoptosis	Inhibitor
Sigma_R 0875	608.69	Reserpine	Serotonin	Inhibitor
Sigma_A 1260	187.71	Amantadine hydrochloride	Dopamine	Releaser
Sigma_A 1755	420.43	Aminophylline ethylenediamine	Adenosine	Antagonist
Sigma_A 1782	466.48	S-(p-Azidophenacyl)glutathione	Multi-Drug Resistance	Modulator
Sigma_A 1784	440.42	Aminopterin	Antibiotic	Inhibitor
Sigma_A 1824	218.26	N-Acetyl-5-hydroxytryptamine	Melatonin	Precursor
Sigma_A 1895	422.35	Aurintricarboxylic acid	Apoptosis	Inhibitor
Sigma_A 1910	183.10	(±)-2-Amino-4-phosphonobutyric acid	Glutamate	Antagonist
Sigma_A 1977	361.53	N-arachidonylglycine	Cannabinoid	Inhibitor
Sigma_A 2129	103.12	GABA	GABA	Agonist
Sigma_A 2169	267.25	3'-Azido-3'-deoxythymidine	Immune System	Inhibitor
Sigma_A 2251	195.69	Acetyl-beta-methylcholine chloride	Cholinergic	Agonist
Sigma_A 2385	244.21	5-azacytidine	DNA Metabolism	Inhibitor
Sigma_A 3085	299.77	5-(N-Ethyl-N-isopropyl)amiloride	Ion Pump	Blocker

Sigma_A 3134	256.26	3-Aminopropionitrile fumarate	Multi-Drug Resistance	Substrate
Sigma_A 3145	270.24	Apigenin	Cell Cycle	Inhibitor
Sigma_A 3539	175.62	Gabaculine hydrochloride	GABA	Inhibitor
Sigma_A 3595	392.24	AC 915 oxalate	Opioid	Ligand
Sigma_A 3711	326.44	AA-861	Leukotriene	Inhibitor
Sigma_A 3773	234.73	9-Amino-1,2,3,4-tetrahydroacridine hydrochloride	Cholinergic	Inhibitor
Sigma_A 3846	402.51	AL-8810	Prostaglandin	Antagonist
Sigma_A 3940	134.14	1-Aminobenzotriazole	Multi-Drug Resistance	Inhibitor
Sigma_A 4147	161.16	3-Amino-1-propanesulfonic acid sodium	GABA	Agonist
Sigma_A 4393	303.79	Apomorphine hydrochloride hemihydrate	Dopamine	Agonist
Sigma_A 4508	218.60	O-(Carboxymethyl)hydroxylamine hemihydrochloride	Biochemistry	Inhibitor
Sigma_A 4562	294.15	5-(N,N-Dimethyl)amiloride hydrochloride	Ion Pump	Blocker
Sigma_A 4638	277.27	Azathioprine	P2 Receptor	Inhibitor
Sigma_A 4669	225.21	Acyclovir	Immune System	Inhibitor
Sigma_A 4687	341.84	Amiprilose hydrochloride	Immune System	Modulator
Sigma_S 9318	465.80	Sandoz 58-035	Lipid	Inhibitor
Sigma_A 4910	169.07	(±)-2-Amino-3-phosphonopropionic acid	Glutamate	Antagonist
Sigma_A 5006	174.20	L-Arginine	Nitric Oxide	Precursor
Sigma_A 5157	225.18	(±)-2-Amino-7-phosphonoheptanoic acid	Glutamate	Antagonist
Sigma_A 5282	197.13	(±)-2-Amino-5-phosphonopentanoic acid	Glutamate	Antagonist
Sigma_A 5330	472.39	L-732,138	Tachykinin	Antagonist
Sigma_A 5376	180.16	Acetylsalicylic acid	Prostaglandin	Inhibitor
Sigma_A 5585	299.77	5-(N-Methyl-N-isobutyl)amiloride	Ion Pump	Blocker
Sigma_A 5626	197.73	Acetylthiocholine chloride	Cholinergic	Agonist
Sigma_A 5791	302.42	4-Androsten-4-ol-3,17-dione	Hormone	Inhibitor
Sigma_A 5879	281.01	2-(2-Aminoethyl)isothiourea dihydrobromide	Nitric Oxide	Inhibitor
Sigma_A 5909	313.83	N-Acetylprocainamide hydrochloride	Na ⁺ Channel	Blocker
Sigma_T 9034	537.70	Sodium Taurocholate	Multi-Drug Resistance	Modulator
Sigma_A 5922	214.22	Amifostine	Cell Stress	Inhibitor
Sigma_A 6011	222.25	Acetazolamide	Biochemistry	Inhibitor
Sigma_A 6134	236.11	Arecoline hydrobromide	Cholinergic	Agonist
Sigma_A 6351	345.47	A-315456	Adrenoceptor	Antagonist
Sigma_G 8543	377.49	GR 4661	Serotonin	Agonist
Sigma_A 6566	265.72	2-Hydroxysaclofen	GABA	Antagonist
Sigma_A 6671	385.51	Actinonin	Biochemistry	Inhibitor
Sigma_A 6770	454.45	Methotrexate	DNA Metabolism	Inhibitor
Sigma_A 6883	384.32	Atropine methyl bromide	Cholinergic	Antagonist
Sigma_A 6976	437.96	Amperozide hydrochloride	Serotonin	Ligand
Sigma_A 7009	246.25	Aminoguanidine hemisulfate	Nitric Oxide	Inhibitor
Sigma_A 7127	228.27	Agmatine sulfate	Imidazoline	Agonist
Sigma_A 7148	208.09	4-Aminobenzamidine dihydrochloride	Biochemistry	Inhibitor
Sigma_A 7162	139.09	3-Aminopropylphosphonic acid	GABA	Agonist
Sigma_A 7250	163.20	N-Acetyl-L-Cysteine	Glutamate	Antagonist
Sigma_A 7275	161.16	L-2-aminoadipic acid	Glutamate	Inhibitor

Sigma_A 7342	202.26	N-Acetyltryptamine	Melatonin	Agonist - Antagonist
Sigma_A 7410	266.09	Amiloride hydrochloride	Na ⁺ Channel	Blocker
Sigma_A 7655	266.34	(±)-Atenolol	Adrenoceptor	Antagonist
Sigma_A 7755	292.47	5alpha-Androstane-3alpha,17beta-diol	Hormone	Metabolite
Sigma_A 7762	115.13	L-allylglycine	Biochemistry	Inhibitor
Sigma_H-123	324.23	H-9 dihydrochloride	Phosphorylation	Inhibitor
Sigma_A 7824	131.18	6-Aminohexanoic acid	Immune System	Inhibitor
Sigma_A 7845	322.26	ATPO	Glutamate	Antagonist
Sigma_A 8003	136.11	Allopurinol	Cell Stress	Inhibitor
Sigma_A 8404	313.87	Amitriptyline hydrochloride	Adrenoceptor	Inhibitor
Sigma_A 8423	681.78	Amiodarone hydrochloride	Adrenoceptor	Agonist
Sigma_A 8456	239.70	4-(2-Aminoethyl)benzenesulfonyl fluoride hydrochloride	Biochemistry	Inhibitor
Sigma_A 8598	261.67	Ancitabine hydrochloride	DNA Metabolism	Inhibitor
Sigma_A 8676	285.82	Alprenolol hydrochloride	Adrenoceptor	Antagonist
Sigma_A 8723	210.28	Altretamine	DNA Metabolism	Inhibitor
Sigma_A 8762	195.22	N-Acetyldopamine monohydrate	Dopamine	Precursor
Sigma_A 8835	110.55	Aminoguanidine hydrochloride	Nitric Oxide	Inhibitor
Sigma_A 9013	566.42	BW 284c51	Cholinergic	Inhibitor
Sigma_A 9251	267.25	Adenosine	Adenosine	Agonist
Sigma_A 9256	133.10	L-Aspartic acid	Glutamate	Agonist
Sigma_A 9335	596.86	Astaxanthin	Cell Stress	Inhibitor
Sigma_A 9345	272.69	N-(4-Amino-2-chlorophenyl)phthalimide	Anticonvulsant	
Sigma_A 9501	329.21	Adenosine 3',5'-cyclic monophosphate	Phosphorylation	Activator
Sigma_A 9512	319.27	L(-)-Norepinephrine bitartrate	Adrenoceptor	Agonist
Sigma_A 9561	311.78	5-(N,N-hexamethylene)amiloride	Ion Pump	Inhibitor
Sigma_A 9630	286.42	4-Androstene-3,17-dione	Hormone	Precursor
Sigma_A 9657	232.28	(±)-p-Aminoglutethimide	Biochemistry	Inhibitor
Sigma_A 9699	116.12	(±)-HA-966	Glutamate	Antagonist
Sigma_A 9755	290.45	Androsterone	Hormone	
Sigma_A 9809	429.93	Amsacrine hydrochloride	DNA Repair	Inhibitor
Sigma_A 9834	166.67	(±)-AMT hydrochloride	Nitric Oxide	Inhibitor
Sigma_P 9623	365.84	Paroxetine hydrochloride hemihydrate (MW = 374.83)	Serotonin	Inhibitor
Sigma_A 9899	299.81	Antozoline hydrochloride	Imidazoline	Agonist
Sigma_A 9950	219.24	Aniracetam	Glutamate	Agonist
Sigma_A-003	284.32	1,3-Diethyl-8-phenylxanthine	Adenosine	Antagonist
Sigma_A-013	336.33	8-(p-Sulfophenyl)theophylline	Adenosine	Antagonist
Sigma_A-022	392.44	1,3-Dipropyl-8-p-sulfophenylxanthine	Adenosine	Antagonist
Sigma_A-023	641.20	2-Methylthioadenosine triphosphate tetrasodium	P2 Receptor	Agonist
Sigma_A-024	294.27	5'-N-Methyl carboxamidoadenosine	Adenosine	Agonist
Sigma_P 0248	381.99	PNU-37887A	K ⁺ Channel	Inhibitor
Sigma_A-129	313.79	Amoxapine	Adrenoceptor	Inhibitor
Sigma_A-138	322.45	Aminobenzotropine	Cholinergic	Ligand
Sigma_A-140	260.13	Arecaidine propargyl ester hydrobromide	Cholinergic	Agonist
Sigma_A-142	266.34	R(+)-Atenolol	Adrenoceptor	Antagonist
Sigma_A-143	266.34	S(-)-Atenolol	Adrenoceptor	Antagonist

Sigma_A-145	376.39	1-Allyl-3,7-dimethyl-8-p-sulfophenylxanthine	Adenosine	Antagonist
Sigma_A-155	173.17	trans-(±)-ACPD	Glutamate	Agonist
Sigma_A-162	179.65	1-Amino-1-cyclohexanecarboxylic acid hydrochloride	Neurotransmission	Substrate
Sigma_A-164	292.21	Alaproclate hydrochloride	Serotonin	Inhibitor
Sigma_P 9872	334.38	Psora-4	K ⁺ Channel	Inhibitor
Sigma_S 0568	304.78	SB 200646 hydrochloride	Serotonin	Antagonist
Sigma_A-167	225.18	D(-)-2-Amino-7-phosphonoheptanoic acid	Glutamate	Antagonist
Sigma_A-178	324.40	Acetohexamide	Hormone	Releaser
Sigma_A-196	173.58	SKF 97541 hydrochloride	GABA	Agonist
Sigma_A-201	101.11	cis-4-Aminocrotonic acid	GABA	Agonist
Sigma_A-202	386.41	N6-2-(4-Aminophenyl)ethyladenosine	Adenosine	Agonist
Sigma_A-206	238.34	Agroclavine	Dopamine	Agonist
Sigma_A-230	127.14	gamma-Acetylinic GABA	GABA	Inhibitor
Sigma_A-236	399.41	AB-MECA	Adenosine	Agonist
Sigma_A-242	214.18	Alloxazine	Adenosine	Antagonist
Sigma_A-243	145.12	cis-Azetidine-2,4-dicarboxylic acid	Glutamate	Modulator
Sigma_A-244	145.12	trans-Azetidine-2,4-dicarboxylic acid	Glutamate	Agonist
Sigma_A-252	189.73	AGN 192403 hydrochloride	Imidazoline	Ligand
Sigma_A-254	221.21	AIDA	Glutamate	Antagonist
Sigma_A-255	365.90	A-77636 hydrochloride	Dopamine	Agonist
Sigma_A-263	228.25	ATPA	Glutamate	Agonist
Sigma_A-265	785.06	ARL 67156 trisodium salt	P2 Receptor	Inhibitor
Sigma_B 0385	408.93	Beclomethasone	Hormone	
Sigma_B 0753	101.11	2,3-Butanedione monoxime	K ⁺ Channel	Blocker
Sigma_S 5192	380.49	SB 222200	Tachykinin	Antagonist
Sigma_B 1183	323.35	1-benzoyl-5-methoxy-2-methylindole-3-acetic acid	Multi-Drug Resistance	Inhibitor
Sigma_B 1266	108.10	p-Benzoquinone	DNA Repair	Inhibitor
Sigma_B 1381	446.09	8-Bromo-cGMP sodium	Cyclic Nucleotides	Activator
Sigma_B 1552	317.18	Bromo-enol lactone	Lipid	Inhibitor
Sigma_B 2009	121.14	Benzamide	Apoptosis	Inhibitor
Sigma_B 2050	242.03	3-Bromo-7-nitroindazole	Nitric Oxide	Inhibitor
Sigma_B 2134	750.72	(+)-Bromocriptine methanesulfonate	Dopamine	Agonist
Sigma_B 2292	241.25	O6-benzylguanine	DNA Repair	Inhibitor
Sigma_B 2377	137.96	N-Bromoacetamide	Na ⁺ Channel	Modulator
Sigma_B 2390	435.32	(±)-Brompheniramine maleate	Histamine	Antagonist
Sigma_B 2417	356.22	Benzamil hydrochloride	Ion Pump	Blocker
Sigma_B 2515	222.31	L-Buthionine-sulfoximine	Multi-Drug Resistance	Inhibitor
Sigma_B 2640	222.31	DL-Buthionine-[S,R]-sulfoximine	Multi-Drug Resistance	Inhibitor
Sigma_B 3023	364.42	Bumetanide	Ion Pump	Inhibitor
Sigma_B 3501	153.61	Betaine hydrochloride	Biochemistry	Metabolite
Sigma_B 3650	137.61	Betaine aldehyde chloride	Cholinergic	Metabolite
Sigma_B 4555	320.37	Benzoline oxalate	Imidazoline	Agonist
Sigma_B 4558	316.34	BWB70C	Leukotriene	Inhibitor

Sigma_B 5002	307.10	5-Bromo-2'-deoxyuridine	DNA Metabolism	Inhibitor
Sigma_B 5016	403.01	Bepridil hydrochloride	Ca ²⁺ Channel	Blocker
Sigma_B 5275	435.32	(+)-Brompheniramine maleate	Histamine	Antagonist
Sigma_B 5399	213.67	(±)-Baclofen	GABA	Agonist
Sigma_S 7067	331.35	SB 202190	Phosphorylation	Inhibitor
Sigma_B 5681	249.33	Bay 11-7085	Cell Cycle	Inhibitor
Sigma_B 5683	343.90	Betaxolol hydrochloride	Adrenoceptor	Antagonist
Sigma_B 6506	156.62	Benzamidine hydrochloride	Biochemistry	Inhibitor
Sigma_B 7005	392.47	Betamethasone	Hormone	
Sigma_B 7148	421.97	Buspirone hydrochloride	Serotonin	Agonist
Sigma_B 7283	293.71	Benserazide hydrochloride	Biochemistry	Inhibitor
Sigma_B 7651	280.37	Brefeldin A from <i>Penicillium brefeldianum</i>	Cytoskeleton and ECM	Inhibitor
Sigma_B 7777	430.55	Budesonide	Hormone	
Sigma_B 7880	430.09	8-Bromo-cAMP sodium	Cyclic Nucleotides	Activator
Sigma_B 8262	403.54	Benztropine mesylate	Cholinergic	Antagonist
Sigma_B 8279	278.35	Ro 20-1724	Cyclic Nucleotides	Inhibitor
Sigma_B 8385	344.84	Bestatin hydrochloride	Biochemistry	Inhibitor
Sigma_B 8406	414.36	Bretylium tosylate	Adrenoceptor	Blocker
Sigma_B 0936	244.27	BRL 50481	Phosphodiesterase	Inhibitor
Sigma_B 9308	417.56	BP 897	Dopamine	Agonist
Sigma_B 9647	333.14	(E)-5-(2-Bromovinyl)-2'-deoxyuridine	Immune System	Inhibitor
Sigma_B 9929	443.42	BRL 15572	Serotonin	Antagonist
Sigma_B-003	408.59	Chloroethylclonidine dihydrochloride	Adrenoceptor	Antagonist
Sigma_B-012	223.63	6-Fluoronorepinephrine hydrochloride	Adrenoceptor	Agonist
Sigma_B-015	481.48	Bromoacetyl alprenolol menthane	Adrenoceptor	Antagonist
Sigma_B-016	397.92	Benoxathian hydrochloride	Adrenoceptor	Antagonist
Sigma_B-019	340.30	Phenoxybenzamine hydrochloride	Adrenoceptor	Blocker
Sigma_B-102	276.21	Bupropion hydrochloride	Dopamine	Blocker
Sigma_B-103	462.30	(-)-Bicuculline methbromide, 1(S), 9(R)	GABA	Antagonist
Sigma_B-112	356.30	(±)-Bay K 8644	Ca ²⁺ Channel	Agonist
Sigma_B-121	305.01	Bromoacetylcholine bromide	Cholinergic	Ligand
Sigma_B-134	458.43	BMY 7378 dihydrochloride	Serotonin	Agonist
Sigma_B-135	455.19	R(+)-6-Bromo-APB hydrobromide	Dopamine	Agonist
Sigma_B-138	335.94	BTCP hydrochloride	Dopamine	Blocker
Sigma_B-152	398.42	N6-Benzyl-5'-N-ethylcarboxamidoadenosine	Adenosine	Agonist
Sigma_B-154	233.70	BU224 hydrochloride	Imidazoline	Antagonist
Sigma_B-161	254.16	B-HT 933 dihydrochloride	Adrenoceptor	Agonist
Sigma_B-168	397.99	(±)-Butaclamol hydrochloride	Dopamine	Antagonist
Sigma_B-169	385.83	BRL 37344 sodium	Adrenoceptor	Agonist
Sigma_B-173	346.39	BRL 54443 maleate	Serotonin	Agonist
Sigma_B-175	322.86	BW 723C86	Serotonin	Agonist
Sigma_C 0253	304.22	Chlorambucil	DNA	Intercalator
Sigma_C 0256	497.29	Citicoline sodium	Lipid	Inhibitor
Sigma_C 0330	289.16	Ciprofibrate	Transcription	Ligand
Sigma_C 0331	266.73	6-Chloromelatonin	Melatonin	Agonist

Sigma_C 0400	214.05	Carmustine	DNA	Intercalator
Sigma_C 0424	352.87	PK 11195	GABA	Antagonist
Sigma_C 0625	180.16	Caffeic Acid	Cell Stress	Inhibitor
Sigma_C 0737	369.47	Cilostazol	Cyclic Nucleotides	Inhibitor
Sigma_C 0750	194.19	Caffeine	Adenosine	Inhibitor
Sigma_C 0768	261.09	Cyclophosphamide monohydrate	DNA	Intercalator
Sigma_C 0862	292.47	CGP-7930	GABA	Modulator
Sigma_C 0987	290.45	CGP-13501	GABA	Modulator
Sigma_C 1112	376.58	CP55940	Cannabinoid	Agonist
Sigma_C 1159	102.09	L-Cycloserine	Sphingolipid	Inhibitor
Sigma_C 1172	361.29	ML-9	Phosphorylation	Inhibitor
Sigma_C 1251	290.28	(+)-Catechin Hydrate	Cell Stress	Inhibitor
Sigma_C 1290	276.74	Chlorpropamide	Hormone	Releaser
Sigma_C 1610	343.81	1-(4-Chlorobenzyl)-5-methoxy-2-methylindole-3-acetic acid	Multi-Drug Resistance	Inhibitor
Sigma_C 1671	352.33	Chlorprothixene hydrochloride	Dopamine	Antagonist
Sigma_C 1754	184.08	Choline bromide	Cholinergic	Substrate
Sigma_C 2137	707.25	Ceramide	Phosphorylation	Inhibitor
Sigma_C 2235	252.19	CB 1954	DNA	Intercalator
Sigma_C 2321	255.15	Carcinine dihydrochloride	Cell Stress	Inhibitor
Sigma_C 2505	346.47	Corticosterone	Hormone	
Sigma_C 2538	371.26	Carboplatin	DNA	Intercalator
Sigma_C 2755	360.45	Cortisone	Hormone	
Sigma_C 2932	383.83	Chelerythrine chloride	Phosphorylation	Inhibitor
Sigma_C 3010	320.05	1-(2-Chlorophenyl)-1-(4-chlorophenyl)-2,2-dichloroethane	Hormone	Inhibitor
Sigma_C 3025	390.87	(±)-Chlorpheniramine maleate	Histamine	Antagonist
Sigma_C 3130	402.49	Cortisone 21-acetate	Hormone	
Sigma_C 3270	478.78	Cephalosporin C zinc salt	Antibiotic	
Sigma_C 3353	422.36	CGP-74514A hydrochloride	Phosphorylation	Inhibitor
Sigma_C 3412	416.95	Cyproterone acetate	Hormone	Antagonist
Sigma_C 3635	250.13	DL-p-Chlorophenylalanine methyl ester hydrochloride	Neurotransmission	Inhibitor
Sigma_C 3662	1202.64	Cyclosporin A	Phosphorylation	Inhibitor
Sigma_C 3909	102.09	D-Cycloserine	Glutamate	Agonist
Sigma_C 3912	493.80	8-(4-Chlorophenylthio)-cAMP sodium	Cyclic Nucleotides	Activator
Sigma_C 3930	687.71	Calmidazolium chloride	Intracellular Calcium	Inhibitor
Sigma_G 5918	393.51	GR 113808	Serotonin	Antagonist
Sigma_C 4024	236.28	Carbamazepine	Anticonvulsant	
Sigma_C 4042	217.29	Captopril	Neurotransmission	Inhibitor
Sigma_C 4238	339.87	CNS-1102	Glutamate	Antagonist
Sigma_C 4382	182.65	Carbachol	Cholinergic	Agonist
Sigma_C 4397	169.57	Chlorzoxazone	Nitric Oxide	Inhibitor
Sigma_C 4418	153.16	L-Cysteinesulfinic Acid	Glutamate	Ligand
Sigma_C 4479	299.35	9-cyclopentyladenine	Cyclic Nucleotides	Inhibitor

Sigma_C 4520	418.43	Cephalothin sodium	Antibiotic	
Sigma_C 4522	252.34	Cimetidine	Histamine	Antagonist
Sigma_C 4542	311.86	Cyclobenzaprine hydrochloride	Serotonin	Antagonist
Sigma_C 4662	525.60	Carbetapentane citrate	Opioid	Ligand
Sigma_C 4895	347.40	Cephalexin hydrate	Antibiotic	
Sigma_C 4911	295.72	Chlorothiazide	Biochemistry	Inhibitor
Sigma_C 4915	390.87	(+)-Chlorpheniramine maleate	Histamine	Antagonist
Sigma_C 5020	476.49	Cefazolin sodium	Antibiotic	
Sigma_C 5040	362.31	Clemizole hydrochloride	Histamine	Antagonist
Sigma_C 5134	301.69	2-Chloroadenosine	Adenosine	Agonist
Sigma_C 5259	196.68	Bethanechol chloride	Cholinergic	Agonist
Sigma_C 5270	368.53	Cinnarizine	Ca ²⁺ Channel	Blocker
Sigma_C 5554	269.60	1-(3-Chlorophenyl)piperazine dihydrochloride	Serotonin	Agonist
Sigma_S 0693	286.36	SB 204741	Serotonin	Antagonist
Sigma_C 5793	598.55	Ceftriaxone sodium	Antibiotic	
Sigma_C 5913	357.16	4-Chloromercuribenzoic acid	Biochemistry	Inhibitor
Sigma_C 5923	176.22	(-)-Cotinine	Cholinergic	Metabolite
Sigma_C 5976	465.80	CL 316,243	Adrenoceptor	Agonist
Sigma_C 5982	256.69	7-Chloro-4-hydroxy-2-phenyl-1,8-naphthyridine	Adenosine	Antagonist
Sigma_C 6019	344.85	Clotrimazole	K ⁺ Channel	Inhibitor
Sigma_C 6022	323.87	Cyproheptadine hydrochloride	Serotonin	Antagonist
Sigma_C 6042	320.31	5'-(N-Cyclopropyl)carboxamidoadenosine	Adenosine	Agonist
Sigma_C 6048	493.52	Cefmetazole sodium	Antibiotic	
Sigma_C 6305	326.83	Clozapine	Dopamine	Antagonist
Sigma_C 6506	199.64	(±)-p-Chlorophenylalanine	Neurotransmission	Inhibitor
Sigma_C 6628	515.87	Chloroquine diphosphate	DNA	Intercalator
Sigma_C 6643	242.70	Clofibrate	Lipid	Modulator
Sigma_C 6645	279.68	Cytosine-1-beta-D-arabinofuranoside hydrochloride	DNA Metabolism	Inhibitor
Sigma_C 6862	438.79	CB34	Benzodiazepine	Ligand
Sigma_C 6895	367.81	Cefaclor	Antibiotic	
Sigma_C 7005	102.09	DL-Cycloserine	Sphingolipid	Inhibitor
Sigma_C 7041	317.22	McN-A-343	Cholinergic	Agonist
Sigma_C 7230	373.89	N-(2-[4-(4-Chlorophenyl)piperazin-1-yl]ethyl)-3-methoxybenzamide	Dopamine	Agonist
Sigma_C 7255	225.20	Cystamine dihydrochloride	Glutamate	Inhibitor
Sigma_C 7291	351.32	Clomipramine hydrochloride	Serotonin	Inhibitor
Sigma_C 7522	523.63	Calcimycin	Intracellular Calcium	
Sigma_C 7632	196.20	Cantharidin	Phosphorylation	Inhibitor
Sigma_C 7861	405.31	Citalopram hydrobromide	Serotonin	Inhibitor
Sigma_C 7897	266.56	Clonidine hydrochloride	Adrenoceptor	Agonist
Sigma_C 7912	477.45	Cefotaxime sodium	Antibiotic	
Sigma_C 7971	342.44	Cilostamide	Cyclic Nucleotides	Inhibitor
Sigma_C 8011	183.12	Chelidamic acid	Glutamate	Inhibitor
Sigma_C 8031	335.37	N6-Cyclopentyladenosine	Adenosine	Agonist
Sigma_C 8088	214.22	Cantharidic Acid	Phosphorylation	Inhibitor

Sigma_C 8138	355.33	Chlorpromazine hydrochloride	Dopamine	Antagonist
Sigma_C 8145	554.54	Cefsulodin sodium salt hydrate	Antibiotic	
Sigma_C 8221	284.31	Caffeic acid phenethyl ester	Cell Cycle	Inhibitor
Sigma_C 8270	445.45	Cephapirin sodium	Antibiotic	
Sigma_C 8395	349.41	Cephadrine	Antibiotic	
Sigma_C 8417	313.07	DSP-4 hydrochloride	Adrenoceptor	Neurotoxin
Sigma_C 8645	262.22	Cinoxacin	Antibiotic	Inhibitor
Sigma_C 8759	260.34	Carisoprodol	Neurotransmission	
Sigma_C 8773	294.18	Centrophenoxine hydrochloride	Nootropic	
Sigma_C 8903	459.97	Clemastine fumarate	Histamine	Antagonist
Sigma_C 9033	160.00	beta-Chloro-L-alanine hydrochloride	Biochemistry	Inhibitor
Sigma_C 9510	110.11	Pyrocatechol	Cell Cycle	Inhibitor
Sigma_C 9511	331.80	Z-L-Phe chloromethyl ketone	Biochemistry	Inhibitor
Sigma_C 9611	247.25	CPCCOEt	Glutamate	Antagonist
Sigma_C 9754	399.45	Colchicine	Cytoskeleton and ECM	Inhibitor
Sigma_C 9758	274.25	L-Canavanine sulfate	Nitric Oxide	Inhibitor
Sigma_C 9847	389.88	Cyclothiazide	Glutamate	Agonist
Sigma_C 9901	349.39	N6-Cyclohexyladenosine	Adenosine	Agonist
Sigma_C 9911	348.36	(S)-(+)-Camptothecin	Apoptosis	Inhibitor
Sigma_C-007	362.92	10-(alpha-Diethylaminopropionyl)-phenothiazine hydrochloride	Biochemistry	Inhibitor
Sigma_C-008	287.14	(+)-cis-Dioxolane iodide	Cholinergic	Agonist
Sigma_C-011	303.21	OXA-22 iodide	Cholinergic	Agonist
Sigma_C-101	304.40	8-Cyclopentyl-1,3-dipropylxanthine	Adenosine	Antagonist
Sigma_C-102	248.29	8-Cyclopentyl-1,3-dimethylxanthine	Adenosine	Antagonist
Sigma_C-104	252.21	(±)-CPP	Glutamate	Antagonist
Sigma_C-106	450.42	CGS-12066A maleate	Serotonin	Agonist
Sigma_C-108	207.75	2-Cyclooctyl-2-hydroxyethylamine hydrochloride	Neurotransmission	Inhibitor
Sigma_C-117	319.32	5-Carboxamidotryptamine maleate	Serotonin	Agonist
Sigma_C-121	223.62	7-Chlorokynurenic acid	Glutamate	Antagonist
Sigma_C-125	315.80	(±)-CGP-12177A hydrochloride	Adrenoceptor	Agonist
Sigma_C-126	226.23	S(-)-Carbidopa	Biochemistry	Inhibitor
Sigma_C-130	410.74	(±)-Chloro-APB hydrobromide	Dopamine	Agonist
Sigma_C-141	535.99	CGS-21680 hydrochloride	Adenosine	Agonist
Sigma_Y 0503	320.26	Y-27632 dihydrochloride	Phosphorylation	Inhibitor
Sigma_C-144	248.12	1-(m-Chlorophenyl)-biguanide hydrochloride	Serotonin	Agonist
Sigma_C-145	629.56	2-Chloroadenosine triphosphate tetrasodium	P2 Receptor	Agonist
Sigma_C-147	271.41	(+)-Cyclazocine	Opioid	Antagonist
Sigma_C-191	376.91	Capsazepine	Vanilloid	Agonist
Sigma_C-192	273.74	Chlormezanone	Neurotransmission	Modulator
Sigma_C-197	330.78	8-(3-Chlorostyryl)caffeine	Adenosine	Antagonist
Sigma_C-199	285.69	CGS-15943	Adenosine	Antagonist
Sigma_C-203	198.60	2-Chloro-2-deoxy-D-glucose	Biochemistry	Analog
Sigma_C-207	378.35	4'-Chloro-3-alpha-(diphenylmethoxy)tropane hydrochloride	Dopamine	Blocker
Sigma_C-223	252.75	Cirazoline hydrochloride	Adrenoceptor	Agonist
Sigma_C-231	590.58	CGP 20712A methanesulfonate	Adrenoceptor	Antagonist

Sigma_C-237	159.14	(2S,1'S,2'S)-2-(carboxycyclopropyl)glycine	Glutamate	Agonist
Sigma_C-239	276.12	CNQX disodium	Glutamate	Antagonist
Sigma_C-271	247.30	CX 546	Glutamate	Modulator
Sigma_C-277	544.74	Chloro-IB-MECA	Adenosine	Agonist
Sigma_D 0411	381.86	WB-4101 hydrochloride	Adrenoceptor	Antagonist
Sigma_D 0540	252.14	DNQX	Glutamate	Antagonist
Sigma_D 0670	586.68	Dihydroouabain	Ion Pump	Inhibitor
Sigma_D 0676	337.85	Dobutamine hydrochloride	Adrenoceptor	Agonist
Sigma_D 1064	229.28	Dihydrokainic acid	Glutamate	Blocker
Sigma_D 1260	418.30	Decamethonium dibromide	Cholinergic	Agonist
Sigma_D 1262	887.49	P1,P4-Di(adenosine-5')tetraphosphate triammonium	Biochemistry	Inhibitor
Sigma_D 1306	448.55	Debrisoquin sulfate	Neurotransmission	Antihypertensive
Sigma_D 1413	224.22	2',3'-didehydro-3'-deoxythymidine	Immune System	Inhibitor
Sigma_D 1414	379.44	Droperidol	Dopamine	Antagonist
Sigma_D 1507	247.68	L-3,4-Dihydroxyphenylalanine methyl ester hydrochloride	Dopamine	Precursor
Sigma_D 1542	169.61	1,4-Dideoxy-1,4-imino-D-arabinitol	Phosphorylation	Inhibitor
Sigma_D 1791	348.24	2,4-Dinitrophenyl 2-fluoro-2-deoxy-beta-D-glucopyranoside	Biochemistry	Inhibitor
Sigma_D 1916	319.15	D-ribofuranosylbenzimidazole	Transcription	Inhibitor
Sigma_D 2064	766.60	Dequalinium analog, C-14 linker	Phosphorylation	Inhibitor
Sigma_D 2521	450.99	Diltiazem hydrochloride	Ca ²⁺ Channel	Antagonist
Sigma_D 2531	352.32	Dextromethorphan hydrobromide monohydrate	Glutamate	Antagonist
Sigma_S 0443	308.81	SB 203186	Serotonin	Antagonist
Sigma_D 2763	679.80	Dihydroergotamine methanesulfonate	Serotonin	Antagonist
Sigma_D 2926	314.55	Diphenyleneiodonium chloride	Nitric Oxide	Inhibitor
Sigma_D 3630	291.82	Diphenhydramine hydrochloride	Histamine	Antagonist
Sigma_D 3634	86.09	2,3-Butanedione	Cytoskeleton and ECM	Inhibitor
Sigma_D 3648	172.19	N,N,N',N'-Tetramethylazodicarboxamide	Cell Stress	Modulator
Sigma_D 3689	183.17	(S)-3,5-Dihydroxyphenylglycine	Glutamate	Agonist
Sigma_D 3768	527.59	Dequalinium dichloride	K ⁺ Channel	Blocker
Sigma_D 3775	388.47	Doxylamine succinate	Histamine	Antagonist
Sigma_D 3900	302.85	Desipramine hydrochloride	Adrenoceptor	Inhibitor
Sigma_D 4007	252.28	5,5-Diphenylhydantoin	Anticonvulsant	
Sigma_D 4268	238.72	N [^] G,N [^] G-Dimethylarginine hydrochloride	Nitric Oxide	Inhibitor
Sigma_D 4434	288.86	Clodronic acid	Cytoskeleton and ECM	Inhibitor
Sigma_D 4505	274.26	Phenytoin sodium	Anticonvulsant	
Sigma_D 4526	315.85	Doxepin hydrochloride	Adrenoceptor	Inhibitor
Sigma_P-152_a	248.33	S(-)-Pindolol	Adrenergic	Antagonist
Sigma_D 5290	183.21	(-)-alpha-Methylnorepinephrine	Adrenoceptor	Agonist
Sigma_D 5294	677.63	Dilazep hydrochloride	Adenosine	Inhibitor
Sigma_D 5385	180.17	1,7-Dimethylxanthine	Adenosine	Antagonist
Sigma_D 5439	218.21	2,3-Dimethoxy-1,4-naphthoquinone	Cell Stress	Modulator
Sigma_D 5564	178.15	Daphnetin	Phosphorylation	Inhibitor
Sigma_D 5689	246.31	DM 235	Nootropic	

Sigma_D 5766	113.16	5,5-Dimethyl-1-pyrroline-N-oxide	Cell Stress	Inhibitor
Sigma_D 5782	211.22	2',3'-dideoxycytidine	Immune System	Inhibitor
Sigma_D 5794	489.59	Diacylglycerol Kinase Inhibitor II	Phosphorylation	Inhibitor
Sigma_D 5814	303.79	Dihyrexidine hydrochloride	Dopamine	Agonist
Sigma_D 5886	203.67	N-Methyldopamine hydrochloride	Dopamine	Agonist
Sigma_D 5891	318.20	1,1-Dimethyl-4-phenyl-piperazinium iodide	Cholinergic	Agonist
Sigma_P 9248	360.35	PD 169316	Phosphorylation	Inhibitor
Sigma_D 6035	437.48	Disopyramide phosphate	K+ Channel	Modulator
Sigma_D 6140	501.32	Demeclocycline hydrochloride	Antibiotic	
Sigma_D 6518	393.35	Diethylenetriaminepentaacetic acid	Biochemistry	Inhibitor
Sigma_D 6899	318.14	Diclofenac sodium	Prostaglandin	Inhibitor
Sigma_D 6908	301.52	DL-erythro-Dihydrosphingosine	Phosphorylation	Inhibitor
Sigma_D 6940	209.72	R(-)-Desmethyldeprenyl hydrochloride	Neurotransmission	Inhibitor
Sigma_D 7505	156.19	2,2'-Bipyridyl	Biochemistry	Inhibitor
Sigma_D 7644	339.48	Disopyramide	Na+ Channel	Blocker
Sigma_D 7802	254.24	Daidzein	Cell Cycle	Inhibitor
Sigma_D 7814	275.31	Dubindine	Anticonvulsant	
Sigma_D 7909	345.96	Dicyclomine hydrochloride	Cholinergic	Antagonist
Sigma_D 7910	215.04	3,4-Dichloroisocoumarin	Biochemistry	Inhibitor
Sigma_D 7938	297.62	DBO-83	Cholinergic	Agonist
Sigma_D 8008	336.56	7,7-Dimethyl-(5Z,8Z)-eicosadienoic acid	Lipid	Inhibitor
Sigma_D 8040	465.44	(±) trans-U-50488 methanesulfonate	Opioid	Agonist
Sigma_D 8065	168.15	Dephostatin	Phosphorylation	Inhibitor
Sigma_D 8190	425.11	3',4'-Dichlorobenzamil	Ion Pump	Inhibitor
Sigma_D 8296	252.23	3-deazaadenosine	Immune System	Inhibitor
Sigma_G 5168	312.46	(Z)-Gugglesterone	Lipid Signaling	Antagonist
Sigma_D 8399	337.47	Danazol	Hormone	Inhibitor
Sigma_D 8555	436.62	N,N-Dihexyl-2-(4-fluorophenyl)indole-3-acetamide	Benzodiazepine	Ligand
Sigma_D 8690	320.44	(R,R)-cis-Diethyl tetrahydro-2,8-chrysenediol	Hormone	Antagonist
Sigma_S 5567	220.23	SP600125	Phosphorylation	Inhibitor
Sigma_D 9035	230.67	Diazoxide	K+ Channel	Activator
Sigma_D 9128	168.15	3,4-Dihydroxyphenylacetic acid	Dopamine	Metabolite
Sigma_D 9175	336.24	Dantrolene sodium	Intracellular Calcium	Inhibitor
Sigma_D 9190	231.08	DCEBIO	K+ Channel	Activator
Sigma_D 9305_a	199.64	1-Deoxynojirimycin hydrochloride	Biochemistry	Inhibitor
Sigma_D 9628	197.19	L-3,4-Dihydroxyphenylalanine	Dopamine	Precursor
Sigma_D 9766	504.64	Dipyridamole	Adenosine	Inhibitor
Sigma_D 9815	547.59	Doxazosin mesylate	Adrenoceptor	Blocker
Sigma_D 9891	480.91	Doxycycline hydrochloride	Antibiotic	
Sigma_D-002	260.13	6,7-ADTN hydrobromide	Dopamine	Agonist
Sigma_D-003	317.82	R(-)-Apocodeine hydrochloride	Dopamine	Agonist
Sigma_D-027	331.85	R(-)-Propylnorapomorphine hydrochloride	Dopamine	Agonist
Sigma_D-029	364.24	R(-)-2,10,11-Trihydroxyaporphine hydrobromide	Dopamine	Agonist
Sigma_D-030	392.30	R(-)-2,10,11-Trihydroxy-N-propylnoraporphine hydrobromide	Dopamine	Agonist

Sigma_D-031	318.26	Dipropyldopamine hydrobromide	Dopamine	Agonist
Sigma_D-033	397.99	(+)-Butaclamol hydrochloride	Dopamine	Antagonist
Sigma_D-042	374.28	R(-)-N-Allylnorapomorphine hydrobromide	Dopamine	Agonist
Sigma_D-044	308.34	Amfonelic acid	Dopamine	Modulator
Sigma_I 9532	311.30	Icilin	Neurotransmission	Agonist
Sigma_D-047	291.78	(±)-SKF-38393 hydrochloride	Dopamine	Antagonist
Sigma_D-052	523.50	GBR-12909 dihydrochloride	Dopamine	Inhibitor
Sigma_D-054	324.25	R(+)-SCH-23390 hydrochloride	Dopamine	Antagonist
Sigma_D-101	357.62	(±)-DOI hydrochloride	Serotonin	Agonist
Sigma_D-103	226.53	(±)-2,3-Dichloro-alpha-methylbenzylamine hydrochloride	Neurotransmission	Inhibitor
Sigma_D-104	451.35	4-DAMP methiodide	Cholinergic	Antagonist
Sigma_D-108	250.30	1,3-Dipropyl-7-methylxanthine	Adenosine	Antagonist
Sigma_D-122	425.92	Domperidone	Dopamine	Antagonist
Sigma_D126608	178.28	Propofol	Cholinergic	Inhibitor
Sigma_D-127	407.47	Dextrorphan D-tartrate	Glutamate	Antagonist
Sigma_D-129	399.32	R(+)-Butylindazone	Ion Pump	Inhibitor
Sigma_E 2031	347.86	Eliprodil	Glutamate	Antagonist
Sigma_D-131	200.11	3,5-Dinitrocatechol	Neurotransmission	Inhibitor
Sigma_D-132	403.48	N,N-Dipropyl-5-carboxamidotryptamine maleate	Serotonin	Agonist
Sigma_D-133	231.04	6,7-Dichloroquinoxaline-2,3-dione	Glutamate	Antagonist
Sigma_D-134	218.22	3,7-Dimethyl-I-propargylxanthine	Adenosine	Antagonist
Sigma_D-138	258.06	5,7-Dichlorokynurenic acid	Glutamate	Antagonist
Sigma_D-142	394.34	4-Diphenylacetoxy-N-(2-chloroethyl)piperidine hydrochloride	Cholinergic	Antagonist
Sigma_D14204	172.32	1,10-Diaminodecane	Glutamate	Agonist (inverse)
Sigma_D-149	356.26	Dihydro-beta-erythroidine hydrobromide	Cholinergic	Antagonist
Sigma_D-155	707.85	Dihydroergocristine methanesulfonate	Dopamine	Agonist
Sigma_D1920-6	126.12	2,6-Diamino-4-pyrimidinone	Phosphorylation	Inhibitor
Sigma_D-193	218.63	DL-alpha-Difluoromethylornithine hydrochloride	Angiogenesis	Inhibitor
Sigma_S 4443	277.33	SCH-28080	Ion Channels	Inhibitor
Sigma_D-206	264.80	S(-)-DS 121 hydrochloride	Dopamine	Antagonist
Sigma_E 0137	223.27	Vanillic acid diethylamide	Vanilloid	Agonist
Sigma_E 0381	344.84	Epibestatin hydrochloride	Biochemistry	Inhibitor
Sigma_E 0516	287.36	Etodolac	Prostaglandin	Inhibitor
Sigma_E 1279	248.31	Enoximone	Cyclic Nucleotides	Inhibitor
Sigma_E 1383	588.57	Etoposide	Apoptosis	Inhibitor
Sigma_E 1779	523.74	ET-18-OCH3	Lipid	Inhibitor
Sigma_E 1896	325.80	Etazolate hydrochloride	Adenosine	Inhibitor
Sigma_C 8863	370.46	7-Cyclopentyl-5-(4-phenoxy)phenyl-7H-pyrrolo[2,3-d]pyrimidin-4-ylamine	Phosphorylation	Inhibitor
Sigma_E 2375	553.58	Emetine dihydrochloride hydrate	Apoptosis	Activator
Sigma_E 2387	308.30	5'-N-Ethylcarboxamidoadenosine	Adenosine	Agonist
Sigma_E 3132	357.41	E-64	Biochemistry	Inhibitor
Sigma_S 3567	359.73	SB 415286	Phosphorylation	Inhibitor
Sigma_E 3149	185.09	S-Ethylisothiurea hydrobromide	Nitric Oxide	Inhibitor

Sigma_E 3256	201.70	Edrophonium chloride	Cholinergic	Inhibitor
Sigma_E 3263	252.75	Efaroxan hydrochloride	Imidazoline	Antagonist
Sigma_E 3380	246.31	Ellipticine	Cell Cycle	Inhibitor
Sigma_E 3520	274.18	Ebselen	Leukotriene	Inhibitor
Sigma_E 3645	522.71	rac-2-Ethoxy-3-hexadecanamido-1-propylphosphocholine	Phosphorylation	Inhibitor
Sigma_E 3770	550.77	rac-2-Ethoxy-3-octadecanamido-1-propylphosphocholine	Phosphorylation	Inhibitor
Sigma_E 3876	125.13	N-Ethylmaleimide	Biochemistry	Inhibitor
Sigma_E 4375	333.30	(-)-Epinephrine bitartrate	Adrenoceptor	Agonist
Sigma_E 4378	380.35	Ethylene glycol-bis(2-aminoethylether)-N,N,N',N'-tetraacetic acid	Biochemistry	Inhibitor
Sigma_E 4642	219.67	(±)-Epinephrine hydrochloride	Adrenoceptor	Agonist
Sigma_E 7138	141.17	Ethosuximide	Anticonvulsant	
Sigma_E 7649	186.17	Endothall	Phosphorylation	Inhibitor
Sigma_E 7881	270.24	Emodin	Phosphorylation	Inhibitor
Sigma_E 8375	275.35	(-)-Physostigmine	Cholinergic	Inhibitor
Sigma_N 3911	434.20	NBI 27914	Neurotransmission	Antagonist
Sigma_E 8875	272.39	beta-Estradiol	Hormone	
Sigma_E 9750	270.37	Estrone	Hormone	
Sigma_E-002	226.24	Methyl beta-carboline-3-carboxylate	Benzodiazepine	Agonist
Sigma_E-006	225.25	N-Methyl-beta-carboline-3-carboxamide	GABA	Antagonist
Sigma_E-007	314.34	Methyl 6,7-dimethoxy-4-ethyl-beta-carboline-3-carboxylate	Benzodiazepine	Agonist
Sigma_E-100	334.38	(-)-Eseroline fumarate	Cholinergic	Inhibitor
Sigma_E-101	377.31	S(-)-Eticlopride hydrochloride	Dopamine	Antagonist
Sigma_E-111	361.40	(S)-ENBA	Adenosine	Agonist
Sigma_E-114	313.83	erythro-9-(2-Hydroxy-3-nonyl)adenine hydrochloride	Adenosine	Inhibitor
Sigma_E-140	609.73	Ergocristine	Dopamine	Agonist
Sigma_F 0778	238.25	Felbamate	Glutamate	Antagonist
Sigma_F 0881	538.71	Fusidic acid sodium	Cell Cycle	Inhibitor
Sigma_F 1016	384.27	Fenoterol hydrobromide	Adrenoceptor	Agonist
Sigma_F 1553	345.80	S-(+)-Fluoxetine hydrochloride	Serotonin	Inhibitor
Sigma_F 1678	345.80	R-(-)-Fluoxetine hydrochloride	Serotonin	Inhibitor
Sigma_F 2802	434.42	Fluvoxamine maleate	Serotonin	Inhibitor
Sigma_F 2927	327.36	1-(4-Fluorobenzyl)-5-methoxy-2-methylindole-3-acetic acid	Multi-Drug Resistance	Inhibitor
Sigma_F 3764	275.24	Furegrelate sodium	Phosphorylation	Inhibitor
Sigma_F 4303	592.12	Fiduxosin hydrochloride	Adrenoceptor	Antagonist
Sigma_F 4381	330.75	Furosemide	Ion Pump	Inhibitor
Sigma_F 4646	183.18	p-Fluoro-L-phenylalanine	Neurotransmission	Substrate
Sigma_F 4765	510.45	Fluphenazine dihydrochloride	Dopamine	Antagonist
Sigma_F 6020	360.84	Fenofibrate	Transcription	Agonist
Sigma_F 6145	296.80	Fenspiride hydrochloride	Adrenoceptor	Antagonist
Sigma_F 6300	303.30	Flumazenil	Benzodiazepine	Antagonist
Sigma_F 6426	307.35	Foliosidine	Anticonvulsant	
Sigma_F 6513	179.22	Fusaric acid	Dopamine	Inhibitor

Sigma_F 6627	130.08	5-Fluorouracil	Cell Cycle	Inhibitor
Sigma_F 6777	474.40	Flecainide acetate	Na ⁺ Channel	Blocker
Sigma_F 6800	386.68	Fenoldopam bromide	Dopamine	Agonist
Sigma_F 6886	410.51	Forskolin	Cyclic Nucleotides	Activator
Sigma_F 6889	337.45	Famotidine	Histamine	Antagonist
Sigma_F 7927	506.56	FSCPX	Adenosine	Antagonist
Sigma_F 8175	358.55	Farnesylthiosalicylic acid	G protein	Antagonist
Sigma_F 8257	477.43	Flunarizine dihydrochloride	Ion Pump	Blocker
Sigma_F 8791	246.20	5-fluoro-5'-deoxyuridine	DNA Metabolism	Inhibitor
Sigma_F 8927	420.40	Flupirtine maleate	Glutamate	Antagonist
Sigma_F 9397	276.22	Flutamide	Hormone	Inhibitor
Sigma_F 9427	501.67	Fexofenadine hydrochloride	Histamine	Antagonist
Sigma_F 9552	804.90	Formoterol	Adrenoceptor	Agonist
Sigma_F 9677	384.26	Felodipine	Ca ²⁺ Channel	Blocker
Sigma_F-100	475.59	Fluspirilene	Dopamine	Antagonist
Sigma_F-114	507.45	cis-(Z)-Flupenthixol dihydrochloride	Dopamine	Antagonist
Sigma_F-124	260.25	Furafylline	Biochemistry	Inhibitor
Sigma_F-131	347.42	FPL 64176	Ca ²⁺ Channel	Activator
Sigma_F-132	345.80	Fluoxetine hydrochloride	Serotonin	Inhibitor
Sigma_D 8816	268.36	N-(3,3-Diphenylpropyl)glycinamide	Glutamate	Blocker
Sigma_G 0639	494.01	Glibenclamide	K ⁺ Channel	Blocker
Sigma_G 0668	395.47	GW2974	Phosphorylation	Inhibitor
Sigma_G 1043	282.56	Guanfacine hydrochloride	Adrenoceptor	Agonist
Sigma_G 2128	183.59	L-Glutamic acid hydrochloride	Glutamate	Agonist
Sigma_G 2536	255.24	Ganciclovir	Cell Cycle	Inhibitor
Sigma_G 3126	146.15	L-Glutamine	Glutamate	Agonist
Sigma_G 3416	699.61	Guanidinylnaltrindole di-trifluoroacetate	Opioid	Antagonist
Sigma_G 4788	398.19	Guanidinoethyl disulfide dihydrobromide	Nitric Oxide	Inhibitor
Sigma_G 5668	495.58	GW1929	Transcription	Agonist
Sigma_G 6416	520.95	GW5074	Phosphorylation	Inhibitor
Sigma_G 6649	270.24	Genistein	Phosphorylation	Inhibitor
Sigma_G 6793	502.77	GW7647	Transcription	Agonist
Sigma_G 7788	189.17	alpha-Guanidinoglutaric acid	Nitric Oxide	Inhibitor
Sigma_G 8134	891.54	Gallamine triethiodide	Cholinergic	Antagonist
Sigma_G 9659	487.52	GBR-12935 dihydrochloride	Dopamine	Inhibitor
Sigma_G-002	163.61	Isoguvacine hydrochloride	GABA	Agonist
Sigma_G-007	163.61	Guvacine hydrochloride	GABA	Inhibitor
Sigma_G-017	267.08	(±)-AMPA hydrobromide	Glutamate	Agonist
Sigma_G-019	195.02	Muscimol hydrobromide	GABA	Agonist
Sigma_G-110	291.14	Guanabenz acetate	Adrenoceptor	Agonist
Sigma_G-111	240.24	gamma-D-Glutamylaminomethylsulfonic acid	Glutamate	Antagonist
Sigma_G-117	445.54	Glipizide	K ⁺ Channel	Blocker
Sigma_G-119	329.79	GYKI 52466 hydrochloride	Glutamate	Antagonist
Sigma_G-120	295.34	GYKI 52895	Dopamine	Inhibitor
Sigma_G-133	530.41	GR-89696 fumarate	Opioid	Agonist
Sigma_G-154	171.24	Gabapentin	Anticonvulsant	

Sigma_H 0126	356.26	DL-Homatropine hydrobromide	Cholinergic	Antagonist
Sigma_H 0131	198.18	(±)-Vanillylmandelic acid	Adrenoceptor	Metabolite
Sigma_H 0627	248.28	6-Hydroxymelatonin	Melatonin	Metabolite
Sigma_H 0879	362.19	Hexamethonium bromide	Cholinergic	Antagonist
Sigma_H 1252	182.18	4-Hydroxy-3-methoxyphenylacetic acid	Dopamine	Metabolite
Sigma_H 1377	454.52	MHPG piperazine	Adrenoceptor	Metabolite
Sigma_H 1384	109.15	Hypotaourine	Cell Stress	Inhibitor
Sigma_H 1512	375.87	Haloperidol	Dopamine	Antagonist
Sigma_H 1753	196.64	Hydralazine hydrochloride	Neurotransmission	Inhibitor
Sigma_H 1877	134.57	4-Imidazolemethanol hydrochloride	Histamine	Inhibitor
Sigma_H 2138	273.29	Hexamethonium dichloride	Cholinergic	Antagonist
Sigma_H 2270	484.53	Hydrocortisone 21-hemisuccinate sodium	Hormone	
Sigma_H 2380	213.19	6-Hydroxy-DL-DOPA	Adrenoceptor	Neurotoxin
Sigma_H 2775	149.10	DL-threo-beta-hydroxyaspartic acid	Glutamate	Inhibitor
Sigma_H 3146	330.34	Hydroxytacrine maleate	Cholinergic	Inhibitor
Sigma_H 4001	362.47	Hydrocortisone	Hormone	
Sigma_L 4408	42.39	Lithium Chloride	Neurotransmission	Inhibitor
Sigma_H 4759	297.74	Hydrochlorothiazide	Biochemistry	Inhibitor
Sigma_S 8817	396.45	SB 218795	Neurotransmission	Antagonist
Sigma_H 5257	246.22	Hispidin	Phosphorylation	Inhibitor
Sigma_H 5752	330.47	17alpha-hydroxyprogesterone	Hormone	Metabolite
Sigma_H 6036	386.45	1,3,5-tris(4-hydroxyphenyl)-4-propyl-1H-pyrazole	Hormone	Agonist
Sigma_H 6892	206.27	1-(4-Hydroxybenzyl)imidazole-2-thiol	Dopamine	Inhibitor
Sigma_H 7250	184.07	Histamine dihydrochloride	Histamine	Agonist
Sigma_H 7258	182.23	Harmane	Imidazoline	Agonist
Sigma_H 7278	250.26	NG-Hydroxy-L-arginine acetate	Nitric Oxide	Metabolite
Sigma_H 7779	391.56	Retinoic acid p-hydroxyanilide	Cell Cycle	Inhibitor
Sigma_H 8034	388.43	HE-NECA	Adenosine	Agonist
Sigma_H 8125	191.62	L-Histidine hydrochloride	Histamine	Precursor
Sigma_H 8250	328.30	(±)-8-Hydroxy-DPAT hydrobromide	Serotonin	Agonist
Sigma_H 8502	189.64	Dopamine hydrochloride	Dopamine	Agonist
Sigma_H 8627	76.06	Hydroxyurea	DNA Metabolism	Inhibitor
Sigma_H 8645	383.40	(+)-Hydrastine	GABA	Antagonist
Sigma_H 8653	328.30	(±)-7-Hydroxy-DPAT hydrobromide	Dopamine	Agonist
Sigma_H 8759	302.35	MHPG sulfate potassium	Adrenoceptor	Metabolite
Sigma_H 8876	191.19	5-Hydroxyindolacetic acid	Serotonin	Metabolite
Sigma_H 9002	289.38	L-Hyoscyamine	Cholinergic	Antagonist
Sigma_H 9003	110.11	Hydroquinone	Leukotriene	Inhibitor
Sigma_B 8433	243.29	BU99006	Imidazoline	Ligand
Sigma_H 9382	211.09	3-Hydroxybenzylhydrazine dihydrochloride	Biochemistry	Inhibitor
Sigma_H 9523	212.68	Serotonin hydrochloride	Serotonin	Agonist
Sigma_L 2167	402.45	L-165,041	Lipid Signaling	Agonist
Sigma_H 9772	220.23	5-Hydroxy-L-tryptophan	Serotonin	Precursor
Sigma_H 9876	69.49	Hydroxylamine hydrochloride	Neurotransmission	Inhibitor
Sigma_H 9882	152.15	4-Hydroxybenzhydrazide	Biochemistry	Inhibitor
Sigma_H-108	574.36	Hemicholinium-3	Cholinergic	Blocker
Sigma_H-120	329.81	HA-1004 hydrochloride	Phosphorylation	Inhibitor

Sigma_H-121	364.30	H-7 dihydrochloride	Phosphorylation	Inhibitor
Sigma_H-127	386.03	Hexahydro-sila-difenidol hydrochloride, p-fluoro analog	Cholinergic	Antagonist
Sigma_H-128	198.10	Histamine, R(-)-alpha-methyl-, dihydrochloride	Histamine	Agonist
Sigma_H-135	210.25	5-hydroxydecanoic acid sodium	K+ Channel	Blocker
Sigma_H-140	328.30	R-(+)-8-Hydroxy-DPAT hydrobromide	Serotonin	Agonist
Sigma_H-168	328.30	R-(+)-7-Hydroxy-DPAT hydrobromide	Dopamine	Agonist
Sigma_G 6043	524.59	GR 125487 sulfamate salt	Serotonin	Antagonist
Sigma_I 0154	428.30	IEM-1460	Glutamate	Inhibitor
Sigma_I 0157	230.31	Ibudilast	Cyclic Nucleotides	Inhibitor
Sigma_I 0375	162.58	Imidazole-4-acetic acid hydrochloride	GABA	Antagonist
Sigma_I 0404	277.28	Indirubin-3'-oxime	Phosphorylation	Inhibitor
Sigma_N 1786	310.39	NSC 95397	Phosphorylation	Inhibitor
Sigma_I 0782	240.27	Imazodan	Cyclic Nucleotides	Inhibitor
Sigma_I 1149	184.96	Iodoacetamide	Biochemistry	Inhibitor
Sigma_I 1392	313.81	HA-100	Phosphorylation	Inhibitor
Sigma_I 1637	412.37	Ipratropium bromide	Cholinergic	Antagonist
Sigma_I 1656	497.51	Idarubicin	DNA Metabolism	Inhibitor
Sigma_I 1899	358.18	2-Iodomelatonin	Melatonin	Agonist
Sigma_S 2318	431.39	SB 228357	Serotonin	Antagonist
Sigma_I 2279	374.68	IMID-4F hydrochloride	K+ Channel	Blocker
Sigma_I 2760	361.35	R(-)-Isoproterenol (+)-bitartrate	Adrenoceptor	Agonist
Sigma_I 2764	452.74	ML-7	Phosphorylation	Inhibitor
Sigma_I 2765	158.11	(±)-Ibotenic acid	Glutamate	Agonist
Sigma_I 2892	801.00	Ifenprodil tartrate	Glutamate	Blocker
Sigma_I 3639	335.42	Isotharine mesylate	Adrenoceptor	Agonist
Sigma_I 3766	256.26	Isoliquiritigenin	Cyclic Nucleotides	Activator
Sigma_I 4883	206.29	(±)-Ibuprofen	Prostaglandin	Inhibitor
Sigma_I 5531	348.45	IIK7	Melatonin	Agonist
Sigma_I 5627	247.72	(±)-Isoproterenol hydrochloride	Adrenoceptor	Agonist
Sigma_I 5879	222.25	3-Isobutyl-1-methylxanthine	Adenosine	Inhibitor
Sigma_I 6138	240.69	Idazoxan hydrochloride	Imidazoline	Ligand
Sigma_I 6391	364.30	1-(5-Isoquinolinylsulfonyl)-3-methylpiperazine dihydrochloride	Phosphorylation	Inhibitor
Sigma_I 6504	247.72	(-)-Isoproterenol hydrochloride	Adrenoceptor	Agonist
Sigma_I 7016	364.30	1-(5-Isoquinolinylsulfonyl)-2-methylpiperazine dihydrochloride	Phosphorylation	Inhibitor
Sigma_I 7378	357.80	Indomethacin	Prostaglandin	Inhibitor
Sigma_I 7379	316.88	Imipramine hydrochloride	Serotonin	Blocker
Sigma_I 7388	179.14	Isoxanthopterin	Cell Stress	Metabolite
Sigma_I 7627	277.22	Iproniazid phosphate	Neurotransmission	Inhibitor
Sigma_I 8005	361.35	S(+)-Isoproterenol (+)-bitartrate	Adrenoceptor	
Sigma_I 8021	223.70	L-N6-(1-Iminoethyl)lysine hydrochloride	Nitric Oxide	Inhibitor
Sigma_I 8250	307.09	3-Iodo-L-tyrosine	Neurotransmission	Inhibitor
Sigma_I 8768	209.68	L-N5-(1-Iminoethyl)ornithine hydrochloride	Nitric Oxide	Inhibitor

Sigma_I 8898	875.12	Ivermectin	Cholinergic	Modulator
Sigma_I 9531	280.76	Imiloxan hydrochloride	Adrenoceptor	Antagonist
Sigma_I 9778	548.66	CR 2945	Cholecystokinin	Antagonist
Sigma_I 9890	648.26	m-Iodobenzylguanidine hemisulfate	Apoptosis	Activator
Sigma_I-106	206.29	S(+)-Ibuprofen	Prostaglandin	Inhibitor
Sigma_I-114	392.46	p-Iodoclonidine hydrochloride	Adrenoceptor	Agonist
Sigma_I-117	357.24	R(+)-IAA-94	Cl- Channel	Inhibitor
Sigma_I-119	328.67	Indatraline hydrochloride	Dopamine	Inhibitor
Sigma_I-120	339.65	Iofetamine hydrochloride	Neurotransmission	Analog
Sigma_I-122	501.84	ICI 204,448 hydrochloride	Opioid	Agonist
Sigma_I-127	313.87	ICI 118,551 hydrochloride	Adrenoceptor	Antagonist
Sigma_I-135	332.06	Imetit dihydrobromide	Histamine	Agonist
Sigma_I-138	161.16	1,5-Isoquinolinediol	Apoptosis	Inhibitor
Sigma_M 1818	312.84	Molindone hydrochloride	Dopamine	Antagonist
Sigma_I-146	510.29	IB-MECA	Adenosine	Agonist
Sigma_I-151	426.90	Indomethacin morpholinylamide	Cannabinoid	Ligand
Sigma_I-160	364.83	3-(1H-Imidazol-4-yl)propyl di(p-fluorophenyl)methyl ether hydrochloride	Histamine	Antagonist
Sigma_I18008	129.16	Isonipecotic acid	GABA	Agonist
Sigma_J 4252	327.43	JWH-015	Cannabinoid	Agonist
Sigma_J-102	307.40	JL-18	Dopamine	Antagonist
Sigma_K 0250	213.24	Kainic acid	Glutamate	Agonist
Sigma_K 1003	531.44	Ketoconazole	Multi-Drug Resistance	Inhibitor
Sigma_K 1136	376.41	Ketorolac tris salt	Prostaglandin	Inhibitor
Sigma_K 1751	254.29	Ketoprofen	Prostaglandin	Inhibitor
Sigma_K 1888	376.50	K 185	Melatonin	Antagonist
Sigma_K 2628	425.51	Ketotifen fumarate	Histamine	Antagonist
Sigma_K 3375	189.17	Kynurenic acid	Glutamate	Antagonist
Sigma_K 3888	327.18	Kenpaullone	Phosphorylation	Inhibitor
Sigma_K 4262	377.53	Karakoline	Cholinergic	Antagonist
Sigma_L 0258	363.80	L-701,324	Glutamate	Antagonist
Sigma_L 0664	246.31	loxoprofen	Prostaglandin	Inhibitor
Sigma_L 1011	364.88	Labetalol hydrochloride	Adrenoceptor	Antagonist
Sigma_L 1415	582.79	L-162,313	Neurotransmission	Agonist
Sigma_L 1788	256.78	Lidocaine N-methyl hydrochloride	Na+ Channel	Blocker
Sigma_L 2037	242.28	beta-Lapachone	Apoptosis	Activator
Sigma_L 2411	452.55	LY-367,265	Serotonin	Antagonist
Sigma_L 2536	430.95	LY-310,762 hydrochloride	Serotonin	Antagonist
Sigma_L 2540	591.24	L-368,899	Neurotransmission	Antagonist
Sigma_L 2906	387.82	Lomefloxacin hydrochloride	Antibiotic	Inhibitor
Sigma_L 3791	256.10	Lamotrigine	Anticonvulsant	
Sigma_L 4376	373.93	alpha-Lobeline hydrochloride	Cholinergic	Agonist
Sigma_L 4762	513.51	Loperamide hydrochloride	Opioid	Ligand
Sigma_L 4900	321.17	Lonidamine	Cell Stress	Inhibitor
Sigma_L 5025	270.21	Leflunomide	Immune System	Inhibitor
Sigma_V 1889	626.39	VER-3323 hemifumarate salt	Serotonin	Agonist

Sigma_L 5647	270.81	Lidocaine hydrochloride	Na ⁺ Channel	Modulator
Sigma_L 5783	343.31	Lidocaine N-ethyl bromide quaternary salt	Na ⁺ Channel	Antagonist
Sigma_L 8397	337.42	L-Leucinethiol, oxidized dihydrochloride	Biochemistry	Inhibitor
Sigma_L 8401	290.41	LE 300	Dopamine	Antagonist
Sigma_L 8533	369.37	Lansoprazole	Ion Pump	Inhibitor
Sigma_L 8539	327.90	L-687,384 hydrochloride	Opioid	Agonist
Sigma_L 8789	360.01	LFM-A13	Phosphorylation	Inhibitor
Sigma_N 0287	564.58	NNC 55-0396	Ca ²⁺ Channel	Inhibitor
Sigma_L 9539	373.86	L-655,240	Thromboxane	Antagonist
Sigma_L 9664	382.89	Loratadine	Histamine	Antagonist
Sigma_L 9756	240.76	(-)-Tetramisole hydrochloride	Phosphorylation	Inhibitor
Sigma_L 9787	341.37	L-655,708	Benzodiazepine	Ligand
Sigma_L 9908	343.81	LY-294,002 hydrochloride	Phosphorylation	Inhibitor
Sigma_L-106	445.91	Loxapine succinate	Dopamine	Antagonist
Sigma_L-107	500.60	LY-53,857 maleate	Serotonin	Antagonist
Sigma_L-109	481.40	Lorglumide sodium	Cholecystokinin	Antagonist
Sigma_L-110	414.47	LY-278,584 maleate	Serotonin	Antagonist
Sigma_P 0618_a	312.25	cis(+/-)-8-OH-PBZI hydrobromide	Dopamine	Agonist
Sigma_L-119	598.49	L-703,606 oxalate	Tachykinin	Antagonist
Sigma_L-121	433.51	Levallorphan tartrate	Opioid	Antagonist
Sigma_L-122	338.46	S-(-)-Lisuride	Dopamine	Agonist
Sigma_L-131	363.29	L-745,870 hydrochloride	Dopamine	Antagonist
Sigma_L-133	527.67	L-750,667 trihydrochloride	Dopamine	Antagonist
Sigma_L-134	391.48	Linopirdine	Cholinergic	Releaser
Sigma_L-135	340.86	L-741,626	Dopamine	Antagonist
Sigma_L-137	439.83	L-733,060 hydrochloride	Tachykinin	Antagonist
Sigma_M 0763	336.26	Metoclopramide hydrochloride	Dopamine	Antagonist
Sigma_M 0814	335.23	R(-)-Me5	Na ⁺ Channel	Antagonist
Sigma_M 1022	307.44	Dihydrocapsaicin	Vanilloid	Agonist
Sigma_M 1275	252.25	(-)-Naproxen sodium	Prostaglandin	Inhibitor
Sigma_M 1387	118.57	4-Methylpyrazole hydrochloride	Biochemistry	Inhibitor
Sigma_M 1404	301.33	Nocodazole	Cytoskeleton and ECM	Inhibitor
Sigma_M 1514	280.28	N-omega-Methyl-5-hydroxytryptamine oxalate salt	Serotonin	Ligand
Sigma_M 1559	278.14	Moxonidine hydrochloride	Adrenoceptor	Agonist
Sigma_M 1692	398.42	MRS 1845	Ca ²⁺ Channel	Inhibitor
Sigma_D 9305_b	199.64	1-Deoxynojirimycin hydrochloride	Biochemistry	Inhibitor
Sigma_M 1809	399.56	MRS 1523	Adenosine	Antagonist
Sigma_M 2011	305.21	Melphalan	DNA Metabolism	Intercalator
Sigma_M 2398	520.60	Metaproterenol hemisulfate	Adrenoceptor	Agonist
Sigma_M 2525	300.83	Mianserin hydrochloride	Serotonin	Antagonist
Sigma_M 2537	390.52	Mevastatin	Antibiotic	Inhibitor
Sigma_M 2547	266.30	8-Methoxymethyl-3-isobutyl-1-methylxanthine	Cyclic Nucleotides	Inhibitor
Sigma_M 2692	494.08	MK-886	Leukotriene	Inhibitor
Sigma_M 2727	215.73	Mexiletene hydrochloride	Na ⁺ Channel	Blocker

Sigma_M 2776	455.52	Methylergonovine maleate	Dopamine	Antagonist
Sigma_M 2901	242.24	Molsidomine	Nitric Oxide	Donor
Sigma_M 2922	278.24	3-Methyl-6-(3-[trifluoromethyl]phenyl)-1,2,4-triazolo[4,3-b]pyridazine	Benzodiazepine	Agonist
Sigma_M 3047	259.22	Mizoribine	DNA Metabolism	Inhibitor
Sigma_M 3127	278.37	S-Methylisothiourea hemisulfate	Nitric Oxide	Inhibitor
Sigma_M 3184	437.37	MG 624	Cholinergic	Antagonist
Sigma_M 3262	147.13	N-Methyl-D-aspartic acid	Glutamate	Agonist
Sigma_M 3281	245.71	alpha-Methyl-DL-tyrosine methyl ester hydrochloride	Neurotransmission	Inhibitor
Sigma_M 3315	514.49	MJ33	Lipid	Inhibitor
Sigma_M 3668	403.53	Metergoline	Serotonin	Antagonist
Sigma_U-106	519.43	(-)-cis-(1S,2R)-U-50488 tartrate	Neurotransmission	Ligand
Sigma_M 3778	308.64	Clorgyline hydrochloride	Neurotransmission	Inhibitor
Sigma_M 3808	459.30	MRS 2179	P2 Receptor	Antagonist
Sigma_M 3935	373.39	Meloxicam sodium	Prostaglandin	Inhibitor
Sigma_M 4008	302.24	Morin	Cell Stress	Inhibitor
Sigma_M 4145	209.25	Minoxidil	K ⁺ Channel	Activator
Sigma_M 4531	318.14	Meclofenamic acid sodium	Prostaglandin	Inhibitor
Sigma_M 4659	211.23	Milrinone	Cyclic Nucleotides	Inhibitor
Sigma_M 4796	209.20	(±)-alpha-Methyl-4-carboxyphenylglycine	Glutamate	Antagonist
Sigma_M 4910	198.10	1-Methylhistamine dihydrochloride	Histamine	Metabolite
Sigma_M 5154	315.84	Moxisylyte hydrochloride	Adrenoceptor	Antagonist
Sigma_M 5171	265.33	S-Methyl-L-thiocitrulline acetate	Nitric Oxide	Inhibitor
Sigma_M 5250	232.28	Melatonin	Melatonin	Agonist
Sigma_M 5379	180.23	L-Methionine sulfoximine	Glutamate	Inhibitor
Sigma_M 5391	684.83	(±)-Metoprolol (+)-tartrate	Adrenoceptor	Antagonist
Sigma_M 5435	229.71	6-Methyl-2-(phenylethynyl)pyridine hydrochloride	Glutamate	Antagonist
Sigma_M 5441	568.56	Mibefradil dihydrochloride	Ca ²⁺ Channel	Blocker
Sigma_M 5501	281.27	N6-Methyladenosine	Adenosine	Agonist
Sigma_M 5560	232.60	(S)-MAP4 hydrochloride	Glutamate	Antagonist
Sigma_M 5644	521.10	(±)-Methoxyverapamil hydrochloride	Ca ²⁺ Channel	Antagonist
Sigma_M 5685	276.29	Metrazoline oxalate	Imidazoline	Ligand
Sigma_M 6191	276.68	GW9662	Transcription	Inhibitor
Sigma_M 6316	486.53	MRS 1754	Adenosine	Antagonist
Sigma_M 6383	302.42	2-methoxyestradiol	Hormone	Metabolite
Sigma_M 6500	113.61	Cysteamine hydrochloride	Somatostatin	Depleter
Sigma_M 6517	517.08	alpha,beta-Methylene adenosine 5'-triphosphate dilithium	P2 Receptor	Agonist
Sigma_M 6524	247.72	Methoxamine hydrochloride	Adrenoceptor	Agonist
Sigma_M 6545	517.41	Mitoxantrone	DNA Metabolism	Inhibitor
Sigma_M 6628	226.71	O-Methylserotonin hydrochloride	Serotonin	Agonist
Sigma_M 6680	218.54	Se-(methyl)selenocysteine hydrochloride	Cell Cycle	Inhibitor
Sigma_M 6690	382.46	MDL 28170	Cell Cycle	Inhibitor
Sigma_M 6760	318.24	Myricetin	Phosphorylation	Inhibitor
Sigma_M 7033	248.28	NG-Monomethyl-L-arginine acetate	Nitric Oxide	Inhibitor
Sigma_M 7065	375.90	MK-912	Adrenoceptor	Agonist

Sigma_M 7277	211.22	(±)-3-(3,4-dihydroxyphenyl)-2-methyl-DL-alanine	Neurotransmission	Inhibitor
Sigma_M 7684	461.21	MRS 2159	P2 Receptor	Antagonist
Sigma_G 5793	534.06	GR 127935 hydrochloride	Serotonin	Antagonist
Sigma_D 8941	402.44	2,6-Difluoro-4-[2-(phenylsulfonylamino)ethylthio]phenoxyacetamide	Glutamate	Agonist
Sigma_M 8046	429.61	Mifepristone	Hormone	Antagonist
Sigma_M 8131	195.22	L-alpha-Methyl-p-tyrosine	Neurotransmission	Inhibitor
Sigma_S 1068	337.81	SB-215505	Serotonin	Antagonist
Sigma_M 8878	82.11	1-Methylimidazole	Prostaglandin	Inhibitor
Sigma_M 9020	203.76	Mecamylamine hydrochloride	Cholinergic	Antagonist
Sigma_M 9125	297.85	Methapyrilene hydrochloride	Histamine	Antagonist
Sigma_M 9292	215.77	Memantine hydrochloride	Glutamate	Antagonist
Sigma_M 9440	168.15	Me-3,4-dephostatin	Phosphorylation	Inhibitor
Sigma_M 9511	492.96	Minocycline hydrochloride	Cell Cycle	Inhibitor
Sigma_M 9651	313.87	Maprotiline hydrochloride	Adrenoceptor	Inhibitor
Sigma_M 9656	338.26	H-8 dihydrochloride	Phosphorylation	Inhibitor
Sigma_M-001	334.42	Proglumide	Cholecystokinin	Antagonist
Sigma_M-104	209.72	(±)-Muscarine chloride	Cholinergic	Agonist
Sigma_M-105	728.77	Methocramine tetrahydrochloride	Cholinergic	Antagonist
Sigma_M-107	337.38	(+)-MK-801 hydrogen maleate	Glutamate	Antagonist
Sigma_M-108	337.38	(-)-MK-801 hydrogen maleate	Glutamate	Antagonist
Sigma_M-109	306.32	2-Methyl-5-hydroxytryptamine maleate	Serotonin	Agonist
Sigma_M-110	306.32	alpha-Methyl-5-hydroxytryptamine maleate	Serotonin	Agonist
Sigma_M-116	365.84	Metolazone	Ion Pump	Inhibitor
Sigma_M-120	396.57	Metaphit methanesulfonate	Opioid	Antagonist
Sigma_M-129	211.22	L-alpha-Methyl DOPA	Biochemistry	Inhibitor
Sigma_M-137	469.54	Methysergide maleate	Serotonin	Antagonist
Sigma_M-140	196.68	Methylcarbamylocholine chloride	Cholinergic	Agonist
Sigma_M-149	452.66	Methiothepin mesylate	Serotonin	Antagonist
Sigma_M-152	539.24	2-Methylthioadenosine diphosphate trisodium	P2 Receptor	Agonist
Sigma_M-153	397.97	Mesulergine hydrochloride	Dopamine	Agonist
Sigma_M-166	280.67	MDL 26,630 trihydrochloride	Glutamate	Agonist
Sigma_Z 4626	367.92	ZM 39923 hydrochloride	Phosphorylation	Inhibitor
Sigma_M-184	206.63	3-Morpholinostydonimine hydrochloride	Nitric Oxide	Donor
Sigma_M-187	293.84	3-Methoxy-morphanin hydrochloride	Glutamate	Antagonist
Sigma_M-204	578.88	p-MPPI hydrochloride	Serotonin	Antagonist
Sigma_M-216	376.20	MDL 105,519	Glutamate	Antagonist
Sigma_M-225	371.40	Metrifudil	Adenosine	Agonist
Sigma_M-226	507.44	p-MPPF dihydrochloride	Serotonin	Antagonist
Sigma_M-231	391.90	(-)-3-Methoxynaltrexone hydrochloride	Opioid	Antagonist
Sigma_N 0630	282.22	Niflumic acid	Prostaglandin	Inhibitor
Sigma_N 1016	308.31	Nimesulide	Prostaglandin	Inhibitor
Sigma_N 1392	298.35	Nialamide	Neurotransmission	Inhibitor
Sigma_N 1530	354.41	Nomifensine maleate	Dopamine	Inhibitor
Sigma_N 1771	734.73	nor-Binaltorphimine dihydrochloride	Opioid	Antagonist
Sigma_N 2001	303.20	Neostigmine bromide	Cholinergic	Inhibitor
Sigma_N 2034	256.35	CR 2249	Glutamate	Agonist

Sigma_N 2255	419.42	S-(4-Nitrobenzyl)-6-thioinosine	Adenosine	Inhibitor
Sigma_N 3136	377.87	Naltrexone hydrochloride	Opioid	Antagonist
Sigma_N 3398	220.25	S-Nitroso-N-acetylpenicillamine	Nitric Oxide	Donor
Sigma_N 3510	327.13	Niclosamide	Antibiotic	
Sigma_N 3529	474.40	NAN-190 hydrobromide	Serotonin	Antagonist
Sigma_N 4034	234.62	NCS-356	GABA	Agonist
Sigma_N 4148	336.33	S-Nitrosogluthathione	Nitric Oxide	Donor
Sigma_N 4159	242.25	NCS-382	GABA	Antagonist
Sigma_N 4382	254.22	Nalidixic acid sodium	Antibiotic	Inhibitor
Sigma_N 4396	393.91	Nalbuphine hydrochloride	Opioid	Antagonist
Sigma_N 4779	300.32	5-Nitro-2-(3-phenylpropylamino)benzoic acid	Cl- Channel	Blocker
Sigma_N 4784	1505.10	NF449 octasodium salt	G protein	Antagonist
Sigma_N 5023	302.37	Nordihydroguaiaretic acid from Larrea divaricata (creosote bush)	Leukotriene	Inhibitor
Sigma_N 5260	462.41	(-)-Nicotine hydrogen tartrate salt	Cholinergic	Agonist
Sigma_N 5501	219.20	NG-Nitro-L-arginine	Nitric Oxide	Inhibitor
Sigma_N 5504	246.74	Naphazoline hydrochloride	Adrenoceptor	Agonist
Sigma_N 5636	119.08	3-Nitropropionic acid	Cell Stress	Toxin
Sigma_N 5751	269.69	NG-Nitro-L-arginine methyl ester hydrochloride	Nitric Oxide	Inhibitor
Sigma_N 7127	219.67	(±)-Normetanephrine hydrochloride	Adrenoceptor	Metabolite
Sigma_N 7261	299.85	Nortriptyline hydrochloride	Adrenoceptor	Inhibitor
Sigma_N 7505	833.36	NADPH tetrasodium	Nitric Oxide	Cofactor
Sigma_N 7510	516.00	Nicardipine hydrochloride	Ca2+ Channel	Antagonist
Sigma_N 7634	346.34	Nifedipine	Ca2+ Channel	Antagonist
Sigma_N 7758	363.84	Naloxone hydrochloride	Opioid	Antagonist
Sigma_N 7778	163.14	7-Nitroindazole	Nitric Oxide	Inhibitor
Sigma_N 7904	363.42	NS 521 oxalate	Glutamate	Modulator
Sigma_N 7906	369.25	2-(alpha-Naphthoyl)ethyltrimethylammonium iodide	Cholinergic	Inhibitor
Sigma_N 8403	175.15	6-Nitroso-1,2-benzopyrone	Transcription	Inhibitor
Sigma_N 8534	317.23	Nilutamide	Hormone	Inhibitor
Sigma_N 8652	1162.89	NF 023	P2 Receptor	Antagonist
Sigma_N 8659	272.70	Nimustine hydrochloride	DNA	Intercalator
Sigma_N 8784	168.15	Norcantharidin	Phosphorylation	Inhibitor
Sigma_N 9007	449.89	Noscapine hydrochloride	Opioid	Ligand
Sigma_N 9765	548.60	(+)-Nicotine (+)-di-p-toluoyl tartrate	Cholinergic	Agonist
Sigma_N-115	450.97	Naltrindole hydrochloride	Opioid	Antagonist
Sigma_S 6319	342.70	Sertraline hydrochloride	Serotonin	Inhibitor
Sigma_N-142	386.88	NO-711 hydrochloride	GABA	Inhibitor
Sigma_N-144	360.37	Nitrendipine	Ca2+ Channel	Antagonist
Sigma_N-149	418.45	Nimodipine	Ca2+ Channel	Antagonist
Sigma_N-151	307.82	Nisoxetine hydrochloride	Adrenoceptor	Blocker
Sigma_N-153	335.88	Nylidrin hydrochloride	Adrenoceptor	Agonist
Sigma_N-154	217.28	N6-Cyclopentyl-9-methyladenine	Adenosine	Antagonist
Sigma_N-156	511.60	Naltriben methanesulfonate	Opioid	Antagonist
Sigma_N-158	465.42	Naftopidil dihydrochloride	Adrenoceptor	Antagonist
Sigma_B 9305	368.48	BW 245C	Prostanoids	Agonist

Sigma_N-165	445.52	Naloxone benzoylhydrazone	Opioid	Agonist
Sigma_N-170	362.23	NS-1619	K+ Channel	Activator
Sigma_N-176	723.70	Naloxonazine dihydrochloride	Opioid	Antagonist
Sigma_N-183	380.25	NBQX disodium	Glutamate	Antagonist
Sigma_N-211	269.06	NS 2028	Cyclic Nucleotides	Inhibitor
Sigma_O 0250	189.64	(±)-Octopamine hydrochloride	Adrenoceptor	Agonist
Sigma_O 0383	325.54	N-Oleoylethanolamine	Sphingolipid	Inhibitor
Sigma_O 0877	261.24	Oxolinic acid	Antibiotic	Inhibitor
Sigma_O 0886	298.35	Olomoucine	Phosphorylation	Inhibitor
Sigma_O 1008	282.47	Oleic Acid	Phosphorylation	Activator
Sigma_O 2378	296.84	Oxymetazoline hydrochloride	Adrenoceptor	Agonist
Sigma_O 2751	111.03	Sodium Oxamate	Biochemistry	Inhibitor
Sigma_O 2881	393.96	Oxybutynin Chloride	Cholinergic	Antagonist
Sigma_O 3011	158.16	Oxiracetam	Nootropic	
Sigma_O 3125	584.67	Ouabain	Ion Pump	Inhibitor
Sigma_O 3636	187.16	ODQ	Cyclic Nucleotides	Inhibitor
Sigma_O 3752	305.85	Orphenadrine hydrochloride	Cholinergic	Antagonist
Sigma_T 5575	249.33	TG003	Cell Cycle	Inhibitor
Sigma_O 8757	361.38	Ofloxacin	Antibiotic	
Sigma_O 9126	760.80	Oxotremorine sesquifumarate salt	Cholinergic	Agonist
Sigma_O 9387	426.57	Oxatomide	Immune System	Modulator
Sigma_S 3442	371.23	SB 216763	Phosphorylation	Inhibitor
Sigma_O 9637	293.33	Oxaprozin	Prostaglandin	Inhibitor
Sigma_O-100	322.19	Oxotremorine methiodide	Cholinergic	Agonist
Sigma_O-111	460.98	(±)-Octoclothepein maleate	Dopamine	Antagonist
Sigma_P 0130	314.47	Progesterone	Hormone	
Sigma_P 0359	299.50	Palmitoylethanolamide	Cannabinoid	Agonist
Sigma_P 0453	244.25	Piceatannol	Phosphorylation	Inhibitor
Sigma_P 0547	592.69	Pentamidine isethionate	Glutamate	Antagonist
Sigma_P 0618_b	312.25	cis-(±)-8-OH-PBZI hydrobromide	Dopamine	Agonist
Sigma_P 0667	248.32	Parthenolide	Serotonin	Inhibitor
Sigma_P 0778	248.33	Pindolol	Adrenoceptor	Antagonist
Sigma_P 0878	185.07	O-Phospho-L-serine	Glutamate	Antagonist
Sigma_P 0884	295.81	(±)-Propranolol hydrochloride	Adrenoceptor	Antagonist
Sigma_P 1061	389.97	SKF-525A hydrochloride	Multi-Drug Resistance	Inhibitor
Sigma_P 1675	602.60	Picrotoxin	GABA	Antagonist
Sigma_P 1726	187.16	4-Phenyl-3-furoxanarbonitrile	Nitric Oxide	Donor
Sigma_P 1784	278.31	Pentoxifylline	Cyclic Nucleotides	Inhibitor
Sigma_P 1793	461.56	Pimozide	Dopamine	Antagonist
Sigma_P 1801	277.24	L-Glutamic acid, N-phthaloyl-	Glutamate	Agonist
Sigma_P 1918	732.69	Pancuronium bromide	Cholinergic	Antagonist
Sigma_P 2016	334.50	3- α ,21-Dihydroxy-5- α -pregnan-20-one	GABA	Modulator
Sigma_P 2116	185.23	Pirfenidone	Immune System	Inhibitor

Sigma_P 2278	256.27	1,3-Dimethyl-8-phenylxanthine	Adenosine	Antagonist
Sigma_P 2607	353.89	PRE-084	Opioid	Agonist
Sigma_P 2738	694.37	PPNDS tetrasodium	P2 Receptor	Antagonist
Sigma_P 2742	217.29	PD 404,182	Biochemistry	Inhibitor
Sigma_P 3510	375.86	Papaverine hydrochloride	Cyclic Nucleotides	Inhibitor
Sigma_P 3520	538.60	Pentolinium di[L(+)-tartrate]	Cholinergic	Antagonist
Sigma_P 4015	235.33	1-Phenyl-3-(2-thiazolyl)-2-thiourea	Dopamine	Inhibitor
Sigma_T 9567	210.30	Thiolactomycin	Antibiotic	Inhibitor
Sigma_P 4394	300.06	Cisplatin	DNA	Intercalator
Sigma_P 4405	414.42	Podophyllotoxin	Cytoskeleton and ECM	Inhibitor
Sigma_S 1693	241.25	SU 9516	Cell Cycle	Inhibitor
Sigma_P 4509	436.08	Palmitoyl-DL-Carnitine chloride	Phosphorylation	Modulator
Sigma_P 4532	385.43	R(-)-N6-(2-Phenylisopropyl)adenosine	Adenosine	Agonist
Sigma_P 4543	166.20	Valproic acid sodium	Anticonvulsant	
Sigma_P 4651	320.89	Promethazine hydrochloride	Histamine	Antagonist
Sigma_P 4668	312.42	Praziquantel	Antibiotic	
Sigma_P 4670	377.92	Propafenone hydrochloride	K ⁺ Channel	Blocker
Sigma_P 5052	332.49	5alpha-Pregnan-3alpha-ol-11,20-dione	GABA	Modulator
Sigma_P 5114	305.37	Pempidine tartrate	Cholinergic	Antagonist
Sigma_P 5295	142.16	Piracetam	Glutamate	Modulator
Sigma_P 5396	182.02	Phosphomycin disodium	Antibiotic	
Sigma_P 5514	401.47	Pyrilamine maleate	Histamine	Antagonist
Sigma_P 5654	331.35	Piroxicam	Prostaglandin	Inhibitor
Sigma_P 5679	194.19	3-n-Propylxanthine	Adenosine	Antagonist
Sigma_P 6126	203.67	Phenylephrine hydrochloride	Adrenoceptor	Agonist
Sigma_P 6402	403.98	Perphenazine	Dopamine	Antagonist
Sigma_P 6500	138.17	Pentylentetrazole	Neurotransmission	Modulator
Sigma_P 6503	244.72	(+)-Pilocarpine hydrochloride	Cholinergic	Agonist
Sigma_P 6628	271.28	Pilocarpine nitrate	Cholinergic	Agonist
Sigma_P 6656	320.89	Promazine hydrochloride	Dopamine	Antagonist
Sigma_P 6777	234.28	Phenelzine sulfate	Neurotransmission	Inhibitor
Sigma_P 6902	356.43	Pheniramine maleate	Histamine	Antagonist
Sigma_P 6909	140.03	Phosphonoacetic acid	DNA	Inhibitor
Sigma_P 7083	166.22	(-)-Perillic acid	G protein	Inhibitor
Sigma_P 7136	123.12	Pyrazinecarboxamide	Antibiotic	
Sigma_P 7295	218.26	Primidone	Anticonvulsant	
Sigma_P 7340	427.03	(±)-threo-1-Phenyl-2-decanoylamino-3-morpholino-1-propanol hydrochloride	Sphingolipid	Inhibitor
Sigma_P 7412	424.33	Pirenzepine dihydrochloride	Cholinergic	Antagonist
Sigma_P 7505	161.08	Putrescine dihydrochloride	Glutamate	Agonist
Sigma_P 7561	377.47	Phentolamine mesylate	Adrenoceptor	Antagonist
Sigma_P 7780	376.95	Propionylpromazine hydrochloride	Dopamine	Antagonist
Sigma_P 7791	419.87	Prazosin hydrochloride	Adrenoceptor	Antagonist
Sigma_P 7912	274.28	Phloretin	Ca ²⁺ Channel	Blocker
Sigma_P 8013	195.69	Pargyline hydrochloride	Neurotransmission	Inhibitor
Sigma_P 8139	616.84	Phorbol 12-myristate 13-acetate	Phosphorylation	Activator

Sigma_P 8227	444.26	1,3-PBIT dihydrobromide	Nitric Oxide	Inhibitor
Sigma_P 8293	562.67	Protoporphyrin IX disodium	Cyclic Nucleotides	Activator
Sigma_P 8352	444.26	1,4-PBIT dihydrobromide	Nitric Oxide	Inhibitor
Sigma_P 8386	308.38	Phenylbutazone	Prostaglandin	Substrate
Sigma_P 8477	376.42	Picotamide	Thromboxane	Antagonist
Sigma_P 8511	169.66	Tranlycypromine hydrochloride	Neurotransmission	Inhibitor
Sigma_P 8688	295.81	(S)-Propranolol hydrochloride	Adrenoceptor	Blocker
Sigma_P 8765	164.29	Ammonium pyrrolidinedithiocarbamate	Nitric Oxide	Modulator
Sigma_P 8782	173.17	(±)-cis-Piperidine-2,3-dicarboxylic acid	Glutamate	Agonist
Sigma_P 8813	299.85	Protriptyline hydrochloride	Adrenoceptor	Blocker
Sigma_P 8828	410.60	Pergolide methanesulfonate	Dopamine	Agonist
Sigma_P 8852	195.22	6(5H)-Phenanthridinone	Transcription	Inhibitor
Sigma_P 8887	318.50	5alpha-Pregnan-3alpha-ol-20-one	GABA	Modulator
Sigma_P 8891	448.40	Propantheline bromide	Cholinergic	Antagonist
Sigma_P 9159	165.21	Piperidine-4-sulphonic acid	GABA	Agonist
Sigma_P 9178	606.10	Prochlorperazine dimaleate	Dopamine	Antagonist
Sigma_P 9233	414.42	Piribedil maleate	Dopamine	Agonist
Sigma_P 9297	713.72	Paromomycin sulfate	Antibiotic	
Sigma_P 9375	180.21	1,10-Phenanthroline monohydrate	Biochemistry	Inhibitor
Sigma_P 9391	271.79	Procainamide hydrochloride	Na ⁺ Channel	Antagonist
Sigma_P 9547	256.78	Prilocaine hydrochloride	Na ⁺ Channel	Blocker
Sigma_P 9689	306.37	Propentofylline	Adenosine	Inhibitor
Sigma_P 9708	377.92	(S)-(-)-propafenone hydrochloride	Adrenoceptor	Blocker
Sigma_P 9797	261.12	Pyridostigmine bromide	Cholinergic	Inhibitor
Sigma_P 9879	272.78	Procaine hydrochloride	Na ⁺ Channel	Blocker
Sigma_P-101	358.36	2-Phenylaminoadenosine	Adenosine	Agonist
Sigma_P-102	255.79	R(+)-3PPP hydrochloride	Dopamine	Agonist
Sigma_P-103	255.79	S(-)-3PPP hydrochloride	Dopamine	Agonist
Sigma_P-105	345.92	(±)-PPHT hydrochloride	Dopamine	Agonist
Sigma_P-106	167.64	3-Phenylpropargylamine hydrochloride	Dopamine	Inhibitor
Sigma_P-107	371.40	N6-2-Phenylethyladenosine	Adenosine	Agonist
Sigma_P-108	343.34	N6-Phenyladenosine	Adenosine	Agonist
Sigma_P-118	249.64	Phaclofen	GABA	Antagonist
Sigma_P-119	480.45	(±)-Pindobind	Adrenoceptors	Ligand
Sigma_P-120	177.21	1-Phenylbiguanide	Serotonin	Agonist
Sigma_S 3317	284.32	SKF 94836	Calcium Signaling	Inhibitor
Sigma_P-126	393.47	Pirenperone	Serotonin	Antagonist
Sigma_I 0658	311.34	IC 261	Phosphorylation	Inhibitor
Sigma_P-152_b	248.33	S(-)-Pindolol	Serotonin	Agonist
Sigma_P-154	245.33	Pinacidil	K ⁺ Channel	Activator
Sigma_P-162	418.53	Pregnenolone sulfate sodium	GABA	Antagonist
Sigma_P-178	599.31	PPADS	P2 Receptor	Antagonist
Sigma_P-183	285.77	S(+)-PD 128,907 hydrochloride	Dopamine	Agonist
Sigma_P-203	401.83	Phenamyl methanesulfonate	Na ⁺ Channel	Inhibitor
Sigma_P-204	335.30	Phenylbenzene-omega-phosphono-alpha-amino acid	Glycine	Antagonist

Sigma_P-209	361.20	Phthalamoyl-L-glutamic acid trisodium	Glutamate	Agonist
Sigma_P-215	267.29	PD 98,059	Phosphorylation	Inhibitor
Sigma_P-216	285.77	(±)-PD 128,907 hydrochloride	Dopamine	Agonist
Sigma_P-233	450.50	PD 168,077 maleate	Dopamine	Agonist
Sigma_S 9692	371.46	SU 6656	Phosphorylation	Inhibitor
Sigma_P63204	167.12	Quinolinic acid	Glutamate	Antagonist
Sigma_Q 0125	302.24	Quercetin dihydrate	Cyclic Nucleotides	Inhibitor
Sigma_Q 0875	746.93	Quinidine sulfate	Na ⁺ Channel	Antagonist
Sigma_Q 1004	445.43	Quipazine dimaleate	Serotonin	Agonist
Sigma_Q 1250	746.93	Quinine sulfate	K ⁺ Channel	Antagonist
Sigma_Q 2128	189.13	(+)-Quisqualic acid	Glutamate	Agonist
Sigma_Q 3251	472.89	Quinacrine dihydrochloride	Neurotransmission	Inhibitor
Sigma_Q 3504	235.67	Quazinson	Cyclic Nucleotides	Inhibitor
Sigma_Q-102	255.79	(-)-Quinpirole hydrochloride	Dopamine	Agonist
Sigma_Q-107	459.46	Quipazine, N-methyl-, dimaleate	Serotonin	Agonist
Sigma_Q-109	374.36	Quipazine, 6-nitro-, maleate	Serotonin	Inhibitor
Sigma_Q-110	319.28	Quinelorane dihydrochloride	Dopamine	Agonist
Sigma_Q-111	292.25	(±)-Quinpirole dihydrochloride	Dopamine	Agonist
Sigma_R 0500	346.47	Cortisolone	Hormone	Precursor
Sigma_R 0758	323.82	Ritodrine hydrochloride	Adrenoceptor	Agonist
Sigma_R 1402	510.06	Raloxifene hydrochloride	Hormone	Modulator
Sigma_R 2625	300.44	Retinoic acid	Apoptosis	Activator
Sigma_R 2751	786.36	Ruthenium red	Ion Pump	Inhibitor
Sigma_R 3255	300.44	13-cis-retinoic acid	Transcription	Regulator
Sigma_R 3277	287.32	Rutaecarpine	K ⁺ Channel	Blocker
Sigma_R 4152	296.84	Ropinirole hydrochloride	Dopamine	Agonist
Sigma_R 5010	228.25	Resveratrol	Prostaglandin	Inhibitor
Sigma_R 5523	335.45	REV 5901	Leukotriene	Antagonist
Sigma_R 5648	516.55	Rottlerin	Phosphorylation	Inhibitor
Sigma_R 6152	500.47	Ranolazine dihydrochloride	Lipid	Inhibitor
Sigma_R 6520	275.35	Rolipram	Cyclic Nucleotides	Inhibitor
Sigma_R 7150	375.94	Ro 25-6981 hydrochloride	Glutamate	Antagonist
Sigma_R 7385	587.48	Phosphoramidon disodium	Biochemistry	Inhibitor
Sigma_R 7772	354.46	Roscovitine	Phosphorylation	Inhibitor
Sigma_R 8875	394.43	Rotenone	Cell Stress	Modulator
Sigma_R 8900	406.89	Ro 8-4304	Glutamate	Antagonist
Sigma_R 9525	270.72	RX 821002 hydrochloride	Adrenoceptor	Antagonist
Sigma_R 9644	244.21	Ribavirin	Cell Cycle	Inhibitor
Sigma_R-101	350.87	Ranitidine hydrochloride	Histamine	Antagonist
Sigma_R-103	477.58	Ritanserlin	Serotonin	Antagonist
Sigma_R-104	390.91	Rauwolscine hydrochloride	Adrenoceptor	Antagonist
Sigma_R-106	235.11	Ro 16-6491 hydrochloride	Neurotransmission	Inhibitor
Sigma_R-107	301.77	Ro 41-1049 hydrochloride	Neurotransmission	Inhibitor
Sigma_R-108	277.21	Ro 41-0960	Neurotransmission	Inhibitor
Sigma_R-115	840.11	Reactive Blue 2	P2 Receptor	Antagonist

Sigma_R-116	234.20	Riluzole	Glutamate	Antagonist
Sigma_R-118	410.50	Risperidone	Dopamine	Antagonist
Sigma_R-121	497.33	S(+)-Raclopride L-tartrate	Dopamine	Antagonist
Sigma_S 4692	514.54	Sobuzoxane	Gene Regulation	Inhibitor
Sigma_R-134	180.25	Rilmenidine hemifumarate	Imidazoline	Agonist
Sigma_D 7815	317.39	R(-)-Denopamine	Adrenoceptor	Agonist
Sigma_R-140	381.29	Ro 04-6790 dihydrochloride	Serotonin	Antagonist
Sigma_S 0278	308.83	(±)-Sotalol hydrochloride	Adrenoceptor	Antagonist
Sigma_S 0441	287.75	SB-366791	Vanilloid	Antagonist
Sigma_S 0501	261.92	Sodium nitroprusside dihydrate	Nitric Oxide	Releaser
Sigma_S 0752	167.21	(±)-Synephrine	Adrenoceptor	Agonist
Sigma_S 0758	314.37	Sulfaphenazole	Multi-Drug Resistance	Inhibitor
Sigma_S 1316	808.99	Seglitide	Somatostatin	Agonist
Sigma_S 1438	372.42	Sulindac sulfone	Prostaglandin	Inhibitor
Sigma_S 1441	612.75	Cortexolone maleate	Dopamine	Antagonist
Sigma_S 1563	232.15	SKF 86466	Adrenoceptor	Antagonist
Sigma_S 1688	248.16	SR 57227A	Serotonin	Agonist
Sigma_S 1875	384.27	(-)-Scopolamine hydrobromide	Cholinergic	Antagonist
Sigma_S 2064	352.75	SC-560	Prostaglandin	Inhibitor
Sigma_S 2201	111.53	Semicarbazide hydrochloride	Neurotransmission	Inhibitor
Sigma_S 2250	380.40	(-)-Scopolamine methyl nitrate	Cholinergic	Antagonist
Sigma_S 2381	464.13	DL-Stearoylcarnitine chloride	Phosphorylation	Inhibitor
Sigma_S 2501	254.63	Spermidine trihydrochloride	Glutamate	Ligand
Sigma_S 2812	449.64	SNC80	Opioid	Agonist
Sigma_S 2816	398.73	SKF 83959 hydrobromide	Dopamine	Agonist
Sigma_S 2876	348.19	Spermine tetrahydrochloride	Glutamate	Antagonist
Sigma_S 2941	350.26	SKF 75670 hydrobromide	Dopamine	Agonist
Sigma_S 3065	331.76	SC 19220	Prostaglandin	Antagonist
Sigma_S 3066	328.23	SKF 89626	Dopamine	Agonist
Sigma_S 3191	419.15	SKF 83565 hydrobromide	Dopamine	Agonist
Sigma_S 3313	419.35	SB 204070 hydrochloride	Serotonin	Antagonist
Sigma_O 2139	417.64	N-Oleoyldopamine	Neurotransmission	Ligand
Sigma_S 3378	416.58	Spirolactone	Hormone	Antagonist
Sigma_S 4063	348.27	SCH-202676 hydrobromide	G protein	Modulator
Sigma_S 4250	105.09	D-Serine	Glutamate	Agonist
Sigma_S 5013	576.71	Albuterol hemisulfate	Adrenoceptor	Agonist
Sigma_S 5890	367.79	Sanguinarine chloride	Ion Pump	Inhibitor
Sigma_S 6633	215.21	N-Succinyl-L-proline	Neurotransmission	Inhibitor
Sigma_S 6879	299.50	Sphingosine	Phosphorylation	Inhibitor
Sigma_S 7389	388.96	SB 269970 hydrochloride	Serotonin	Antagonist
Sigma_S 7395	431.94	Spiperone hydrochloride	Dopamine	Antagonist
Sigma_S 7690	370.41	SR 2640	Leukotriene	Antagonist
Sigma_S 7771	341.43	(-)-Sulpiride	Dopamine	Antagonist
Sigma_S 7809	402.93	SKF 96365	Ca ²⁺ Channel	Inhibitor
Sigma_S 7882	440.38	(-)-Scopolamine,n-Butyl-, bromide	Cholinergic	Antagonist
Sigma_S 7936	330.41	SB 205384	GABA	Modulator

Sigma_S 8010	341.43	(±)-Sulpiride	Dopamine	Antagonist
Sigma_C 7238	592.78	CV-3988	Cytokines & Growth Factors	Antagonist
Sigma_S 8139	356.42	Sulindac	Prostaglandin	Inhibitor
Sigma_S 8251	361.31	Succinylcholine chloride	Cholinergic	Antagonist
Sigma_S 8260	239.32	Salbutamol	Adrenoceptor	Agonist
Sigma_S 5068	603.76	Salmeterol xinafoate	Adrenoceptor	Agonist
Sigma_S 8442	238.29	SU 5416	Phosphorylation	Inhibitor
Sigma_S 8502	398.30	(-)-Scopolamine methyl bromide	Cholinergic	Antagonist
Sigma_S 8567	264.33	SU 4312	Phosphorylation	Inhibitor
Sigma_S 8688	415.49	SR 59230A oxalate	Adrenoceptor	Antagonist
Sigma_B 5559	391.77	BRL 52537 hydrochloride	Neurotransmission	Agonist
Sigma_S 9066	371.91	SKF 89976A hydrochloride	GABA	Inhibitor
Sigma_S 9186	213.24	SIB 1757	Glutamate	Antagonist
Sigma_S 9311	195.27	SIB 1893	Glutamate	Antagonist
Sigma_S-003	248.76	1-(1-Naphthyl)piperazine hydrochloride	Serotonin	Antagonist
Sigma_S-006	545.53	Ketanserin tartrate	Serotonin	Antagonist
Sigma_S-008	228.72	1-(2-Methoxyphenyl)piperazine hydrochloride	Serotonin	Agonist
Sigma_S-009	349.40	PAPP	Serotonin	Agonist
Sigma_S-103	379.46	Spiroxatrine	Serotonin	Agonist
Sigma_S-106	368.23	SR-95531	GABA	Antagonist
Sigma_S-143	370.68	(±)-6-Chloro-PB hydrobromide	Dopamine	Agonist
Sigma_S-145	248.22	SKF 91488 dihydrochloride	Histamine	Inhibitor
Sigma_S 2671	1429.19	Suramin hexasodium	P2 Receptor	Antagonist
Sigma_S-153	205.22	SQ 22536	Cyclic Nucleotides	Inhibitor
Sigma_S-154	237.22	Sepiapterin	Nitric Oxide	Cofactor
Sigma_S-159	413.47	R(-)-SCH-12679 maleate	Dopamine	Antagonist
Sigma_S-168	376.30	(±)-SKF 38393, N-allyl-, hydrobromide	Dopamine	Agonist
Sigma_S-174	337.25	SDZ-205,557 hydrochloride	Serotonin	Antagonist
Sigma_S-180	328.80	SB 206553 hydrochloride	Serotonin	Antagonist
Sigma_S-201	557.10	SB 224289 hydrochloride	Serotonin	Antagonist
Sigma_T 0254	204.23	L-Tryptophan	Serotonin	Precursor
Sigma_T 0318	327.34	Tranilast	Leukotriene	Inhibitor
Sigma_T 0410	364.89	Tiapride hydrochloride	Dopamine	Antagonist
Sigma_T 0625	125.15	Taurine	Glycine	Agonist
Sigma_T 0780	480.10	Thiothixene hydrochloride	Dopamine	Antagonist
Sigma_T 0891	270.35	Tolbutamide	Hormone	Releaser
Sigma_T 1132	296.54	Tetraethylthiuram disulfide	Biochemistry	Inhibitor
Sigma_T 1443	402.07	TCPOBOP	Transcription	Agonist
Sigma_T 1505	342.36	Tetraisopropyl pyrophosphoramidate	Biochemistry	Inhibitor
Sigma_T 1512	240.76	Tetramisole hydrochloride	Phosphorylation	Inhibitor
Sigma_T 1516	337.94	Trihexyphenidyl hydrochloride	Cholinergic	Antagonist
Sigma_T 1633	179.18	Theophylline	Adenosine	Antagonist
Sigma_T 1694	101.11	(E)-4-amino-2-butenoic acid	GABA	Agonist
Sigma_T 1698	288.50	Tetradecylthioacetic acid	Transcription	Agonist
Sigma_T 2057	441.96	Trequinsin hydrochloride	Cyclic Nucleotides	Inhibitor

Sigma_T 2067	316.47	Tyrphostin AG 879	Phosphorylation	Inhibitor
Sigma_T 2265	165.71	Tetraethylammonium chloride	Cholinergic	Antagonist
Sigma_T 2408	311.41	Tolazamide	Hormone	Releaser
Sigma_T 2528	548.66	Terbutaline hemisulfate	Adrenoceptor	Agonist
Sigma_T 2879	173.64	4-Hydroxyphenethylamine hydrochloride	Dopamine	Agonist
Sigma_T 2896	388.89	Triflupromazine hydrochloride	Dopamine	Antagonist
Sigma_T 3146	410.52	Trimipramine maleate	Serotonin	Inhibitor
Sigma_T 3434	294.31	Tyrphostin AG 490	Phosphorylation	Inhibitor
Sigma_T 3757	348.49	TTNPB	Transcription	Ligand
Sigma_L 3040	522.61	L-765,314	Adrenoceptor	Antagonist
Sigma_T 4143	253.27	Triamterene	Na ⁺ Channel	Blocker
Sigma_T 4182	315.76	Tyrphostin AG 1478	Phosphorylation	Inhibitor
Sigma_T 4264	236.75	Tetrahydrozoline hydrochloride	Adrenoceptor	Agonist
Sigma_T 4318	280.29	Tyrphostin AG 494	Phosphorylation	Inhibitor
Sigma_T 4376	351.85	N-p-Tosyl-L-phenylalanine chloromethyl ketone	Biochemistry	Inhibitor
Sigma_T 4425	314.17	(6R)-5,6,7,8-Tetrahydro-L-biopterin hydrochloride	Neurotransmission	Cofactor
Sigma_T 4443	308.34	Tyrphostin AG 527	Phosphorylation	Inhibitor
Sigma_T 4500	180.17	Theobromine	Adenosine	Antagonist
Sigma_T 4512	304.26	(±)-Taxifolin	Cell Stress	Inhibitor
Sigma_T 4568	308.34	Tyrphostin AG 528	Phosphorylation	Inhibitor
Sigma_T 4680	423.90	Terazosin hydrochloride	Adrenoceptor	Antagonist
Sigma_T 4693	448.44	Tyrphostin AG 537	Phosphorylation	Inhibitor
Sigma_T 4818	322.37	Tyrphostin AG 555	Phosphorylation	Inhibitor
Sigma_T 5193	308.34	Tyrphostin AG 698	Phosphorylation	Inhibitor
Sigma_T 5318	304.31	Tyrphostin AG 808	Phosphorylation	Inhibitor
Sigma_T 5515	781.46	Thio-NADP sodium	Intracellular Calcium	Blocker
Sigma_T 5568	308.34	Tyrphostin AG 835	Phosphorylation	Inhibitor
Sigma_T 5625	206.33	(±)-alpha-Lipoic Acid	Cell Stress	Coenzyme
Sigma_T 6031	253.32	DL-Thiorphan	Neurotransmission	Inhibitor
Sigma_T 6050	264.20	Tulobuterol hydrochloride	Adrenoceptor	Agonist
Sigma_T 6154	408.33	Trazodone hydrochloride	Serotonin	Inhibitor
Sigma_T 6318	216.20	Tyrphostin AG 34	Phosphorylation	Inhibitor
Sigma_T 6376	394.44	Triamcinolone	Hormone	Agonist
Sigma_T 6394	432.50	S(-)-Timolol maleate	Adrenoceptor	Antagonist
Sigma_T 6692	423.34	N,N,N-trimethyl-1-(4-trans-stilbenoxy)-2-propylammonium iodide	Cholinergic	Antagonist
Sigma_T 6764	314.86	Triprolidine hydrochloride	Histamine	Antagonist
Sigma_T 6943	236.23	Tyrphostin AG 112	Phosphorylation	Inhibitor
Sigma_T 7040	184.20	Tyrphostin 1	Phosphorylation	Inhibitor
Sigma_T 7165	186.17	Tyrphostin 23	Phosphorylation	Inhibitor
Sigma_T 7188	284.73	TFPI hydrochloride	Nitric Oxide	Inhibitor
Sigma_T 7254	369.31	Na-p-Tosyl-L-lysine chloromethyl ketone hydrochloride	Cyclic Nucleotides	Inhibitor
Sigma_T 7290	202.17	Tyrphostin 25	Phosphorylation	Inhibitor
Sigma_T 7313	212.18	1-[2-(Trifluoromethyl)phenyl]imidazole	Nitric Oxide	Inhibitor
Sigma_T 7402	853.93	Taxol	Cytoskeleton and ECM	Inhibitor

Sigma_T 7508	300.83	Tetracaine hydrochloride	Na ⁺ Channel	Modulator
Sigma_T 7540	220.25	Tyrphostin 47	Phosphorylation	Inhibitor
Sigma_T 7665	268.23	Tyrphostin 51	Phosphorylation	Inhibitor
Sigma_T 7692	665.68	T-1032	Cyclic Nucleotides	Inhibitor
Sigma_T 7697	437.19	I-OMe-Tyrphostin AG 538	Phosphorylation	Inhibitor
Sigma_T 7822	297.27	Tyrphostin AG 538	Phosphorylation	Inhibitor
Sigma_T 7883	290.32	Trimethoprim	Antibiotic	Inhibitor
Sigma_T 7947	255.36	Tomoxetine	Adrenoceptor	Inhibitor
Sigma_T 8067	620.07	T-0156	Cyclic Nucleotides	Inhibitor
Sigma_T 8160	314.21	3-Tropanyl-3,5-dichlorobenzoate	Serotonin	Antagonist
Sigma_T 8516	480.43	Trifluoperazine dihydrochloride	Dopamine	Antagonist
Sigma_T 8543	266.47	D-609 potassium	Lipid	Inhibitor
Sigma_T 9025	407.04	Thioridazine hydrochloride	Dopamine	Antagonist
Sigma_T 9033	650.77	Thapsigargin	Intracellular Calcium	Releaser
Sigma_T 9177	215.17	Tyrphostin AG 126	Phosphorylation	Inhibitor
Sigma_T 9262	563.65	Tamoxifen citrate	Phosphorylation	Inhibitor
Sigma_T 9652	471.69	Terfenadine	Histamine	Antagonist
Sigma_T 9778	284.36	Tropicamide	Cholinergic	Antagonist
Sigma_T-101	176.60	THIP hydrochloride	GABA	Agonist
Sigma_T-103	445.89	Trifluoperidol hydrochloride	Dopamine	Antagonist
Sigma_T-104	320.82	3-Tropanyl-indole-3-carboxylate hydrochloride	Serotonin	Antagonist
Sigma_T-112	304.40	Tracazolate	GABA	Modulator
Sigma_T-113	426.30	3-Tropanylindole-3-carboxylate methiodide	Serotonin	Antagonist
Sigma_T-122	443.40	Telenzepine dihydrochloride	Cholinergic	Antagonist
Sigma_T-123	408.52	Thioperamide maleate	Histamine	Antagonist
Sigma_T-144	258.24	(±)-Thalidomide	Cytoskeleton and ECM	Inhibitor
Sigma_T-165	340.47	R(+)-Terguride	Dopamine	Agonist
Sigma_T-173	191.25	Thiocitrulline	Nitric Oxide	Inhibitor
Sigma_T-182	282.39	Tyrphostin A9	Phosphorylation	Inhibitor
Sigma_T-200	161.14	TPMPA	GABA	Antagonist
Sigma_U 1508	361.53	U-75302	Leukotriene	Agonist
Sigma_U 4125	448.13	Uridine 5'-diphosphate sodium	P2 Receptor	Agonist
Sigma_U 5882	726.92	U-74389G maleate	Cell Stress	Inhibitor
Sigma_U 6007	593.65	U-83836 dihydrochloride	Cell Stress	Inhibitor
Sigma_U 6756	464.65	U-73122	Lipid	Inhibitor
Sigma_S 5317	613.69	SKF 95282 dimaleate	Histamine	Antagonist
Sigma_U 7500	138.13	4-Imidazoleacrylic acid	Histamine	Inhibitor
Sigma_U-100	423.95	Urapidil hydrochloride	Adrenoceptor	Antagonist
Sigma_U-101	401.51	Urapidil, 5-Methyl-	Adrenoceptor	Antagonist
Sigma_U-103	356.51	U-69593	Opioid	Agonist
Sigma_U-104	292.14	UK 14,304	Adrenoceptor	Agonist
Sigma_U-105	521.51	U-62066	Opioid	Agonist
Sigma_U-108	301.84	S(-)-UH-301 hydrochloride	Serotonin	Antagonist
Sigma_U-109	301.84	R(+)-UH-301 hydrochloride	Serotonin	Agonist

Sigma_U-110	405.80	(+)-trans-(1R,2R)-U-50488 hydrochloride	Opioid	Agonist
Sigma_U-111	405.80	(-)-trans-(1S,2S)-U-50488 hydrochloride	Opioid	Agonist
Sigma_U-115	455.56	U-101958 maleate	Dopamine	Antagonist
Sigma_U-116	393.48	U-99194A maleate	Dopamine	Antagonist
Sigma_U-120	380.50	U0126	Phosphorylation	Inhibitor
Sigma_V 1377	909.07	Vinblastine sulfate salt	Cytoskeleton and ECM	Inhibitor
Sigma_V 4629	491.08	(±)-Verapamil hydrochloride	Ca ²⁺ Channel	Modulator
Sigma_V 5888	371.40	VUF 5574	Adenosine	Antagonist
Sigma_V 6383	350.46	Vinpocetine	Cyclic Nucleotides	Inhibitor
Sigma_V 8138	1485.75	Vancomycin hydrochloride from <i>Streptomyces orientalis</i>	Antibiotic	
Sigma_V 8261	129.16	(±)-gamma-Vinyl GABA	GABA	Inhibitor
Sigma_V 8879	923.06	Vincristine sulfate	Cytoskeleton and ECM	Inhibitor
Sigma_V 9130	293.41	N-Vanillylnonanamide	Vanilloid	Ligand
Sigma_V-100	295.86	(±)-Vesamicol hydrochloride	Cholinergic	Inhibitor
Sigma_X 3628	366.74	XK469	Apoptosis	Inhibitor
Sigma_W 1628	428.44	Wortmannin from <i>Penicillium funiculosum</i>	Phosphorylation	Inhibitor
Sigma_W 4262	250.17	1400W dihydrochloride	Nitric Oxide	Inhibitor
Sigma_W 4761	808.66	WB 64	Cholinergic	Ligand
Sigma_W-102	522.63	(R)-(+)-WIN 55,212-2 mesylate	Cannabinoid	Agonist
Sigma_W-104	438.58	WIN 62,577	Tachykinin	Antagonist
Sigma_W-105	199.17	S(-)-Willardiine	Glutamate	Agonist
Sigma_W-108	538.65	WAY-100635 maleate	Serotonin	Antagonist
Sigma_W-110	325.06	S-5-Iodowillardiine	Glutamate	Agonist
Sigma_X 1251	256.80	Xylazine hydrochloride	Adrenoceptor	Agonist
Sigma_X 3253	794.86	Xamoterol hemifumarate	Adrenoceptor	Agonist
Sigma_X 6000	280.84	Xylometazoline hydrochloride	Adrenoceptor	Agonist
Sigma_X-103	428.50	Xanthine amine congener	Adenosine	Antagonist
Sigma_Y 3125	390.91	Yohimbine hydrochloride	Adrenoceptor	Antagonist
Sigma_Y-101	395.93	YS-035 hydrochloride	Ca ²⁺ Channel	Blocker
Sigma_Y-102	304.35	YC-1	Cyclic Nucleotides	Activator
Sigma_Z 0878	271.28	Zaprinast	Cyclic Nucleotides	Inhibitor
Sigma_Z 2001	234.21	Zonisamide sodium	Anticonvulsant	
Sigma_Z 3003	268.22	Zardaverine	Cyclic Nucleotides	Inhibitor
Sigma_Z-101	390.15	Zimelidine dihydrochloride	Serotonin	Inhibitor

6.4.4. Liquid class programs

- Program 1 (20-201 μ l)

	Aspiration	Dispensing
Speed (μl/s)	100	100
Delay (ms)	500	200
System Trailing Air gap (μl)	0	
Leading air gap (μl)	15	
Trailing air gap (μl)	10	
Aspiration/Dispensing position	z-max \pm offset, with tracking 0 mm, x: center	z-max \pm offset, no tracking 0 mm, x: center
Retract tip to	z-start 0 mm	z-start 0 mm
Retract speed (mm/s)	100	100

- Program 2 (20-201 μ l)

	Aspiration	Dispensing
Speed (μl/s)	200	200
Delay (ms)	500	200
System Trailing Air gap (μl)	0	
Leading air gap (μl)	15	
Trailing air gap (μl)	0	
Aspiration/ Dispensing position	z-max \pm offset, with tracking 0 mm, x: center	z-dispense \pm offset, no tracking -10 mm, x: center
Retract tip to	z-start 0 mm	z-start 0 mm
Retract speed (mm/s)	42	42

- Program 3 (20-201 μ l)

	Aspiration	Dispensing
Speed (μl/s)	100	100
Delay (ms)	500	200
System Trailing Air gap (μl)	0	
Leading air gap (μl)	15	
Trailing air gap (μl)	10	
Aspiration/ Dispensing position	z-max \pm offset, with tracking 0 mm, x: center	z-max \pm offset, no tracking -10 mm, x: center
Retract tip to	z-start 0 mm	z-start 0 mm
Retract speed (mm/s)	100	100

▪ Program 3 (7.5-15 μ l)

	Aspiration	Dispensing
Speed (μl/s)	10	20
Delay (ms)	200	200
System Trailing Air gap (μl)	0	
Leading air gap (μl)	10	
Trailing air gap (μl)	1	
Aspiration/ Dispensing position	z-max \pm offset, no tracking 0 mm, x: center	z-max \pm offset, no tracking 0 mm, x: center
Retract tip to	z-start 0 mm	z-start 0 mm
Retract speed (mm/s)	5	42

Acknowledgment

7. Acknowledgment

Even a lot of books cannot replace a good teacher. Hence, I would like to thank my supervisor Prof. Rita Bernhardt that gives me the chance to be one of her interesting team. During the last couples of years, I had the honour to be one of your team, a member in this big family, which is called AK Bernhardt. I will not forget theses years and every moment you spent to give me the scientific advice. Although every person has only two parents, I feel that I am somewhat different!

I thank the German Academic Exchange Service (DAAD; Deutscher Akademischer Austausch Dienst) for the financial support of this work.

Special thank to Prof. Dr. Mohyden Jumaa and Prof. Dr. Friedrich Sitzmann for every effort that they spent to help me to achieve this academic level.

Many thanks to PD Dr. Matthias Bureik, Dr. Frank Hannemann and Dipl. Biol. Calin-Aurel Dragan for countless scientific conversation and for giving me lots of valuable information. Additionally, I would like to thank PD Dr. Matthias Bureik and Dipl. Biol. Calin-Aurel Dragan that introduced me in the interesting world of *S. pombe*.

Special thanks to Dr. Frank Hannemann and PD Dr. Matthias Bureik for the proof reading of the present manuscript and to our cooperation partners at the Max-Planck-Institute of Molecular Physiology, Dortmund; Prof. Herbert Waldmann and Dr. Katja Hübel.

Many thanks also to our other cooperation partners from the University of Ljubljana, Slovenia; Prof. Bronislava Cresnar and Ms. Spela Petric.

Special thank to our nice secretary Ms. Gabi Schon! Frau Schon es war schön mit dir zu arbeiten!

At this point, I would like to thank my parents Mrs. Ghada Al Ghrawi and Dr. Farouk Hakki and my lovely brother Talal. I am very thankful for having such wonderful family. Although you are **2984** kilometers away from me, you have been all the time with me.

Acknowledgment

Special thank to my officemate Dr. Andreas Bichet and my good smoking partner Calin-Aurel Dragan, and many thanks to each member of our group for the excellent working climate!

Curriculum Vitae

- **Personal data**

Last Name: Hakki

First Name: Tarek

Place of birth and date: Schlüchtern, Germany, 15. 01.1975

Nationality: Syrian

Gender: Male

Address: Hanna-Kirchner Straße 6, 66123 Saarbrücken, Germany

eMail: t.hakki@mx.uni-saarland.de

[phm t hakki@hotmail.com](mailto:phm_t_hakki@hotmail.com)



- **Academic background**

2004 -Present Department of biochemistry, University of Saarland, Saarbrücken, Germany.

PhD student.

- Research topic: Development of efficient P450-dependent whole-cell biotransformation reactions for steroid hydroxylation and drug discovery
- Supervisor: Prof. Dr. Rita Bernhardt

2000-2003 Faculty of Pharmacy, University of Damascus, Damascus, Syria.

Master degree of Laboratory diagnosis (Clinical biochemistry)

overall GPA: 90%.

- Research topic: Deep vein thrombosis, environmental and inherited risk factors.
- Internal supervisor: Prof. Dr. M. Jouma. Damascus, Syria.
- External supervisor: Prof. Dr. W. Herrmann. Homburg, Saarland, Germany.
- Publication: Obeid, R., Hakki, T., Jouma, M. and Herrmann, W., 2003. The risk of venous thromboembolism associated with the factor V Leiden mutation and low B-vitamin status. Clin Chem Lab Med. 41, 1357-1362.

Curriculum Vitae

1998-2000 Faculty of Pharmacy, University of Damascus, Damascus, Syria.
Diploma of Laboratory diagnosis overall GPA: 75%.

1993-1998 Faculty of Pharmacy, University of Damascus, Damascus, Syria.
Bachelor of pharmacy overall GPA: 69 %

- **Language skills**

Arabic, English, German

- **Honours & Awards**

DAAD scholarship 2004-2007

“Ich denke niemals an die Zukunft.

Sie kommt früh genug“

Albert Einstein

Affidavit

I hereby swear in lieu of an oath that I have independently prepared this thesis and without using other aids than those stated. The data and concepts taken over from other sources or taken over indirectly are indicated citing the source. The thesis was not submitted so far either in Germany or in another country in the same or a similar form in a procedure for obtaining an academic title.

Place, date

(signature)